DOCTORAL DISSERTATION SERIES

PUBLICATION: 7607

AUTHOR: Philip Edmund Bocquet, Ph. D., 1953
University of Michigan

TITLE: THE STREAMING POTENTIAL CONCEPT

University Microfilms, Ann Arbor, Michigan

THE STREAMING POTENTIAL CONCEPT

by
Philip E. Bocquet

A dissertation submitted in partial fulfillment
of the requirements for the degree of
Doctor of Philosophy in the
University of Michigan
1952

Committee in charge:

Associate Professor Cedomir M. Sliepcevich, Chairman
Associate Professor David F. Bohr
Professor Russell A. Dodge
Associate Professor Sibley W. Hoobler
Professor Donald L. Katz
Professor Melville B. Stout

Abstract

THE STREAMING POTENTIAL CONCEPT

by Philip E. Bocquet

"The Streaming Potential Concept" is a study which is directed toward the clarification of this concept with emphasis placed on its relation to fluid flow.

A review of the literature includes articles by Helmholtz, Smoluchowski, Stern, and Reichardt, as well as many later authors. The bibliography contains 73 references.

Equipment is described in which the streaming potential, pressure differences, temperature, flow rate, and electrical resistance of the solution can be measured for streaming potential tubes which may be any length up to about one meter. There are 30 tables of experimental data.

The results of the experiments show that the Helmholtz-Smoluchowski streaming potential equation is valid for either turbulent or laminar flow, but that the flow must be "established". An established flow is defined as one whose pressure gradient is independent of the axial distance along a tube. The existence of the laminar film for turbulent flow is confirmed.

An hypothesis is presented for the day-to-day variation of the zeta-potential, depending on the rate of adsorption of the positive and negative ions on the surface.

Several mathematical analyses on the effect of the surface conductance and the electroosmotic countereffect on electrokinetic phenomena are included.

Since the velocity gradient at the wall is proportional to the streaming potential gradient, the streaming potential can be used to evaluate the velocity gradient at the wall for a nonestablished flow.

PREFACE

While the writing of a doctoral dissertation may be the culmination of a formal education, the basis has been the exchange of ideas between the student and his teachers. If one professor can be singled out, it would be the late Professor George Bauer of Texas A and M, who taught this writer more than the context of his courses.

Should this study have significance, it is not primarily the discovery of new concepts, but more the clarification of old ones by combining the viewpoints of several fields of science. Actually, this goal was the original intent of Professor Cedomir M. Sliepcevich and the writer when interdepartmental research was investigated as possible doctoral research in chemical engineering.

The meeting with Dr. David F. Bohr of the Physiology Department was very fortunate for he became the director of the project as well as arranged funds for equipment and personnel. His daily interest, even though this problem developed outside his personal field, was a source of encouragement throughout these past four years. The close cooperation and coordination between these professors and their willingness to give needed advice have eased the task.

This study evolved from the original ideas of Dr. W. John Kenfield. Professor Donald L. Katz, Professor Melville B. Stout, and Dr. Sibley W. Hoobler, as members of the doctoral committee, have contributed the viewpoints of their fields of specialization. It was Professor Russell A. Dodge, also a member of the committee, who first introduced to this writer the concept of a nonestablished flow, which is an essential idea of this presentation.

The author's interpretation of Helmholtz' concepts of electrokinetics would not have been possible without the generous help of Dr. B. A. Uhlendorf in the translation of the involved German. Harold J. Kitto, Norman A. Obrien, Enrique Perez, and Lester E. Vocke, fellow students, each had his patience well tested by his part in the operation of the equipment which, at times, could best be described as fickle or temperamental.

Much time and effort was saved by the construction of many of the essential components of the equipment by Earl N. Bryant, a skilled craftsman, whose technical knowledge and experience enable him to convert ideas into workable apparatus.

The life of this graduate student was made more pleasant by the financial assistance in the form of the American Cynamid Fellowship in Chemical Engineering (1947-1948), a Research Assistantship in Physiology from Public Health Project H-670 (1949-1951), and the Michigan Heart Fellowship in Chemical Engineering (1951-1952).

This writer is grateful for his association with all these people and their aid to him, to the other members of the chemical engineering faculty, to the librarians particularly for their help in locating the older references, to the typists of this dissertation, and to Dr. Ruth B. McVaugh, who unravelled many of the ambiguities of the text in its final stages.

TABLE OF CONTENTS

	Page
Preface	ii
Purpose	vii
Summary	viii
List of Tables	x
List of Figures	xi
A General Discussion of the Electrokinetic Effects and the Liquid Flow through Small Tubes	1
Electric Double Layer	3
Stern's Theory	4
Condenser Analogy	8
Zeta-Potential	9
Moment	10
Dielectric Constant	11
Previous History of the Surface	12
Formation of the Double Layer	13
Rate of Formation	14
Electrokinetic Effects	15
Electroosmosis	17
Electrophoresis	25
Electrophoretic Potential	26
Streaming Potential	26
(1) Helmholtz-Smoluchowski Equation	27
(2) Effect of Surface Conductance	31
(3) Double Layer Thickness	36
(4) Electroosmotic Countereffect	37
(5) Hydrostatic Factors	40
Interrelationships of Electrokinetic Effects	44
Liquid Flow in Small Tubes	47
Energy of Motivation	48
Flow Resistance	49
Laminar Flow	52
Turbulent Flow	52
Reynolds Number	53
Established Flow	54
Entrance and Exit Effects	60
Experimental Work	64
Theoretical Background for Experimental Work	65

Page

The Basic Concept of the Streaming Potential 66
The Significance of the Basic Equation 74
Velocity Gradient at the Wall 76
Shearing Stress 78
Contraction and Expansion Losses 79

Equipment 80

Solution System 82
(1) Streaming Potential Tubes 84
(2) Electrode Chambers 89
(3) Reservoirs 90
(4) Thermometers and Thermocouples 91
Nitrogen System 92
(1) Nitrogen Flow Components 92
(2) Manometers 93
Electrical Measurement Equipment 95
(1) Electrodes 96
(2) Electrometer Detector 98
(3) Sanborn Amplifier and Recorder 105
(4) Shorting Mechanism 108
(5) Variable-Voltage Supply 111
(6) Resistance Box 115
(7) Shielding 118

Calibration of Equipment 121

Variable-Voltage Supply 121
Resistance Box 122
Thermometers and Thermocouples 123

Procedure 123

Preparation 123
Operation 127

Accuracy of Measurements 131

Streaming Potential 131
Pressure Difference 134
Resistance of Solution 136
Temperature 137

Results and Discussion 138

Effect of the Flow Rate on the Ratio of the Streaming Potential to the Pressure Difference Measured between Points in Front of the Tube Entrance and beyond the Exit of the Tube 138

Effect of an Established Flow on the Ratio of the Streaming Potential to the Pressure Difference 143

Laminar Film in Turbulent Flow 145

Effect of Expansion and Contraction Losses on the Ratio of the Streaming Potential to the Pressure Difference 146

Page

The Streaming Potential Gradients of Tube 7 151

Shearing Stress along Tube 7 165

Use of Streaming Potential in Evaluating Boundary Conditions 167

Change of the Ratio of the Streaming Potential to the Pressure Difference with Time 169

Formation of the Double Layer 173

Rate of Formation of the Double Layer 175

Use of Streaming Current to Measure the Resistance of the Solution in the Streaming Potential Tube 182

Observations of the Streaming Potential Oscillations in Turbulent Flow and Streaming Potential Pulsations in Transient Flow 184

Other Theoretical Considerations 189

Electroosmotic Countereffect in Electroosmosis and in Streaming Potential 189

Effect on Electroosmosis 190
Effect on Streaming Potential 191
Relationship between the Effect on Electroosmosis and the Effect on Streaming Potential 193

Effect of Surface Conductance on the Streaming Current through Porous Diaphragms 197

An Interpretation of Other Experiments in View of the Results of This Study 201

Clark 201

Cameron and Ottinger 202

Bishop, Urban, and White 204

Jones and Wood 206

Considerations of the Streaming Potential as a Tool in the Measurement of Blood Flow 210

Streaming Current in Blood Flow 211

Zeta-Potential 211
Velocity Near the Wall 213

Streaming Potential in Blood Flow 214

Complications of Catheterization 214

Page

Conclusions 216

Conclusions 217

Symbolization 219

Appendix 221

Tables of Experimental Data (See List of Tables) 223

Analysis 1. Velocity Distribution Near the Wall of a Tube 322

Analysis 2. The Streaming Current Expressed as the Product of the Velocity at a Particular Distance from the Wall and the Total Displaceable Charge per Unit Length 326

Analysis 3. Evaluation of the Resistance of the Solution between Electrodes by Shunting the Streaming Potential with Known Fixed Resistors 329

Analysis 4. Effect of Surface Conductance on Streaming Current 332

Bibliography 338

PURPOSE

The original intent of this study was to investigate the possibility of using the streaming potential as a measure of the blood flow in its vessels. Early experimentation and review of references indicated that this present study would be a necessary prerequisite. The selection of equipment and procedures was influenced by their adaptability to the original goal.

SUMMARY

Preliminary measurements of the streaming potential showed that the ratio of the streaming potential to the pressure difference was almost the same whether the flow was laminar or turbulent. Since this finding was in direct conflict with the opinion expressed in all current articles and since the classical Helmholtz (31) article was always cited as the reference for this opinion, this writer translated the article. This translation, along with that of the review of electrokinetics from its beginning until the end of 1913 by Smoluchowski, were published as Bulletin 33 by the Engineering Research Institute of the University of Michigan. These translations were part of an extensive literature survey in which conflicts of opinion and ambiguities constantly occurred. Essential parts of this survey are summarized in this dissertation.

In order to obtain the required degree of accuracy of results, refinements of the preliminary equipment and of the methods of others were necessary. This equipment included precision-bore streaming potential tubes along with apparatus for measuring the streaming potential, the pressure difference, the temperature, the flow rate, the electrical resistance, and the specific resistance of the solution.

When a commercial electronic concern failed to manufacture an amplifier for the streaming potential which would meet the specifications necessary for this study and which would also be adaptable for an anticipated study of pulsatile flow, an electronic detector was designed and constructed by the writer. It is an adaptation of a circuit for the detection of atomic radiation.

Helmholtz' discussion of his assumptions and analyses present a view more fundamental than ostensibly realized by most modern writers. However, his conclusion that the liquid flow must always comply with the Poiseuille law for his streaming potential equation to be valid is incorrect. The results of the experiments presented in this dissertation confirm the findings of Reichardt (48) that the Helmholtz-Smoluchowski streaming potential equation applies to turbulent flow as well as to laminar flow. The primary requirement is that the flow be "established". An established flow is defined as one whose pressure gradient is independent of the axial length along the tube. This condition is not approximated unless the ratio of the length to the diameter is sufficiently great for the flow rate being studied.

The validity of the Helmholtz-Smoluchowski equation for both turbulent and laminar flow confirms the existence of the laminar film for turbulent flow. Since the Hagen-Poiseuille law requires that the flow be established, as well as laminar, most modern writers of electrokinetics have misinterpreted Helmholtz' conclusion by assuming that a Reynolds number less than 2000 is the proper flow condition.

In an attempt to find streaming potential tubes which would not be susceptible to the usual day-to-day variation in the zeta-potential, tubes were made from teflon. However, the same type of variation occurs in these tubes as that usually observed in glass and vitrous-silica tubes. This observation led to the development of a hypothesis that the variation of the zeta-potential is due to the relative adsorption rates of the positive and negative ions on the surface.

The need for a simple method to measure the resistance of the solution led to the construction of a switching device so that various known resistors could be placed directly between the electrodes used to measure the streaming potential. The radius of the tube can be evaluated from the relation between the electrical resistance in the tube and the specific electrical resistance of the solution. The evaluation of the radius in this way, along with that from the flow rates, is a method of verifying the tube specifications. A mathematical analysis to show that the resistance measured by using the streaming current as the only source of energy is relatively correct led to a different conclusion. The macroscopic resistance measured in this way actually includes the electroosmotic countereffect and the effect of the surface conductance in their exact relation to the streaming potential. In other mathematical analyses, several conflicts in the literature concerning the effect of the surface conductance and the electroosmotic countereffect on electrokinetic phenomena are resolved.

Through the larger-bore tubes, different flow rates produced different ratios of the streaming potential to the pressure difference when each was measured between points in front of the entrance and beyond the exit of the tube. Fluid mechanics was studied for the possibility of developing an empirical method for correcting the deviations of this ratio. This study led to the conclusion that the ratio is influenced by uninvestigated characteristics of the flow very near the tube wall. The streaming potential will be a useful tool in the evaluation of the velocity gradient at the wall, even in a nonestablished flow. The streaming potential was measured between points along one tube to demonstrate a method for this use of the streaming potential.

LIST OF TABLES

Page

1. Composition and Dimensions of Streaming Potential Tubes 223

Streaming Potential, Pressure Difference, Temperature:

2. 10^{-3} N KCl in Tube 1 223
3. 10^{-3} N KCl in Tube 3a 226
4. 10^{-3} N KCl in Tube 3b 227
5. 10^{-3} N KCl in Tube 4 229
6. Physiological Saline in Tube 1 230
7. Physiological Saline in Tube 2 232
8. 10^{-2} N NaCl in Tube 1 234
9. 10^{-3} N NaCl in Tube 1 236
10. 10^{-3} N NaCl in Tube 2 237
11. 10^{-3} N NaCl in Tube 3a 244
12. 10^{-3} N NaCl in Tube 3b 247
13. 10^{-3} N NaCl in Tube 4 250
14. 10^{-3} N NaCl in Tube 4 255
15. 10^{-3} N NaCl in Tube 5 265
16. 10^{-3} N NaCl in Tube 6 273
17. 10^{-3} N NaCl in Tube 7 283
18. 10^{-4} N NaCl in Tube 1 287
19. 10^{-4} N NaCl in Tube 7 289

20. Pressure Difference between Taps and Tube 7 and Reservoir Pressure Difference 301

21. Specific Resistance of Solutions 313

22. Calibration of Right Reservoir 314

Time, Right-Reservoir Level, Pressure Difference, Temperature:

23. Tube 1 315
24. Tube 2 316
25. Tube 3 317
26. Tube 4 318
27. Tube 5 318
28. Tube 6 319
29. Tube 7 319

30. Calculated from Data in Tables 19, 20, and 29 320

LIST OF FIGURES

		Page
1.	Distribution of the Ions of the Double Layer (Sketch)	3
2.	Diagram Showing Direction of Electric Currents and Velocity for Streaming Potential (Schematic Diagram)	18
3.	Radial Distribution of the Shearing Stress for an Established Turbulent Flow (Sketch)	58
4.	Velocity Distribution Along an Ordinary Tube with a Sharp-Cornered Entrance (Sketch)	62
5.	Effect of Velocity Near the Wall on the Conduction Current of the Streaming Potential (Sketch)	70
6.	The Solution System of the Streaming Potential Apparatus (Photograph)	81
7.	The Measurement and Control Equipment (Photograph)	81
8.	Apparatus for the Measurement of the Streaming Potential (Schematic Diagram)	83
9.	Circuit Diagram of Electrometer Detector	99
10.	Circuit Diagram of Shorting Mechanism	108
11.	Circuit Diagram of Variable-Voltage Supply	112
12.	Circuit Diagram of Resistance Box	117
13.	Streaming Potential vs Time. Reading the Tape for Data (Photograph of Sanborn Recorder Tape)	129
14.	Streaming Potential vs Time. Change from Transient to Laminar Flow (Photograph of Sanborn Recorder Tape)	134
15.	Ratio of Streaming Potential to Pressure Difference Measured between Points in Front of Tube Entrance and Beyond Exit vs Reynolds Number (Graph)	139
16.	Tube Diameter vs Ratio of Maximum Valid Reynolds Number for Helmholtz-Smoluchowski Streaming Potential Equation to Tube Length (Graph)	142
17.	Ratio of Streaming Potential to Pressure Difference for an Established Flow vs Reynolds Number (Graph)	144
18.	Attempted Corrections for Ratio of Streaming Potential to the Pressure Difference for Various Flow Rates (Graph)	150

Page

19a. Streaming Potential Gradient Between Points Along the Length of Tube 7 for Four Flow Rates (Graph) 153

19b. Streaming Potential and Pressure Difference Between Taps F and E and Between Taps H and G of Tube 7 vs Reynolds Number (Graph) 159

20. Hypothetical Shearing Stress vs Radial Distance for Entrance Flow at End I of Tube 7 for Reynolds Number of 950 (Sketch) 166

21. Ratio of the Streaming Potential to the Pressure Difference vs Time (Graph) 171

22. Hypothetical Distribution of Charge of the Double Layer for a Minus Zeta-Potential (Sketch) 174

23. Hypothetical Adsorption of Charge at a Solid-Liquid Interface for a Negative Zeta-Potential vs Time (Sketch) 179

24. Tape Records of Streaming Potential vs Time (Photographs) 185

25. Wijga's Zeta-Potentials vs Concentration of Solutions from Measurements of Streaming Potential and of Electroosmosis through Porous Diaphragms (Graph) 196

A GENERAL DISCUSSION OF THE ELECTROKINETIC EFFECTS AND THE LIQUID FLOW THROUGH SMALL TUBES

Electrokinetic phenomena have been an intellectual curiosity since Reuss (50) and Porrett (45) observed an electrokinetic effect in the early nineteenth century. The classical analysis, which Helmholtz (31) formulated in 1879, is still considered to be fundamentally correct; however, certain of its concepts have been modified as our more detailed knowledge of the phenomena have been developed.

With the well-known Helmholtz analysis as a basis, the study of the electrokinetic phenomena should probably have proceeded in a more methodical manner. However, many investigations subsequent to his analysis were directed toward some particular point, and Helmholtz' broad concept of the fundamentals was usually misinterpreted, if not misunderstood.

Helmholtz' analysis was published a few years before Reynold's (51,52) articles which first formally defined the factors which determine whether streamline or turbulent flow exists when a fluid flows through a tube. Subsequent writers have applied Reynold's development to the Helmhlotz theories and interpretations in order to simplify them. In this simplification process, Helmholtz' concern for the deviations of his formula for certain flow conditions have been ignored. If one correlates present-day knowledge of fluid mechanics with electrokinetics, it is evident that his concern for these deviations is important and should be studied in more detail.

A compilation of the early investigations of electrokinetics has been made by Smoluchowski (59) in his review of the subject from its beginning until 1913. While some of his interpretations may be questioned, his bibliography and discussions are comprehensive. Gouy's (1910) and Chapman's (1913) double layer theories are probably the only important omissions. There is no review of comparable completeness on the investigations from 1913 to the present date.

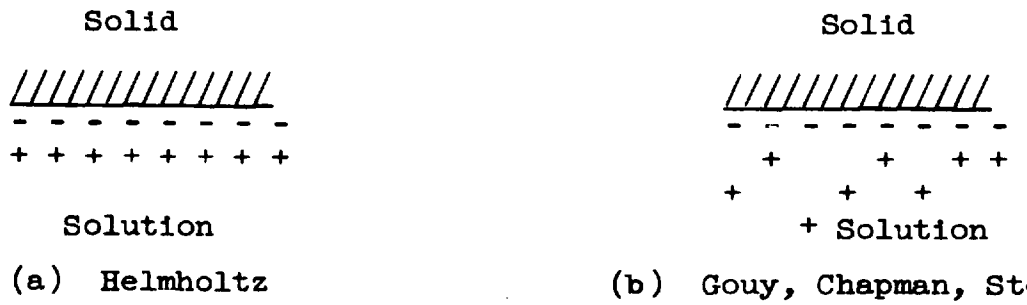
Electrokinetics is not an easily understood subject. This fact becomes more apparent as one reads conflicting opinions on a particular point by well-informed persons. For example, in different articles, the same electrokinetic equation can be found with, or without, a minus sign. This inconsistancy is due to the arbitrary selection of either different or the same reference points for the hydrostatic and electrical differences. Also, it is impossible to determine the direction of the electric current with respect to the direction of the liquid flow, from such equations. Since the sign of the electrical and hydrostatic quantities and their direction is important in electrokinetics, the reference points and directions of movement should be more accurately defined.

Before a discussion of the electrokinetic effects and their relation to fluid mechanics is presented, the basic theories of the phenomena will be described. The fundamental concept in the explanation of the electrokinetic effects is the formation of an electric double layer. All the phenomena of electrokinetics are dependent on the displacement of one of these layers of the double layer with respect to the other.

Electric Double Layer

When a liquid and solid come into contact, there is an accumulation of ions of the liquid near the surface of the solid to produce what is called an electric double layer, an electrolytic double layer, or simply a double layer. Pure water, benzene, toluene, and other liquids which are usually considered as being non-ionized, must have sufficient ions present to form a double layer if they are to conform with the present theories of electrokinetics. However, another explanation based on the orientation of their molecules at the interface may prove to be correct for non-ionized liquids.

In his analysis of electrokinetics, Helmholtz envisaged the double layer as parallel planes of oppositely charged ions. For the case of a glass-water interface, his theory assumes that the OH^- ions adhered immovably to the glass, while the H_3O^+ ions form a mobile plane of positive charge parallel to the glass surface at a small finite distance from it as shown in Figure 1a. Subsequent development of double layer theory by Gouy (22), Chapman (15), Stern (60), and others have shown that the layers of charge do not lie only in a plane but also in an ionic atmosphere because thermal agitation of the ions disperses them away from the planes as illustrated in Figure 1b.



(a) Helmholtz (b) Gouy, Chapman, Stern

Figure 1. Distribution of the Ions of the Double Layer.

Stern's Theory: This theory for the distribution of charge of the double layer is usually accepted today, but even Stern admits that it needs further development; yet no important modifications have been added since its publication in 1924. However, the interpretation of this theory by Verwey (64) might be considered at least an amplification. Wood (72), while not mentioning Stern's theory, states that there is at present no generally accepted theory explaining the origin of the double layer potential difference upon which the electrokinetic effects depend. This author's concept of the distribution of charge in the double layer within a solution in contact with a nonconducting wall is pictured in Figure 22 under Results of the Experimental Work.

Without doubt, the determination of the potential pattern for a solid-liquid interface is a very complicated process. The total difference of potential occurs very near the interface within molecular dimensions. It is known that the overall potential difference, the Nernst potential, between glass and aqueous solutions is dependent only on the concentration of the H_3O^+ ion in the bulk of the solution. This fact is the basis of the glass electrode pH meter.

Also, it is known that the addition of an electrolyte such as potassium chloride to pure water has practically no effect on the pH. Therefore, when a potassium chloride solution is in contact with glass, it has the same effect as that of pure water on the overall potential difference. However, such an addition greatly reduces the potential gradient of the double layer on the liquid side. Therefore, with such an addition the potential gradient must increase to offset this decrease

as the wall is approached since the wall potential with respect to the bulk liquid is the same if either potassium chloride solution or pure water is present.

According to Stern's theory, both positive and negative ions of the liquid are adsorbed on the surface of a heteropolar solid such as glass in a monoionic layer. There is an ionic atmosphere, or diffused layer, consisting of both positive and negative ions and whose charge is greatest near the adsorbed layer and decreases asymptotically to zero toward the interior of the liquid within the distance of a few molecular dimensions from the wall.

The ions of the adsorbed layer are held immovably on the surface. The exact kind of forces which attract and hold the adsorbed ions has not been explained. The adsorption of molecules on solids is usually divided into two types, i.e., physical or van der Waal adsorption and activated adsorption or chemisorption. The direct application of either of these concepts to the adsorption of ions at the interface has not been successful. Since the ions are electrically charged, one would expect that electrostatic attraction should be the dominant force. However, the formation of the double layer cannot be explained by electrostatic forces, and, in fact, they must play a minor role.

The concept of the double layer formation simply assumes a adsorption without an explanation of the forces involved. The concentration of each ion in the adsorbed layer is assumed to be a function of the electrical potential of the layer, the "adsorption potential", the concentration of the ion in the bulk of the solution, and other factors.

This "adsorption potential", so called by Stern, represents the unknown factors of the attraction of an ion for the surface. It is expressed in the maximum concentration of the ion that can be adsorbed on a given surface. This term encompasses those factors which, for example, permit Th^{++++} ions to be more readily adsorbed on glass surfaces than H_3O^+ or Na^+ ions. For an example of greater contrast to our usual concepts of electrostatic attraction, it includes factors which permit OH^- ions to be more readily adsorbed than H_3O^+ ions on glass surfaces, which become negative with respect to water in contact with it. But for this example, it might be said that the glass is negative with respect to the water because the OH^- ions are adsorbed on the glass.

The total concentration of ions in the adsorbed layer relative to that of the diffused layer is assumed to be greater as the bulk solution becomes more concentrated. Furthermore, the concentration of ions in the entire double layer has been found to be greater than that in the bulk liquid, but this relation is proportionally greater as the solution becomes more dilute. Since electric conductance is greater when the concentration of ions is greater, this condition is used to explain why the surface conductance, rather than the conductance of the bulk solution, determines the total conductance of the solution if the solution is very dilute and present in small bore capillaries. Since the double layer is so thin, the specific surface conductance k_s is defined as the conductance of a unit area of surface, while specific conductance k is the conductance of a unit volume of solution. Therefore the total conductance K of a tube with a radius a and length L becomes

$$K = \pi a^2(k + 2k_s/a)/L. \qquad (1)$$

Another factor considered in the theory is the effect of temperature. Since the quantity and spacing of the ions in the diffused layer is due to their thermal agitation, at absolute zero the ions are assumed to be in parallel planes of charge, identical with Helmholtz' concept of the double layer for any temperature.

In the Stern article, most of the discussion of the double layer deals with a silver-silver nitrate solution interface where Ag^+ ions become an integral part of the surface and give the silver plate a positive charge, η_o (Stern's symbolization). In the case of a heteropolar substance such as glass, the charge of the glass is independent of the ions which are adsorbed near its surface; therefore, η_o is equal to zero. Apparently Urban and White (63) do not interpret η_o in this manner. In a mathematical analysis of surface conductance on a glass surface, they give η_o a value without an explanation, even though they use Stern's definition of it. Perhaps an exception for the OH^- and H_3O^+ ions should be made here, since the potential of the glass with respect to the bulk solution is dependent on them as stated above.

For the case of a glass-solution interface where ions do not become an integral part of the surface, the algebraic sum of the charges of the double layer is zero. Therefore, a surplus of charge in the adsorbed layer must be equal, and of opposite sign, to the surplus of charge in the diffused layer. Usually the surplus of charge is referred to as the charge. However, in the discussion of the double layer it seems more explicit to use the term surplus of charge, since ions of both positive and negative charge are present in each layer.

Verwey (64), in studies on a silver iodide colloid, concludes that several types of adsorption take place during the formation of its double layer. That is, the adsorption of I^- ions of a silver iodide solution on the surface of a silver iodide solid is true adsorption. While, with an addition of a "potential-determining electrolyte" such as potassium nitrate, the accumulation of K^+ and NO_3^- ions in the adsorbed layer very near, but not an integral part of, the surface, should take place by a process called assimilation. Perhaps, then, in this author's opinion the formation of a double layer between glass and aqueous solution could, by analogy, be divided into two types of adsorption. That is, the H^+ ions would control the adsorption immediately at the surface as the I^- ions do in the colloidal silver-iodide double layer. Then the ions of the electrolyte would affect only that portion of the adsorbed layer nearest the liquid. To discriminate between parts of the adsorbed layer which at most is only several ions thick, is possibly carrying conjecture too far. More important, as will be shown later, the electrokinetic effects are dependent only on the surplus of charge in the diffused layer, and are unaffected by the distribution within the adsorbed layer.

Condenser Analogy: Almost from its inception, the double layer has been compared to a condenser. The analogy is more exact for the Helmholtz concept of the double layer, but it makes for convenience in mathematical manipulation and presentation of discussion to apply the analogy to the diffused double layer.

In this analogy the layers of charge simply become the charged plates of a condenser. The distance between the electrical centers of gravity of the

two layers is equivalent to the spacing of the condenser. This distance is usually referred to as the thickness δ of the double layer.

The double layer does have a capacitance which can be measured in certain cases. Since it is difficult to measure the charge of the adsorbed layer formed on most surfaces, its evaluation has been limited to the double layers formed between two liquids, particularly mercury-aqueous solutions.

In a series of recent articles, Grahame (23, 24, 25, 26, 27, 28, 29) has analyzed the double layer of various solutions at a mercury interface by the capillarity method, which he has improved. The capillarity method evaluates the capacitance of the double layer by varying an applied voltage across the double layer and observing the change in surface tension of mercury in contact with the solution. The applied voltage changes the charges of the double layer, and the surface tension is a means of determining the charge of a surface as shown by Gibbs and others. While one of Grahame's (24) articles on the double layer is very comprehensive, the theory of electrokinetic effects is not discussed.

Zeta-potential: The potential difference between the adsorbed and diffused layer is sometimes called the electrokinetic potential, but it is usually referred to as the zeta-potential, ζ. It is defined as the potential of the adsorbed layer with respect to that of the diffused layer. Therefore, the zeta-potential is negative when the diffused layer has a surplus of positive ions.

Moment: Bull and Gortner (11) in 1932, Guggenheim (30) in 1940, and others objected to the use of the zeta-potential to define the electric intensity of the double layer. By the use of dimensional analysis, Guggenheim

maintained that the moment M, i.e., the surface charge density σ_s times the thickness δ of the double layer, is a more fundamental definition. However, as pointed out by Wood (72) in 1946, Guggenheim's application of dimensional analysis can be questioned in that he gave dimensions to the constant 4π of the electrostatic equations.

Wood showed that the electric moment can be used in electrokinetic equations if only two assumptions concerning the electric charge are valid: (1) The system as a whole is electrically neutral, and (2) The thickness of the double layer is small compared to the radius of the tube, so that the charge is zero except very near the wall.

Continuing the same development, he established that the use of zeta-potential in the electrokinetic equations requires four additional assumptions: (3) The solution charges may be treated as continuously distributed over the volume of the tube, and the wall charges may be treated as uniformly distributed over the wall. (4) The volume charge density σ is a function of the radial distance r but independent of the angle θ about the axis in a given cross section of the tube. (5) The potential ψ caused by the wall charges and the solution charges is additive to any applied or generated potential parallel to the surface, so that the superposition of the applied or generated potential does not affect the distribution of the charges in a given cross section of the tube. (6) Poisson's equation holds.

With these assumptions Wood developed the relation,

$$\zeta = 4\pi M/\epsilon \ , \qquad (2)$$

in which ϵ is the dielectric constant, and which Perrin (44) used as early as 1904. The relation has a minus sign as developed by Wood, but it is dependent on his selection of different reference points for the electric charge and zeta-potential.

Dielectric Constant: The conflict of opinion between Wood and Guggenheim is, in a sense, beyond the scope of electrokinetics and apparently depends on the definition of the dielectric coefficient and its units. However, Guggenheim's statement that the dielectric coefficient can only be constant when it is independent of the field strength is the fundamental basis of his argument. Since the potential gradient across the double layer is extremely large, and, as shown by Grahame (28) in 1950 in a detailed analysis, the dielectric constant of the double layer in aqueous solutions is much less than that of pure water. Also since the potential gradient is not constant across the double layer but increases very rapidly as the adsorbed layer is approached, the dielectric coefficient probably varies considerably within the double layer even though only molecular dimensions are concerned.

If the dielectric coefficient is not constant in Poisson's equation, which is assumption (6) of Wood's development for the relation between the zeta-potential and the moment, Wood's development is no longer exact. Then the development becomes more complex but not impossible as pointed out by Grahame (28).

Most investigators of electrokinetic phenomena assume the dielectric constant of the double layer to be that of pure water (ϵ = 81 at 25°C) since very dilute solutions are usually used. However, Verwey (64)

has noted that the ions determine the dielectric constant within the double layer, and therefore, it should be of the order of 2 instead of 80. By using the electric moment to define the electric intensity of the double layer, the dielectric constant does not enter the calculations for electrokinetic effects, so one unknown can be eliminated.

Previous History of the Surface: To reproduce a given surface is almost impossible today. The elimination of contaminants, which requires meticulous care, probably is not the only factor controlling the reproduction of a surface. The process by which molecules are adsorbed is not well understood; that for the adsorption of ions at solid-liquid interfaces is even less well understood.

Taylor (33) has proposed that adsorption in catalytic processes takes place at active centers. These centers constitute a small portion of the surface, and therefore a small amount of contaminant can "poison" a catalyst very easily. Verwey (64) concluded from the application of mathematical analysis, as well as the results of X rays, that the aging process of silver iodide sols is controlled by the adsorption and desorption of I^- ions at particular active spots with some spots being more active than others.

Perhaps the activity of these spots is also influenced by the physical treatment of the clean surface. For example, heating vitrous silica to a dull red glow during the cleaning process may lower the activity of the spots, which would reduce the adsorption of ions when it comes into contact with a solution.

Therefore, the lack of agreement between the data of different studies of electrokinetics can probably be accredited to the adsorption of different quantities of ions at the surface. This adsorption, in turn, is greatly affected by the previous history of the solid surface.

Formation of the Double Layer: For the glass-water interface, most of the ions of the adsorbed layer are OH^- ions, leaving the H_3O^+ ions to be the surplus ions of the diffused layer. Therefore, the zeta-potential is negative. However, as a salt such as sodium chloride is added to the water, proportionally more Na^+ ions are adsorbed on the glass than remain in the diffused layer, reducing the surplus of positive ions in the diffused layer. In this way the zeta-potential becomes less negative to approach zero asymptotically as the concentration of sodium chloride of the bulk solution is increased.

When the zeta-potential is zero, the condition is defined that the solution is at its isoelectric point. At this condition the charge of the positive ions and the charge of the negative ions are numerically equal in the diffused layer, and in the adsorbed layer.

When a thorium chloride solution is present, the Th^{++++} ions are so readily adsorbed that the zeta-potential becomes rapidly less negative until it reaches zero as the concentration of thorium chloride is only slightly increased. As more thorium chloride is added so many Th^{++++} ions are adsorbed that a surplus of negative ions is present in the diffused layer, and the zeta-potential becomes positive. However, as still more thorium chloride is added, the adsorption of both positive and negative ions is increased in such proportion that the surplus of

negative ions in the diffused layer is decreased; therefore, the zeta-potential becomes less positive to approach zero asymptotically.

In these explanations, it is noted that the zeta-potential of sodium chloride solutions is always negative while that of the more concentrated thorium chloride solutions is positive. Recalling that the overall potential, or Nernst potential, has practically the same negative value for both solutions, it becomes apparent that the zeta-potential and the Nernst potential are quite independent of one another, a view expressed by Freundlich (19) as early as 1909.

Rate of Formation: From the above discussion of the double layer one would assume that the formation of the double layer happened almost at the instant when the solution and solid come into contact. For most cases, this formation is a rather slow one, and to make its evaluation more difficult, it usually changes in an irregular manner.

Most investigators have found that the zeta-potential slowly decreases with time. However, this observation was not evident in a study of the zeta-potential by Jones and Wood (34). They found that the zeta-potential slowly increased for a period sometimes of several weeks duration. When it reached a leveling-off or a maximum value, they considered that an equilibrium value had been reached and that this value was the most definitive. Usually no more than one or two points were presented in their published papers after a maximum value of the zeta-potential was reached; therefore it cannot be ascertained whether Wood and his coworkers observed the usual decrease in zeta-potential with time.

Wood (72) suggested an explanation for the slow increase of the zeta-potential that he had observed. When a potassium solution is first brought in contact with a perfectly dry and uncontaminated vitrous silica surface, he hypothesized that Cl^- ions are adsorbed on the surface of the silica. When sufficient of them are adsorbed, their charge develops a potential sufficiently negative so that it becomes increasingly more difficult for the Cl^- ions of the bulk solution to approach the adsorbed layer. Therefore equilibrium is attained very slowly.

Further, he stated that his hypothesis is untenable for a vitrous silica-water interface because no ions other than those supplied by the water are present and that another explanation must be sought for this particular case. In his original hypothesis the entire effect was based on the adsorption of the Cl^- ion with no other ions playing an active part. Yet, in continuing his discussion, he failed to discriminate in the way by which the adsorption of the OH^- ion of the vitrous silica-water interface is different from that of the Cl^- ion of the vitrous silica-potassium chloride solution.

Also he suggested that no real distinction can be made between a process by which the OH^- ions are adsorbed and a process by which the glass slowly forms a monolayer of partly ionized silicic acid gel. The latter process is a refinement of the "classic" one, the dissolving of the glass surface, for the explanation for changes in the zeta-potential.

Electrokinetic Effects

Whenever one of the layers of the double layer is displaced relative to the other, an electrokinetic effect, or an electrokinetic

phenomenon, occurs. This displacement may be produced by either electrical or mechanical means. When the displacement is produced by electrical means, a mechanical motion results; conversely, when a mechanical force is applied, an electric current is generated.

Each of these inverse effects is further divided depending on whether the liquid moves relative to the solid, or conversely. Therefore, the phenomena of electrokinetics may be divided into four categories: electroosmosis, or electroendosmosis, the displacement of a liquid relative to a solid by means of an electrical force; electrophoresis, or cataphoresis, the displacement of a solid relative to a liquid by means of an electrical force; electrophoretic potential, cataphoretic potential, or Dorn effect, the generation of a voltage by the displacement of solid particles through a solution, usually activated by gravity; and streaming potential, the generation of voltage by the displacement of a liquid past a solid by means of mechanical force, usually the hydrostatic pressure.

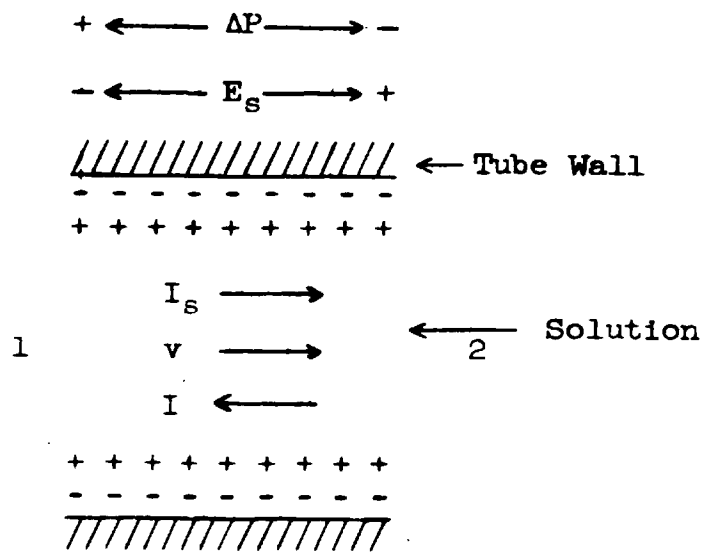
The sign of the generated potential or the direction of the resulting mechanical motion will depend on the category of electrokinetics and the sign of the zeta-potential. In the following description of the categories, a glass-water interface with a negative zeta-potential is usually used as an example. The resulting actions of other interfaces with negative zeta-potentials will have the same sign or direction as those described for the glass-water interface. The resulting actions of interfaces with positive zeta-potentials will have the opposite sign or direction to those of the glass-water interface.

It is not surprising to find the same electrokinetic equation sometimes written with a minus sign and sometimes without. The reason for this is the arbitrary selection of reference points for the hydrodynamic and electrical quantities by the different writers. Most of the more recent authors have recognized this point of confusion and have usually defined the sign of the hydrostatic and electrical quantities. However, few think of their definitions as selections of physical reference points.

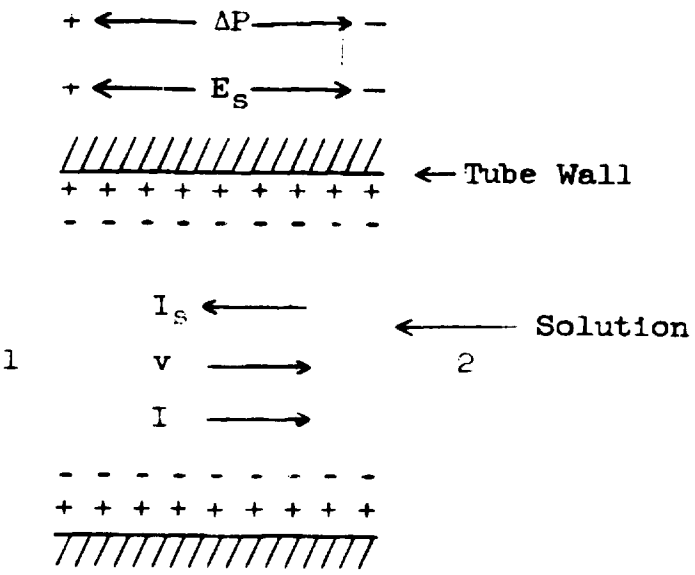
In order to avoid further confusion, the following conventions will be used in this presentation. Denote arbitrary reference points as 1 and 2, which may be any points on a path along the displacement of a double layer (1 is usually the entrance of a tube and 2, the exit): Then $E = E_2 - E_1$. $\Delta P = P_2 - P_1$. The velocity v and volume rate of flow V are positive when flowing from 1 to 2. The conventional current I is positive when flowing from 1 to 2 as shown in Figure 2b.

The symbol I_s is used to represent the convectional flow of positive or negative ions; the flow of negative ions will be negative when flowing from 1 to 2 as shown in Figure 2b, while that of the positive ions will have the same sign as the conventional current when flowing from 1 to 2 as shown in Figure 2a. The ions of the diffused layer actually move in the same direction as the velocity in streaming potential, but the sign must also include the polarity of the ions.

Electroosmosis: When a direct current voltage is applied to the ends of a glass capillary which is filled with water, the water flows toward the end of the tube at which the negative potential is applied: The diffused



(a) For a Negative Zeta-Potential



(b) For a Positive Zeta-Potential

Figure 2. Diagram Showing Direction of Electric Currents and Velocity for Streaming Potential.

layer of the glass-water interface has a surplus of positive ions which are attracted toward the cathode, and these positive ions simply pull the liquid along.

There are some negative ions in this diffused layer, but their effect is counterbalanced by positive ions of equal charge, and it is the surplus of positive ions in any given stratum of the diffused layer which controls the movement of that stratum. A stratum in this case is considered to be a diminishingly thin cylindrical layer concentric about the axis of the tube. The molecules of water in this stratum are simply pushed and pulled along with the ions.

All strata of the tube are coupled to one another by viscous forces, and these viscous forces tend to retard any difference of velocity between the adjacent strata. In counteraction, the electrical forces tend to give an individual stratum a velocity. The electrical force in this case is the product of applied potential gradient and the electrical charge density. Since for electroosmosis the pressure gradient along the tube must be zero by definition, the only forces present are the viscous and electrical; therefore they must be equal and opposite.

The surplus of charge of the ions of the adsorbed layer do not play a part in electroosmosis. The ions are so securely attached to the surface that they are not displaced by the electrical forces. The entire adsorbed layer is so close to the surface and is so thin that its velocity is zero, even when there is motion in the interior of the solution.

The entire interior core of the liquid in the tube is pulled along by the viscous forces which hold this liquid to the liquid side of the diffused layer. The velocity of all strata in this region is the same since the only forces which can be present here are the viscous forces. Therefore the velocity profile of the liquid for electroosmosis is zero at the wall, sharply increasing across the diffused layer, and exactly level from the diffused layer to the axis of the tube.

By assuming that a porous diaphragm is composed of many capillaries, Helmholtz (31) applied the formula he had derived for electroosmosis in capillary tubes to porous diaphragms. Smoluchowski (59) generalized Helmholtz' analysis and the resulting equation, referred to as the Helmholtz-Smoluchowski electroosmosis equation is

$$\frac{V_e}{I} = -\frac{\zeta \varepsilon}{4\pi\mu k} \qquad (3)$$

As described in the example of glass-water interface with a negative zeta-potential, the electroosmosis or the <u>electroosmotic volume rate of flow</u> V_e has the same direction as the conventional current I (both flow toward the cathode). Therefore, equation (3) needs a minus sign since for the described example, the left side of the equation is positive, and the value of the terms of the right side is negative.

As stated above, the electrical force which propels the liquid is proportional to the potential gradient. If equation (3) is always valid, the potential gradient must be proportional to the current I divided by the specific conductance k of the solution.

Because Ohm's law must be satisfied, this condition is not true when the surface conductance is sufficiently large to affect the total conductance, and therefore equation (3) must be modified to account for the effect of surface conductance on the potential gradient.

Taking into account the effect of surface conductance according to equation (1), the equation then becomes

$$\frac{V_e}{I} = -\frac{\epsilon \zeta}{4\pi\mu(k + 2k_s/a)}, \tag{4}$$

or expressed with the moment of the double layer,

$$\frac{V_e}{I} = -\frac{M}{\mu(k + 2k_s/a)}. \tag{5}$$

Accurate measurement of electroosmosis are very difficult since the volume rate of flow is very small. Experimental errors are usually quite large. The deviations from the theoretically expected results are usually attributed to turbulent flow without explaining just where the turbulence originates. However, Wigga (71) has recently made some measurements of electroosmosis which closely agree with the theoretically expected.

Dividing both sides of electrocsmosis equation (4) by the electrical resistance of the liquid in a capillary tube makes it possible to express the ratio of the electroosmosis to the applied voltage. The resulting equation is

$$\frac{V_e}{E} = \frac{\epsilon \zeta a^2}{4\mu L} \tag{6}$$

The important aspect of this equation is that since the ratio is independent of the conductance, the zeta-potential can be evaluated without knowing the value of the conductance. The equation is written for a single capillary of radius a and length L, but can be generalized to diaphragms by the assumption of a mean radius and length for the pores of the diaphragm.

If one considers the average velocity produced by electroosmosis, i.e., the <u>electroosmotic velocity</u> v_e, instead of the volume rate of flow, the electroosmotic equation becomes

$$\frac{v_e}{E} = \frac{\epsilon \zeta}{4\pi\mu L} . \qquad (7)$$

In this equation also, the zeta-potential can be evaluated independently of the conductance. Since surface conductance cannot be measured directly Rutgers and DeSmet (56) have combined the electroosmotic velocity method with that of another electrokinetic effect which is dependent on the conductance to evaluate the conductance. They then used the relation found in equation (1) to evaluate the specific surface conductance.

However, equation (7) is usable only for a single capillary of constant radius since the usual definition of velocity limits it to a tube of constant radius.

If the electroosmotic liquid flow is not removed at the exit, the pressure will increase at the exit. Since the pressure gradient along the tube must be zero for electroosmosis, the equations for it are no longer valid.

When sufficient pressure, the electroosmotic pressure, has built up, the net volume rate of flow becomes zero. However, there are two countercurrent liquid flows within the tube. The electrical force produces a flow near the wall of the tube; the resulting hydrostatic pressure produces a countercurrent flow through the interior of the tube.

The strata of the diffused layer have three forces applied to them. The electrical forces pull them along, while the hydrostatic forces oppose the electrical forces, and the viscous forces tend to retard any difference of velocity between the strata. Therefore, in this region the differences of the electrical forces and the hydrostatic forces are equal and opposite to the viscous forces. From the diffused layer to the axis of the tube, the hydrostatic forces tend to push the liquid in the opposite direction, while the viscous forces tend to retard this motion. Therefore in the interior of the tube the hydrostatic forces are equal and opposite to the viscous forces.

Consequently, the velocity profile is zero at the wall, increases sharply upon entering the diffused layer, reaches a maximum within the diffused layer at the point where the electrical and hydrostatic forces are equal, begins to decrease before leaving the diffused layer, continues to decrease to reach zero, and then begins to increase again in the opposite direction. Assuming a streamline flow, the velocity profile from the edge of the diffused layer to the axis of the tube is a parabola. If the thickness of the double

layer is diminishingly small when compared to radius of the tube, the radial distance, at which the liquid point velocity is zero, is $a/\sqrt{2}$, as well as at the wall.

The equation resulting from the Helmholtz-Smoluchowski analysis of this effect is

$$\frac{\Delta P_e}{E} = \frac{2\epsilon\zeta}{\pi a^2} \quad (8)$$

While several of the earlier investigators measured the electroosmotic pressure instead of the electroosmosis, it has not been used recently.

Smoluchowski (59), Bikerman (3), and others have evaluated an effect of the convection current of ions on electroosmosis. They considered that the convection current flows through a conductance which affects the applied voltage in the same way a surface conductance would. The effect was expressed as a ratio of convection current to the conduction current, e.g., Smoluchowski's equation (43)

$$\frac{I_s}{I} = \frac{\epsilon^2\zeta^2}{8\pi^2 a\delta\mu k} \cdot \quad (9)$$

While Smoluchowski apparently considered the convection curent to be the dominant factor in determining the surface conductance, Bikerman considered that the concentration of ions at the interface, which is greater than that in the bulk of the solution, would also be an appreciable factor.

In the terminology of this study, the total conductance of a solution in a tube, or any orifice, would be constituted of three components:

the conductance of the bulk solution, the surface conductance, and the electroosmotic conductance. The conductance of the bulk solution is a conductance evaluated in the absence of surface effects. The surface conductance is due to the ionic concentration being greater at the surface than in the bulk of the solution, and the electroosmotic conductance is due to the convection current of ions which results when a voltage is applied across a tube.

Electrophoresis: If a voltage is applied across a suspension of small solid particles which have an adsorbed layer of ions on them so that they have a surplus of charge, the particles will move. If the surplus of charge is negative, they will move to the anode. The analysis of this phenomenon is even more complicated than that of electroosmosis since one must take into account the eddy currents of liquid flow around the particles and a complicated distribution of electrical forces due to the curvature of the particles.

Experimental technique is also hindered by the fact that electroosmosis takes place between the container holding the liquid and the liquid itself. But even with these handicaps of forming an exact analysis, electrophoresis has been developed from a macroscopic viewpoint, so that today it is the most useful of the electrokinetic effects.

Medical researchers have found it beneficial in the evaluation of proteins. Bull (9) discussed the important aspects of electrophoresis from a medical standpoint, including the various

techniques which have been perfected. Svensson (61) reviewed much of the same material but in more detail.

The deposition of liquid latex on molds of sundry shapes is an electrophoretic process, and the one which has attained the greatest commercial development of any of the electrokinetic processes.

Electrophoretic Potential: If small solid particles, which can adsorb a surplus of one charge on their surface, move through a liquid, a potential gradient is set up along their path through the liquid. The potential generated in this way is the electrophoretic potential. The usual motivating force for the particles is gravity. If the particles adsorb a surplus of negative charge, the potential at the bottom of the liquid will be negative with respect to that at the top.

To obtain reproducible results one would have to control the number and spacing of falling particles. Also as discussed above, the double layer requires time to be formed; therefore, the dropping of dry particles into a liquid will give different results from those obtained when particles wetted with the solution are used. These factors, in addition to others, such as that the velocity of the particles may be constantly increasing as it approaches the bottom of the liquid, eddy flows, etc., cause experimental equipment and technique to be so exacting that probably no published data are reliable.

Streaming Potential: About 1860 Quincke (46) discovered that when he forced water through a clay diaphragm a potential

developed across it. He also realized that this effect was an inverse phenomenon to electroosmosis. Early investigations were handicapped by the polarization of electrodes and the lack of suitable instruments to measure the generated potential. Quadrant electrometers were used, but most early data is not reproducible.

The development of the electrometer vacuum tube as a measuring device for the potential and the perfection of techniques to produce nonpolarizing, or reversible, electrodes have made possible very exacting studies of this potential. So that today, the streaming potential, so called because it is produced by a streaming liquid, is probably the most satisfactory of the categories of electrokinetics with which to analyze the entire electrokinetic phenomena.

(1) Helmholtz-Smoluchowski Equation: When a liquid flows through an orifice, the ions of the diffused layer are carried along with the liquid flow. If there is a surplus of charge in the diffused layer, this displacement of ions is the streaming current. According to Helmholtz' interpretation, this ionic convection current, if it maintains a constant velocity parallel to the wall, causes a deficiency of charge at the entrance of a tube and a surplus of charge at its exit. To offset the deficiency and surplus of charge at the opposite ends of the tube, a conduction current develops through any electrical path which may be present.

If no external path exists and the walls of the tube are a nonconductor, the only path for the conduction current is

through the bulk of the solution. These conditions are assumed in the development of the streaming potential equation.

The streaming potential is the voltage generated by the ionic convection current when all this current is converted into a galvanic conduction current which flows through the solution of the tube. The streaming current can be compared to the current which flows in the interior of a battery between its terminals, while the conduction current would be the current which flows through the external circuit connected to the same battery.

When Helmholtz (31) analyzed the streaming potential phenomena in 1879, he was able to develop an equation in which there is only one term, the displacable charge, which cannot be measured directly or whose value cannot be evaluated in some other independent manner. With the introduction of the dielectric constant into the equation, this term becomes the zeta-potential.

While the equation has been confirmed many times experimentally, his derivation is not easily interpreted because it is difficult to place readily understood physical meanings on his second order differential equations and is often referred to as the complicated Helmholtz treatment. However, his basic assumptions are adequately explained in his discussion. They are:

a. The liquid is galvanically opposite to the wall of the vessel, and the two form an electric double layer along their boundary surface, i.e., there are two layers of charge near the wall whose electrical properties are defined by their electric

moment, the product of the distance between the charge and the quantity of charge per unit of area in each layer. (Some authors, e.g., Guggenheim (30) in 1940, believed that this Helmholtz definition of the double layer is the most rigorous. However, the analogy of the double layer to a condenser as first suggested by Pellat (44) about 1900 makes it possible to place a more easily interpreted physical concept on the double layer. Wood (72) showed in 1946 that additional assumptions are needed when the double layer is compared to a condenser instead of defining it by Helmholtz' moment.)

b. The electrical equilibrium of the electrically charged boundary layer is not disturbed by the displacement of its inner portion, i.e., the moment of the double layer, or its zeta-potential, is unaffected by the generation of a streaming potential; the streaming potential is simply superimposed upon the zeta-potential.

c. The vessel wall, when compared to the streaming liquid, can be regarded as an insulator, i.e., the conductance between the ends of the tube is the conductance of the bulk liquid.

d. The double layer has an extraordinarily small, but not disappearing, thickness, i.e., the thickness of the double layer is diminishingly small when compared to the radius of the tube.

e. The hydrodynamic laws which are valid for the entire liquid flow are valid for the double layer, i.e., the viscosity of the liquid in the double layer is the same as that of the bulk liquid.

f. The liquid motion is such that the actions of the rubbing liquid have time to be developed completely so as to cause a steady state,

and the displaced charged particles are moved with a constant velocity parallel to the wall; and such a velocity can only exist if the entire liquid flow is such that the Poiseuille law is valid, i.e., the entire liquid flow is laminar.

In 1928 Reichardt (48) showed in his doctoral research that it is not necessary to assume that the entire liquid flow be laminar in order that the displaced ions be moved with constant velocity parallel to the wall. The basis of his presentation was that a film exists at any liquid-solid interface whose flow is always laminar even if the flow in the interior of the liquid is turbulent. Therefore, the necessary criterion is that the flow be "established", or be developed so as to cause a steady state.

The resulting equation, which is now usually called the Helmholtz-Smoluchowski equation because Smoluchowski added the condenser analogy, with its dielectric constant, and generalized the equation to be valid for any shape of conduit, is

$$\frac{E_s}{\Delta P} = \frac{\epsilon \zeta}{4\pi \mu k} . \qquad (10)$$

Wood (72) put a minus sign in this equation; however, his reasoning is based on the selection of opposite ends of the tube for the reference points for the generated voltage and the applied pressure. If the entrance of the tube is point 1 and the exit, 2, by Wood's definitions $E = E_2 - E_1$, and $\Delta P = P_1 - P_2$. This selection of reference point for the pressure difference is contrary to that which has been established in fluid mechanics, chemical

engineering, etc. If $E = E_2 - E_1$ and $\Delta P = P_2 - P_1$, no minus sign is needed in equation (10).

Under certain conditions, it may be more desirable to measure the streaming current than the streaming potential. The streaming current is measured by connecting a low resistance galvanometer across the ends of the tube. This connection causes the conduction current to flow through the galvanometer instead of through the solution in the tube. Consequently, the potential across the tube becomes zero.

The equation for streaming current is actually one of the steps in Helmholtz' analysis, but can be derived from the streaming potential equation by dividing each side of equation (10) by the electrical resistance of the liquid flowing in the tube. The resulting equation is

$$\frac{I_s}{\Delta P} = \frac{\epsilon \zeta a^2}{4\pi\mu L} . \qquad (11)$$

This equation is written for a single tube, but can be generalized to a diaphragm with the assumption of a mean radius and a mean length for the pores of a diaphragm.

(2) Effect of Surface Conductance: While Smoluchowski and others realized that surface conductance would affect the electrokinetic phenomena, they did not formulate the effect. In 1928 when Briggs (6) measured the streaming potential by forcing distilled water through cellulose diaphragms, he discovered that the ratio of the streaming potential to the pressure difference was not constant when the tightness of the diaphragm was varied. After studying the

possibility that the deviation might be due to different flow rates, he attributed the deviation to the effect of surface conductance. He then modified equation (10) by substituting an experimentally dependent conductivity for the conductivity of the bulk solution. When the modification is expressed as a ratio of electrical resistances, the equation becomes

$$\frac{E_s}{\Delta P} = \frac{\epsilon \zeta R_{exp}}{4\pi\mu k R_{calc}}, \qquad (12)$$

where R_{exp} is the experimentally measured electrical resistance of the diaphragm and R_{calc} is the resistance to be expected in the absence of surface conductance.

When equation (12) is written for a single capillary it is

$$\frac{E_s}{\Delta P} = \frac{\epsilon \zeta}{4\pi\mu(k + 2k_s/a)}. \qquad (13)$$

In order to prove equation (13) experimentally, in the early 1940's Rutgers (54) measured the streaming potential generated by flowing solutions through three capillary tubes of different radius. Since there are two values, the zeta-potential and specific surface conductance k_s, in equation (13) which they either could not experimentally measure directly or did not know from accepted measurements, it was necessary to use the data from any two capillary tubes to evaluate the unknowns.

Close agreement was obtained for the value of surface conductance and zeta-potential by calculations on any two tubes. This agreement indicates that equation (13) is valid for the tubes studied by Rutgers.

However, White, Urban, and Monaghan (69) did not accept the results of these experiments. They stated that the relation of electrokinetics to surface conductance is more complicated than that expressed by equation (13). They admitted that Rutger's streaming potential measurements were probably substantially correct but believed that the close agreement of the value for surface conductance calculated by Rutgers with that of other investigators using non-electrokinetic methods is "fortuitous".

To develop the proof further, more recently Rutgers and DeSmet (55, 56) have measured the electroosmotic velocity, along with the streaming potential, on the same tube and solution. Close agreement was again obtained for the zeta-potential and surface conductance for several tubes, indicating that both equations (7) and (13) are valid for the tubes studied.

In another study in 1946, when Wijga (71) measured the streaming potential of the same liquid in glass capillary tubes and across diaphragms made of powdered glass, he found that the zeta-potential evaluated by equation (12) was less for the diaphragms than for the capillaries. In addition, this deviation was greater when the more dilute solutions were used.

To aid in the explanation of this deviation Overbeek and Wijga (43) in 1946 made an adept mathematical analysis of the effect of surface conductance on the streaming potential in diaphragms. They considered that a diaphragm can be compared to capillary tubes connected in parallel and in series. To simplify the mathematics,

they analyzed the tubes in parallel separately from those in series. It was shown that equation (12) expressed the correct effect of surface conductance for tubes connected in parallel. However, for the case of tubes in series, the zeta-potential calculated by equation (12) was found to be always less than it should be, if the surface conductance is effective at all, i.e., twice the specific surface conductance divided by the radius is appreciable when compared to the specific conductance of the bulk solution.

Their analysis showed why the ratio of streaming potential to the pressure difference can be less for a diaphragm than a capillary tube only as far as the effect of surface conductance is concerned. It did not show why the ratio was less for a diaphragm than for a capillary tube when the surface conductance plays no part.

The unfortunate aspect of this analysis is that the effect of surface conductance on streaming potential in diaphragms cannot be accurately expressed. That is, the effect depends on the exact dimensions and interconnections of the various pores of the diaphragm which cannot be evaluated, experimentally or theoretically, with our present knowledge of porous diaphragms and beds.

Almost simultaneously with the publication of Overbeek and Wijga's analysis, Neale (41) presented a derivation of a streaming current equation for a packed diaphragm based on the porosity and surface per unit volume of packing. He maintained that the resulting equation is independent of the surface conductance. Neale used the term, surface potential, to define the electric potential of an

interface instead of the zeta-potential. He did not directly state the advantage of his terminology, but apparently, the two terms are nearly synonymous. The surface potential could be interpreted as being the Nernst potential, but his discussion does not warrant this interpretation.

Therefore, if Overbeek and Wijga's and Neale's analyses are both correct, it will be possible to gain additional knowledge of the dimensions of the pores of a diaphragm by comparing the results obtained by measuring both the streaming potential and the streaming current of the same diaphragm.

In order to substantiate Neale's development, Neale and Peters (42) investigated the streaming currents generated by flowing solutions through diaphragms of various fibers. The solutions were varied in composition and concentration. Figure 2 of their article is a graph of the surface potential of cotton fibers versus the concentration of the solutions used. The theoretically expected points in accord with Neale's equation are also indicated. For the more concentrated solutions, the curves for the salt solutions agree with those theoretically expected. But when the concentration is sufficiently dilute for the surface conductance to be effective, the experimental surface potentials are less than those theoretically expected.

However, Neale and Peters suggested that this deviation may be due to interference of ions of the water itself, or ions of adventitious impurities, since ordinary laboratory distilled water was used in making the solutions. Such reasoning is not very convincing when

compared with Overbeek and Wijga's conclusions. Neale's analysis warrants further study.

(3) Double Layer Thickness: The assumption that the thickness of the double layer must be diminishingly small when compared to the thickness of the liquid adjacent to the solid is essential in usual developments of the electrokinetic equations.

Much has been written about how to determine when this assumption is valid, but concrete conclusions are few. White, Urban, and Krick (68) in a frequently quoted reference found that the streaming potential per unit pressure difference decreased rapidly when measured in decreasingly smaller capillaries of less than forty micron diameters. The solutions used were sufficiently dilute so that surface conductance could have produced the effect they observed. However, White, Urban, and VanAtta (70) repeated these experiments after changing their potential measuring device and found much lower values for the smaller capillaries. They attributed these very low values to the change of zeta-potential which they believed to be a function of the surface conductance.

Experiments concerning the effect of orifice size, e.g., Bull and Gortner's (12) study of the effect of particle size in packed beds, usually show a decrease of streaming potential per unit pressure difference as the orifice size is reduced. However, in these experiments solutions have been used which were sufficiently dilute so that the effect of surface conductance cannot be eliminated.

Since the actual thickness of the double layer is a matter of much speculation, it is difficult to determine whether or not its thickness in relation to the thickness of the liquid adjacent to the solid is the factor affecting a given electrokinetic experiment.

Bull and Moyer (13) have shown theoretically that the electrokinetic effect would be decreased as the radius of the tube is decreased by comparing the double layer to two concentric layers instead of the usual assumption of paralell layers of charge. By their analysis a five-percent decrease of electrokinetic effect, e.g., streaming potential, would occur when the radius is ten times the thickness of the double layer, and then the effect decreases very rapidly as the radius is further decreased. Ascertaining the size of such small capillaries may be difficult; in any case, experimental proof of their analysis is lacking.

Therefore, the effect of the thickness of the double layer has not been adequately explained, either theoretically or experimentally.

(4) Electroosmotic Countereffect: As stated above, the generation of the streaming potential is dependent on the development of an ionic convection current and a consequent conduction current. By the nature of the phenomenon, the convection current is opposed by the field of the streaming potential and the conduction current. An electric force, equal to the product of the streaming potential gradient and the surplus of charge of the moving ions, opposes the movement of these ions. This force is

identical to the motivating force in electroosmosis. Therefore, the countereffect has been expressed in units equivalent to any of the variables of the electroosmotic equations (3), (4), (5), (6), and (7), as well as the viscosity.

Abramson (1) in 1932 choose to express this effect as a ratio of the volume of liquid that would be conveyed by electroosmosis to the volume forced through a tube by the hydrostatic pressure. His concern about this effect resulted from his realizing that the viscosity of certain liquids measured in small tube viscometers would be incorrect because of it. Also concerned with its effect on flow rates, Elton (18) in 1948 called the electroosmotic countereffect an electroviscous effect and expressed it as a viscosity increase, which he called the electroviscosity.

White, Monaghan, and Urban (66) studied the filtration rates of thorium chloride solutions through cellophane in 1935. The selection of this solution in an investigation of electroosmotic countereffect is very suitable because dilute solutions of thorium chloride have a negative zeta-potential in contact with cellophane while that of the more concentrated solution is positive. They found that a maximum filtration rate occurs at the isoelectric point: the filtration rate was higher for a thorium chloride solution at the isoelectric point than for pure water, or any other concentration of thorium chloride. Their results showed that the filtration rate was some inverse function of the magnitude of the zeta-potential. While

realizing this relation, they believed that the effect was due in part to a reduction of the effective size of the capillaries of the cellophane by polarization causing orientation of the water molecules along the capillary walls.

In a study of streaming potential of organic liquid-cellulose interfaces, Lauffer and Gortner (36) found the electroosmotic effect to be appreciable, and they expressed it as a pressure difference. Their mathematic analysis was for their special case in which they measured the streaming potential by an indirect method.

Using a different approach in the evaluation of the electroosmotic countereffect, Bull and Moyer (13) expressed the effect as a ratio of the electrical work required to drive the streaming current against the streaming potential gradient to the mechanical work producing the liquid flow. When the electrical work and mechanical work are expressed in equivalent terms which include pressure differences, the relation is an expression of the electroosmotic counter pressure to the total pressure difference.

Since the volume rate of flow does not appear in the usual equation for streaming potential, Abramson's analysis cannot be directly introduced into the equations.

If the electroosmotic pressure is used to express the counteraction, the streaming potential equation is

$$\frac{E_s}{\Delta P} = \frac{\epsilon\zeta\left[1 - \epsilon^2\zeta^2/2\pi^2a^2\mu(k + 2k_s/a)\right]}{4\pi\mu(k + 2k_s/a)} \quad . \qquad (14)$$

However, if Elton's apparent viscosity, expressed as a function of the true viscosity, is used, the equation becomes

$$\frac{Es}{\Delta P} = \frac{\epsilon \zeta}{4\pi\mu(k + 2k_s/a)\left[1 + \epsilon^2\zeta^2/2\pi^2a^2\lambda(k + 2k_s/a)\right]} . \qquad (15)$$

Equations (14) and (15) are not identical. It is true, however, that when the counteraction is small, the two equations are mathematical approximations of each other.

According to Elton's analysis, the numercial coefficient of the denominator of the second term of the denominator of the right-hand side of equation (15) should be 2, as shown, only for the assumption that parallel layers of charge form the double layer. If the layers of charge are concentric about the axis, as they are in a capillary tube, the numerical coefficient should be 3.

While there is experimental evidence that an electro-osmotic countereffect of appreciable magnitude does exist when a streaming potential is generated in very small orifices, the modification of the streaming potential equation to account for this effect shows a conflict of opinion in its theoretical analysis.

(5) Hydrostatic Factors: In Helmholtz' (31) discussion on the deviations in wider tubes, he states, "For the experiments where one allowed water to flow through glass tubes, and measured the potential difference arising this way, we must repeat that the theory given above assumes that the action of the friction is completely developed through the whole tube and that every individual water stratum parallel to the axis of the tube moves as it

would continue to move in an infinitely long tube. This assumption, however, does not prove true in the entrance of a tube when the water enters it from a wider vessel." He continued by analyzing the way in which the diameter, the velocity, and the shape (trumpet-shaped or sharp-edged) of the entrance affect the entrance flow.

The only criterion most investigators have applied to fluid flow of their experiments is that the Raynolds number be less than 2000 since with this criterion laminar flow exists. Throughout the literature, results which deviate from those expected theoretically are explained by suggestions that probably the flow was turbulent.

This explanation has been used both before and since Reichardt (48) found that the streaming potential is independent of the type of flow. This independence was attributed to the assumptions, (a) that the double layer is thinner than a liquid film near the wall and (b) that the flow in this film is always laminar. His analysis of these assumptions proved them to be valid within the limits imposed by the usual streaming potential apparatus and experimental procedure.

Basing his treatment on these assumptions, he concluded that the streaming current for either type of flow is a displacement of the charged ions within a laminar region, and that the only effect of turbulence is that it causes a fluctuation in the hydrostatic pressure producing the laminar flow.

Reichardt's experimental data confirmed the independence of streaming potential from the type of flow. However, he was unable

to observe the fluctuations of the streaming potential which he had expected the effect of turbulence to superimpose on the average streaming potential. This lack of fluctuations was attributed to the high inertia of his quadrant electrometer with which he measured the streaming potential.

The only deviation from the Helmholtz-Smoluchowski equation, i.e., the ratio of the streaming potential to the pressure difference, which he observed, was in the transient region between laminar and turbulent flow. The ratio for this region was slightly greater than for either turbulent or laminar flow, once they were "established". Since in the transient region, the flow oscillates between laminar and turbulent, he believed that it did not have time to become established in either type of flow, causing the deviation.

Since some of the older experiments are referred to for the effect of radius size, one will be selected to suggest why the accepted concepts about it are inexact. In 1877 Clark (16) measured the streaming potential generated by connecting glass capillary tubes in a vertical position to the water supply of Heidelberg. Electrodes were placed in side arms of larger connector tubes which were at the top and bottom of the capillary. The outlet of the lower connector tube was tapered to a small hole so that air would not enter the system once water was run in it. The size of the small hole was not recorded.

A series of experiments were run using tubes of different diameters and lengths. Clark measured the hydrostatic pressure of

the Heidelberg water main and considered that this constant pressure was generating the streaming potential. He found that the streaming potential was different for each tube; he had expected it to be nearly the same for all tubes so that the ratio of the streaming potential to the pressure difference would be constant, and therefore independent of the tube dimensions.

In reviewing this experiment in 1913, Smoluchowski (59) states, "In all these experiments, however, it is very difficult to obtain constant value, since imperceptible impurities of the water or of the tubes cause great differences, and since, besides, after some time, probably due to the dissolving of the glass, a decrease of the effect occurs."

No mention is made that perhaps the pressure losses, which occur in the parts of the flow system other than in the capillary itself, may have no effect on the generation of the streaming potential in the capillary.

A 1911 study by Riety (53) is quoted as an example of the effect of turbulence on the ratio of the streaming potential to the pressure difference. He found that there was a gradual decrease in the ratio as the pressure difference increased. The ratio at ninety atmospheres pressure difference was ten percent less than that at five atmospheres. However, no dimensions were given on the capillary tube; therefore, it is impossible to determine at what pressure the flow became turbulent.

When Bishop, Urban, and White (4) measured the streaming potential of flow through small capillaries with very short length in 1931, they could not obtain a constant ratio of the streaming potential to the pressure difference. In referring to their results, they suggest that there might be an optimum diameter for the development of the streaming potential, and then they wrote, "...there appears to be a relation between capillary diameter and stream potential but it apparently is not a simple one." They quote Helmholtz as a reference in their article, but apparently do not share his concern for deviations that may be due to entrance conditions.

Interrelationship between Electrokinetic Effects

While Quincke recognized in 1859 that electroosmosis and streaming potential are correlated inverse phenomena, he did not express the relationship in an exact form. It was only after Helmholtz'formulation of the electrokinetic effects that a theoretical basis was available for this purpose.

In comparing the equations (4) and (13) expressing electroosmosis and streaming potential respectively, one notices that the terms of the right-hand side are identical. In 1892 Saxen (57) first performed the experiments which showed that the left-hand quantities of these equations are equal, and the relationship is usually called Saxen's law.

This relation has been confirmed within the limits of small experimental errors. Probably, Wijga's (71) studies of 1946 are the most accurate, and have been the basis of further theoretical development.

Treating the relationship from a thermodynamic viewpoint, in 1938 Maturo (38) showed that there are also three other relations besides Saxen's which can be written between electroosmosis and streaming potential.

In a recent macroscopic analysis, Lorenz (37) combined the relations between electroosmosis, electroosmotic pressure, streaming potential, and streaming current into two equations with four variables, current, flow, pressure, and potential. His treatise was that only three parameters are necessary to define the effects. These parameters are not independent of one another, and when combined in particular manner, the resulting number must always be less than one. When this restriction is applied to equation (14), it requires that the second term of the numerator of the right-hand side has to be less than one. According to Lorenz, it places definite restrictions on the theoretical values such quantities as conductivity, zeta-potential, viscosity, etc. can have in any given example, and this factor was not previously understood.

Mazur and Overbeek (39) have recently considered the relationship between electroosmosis and streaming potential from a macroscopic viewpoint, along with an analysis depending on the exact kinetic relations at the interface and in the bulk of the solution.

While differences of concept are expressed in each article, Maturo, Lorenz, and Mazur and Overbeek reached the same conclusions that Saxen's law is valid and that the relationship between electroosmosis and streaming potential can be expressed by three additional relations.

The relations for any given capillary or diaphragm and any given solution are:

Saxen's law. The ratio of the streaming potential to the pressure difference is equal to the ratio of the electroosmotic volume rate of flow to the electric current.

$$\left(\frac{E_s}{\Delta P}\right)_{I=0} = -\left(\frac{V_e}{I}\right)_{\Delta P=0} . \tag{16}$$

The ratio of the streaming potential to the hydrostatic volume rate of flow is equal to the ratio of the electroosmotic pressure to the electric current.

$$\left(\frac{E_s}{V}\right)_{I=0} = \left(\frac{\Delta P_e}{I}\right)_{V=0} . \tag{17}$$

The ratio of the streaming current to the pressure difference is equal to the ratio of the electroosmotic volume rate of flow to the applied potential.

$$\left(\frac{I_s}{\Delta P}\right)_{E=0} = \left(\frac{V_e}{E}\right)_{\Delta P=0} . \tag{18}$$

The ratio of the streaming current to the volume rate of flow is equal to the ratio of the electroosmotic pressure to the applied potential.

$$\left(\frac{I_s}{V}\right)_{E=0} = -\left(\frac{\Delta P_e}{E}\right)_{V=0} . \tag{19}$$

Since all the electrokinetic effects have in common the displacement of the double layer, it should be possible to develop simple relations between the electrophoresis and the streaming potential, or

between any two electrokinetic effects. In 1934 Bull (8) compared the zeta-potentials calculated from electrophoresis, streaming potential, and electroosmosis studies and found close agreement for the protein-solution interfaces. However, the lack of agreement for quartz and cellulose interfaces was so great that Bull suggested the theories of electrophoresis may need modification.

Liquid Flow in Small Tubes.

Although fluid mechanics embraces the entire field of fluid flow, the following discussion will be limited to the flow of liquids within conduits since the streaming potential concept is concerned only with this special case.

Even though a complete knowledge is still lacking for certain conditions of liquid flow, the concepts of the mechanics of flow have become better established, both theoretically and experimentally, than those accepted at the time at which the fundamental equations of electrokinetics were developed in 1879.

Basing his opinion on the lectures of Prandtl, in 1934 Tietjens (62) wrote, "In classical hydrodynamics everything was sacrificed to logical construction; hydraulics on the other hand treated each problem as a separate case and lacked an underlying theory by which the various problems could be correlated. Theoretical hydrodynamics seemed to lose all contact with reality; simplifying assumptions were made which were not permissible even as approximations. Hydraulics disintegrated into a collection of unrelated problems. . .hydraulics seemed to become more and more a science of coefficients."

It must be remembered that Helmholtz' analysis of electrokinetics is based on classical hydrodynamics. His imposition of conditions, which he placed on his conclusions, implies that he realized that classical hydrodynamics was inexact, but that the proper corrections were unknown. Unfortunately, many of these corrections are still unknown. However, in many instances the conclusions of Helmholtz have been used by others without due regard for his imposed conditions.

Perhaps Bakhmeteff (2) in 1941 gave the best presentation of the development of fluid mechanics for turbulent flow in its transition from hydrodynamics and hydraulics into a more exacting science. The contributions of Reynolds, Prandtl, von Karman, Nikuradze, and many others are combined in an apropos, nonchronologic sequence in a simplified mathematical analysis. Dodge and Thompson (17) have more adequately covered the accepted concepts of the mechanics of liquid flow from a broader viewpoint in that Bakhmeteff directed his analysis to only some of the problems involved in turbulent flow.

However, only a brief summary of the factors which most directly affect electrokinetics is presented here. The discussion is confined to liquid flow through smooth cylindrical tubes with sharp-cornered entrances and exits since the experimental work of this investigation was limited to these conditions.

Energy of Motivation: If the electrokinetic effects are neglected, the flow of a liquid through a tube is motivated by the difference of the conditions between its ends, i.e., the pressure, the kinetic energy, and the potential energy.

Pressure is an intensity factor. A pressure difference motivating a volume rate of flow is energy. It may be called a "pressure-volume" energy since it is equal to the product of the pressure and volume. A difference of the pressure-volume energy for a noncompressible liquid is equal to the product of the pressure difference ΔP and the moving volume, which is equal to the product of the volume rate V and the time t.

The kinetic energy is that energy which a mass has because of its motion; it is equal to the product of the mass m and the point velocity u squared divided by two times the conversion factor g_c.

The potential energy is that energy due to the force of gravity; it is measured as the product of the mass and the elevation z with respect to some datum plane.

The generalized equation for liquid flow between any two points, not necessarily the ends of the tube, in which no useful work is done, e.g., only the liquid is moved without any turbines being turned, is

$$V(P_2 - P_1)t + m(v_2^2 - v_1^2)/2g_c + m(z_2 - z_1) = (lw) \qquad (20)$$

where the first term represents the change in pressure-volume energy; the second, the change in the kinetic energy; and the third, the change in potential energy.

Flow Resistance: The (lw) of equation (20) represents the work lost in overcoming the resistance to flow. It includes all the irreversibilities and is ultimately lost as heat to the surroundings

although the temperature of the flowing liquid may be increased momentarily. This energy is principally dissipated by offsetting (1) the resistance of one lamina of liquid moving past another, i.e., the viscous forces, and (2) the resistance to a change of velocity due to the interchange of momentum when particles of liquid collide, i.e., the inertial forces.

The resistance to flow at any point may be expressed as the shearing stress τ. It is equal to the sum of the viscous and inertial forces per unit of lamina area at that point.

The viscous forces are dependent on the rate of deformation of the liquid. For a liquid flow, the viscous forces are closely related to forces of attraction. However, viscous forces are not completely dependent on forces of attraction. Particularly for gases, the transfer of momentum between adjacent layers is an important, and probably the controlling, factor. Perhaps, a discrimination should be made between the transfer of momentum opposed by the viscous forces and the transfer of momentum opposed by the inertial forces. The opposition of the viscous forces could result in an orderly transfer, while the inertial forces could oppose a more active transfer, which produces a momentary instability across several laminae.

The shearing stress τ_v due to the viscous forces is equal to the product of the coefficient of viscosity, or simply the viscosity μ, and the rate of change of the velocity measured perpendicular to the direction of flow, e.g., in a tube this velocity gradient is along the radial distance;

$$\tau_v = -\mu du/dr \ . \qquad (21)$$

A force is required to give any mass an acceleration, the rate of change of velocity. When a force is applied to a particle of liquid, there is a resultant acceleration of the particle. But since this particle transfers its resultant energy to the surrounding particles in a haphazard manner, it has not been possible to evaluate theoretically the exact energy losses which occur in overcoming the inertia of the particles, i.e., counteracting the inertial forces.

The inertial forces are additive to the viscous forces, and their total effect has been evaluated experimentally for most cases of liquid flow.

An energy loss may be measured as a pressure difference only if there is no change in kinetic or potential energy as shown by equation (20). If a tube is maintained at a constant level, the potential energy remains constant throughout the tube, and consequently, does not affect the pressure difference. However, an increase in kinetic energy between two points tends to produce a decrease in the pressure difference, and conversely, a decrease in kinetic energy tends to produce an increase in the pressure difference.

Therefore, for constant potential energy and constant temperature, the pressure difference is a measure of the loss of energy as heat with the effect of a change in kinetic energy superimposed upon it.

Laminar Flow: If all liquid laminae, which are concentric about the axis of a tube, move parallel to the axis of the tube, i.e., there is no transverse motion, the flow is said to be laminar or streamline. Since a molecular layer of liquid always adheres immovably to the wall, all the laminae cannot have the same velocity. In addition, since the viscous forces tend to maintain adjacent lamina at the same velocity, there must be a gradual and continuous increase in velocity as the distance from the wall is increased, reaching a maximum at the tube axis.

Since all resistance to laminar flow may be expressed as the shearing stress due to the lamina moving past one another, the resistance to laminar flow is entirely due to the viscous forces. The viscous forces are proportional to the viscosity; therefore, for a given pressure drop and a given tube, the laminar flow rate is inversely proportional to the viscosity.

Turbulent Flow: When the flow rate gets sufficiently large, a transverse motion begins, and there are random interchanges of momentum between the laminae. The resulting flow is called turbulent. Just what initiates the transverse motion is not known. However, in turbulent flow each lamina may be considered as having an average velocity. In addition, this average velocity has a fluctuating velocity superimposed upon it which varies both in the direction of the flow and transverse to the direction of the flow.

The effect of turbulence on fluid flow has not been theoretically evaluated to an exact degree, but it has been determined experimentally and correlated empirically for most cases. Since in turbulent

flow most of the particles are constantly changing their velocity, both in amplitude and in direction, the resistance to turbulent flow becomes principally an overcoming of the inertia of the particles. As the flow rate continues to increase, the resistance due to the viscous forces becomes proportionally less, and the resistance due to the inertial forces continues to increase.

Reynolds Number: By observing the effect of the flow rate on the diffusion of a jet of dye inserted at the inlet of various tubes, Reynolds (51, 52) was able to correlate his data in such a way that a dimensionless number resulted whose value indicates whether the flow is laminar or turbulent. This number is now called the Reynolds number Re, which is the product of the tube diameter D, the average velocity v, and the density ρ divided by the viscosity μ, i.e.,

$$Re = Dv\rho/\mu . \qquad (22)$$

While Reynolds did not realize the full significance of his criterion, others have interpreted it in a unique way. It can be considered as a ratio of the inertial forces, which are an indication of instability of flow, to the viscous forces, which represent a stabilizing influence. Therefore, when the Reynolds number is small, the viscous forces are dominant, and the flow is laminar. When the Reynolds number is large, the inertial forces are dominant, and the flow is turbulent.

The critical value of the Reynolds number is approximately 2000. When the Reynolds number is less than 2000, laminar flow must exist. When it is greater than 2000, the flow is ordinarily turbulent; but with exacting care in producing the flow, a laminar flow is possible.

"Established" Flow: Since the velocity of the liquid adhering to the wall is always zero, the effect of the wall on the entire flow through the tube is very pronounced. Also, if the liquid flowing into a tube comes from a sufficiently large vessel, the velocity of each lamina outside of the tube may be considered to be zero. Therefore, a distance into the tube will be required before all the moving laminae reach their steady velocity for laminar flow, or their average velocity for turbulent flow, i.e., before the flow becomes "established".

The term "established" is introduced by this writer from his translation of the German work "ausgebildet" used by Reichardt (48). A more literal translation of "ausgebildet" would be "formed" or "developed", but these words imply that a condition has been reached, while "established" implies that the condition reached will remain constant. From the viewpoint of fluid mechanics, the flow is established when the "boundary layer" fills the entire tube. The "boundary layer" is the resultant of the stabilizing effect of the wall on the fluid flow. It is zero at the entrance of the tube and increases from point to point along the entrance length until it fills the entire tube. (In this writer's translation of Helmholtz (31), Helmholtz' terminology for an established flow is worded "fully developed under the influence of eddy currents").

When a flow is established, the pressure gradient is independent of the axial length.

When a laminar flow becomes established, each lamina has a characteristic or point velocity u which is determinable by the equation,

$$u = (-\Delta P)(a^2 - r^2)/4\mu L , \qquad (23)$$

where ΔP is the pressure difference for the length L of the tube; a, the tube radius; r, the radial distance from the tube axis; and μ, the viscosity. In this equation the point velocity is a parabolic function of the radial distance, i.e., the velocity distribution or velocity profile, is a parabola.

If the point velocity of equation (23) is integrated over the cross-sectional area of a tube, the flow rate V, as expressed in the Hagen-Poiseuille law for laminar flow, results,

$$V = \pi(-\Delta P)a^4/8\mu L . \qquad (24)$$

When a turbulent flow becomes established, a more complicated velocity distribution occurs than that for laminar flow. In the immediate vicinity of the wall, a laminar film exists. The flow within this laminar film is almost identical to the flow in the same region when laminar flow exists throughout the tube. A difference results in that there are momentary fluctuations of the pressure gradient along the tube due to turbulence in the interior of the tube. These momentary fluctuations of pressure difference affect

the velocity of each of the lamina of the laminar film; therefore, there is a fluctuating laminar flow in this region when the flow in the interior is turbulent. The thickness of this laminar film is extremely small, probably never more than several thousandths of an inch, and it decreases as the Reynolds number increases.

Another criterion for either type of flow becomes useful in the analysis of the velocity distribution within the turbulent region. This criterion is that the tangential shearing stress τ, at least for an established liquid flow, is always proportional to the radial distance r as shown in Figure 3 and is equal to zero at the axis of the tube, or

$$\tau = - (dP/dx)r/2 , \qquad (25)$$

where dP/dx is the pressure gradient in the direction of flow.

In order to evaluate the shearing stress as a function of the velocity, Prandtl expressed that part of the shearing stress τ_i due to the inertial force as a function of the radial velocity gradient du/dr in the following equation,

$$\tau_i = \rho l^2 (du/dr)^2 , \qquad (26)$$

in which ρ is the density of the liquid and l is the "mixing length". The mixing length is an empirical factor which more or less expresses the distance to which a transverse impulse can reach due to an interchange of momentum between the laminae. It is zero at the wall and increases with the distance from the wall. Also, the mixing length

decreases as the flow rate increases, but this decrease is very small, and for Reynolds numbers over 10^5 it is practically constant with respect to the flow rate.

Therefore, in accord with equation (26) and considering the relation of the mixing length to the radial distance and the fact that the radial velocity gradient is zero at the axis and has a finite value elsewhere, the shearing stress τ_i due to turbulence will be zero both at the wall and at the axis of the tube and will have a maximum value somewhere in between them. Following this pattern, τ_i is sketched in Figure 3.

Since the shearing stress is equal to the sum of its parts, that due to the viscous forces, equation (21) and that due to the inertial forces, equation (26), the relation of the shearing stress to the velocity grandient at any point is

$$\tau = -\mu \, du/dr + \rho l^2 (du/dr)^2 \, . \qquad (27)$$

The velocity distribution for an established turbulent flow has been found to be U-shaped: While the velocity at the wall is zero, the velocity gradient du/dr is greatest at the wall and almost constant through the laminar film. In the outer turbulent regions, the velocity gradient sharply decreases until the center core of the liquid has almost the same average velocity.

Therefore, the viscous shearing stress τ_v, represented by the first term of the right-side of equation (28) or by equation (21), has its maximum value at the wall. It decreases proportionally faster

for turbulent flow than for laminar flow as the distance from the wall is increased as sketched in Figure 3.

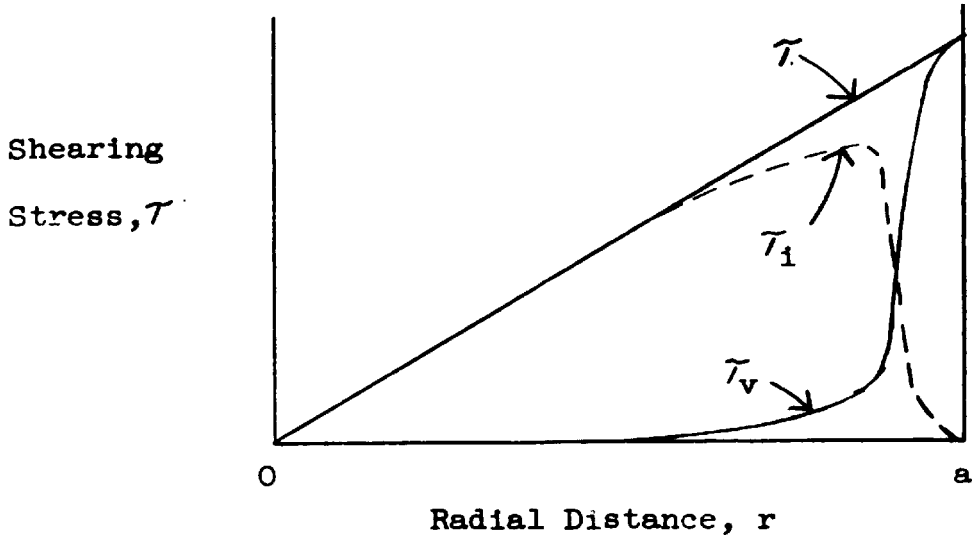


Figure 3. Radial Distribution of the Shearing Stress for an Established Turbulent Flow.

When equations (25) and (27) are equated, the resulting equation is

$$-(dP/dx)r/2 = -\mu du/dr + \rho l^2 (du/dr)^2 \qquad (28)$$

By assuming the pressure gradient dP/dx to be constant and integrating equation (28), the velocity distribution could be theoretically evaluated. However, this integration will be only a close approximation, not an exact solution, since the relation between the mixing length and the radial distance is empirical and has not been expressed mathematically. Therefore, the present solution of equation (28), and the velocity distribution, is based on experimental data.

Another empirical correlation for an established flow which has proved to be of much more importance and usefulness, is that of the friction factor and the Reynolds number. The friction factor, like the Reynolds number, is dimensionless; nevertheless, it is an expression which contains a ratio of the pressure difference ΔP for a given length L of the tube to the square of the average velocity v for any type of flow. The friction factor f, as defined by Moody (7), is

$$f = 2g_c D(-\Delta P)/\rho v^2 L \ , \qquad (29)$$

where g_c is a conversion factor and ρ is the density of the liquid.

It has been found that smooth curves express the relation between the log of the friction factor and the log of the Reynolds number as illustrated in Fig. 125 of Brown's (7) text on chemical engineering unit operations.

The graph of this correlation is useful for both laminar and turbulent flow. The laminar flow rate can be expressed as an exact function of the pressure difference as shown in equation (24), and is apparent on the friction factor graph. This linear relationship is expressed as $f = 64/Re$ for laminar flow.

Less is known of the transient region between laminar and turbulent flow rates than about either one of them; therefore, this region is usually represented on a friction factor graph with dashed lines connecting the known laminar region to the known turbulent region.

Entrance and Exit Effects: The entrance effects may be considered to include the effect of the entrance on the flow from the entrance to the point at which the flow becomes established, as well as its effect on the flow immediately at the entrance.

When the kinetic energy term of the generalized equation (20) for the energy balance in liquid flow is more closely analyzed, it becomes apparent that if the velocity used to evaluate the term is the average velocity of the flow in a tube, the term is actually an approximation of the kinetic energy for turbulent flow. The equation is only exact when the mass m is a very small quantity of liquid whose volume is the produce of its volume rate and time t.

The reason for this deviation is that the kinetic energy of the liquid passing any cross section will always be greater when the velocity distribution is nonuniform than when each particle of liquid has the same velocity. Therefore, an average velocity which is calculated by dividing the volume rate by the cross-sectional area cannot be used in the accurate evaluation of the kinetic energy for an established liquid flow in a tube.

However, if the average velocity is used, the correct evaluation of the kinetic energy for laminar flow is obtained when the term $mv^2/2g_c$ is multiplied by 2. For an established turbulent flow, it should be multiplied by approximately 1.1. The kinetic energy of turbulent flow is affected by the fluctuating average velocity and fluctuating transverse velocity, as well as by the nonuniform velocity distribution.

If the vessel from which the liquid flows is sufficiently large, the velocity may be considered zero before it enters the tube. Immediately at the entrance the velocity of each lamina is nearly the same as shown in Figure 4a; therefore, the kinetic energy at this point will be equal to $mv^2/2g_c$ for either laminar or turbulent flow. If the entrance is sharp-edged, or sharp-conrnered, the velocity of each lamina at the entrance is equal to the average velocity through the tube.

For any change of kinetic energy, there is an energy loss since the inertia of the particles resist such a change. For a sharp-edged entrance from a sufficiently large vessel, the change is very rapid, and the loss is equal to approximately one half of the increase in kinetic energy.

Considering that the velocity distribution immediately at the entrance is assumed to be uniform and that the velocity distribution of an established flow is nonuniform, an additional increase in kinetic energy is required between the entrance and the point at which the flow becomes established. For laminar flow and its parabolic velocity distribution this additional requirement is equal to the increase for a sharp-edged entrance, while for turbulent flow the additional requirement is only about ten percent of that required for laminar flow.

For the special case of a sharp-edged entrance, the forces exerted by the liquid just outside of the entrance on the liquid just inside the entrance are directed in the direction of flow and toward the axis of the tube. The resultant of these forces produces a

high-velocity jet of liquid near the axis of the tube inside of the entrance as illustrated in Figure 4b. This jet has a much greater velocity than the average velocity. Consequently, the kinetic energy of the flow at the point where the jet has its greatest velocity is greater than at any other point along the length of a constant diameter tube. Therefore, a very large loss of energy occurs when the flow of this jet spreads to fill the cross section of the tube since there is a large decrease in the kinetic energy.

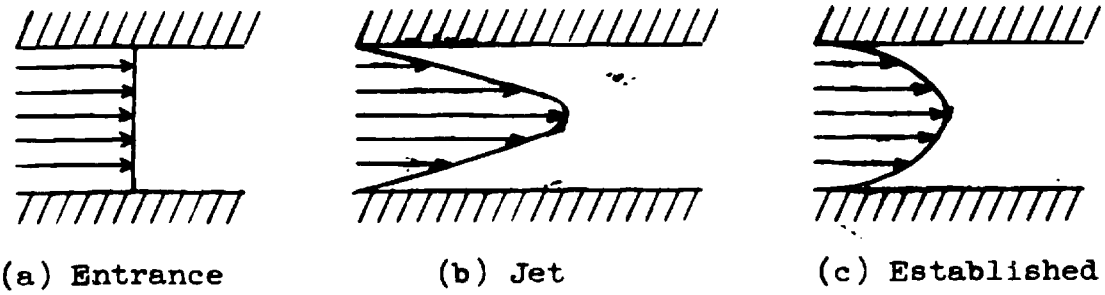


Figure 4. Velocity Distribution Along an Ordinary Tube with a Sharp-Cornered Entrance.

After the flow from the jet fills the cross section again, the effect of the wall, and its adhering layer of liquid with zero velocity, slows the laminae near the wall until an established flow is developed as shown in Figure 4c. The distance, which is required for the flow to become established when the shape of the entrance is such that no appreciable jet is formed, has been found to be 0.065DRe, where D is the tube diameter and Re is the Reynolds number. The effect of the jet due to a sharp-edged entrance on this distance has not been evaluated.

At the exit, there is a reduction in the kinetic energy which, if the receiving vessel is sufficiently large, will become zero. A loss of energy, approximately equal to and caused by the decrease in kinetic energy, is required to slow the liquid at the exit. This loss may be termed the exit loss.

EXPERIMENTAL WORK

This study is directed toward the clarification of the streaming potential concept. Emphasis is placed on the relation of fluid flow to the generation of this potential. In contrast, most investigators have been primarily concerned with the use of the streaming potential as one of the means of evaluating the zeta-potential.

A review of the literature revealed that most of the factors which can affect the streaming potential have been considered, at least theoretically. However, experimental correlations, and even theoretical analyses, for the effect of such factors as the diameter of a tube have been unsuccessful, particularly for a tube of greater diameter than about one mm. In electrokinetics, for the results of any one study to be reproduced by others is an oddity, instead of the rule. Perhaps this lack of experimental agreement can be traced principally to the difficulty of reproducing a given surface upon which the ions of a solution are adsorbed to form a double layer.

The simplicity of the Helmholtz-Smoluchowski equation (10), which expresses the ratio of the streaming potential to the pressure difference as being independent of the dimensions of the tube, has obviously caused some misunderstanding of the streaming potential concept.

In the Theoretical Background for the Experimental Work, emphasis is placed on the fact that factors other than the pressure difference may control the generation of the streaming potential.

Subsequent sections describe the selection, the design, and the construction of the equipment, along with the experimental procedure. The streaming potential and the pressure difference are measured at points in front of the entrance and beyond the exit of six different tubes. These tubes are composed of vitrous silica, borosilicate glass, or teflon. A seventh tube, composed of butyl acetate, is tapped at seven points so that the streaming potential and the pressure difference can be measured between any of the taps. Measurements can also be made between the ends of the tube. The tubes vary in diameter from 0.31 to 4.9 mm and in length from 11.57 to 93.75 cm.

Theoretical Background for Experimental Work

Since Reichardt's (48) article of 1935 was not included among the hundreds of articles reviewed before the experimental portion of this study was completed, a large part of the work was directed toward the clarification of the concepts which Reichardt had already verified. He showed both theoretically and experimentally that the Helmholtz-Smoluchowski equation for streaming potential was valid for turbulent, as well as laminar, flow. Subsequent articles on streaming potential have ignored his analysis. Authors have consistently referred to the incorrect conclusion by Helmholtz that for his streaming potential equation to be valid laminar flow must exist in the entire cross section of a tube.

Unfortunately, the concept of a laminar film for turbulent flow had not yet been developed in Helmholtz' time. In accord with this concept, Helmholtz' assumption that the velocity of the liquid near the wall

proportional to the pressure difference is just as valid when the flow in the tube is turbulent as when it is entirely laminar.

In fact, Helmholtz (31) was so uncannily correct in his analysis that the clarification of the streaming potential concept presented in this study is simply a modification, or perhaps more exactly expressed a modernization, of his assumptions and conclusions.

Probably, with the exception of Helmholtz and Reichardt, no other investigators of streaming potential have placed the proper significance on the fact that the velocity distribution is different at consecutive points along a given entrance length before it becomes more or less stable further along the tube. As Reichardt has shown, the Helmholtz-Smoluchowski equation is valid for either turbulent or laminar flow, but, as both he and Helmholtz maintained, the flow must be established, or fully developed; i.e., when the pressure gradient is independent of the axial length, the flow is established.

The distance through which a nonestablished flow exists near the entrance of a tube has been found to be approximately proportional to the diameter of the tube and to the Reynolds number. However, the exact velocity distributions and energy losses along this nonestablished flow length have not been successfully investigated.

Each of the sections of the Theoretical Background presents the basic concepts of Helmholtz and Reichardt, or a modification of these concepts in the light of current information.

The Basic Concept of Streaming Potential: The source of energy for the generation of a streaming potential is the tangential flow of

liquid very near the wall of a tube. The laminae of this flow contain a surplus of ions of one particular charge because an electric double layer of ions has formed at the solid-liquid interface. A surplus of the other charge is held immovably to the wall of the tube. The two layers of ions taken as a whole must be electrically neutral. The ions in the laminae, which are next to the immovable layer, are carried along by the movement of these laminae to form a convection current of ions, which is called the streaming current.

For simplification of discussion, it will be assumed that all ions in a solution are monovalent and that a surplus of negative ions is adsorbed to form the immovable part of the double layer, leaving a surplus of positive ions to form its displaceable charge.

Any positive ions which are displaced must be replaced immediately by other positive ions because the negative ions, which adhere immovably to the wall of the tube, cannot exist unless there is an externally applied potential gradient or unless they are "paired," or potentially neutralized, with positive ions. The latter is the case here. The immovable negative ions attract another positive ion at the instant any positive ion is displaced. Therefore, the distribution of the charge of the double layer is unaffected by the flow of liquid which displaces part of its ions.

If this condition were not true and assuming that the negative ions are held immovably at the wall by other than electrostatic forces, either the negative ions would have to react with the wall, or atoms or molecules would have to form from the negative ions. Neither the reaction between the adsorbed ions and the wall, which is dependent on the flow of

the liquid, nor that between adsorbed ions has been detected.

Now, if it is assumed that the positive ions are displaced at a constant velocity parallel to the wall, there would tend to be an accumulation of positive ions at the exit of the tube and a deficiency of positive ions at the entrance. Since surpluses of opposing charge cannot exist at a distance from one another unless a capacitive impedance is present, and since there is a very limited capacitance between the ends of a tube filled with solution, there is a very limited accumulation and deficiency of positive ions at the ends of the tube.

In this discussion, it will be assumed that the electroosmotic countereffect is negligible for streaming potential. In fact, the electroosmotic countereffect has been found to be negligible when the radius of the tube is larger than approximately 0.1 mm or when the solution is more concentrated than 0.0001 N because then the conductivity of the solution is great.

Instead of an accumulation and an equal deficiency at the ends of the tube, a positive ion upon reaching the exit will attract a negative ion from the bulk solution at the exit. At the same instant, another positive ion will take its place in the double layer, leaving a negative ion free at the entrance. If there is no electrical path present other than through the solution of the tube, all the negative ions of the solution will simply move with their speed of migration toward the exit, and all the positive ions toward the entrance, so that the distribution of ions within the solution remains unchanged. This shifting of position of the ions in the solution is an electrolytic conduction current. It must, of

course, be equal to the convection current of ions along the wall, since the entire system is electrically neutral. The conventional current, in this case, will flow from the exit to the entrance of the tube.

When this conduction current flows through the electrical resistance of the liquid, a voltage results, and it is called the streaming potential. The use of the term streaming potential will be limited in this discussion, as it usually is, to the potential which is generated by the flow of a liquid when the only electrical path present is through the solution in the tube. It is assumed that the tube wall is an insulator and that no external path, such as a voltmeter drawing an appreciable current, exists between the ends of the tube.

In the above discussion, the velocity of the liquid near the wall has been considered to be constant and parallel to the wall. This condition will exist only when the velocity distribution of the cross section of a tube is that which is present in an infinitely long tube, which is referred to here as an established flow. However, it has been found that for a trumpet-shaped entrance an established flow is approximated only after the liquid has traversed an entrance length equal to 0.065 D Re, where D is the diameter of the tube and Re is the Reynolds number.

For a sharp-cornered entrance, the entrance length traversed before an approximate established flow exists has not been formulated; however, it is probably of the same order of magnitude as that for a trumpet-shaped entrance. In any case, the velocity distribution, and consequently the velocity near the wall, are different at consecutive points along a given entrance length until the flow becomes established.

To analyze the case where the velocity v_δ near the wall is not constant, let us assume that the velocity at the wall through a given entrance length is constant and, at the same time, greater than the velocity at the wall along the remainder of the tube, which is also constant. This particular case is illustrated in Figure 5, in which the entrance-length velocity is arbitrarily selected to be twice that of the remainder of the tube.

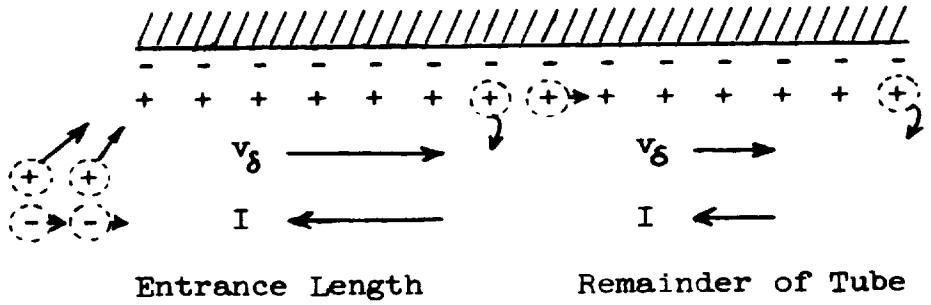


Figure 5. Effect of Velocity Near the Wall on the Conduction Current of the Streaming Potential

Then the displaced positive ions upon reaching the end of the entrance length may take either of two paths: they may move along the wall to replace displaced positive ions in the double layer of the remainder of the tube, or they may be forced away from the wall with the liquid, and consequently away from the double layer, by the slowing liquid. As soon as they are torn from the attractive influence of the adsorbed negative ions of the double layer, a momentary accumulation of positive ions will occur at the point between the entrance length and the remainder of the tube.

The positive ions which remain in the double layer for their entire path through the tube will produce a momentary accumulation of positive ions upon reaching the end of the tube. The positive ions replacing displaced ions in the double layer at the entrance of the tube must leave behind a

momentary surplus of negative ions in the bulk solution. Then, with the speed of electrolytic conduction, the surpluses and deficiencies are eliminated. The negative ions in the solution shift toward the exit, and the positive ions toward the entrance, until their distribution in the solution is identical to that before the flow began in the tube.

Since there was a momentary accumulation at the point between the entrance length and the remainder of the tube, more ions will have to shift in the entrance length than in the remainder of the tube. The conduction current in each section must be exactly equal to the convection current of ions in that section.

Generalizing from this analysis, the tube may be divided into incremental lengths sufficiently short so that the velocity of each increment can be considered as being constant; the conduction current of each increment will be exactly equal to the convection current of ions in that increment. As a consequence, the streaming potential across each incremental length is equal to the product of the convection current of ions, i.e., the streaming current, and the electrical resistance of each incremental length. No assumption has been made as to whether the type of liquid flow in each incremental length is established or nonestablished. This point will be further amplified in subsequent paragraphs.

In this discussion, expressions such as "... ions, which remain in the double layer for their entire path through the tube, ..." are used quite often. They cannot be interpreted literally since the ions of a solution, whether in the double layer or in the bulk of the solution, are constantly migrating about and exchanging their positions. Consequently,

to state that an ion is at some particular place actually means that by a statistical average or from a probability viewpoint an ion should be at that particular place.

Also, since it is believed that there are no free electrons in solutions, such as are found in metals, the ions are the means of transmitting an electric conduction current. Even those ions which constitute the convection current transmit their portion of the conduction current, but this constitutes the electroosmotic countereffect which is considered to be negligible for the purposes of this discussion.

In this same line of thought, the liquid flow producing the streaming potential does not, in a sense, pull the oppositely charged layers of the double layer away from one another. A true separation requires the energy expended in electrolysis. Here, the liquid flow merely tangentially slips one ion in to take the place of another ion. A very small amount of energy is required to do this slipping, and consequently, the resulting energy of the streaming potential and the conduction current is very small, i.e., billionths of a watt.

The streaming current is equal to the summation of the products of the velocity of each lamina containing a surplus of charge and that lamina's surplus charge per unit length. Since the thickness of the double layer is of the order of 10^{-7} cm and the diameter of a water molecule is about 2×10^{-8} cm, the number of laminae containing displaceable charge is quite limited, but the possibility exists that there may be more than one. It should be noted that the thickness of the displaceable layer is the quantity of actual concern here. It is greater than the thickness of the double

layer, as illustrated in Figure 22, but even the thickness of the double layer is known only to order of magnitude. The thickness of the displaceable layer is more indefinite.

The objective here is to formulate an equation for the streaming potential which is valid for any type of flow. Since the usual assumption that the velocity of the laminae near the wall is proportional to the pressure gradient is not always valid for a nonestablished flow (as shown in Analysis 1 of the Appendix), this assumption cannot be used here.

In Analysis 2 of the Appendix, it is shown that the streaming current can be expressed as the product of the velocity at a particular distance δ from the wall and the total displaceable charge per unit tube length. However, in Analyses 1 and 2 it is necessary that the tube be thought of as divided into a sufficient number of increments so that the velocity u near the wall, or the pressure gradient dP/dx, can be considered constant for each increment. Also, the following assumptions must be valid:

1. An electric double layer is formed at a solid-liquid interface. The outer layer of charge, i.e., ions, adheres immovably to the wall, while the inner layer can be displaced by the liquid streaming past the solid surface.

2. The distribution of charge of the double layer is homogeneous over the surface of the increment, is unaffected by the displacement of the inner layer of charge since any displaced ion must be replaced immediately, and is a continuous function of the radial distance.

3. The system as a whole is electrically neutral.

4. The thickness of the double layer is small compared to the radius of the tube.

5. The flow near the wall is laminar, and the viscosity of the double layer is the same as that of the bulk solution.

6. The tube is circular, and its radius is constant.

7. The electroosmotic countereffect is negligible.

Then, to comply with the definition of the streaming potential, it must be assumed that

8. The tube wall can be considered an insulator with respect to the solution, and no other electrical path exists between the ends of the incremental length.

Since all these assumptions can be fulfilled or shown to be valid within definable limits, a generalized equation for the streaming potential E_s for a tube may be written:

$$E_s = \sum_{1}^{j} 2 \pi a_j \sigma_{s_j} u_{s_j} R_j \quad , \tag{30}$$

where j is the number of incremental lengths in which the tube is divided, a is the radius, σ_s is the displaceable surface charge density, u_s is the velocity at the distance δ from the wall, and R is the electrical resistance of the solution in the tube.

The Significance of the Basic Equation: If the radius a, the displaceable charge density σ_s, and the electrical resistance R are constant for a unit length, the streaming potential across the unit length becomes a relative measure of the average velocity at a fixed, but indeterminate, distance δ from the wall. For the experimental application of equation (30), a

sufficient number of adjacent incremental lengths must be combined to give a finite unit length. Therefore, the velocity u_s, which generates the streaming potential, is an average of all the constant velocities of the incremental lengths as expressed by the following relation:

$$u_s = \sum_{1}^{j} u_{s_j} \underline{L}_j \Big/ \sum_{1}^{j} \underline{L}_j \quad , \tag{31}$$

where j is the number of incremental lengths of length $\underline{L}$ in a unit length.

The usefulness of equation (30) is limited to a comparison of the average velocities for the different unit lengths of a tube. The absolute value for these velocities cannot be determined by any present method.

The streaming potential cannot be used to measure this velocity, since the quantity of displaceable charge cannot be measured directly. This charge is simply the displaceable part of a continuous layer of charge, which exists near the wall and which probably extends into the boundary film of liquid which adheres immovably to any wetted solid.

Since the velocity producing the streaming potential occurs so close to the surface, no measuring device, such as a pitot tube, is sufficiently small to measure it accurately. Also, the fact that the distance δ is indeterminate makes it impossible to use the accepted velocity distribution for an established flow to evaluate the velocity producing the streaming potential.

The principal condition necessary for maintaining the resistance constant per unit length is for the radius a to be constant and the tube to be circular. The effect of surface conductance on the resistance is also dependent on there being a homogeneous charge distribution, but the surface

conductance, like the electroosmotic countereffect, is not appreciable except for tubes of less than several tenths of a millimeter diameter or with solutions of less than 0.0001 normality.

In order for the displaceable charge density to be constant, the charge must be homogeneously distributed over the entire surface. A theoretical confirmation of the assumption of homogeneous distribution of charge depends on a more complete knowledge of the process of adsorption than has been established; however, the previous history is probably one of the most important factors.

The previous history, i.e., the process of cleaning, former solutions and ions in contact with it, etc., of the different portions of the surface for any one tube is more likely to be the same than the previous history of the entire surfaces of two different tubes. Therefore, while the assumption that the displaceable charge density is constant for any given tube cannot be verified, it should be more reliable for any one tube than among different tubes.

Velocity Gradient at the Wall: One of the most important factors in the solution of any problem of fluid flow is the establishment of boundary conditions. The fact that the velocity of the liquid at the wall is zero is a boundary condition which is usually accepted for any type of flow. However, the velocity gradient $(du/dr)_a$ at the wall with respect to the radial distance has been evaluated only for an established flow. (The subscript a indicates that the radial distance is equal to the radius a of the tube; the term $(du/dr)_a$ is sometimes written $(du/dN)_0$, or $(du/dy)_0$, where N, or y, is the normal, or perpendicular, distance from the wall.) Of course,

the evaluation of this velocity gradient even for an established flow depends on certain conditions, such as the viscosity of the liquid near the wall being identical with that of the bulk liquid, which are usually accepted as very close approximations.

Since the velocity at the wall is zero and since the thickness δ of the double layer is so small, the velocity gradient at the wall will be directly proportional to the velocity generating the streaming potential, i.e.,

$$- (du/dr)_a = u_s/\delta \quad . \tag{32}$$

If the velocity is considered positive, the velocity gradient with respect to the radial distance is negative; i.e., the velocity decreases as the radial distance increases. Therefore, the minus sign is necessary in equation (32), since δ is simply a dimension, a positive constant analogous to the length and the radius.

If the average velocity gradient for a unit of tube length is expressed in accordance with equations (30) and (32), the following relationship is obtained:

$$(du/dr)_a = - E_s/2\pi a \sigma_s R \delta \quad . \tag{33}$$

The factors in the denominator of the right side of this equation can be maintained constant under the same conditions as those discussed above. Therefore, if these factors are maintained constant and if the streaming potential is measured and the velocity gradient calculated in a section of the tube where the flow is established, the velocity gradient in any other section of the tube can be calculated from their relative streaming

potential gradients. Consequently, an important boundary condition, the velocity gradient at the wall, can be evaluated for a nonestablished flow by the measurement of its streaming potential.

If the resistance R of equation (33) is expressed as a function of the electrical conductance k and the surface conductance k_s of the solution, along with the radius a and the axial distance x of the tube, the streaming potential gradient is clearly shown. That is,

$$(du/dr)_a = - \frac{(E_s/x)\ a\ (k + 2k_s/a)}{2\ \sigma_s\ \delta} \quad . \tag{34}$$

Shearing Stress: The shearing stress at any point is the force per unit area which resist the movement between two adjacent layers of liquid. Since the flow adjacent to the wall is always laminar, the shearing stress τ_a at the wall may be expressed for any type of flow along the tube by the following equation:

$$\tau_a = - \mu (du/dr)_a \quad . \tag{35}$$

Or, expressing the velocity gradient at the wall as a function of the streaming potential in accord with equation (33), the average shearing stress along a unit length of the tube is

$$\tau_a = \mu E_s / 2\pi a \sigma_s R \delta \quad . \tag{36}$$

Then, since the shearing stress for an established flow is directly proportional to the radial distance, the shearing stress at the wall for an established flow may be evaluated from the pressure gradient dP/dx and the tube radius a by the following equation:

$$\gamma_a = - (dP/dx)a/2 \quad . \tag{37}$$

Consequently, the shearing stress at the wall can be evaluated in the same manner as that shown for the velocity gradient, i.e., by a ratio of the streaming potential gradients.

However, since the shearing stress for a nonestablished flow is not proportional to the radial distance, the shearing stress at the wall does not have the same significance (e.g., its relation to the velocity distribution) for a nonestablished flow as for an established flow. If the effect of the tangential forces of the liquid on the wall were being studied, then the evaluation of the shearing stress would be important.

Contraction and Expansion Losses: One of the energy losses of liquid flow is due to the contraction at the entrance and expansion at the exit of a tube; i.e., a loss of energy occurs with any change in the kinetic energy of the liquid. Since the ΔP of the Helmholtz-Smoluchowski equations is usually defined as the pressure which produces the flow, perhaps this loss may be ignored from a theoretical viewpoint. However, in an experimental procedure, it must be considered, since the pressure difference is usually measured between points in front of the entrance and beyond the exit.

The exit loss is approximately equal to the loss of kinetic energy due to the decrease of velocity at the exit. Therefore, no appreciable pressure drop occurs at the exit.

For sharp-cornered entrances, the entrance loss has been found to be equal to approximately one-half the increase in kinetic energy. Therefore,

the pressure drop at the entrance will be equal to about one and one-half times the increase in kinetic energy when the kinetic energy is expressed as an equivalent pressure difference.

The pressure losses due to the entrance and the exit effects are related to the flow rate and to the dimensions of the tube. The other pressure losses resulting from a flow are also related to the same factors. These relations have not been evaluated for all cases. For a tube of infinite length and finite diameter, the pressure losses due to the entrance and exit effects will be negligible when compared to the other pressure losses. However, a minimum ratio of the tube length to the diameter, at which the pressure losses due to entrance and exit effects are negligible, cannot be determined for both laminar and turbulent flow.

Equipment

While the equipment of this study conforms to the standards established as necessary by other investigators, it is different from their equipment in several aspects: (1) The tubes can be interchanged with comparative ease. (2) No sealing compounds are used in connecting the various components of the flow system, eliminating a possible source of contamination of the solutions. (3) The electrometer detector and the amplifying system have a higher frequency response, up to 50 cycles per second. (4) Fixed resistors can be connected across the streaming potential tube by turning a switch, permitting the use of the streaming current as the source of energy to measure the electrical resistance of the flowing liquid in the tube.



Figure 6. The Solution System of the Streaming Potential Apparatus



Figure 7. The Control and Measurement Equipment

Figure 8 is a schematic diagram of the entire streaming potential equipment. For the purpose of description, the equipment is divided into three categories: (1) the solution system, (2) the nitrogen system, and (3) the electrical measurement equipment.

The solution system is pictured in Figure 6. For comparative size, the steel shield is 6 feet long. Its top and front panels are open so that the streaming potential tube and electrode chambers can be seen. Figure 7 pictures the nitrogen system with its pressure stabilizing tank, the pressure control valves (mounted on the side of the table very close to the Sanborn Twin-Viso), and the manometers, as well as the components of the electrical measurement equipment with their interconnecting cables.

The Solution System: The streaming potential tube pictured in Figure 6 is tube 7, while the streaming potential tube shown in the schematic diagram of Figure 8 represents any of the other tubes. When the streaming potential is measured at the ends of tubes 1-6, the electrode chambers which contain the electrodes are located at each end of the streaming potential tube so that the solution flow through them. The apparatus has to be assembled in a slightly different way from that of Figure 8 for tube 7, as is illustrated in Figure 6. The electrode chambers are needed at the taps when the streaming potential is measured between the taps of tube 7.

While the streaming potential tubes are composed of several materials, the remainder of the components of the system which come into contact with the solution are composed of either pyrex glass or teflon. This limitation of materials prevents the contamination of the solutions being studied. Teflon was selected because of its chemical inertness and because it can be

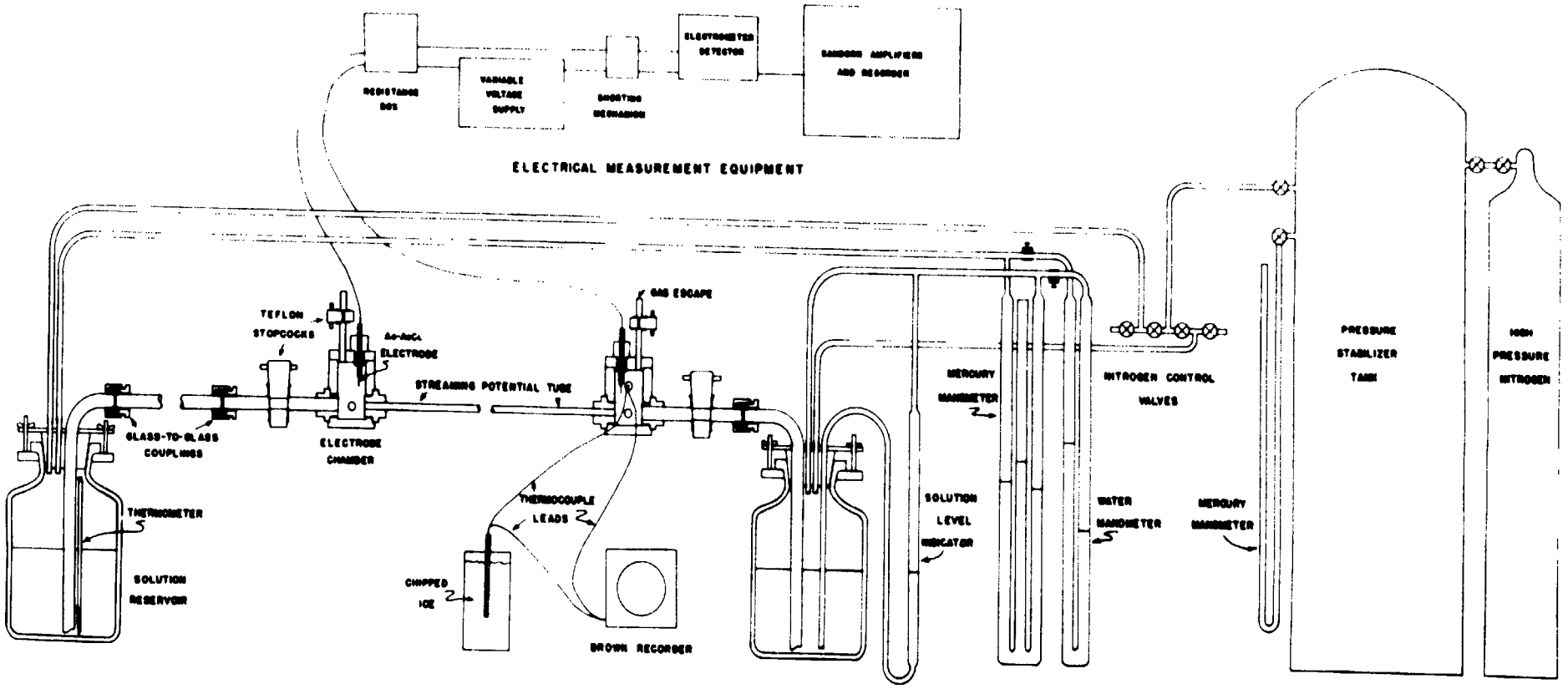


FIGURE 8. APPARATUS FOR THE MEASUREMENT OF STREAMING POTENTIAL

achined to precision dimensions. Its use made it possible to fit the various components of the solution system together without the use of the usual sealing compounds and stopcock grease, which permit the possibility of contamination.

Also, the apparatus can be dismantled so that the relatively smaller components can be cleaned. However, the entire flow apparatus is larger than that of the usual study. For example, 14-liter pyrex bottles are used as reservoirs to store the solution at either end of the system.

The reservoir is coupled to the tubes containing stopcocks with 1/2-inch pyrex tubing and pyrex pipe fittings, which were obtained from Fisher and Porter, Hatboro, Pennsylvania. The stopcock plugs were machined from teflon rods, eliminating the use of stopcock grease, since the surface of the teflon does not stick to that of the glass. Also, the asbestos washers of the Fisher and Porter glass-to-glass couplings were replaced with teflon washers.

One end of the tubes containing the stopcocks are slip fitted into plugs which screw into the electrode chambers. This assembly is the case for tubes 1-6; however, for tube 7, which has an enlarged chamber sealed on each of its ends, the plugs are screwed into this enlarged chamber.

The four principal components of the solution system which will be described in detail are (1) the tubes, through which the streaming potential is generated, (2) the electrode chambers, (3) the reservoirs, and (4) the solution temperature measurement devices.

(1) Streaming Potential Tubes: Tubes are used in this study which are composed of vitrous silica, borosilicate glass, teflon, and butyl acetate, whose diameters vary from 0.3 mm to 4.9 mm, and whose lengths vary from 11.5

cm to 94 cm.

Jones and Wood (34) maintained that much of the lack of agreement between different studies can be traced to the fact that the composition of the tubes, in which the streaming potentials were generated, has not always been known or has not always been recorded. They selected vitrous silica because the tubes would then be composed of a single pure substance, instead of the multiple substances which compose glass, the usual material selected. The close agreement of the results obtained from the two tubes of their equipment is probably the most consistent in the literature.

When it was found that vitrous silica tubes could not be obtained with precision dimensions, only one vitrous tube (tube 1) was purchased. It is a "vitreosil" tube from the Thermal Syndicate Ltd., New York, whose diameter is 1 mm, tolerance 0.25 mm, and length 89.35 cm. This tube is used as a control for the comparison of the results of this study with those of Jones and Wood.

Precision-bore tubes made of borosilicate glass by the "Glo-Tech" process were obtained from Fisher and Porter Company. This company maintains that bore dimensions are within 0.005 mm of the size specified. Tubes are used whose diameters are 0.475 mm (tube 2), 1.00 mm (tube 3a), and 3.08 mm (tube 4) and whose lengths are each 83.82 cm. A piece was inadvertently broken off of tube 3a in January, 1951, and thereafter it is referred to as tube 3b, whose length is 76.53 cm. (A mix-up in tubes apparently occurred at Fisher and Porter on tube 2, since it was specified as having a 0.308-mm diameter. Measurement of the electrical resistance and flow rates, as well as physical measurement by the insertion of rods in its ends, confirm the

0.475-mm diameter. However, this diameter is not one of the standard sizes listed by Fisher and Porter for this type of tube.)

The "classic" explanation for the continuous change of the zeta-potential with time is the dissolving of the glass tube or the formation of silicic acid gels. Therefore, the streaming potential generated in tubes made of DuPont teflon, which at least can only dissolve, but not form silicic acid gels, is also studied. The 1.33-mm diameter teflon tube (tube 6), whose length is 12.75 cm, was machined by drilling a teflon rod. The 0.305-mm diameter tube (tube 5), whose length is 11.75 cm, was made by molding teflon powder around a 0.3-mm stainless-steel wire.

The design of the mold was complicated because of the high coefficient of expansion of the teflon, the necessity for putting the teflon under pressure, and the desirability of the steel wire being kept taut so that the resulting hole would be straight.

A 1/2-inch brass pipe about 12 inches long was used as a mold. Both ends of the pipe were threaded. The steel cap on one end had a hole in its center just big enough for the 0.3-mm wire to be passed through it. The wire then was passed over a pulley and a weight fastened to its end so that the wire would be taut at all times. The other end of the wire was passed through a small hole in a plug and then fastened to the back side of the plug, which was machined to fit inside the molding tube. The cap on the end at which the plug was located was fitted with a screw so that pressure could be applied to the plug.

Teflon molding powder has a very high porosity, so that a much larger volume of it was needed than the final solid volume. A hole was drilled in

the mold so that the plug could be pulled back by an auxiliary wire to allow a slug of teflon powder to be fed into the mold. The elimination of the air between the teflon powder particles was accomplished by applying pressure, pulling back the plug, adding more powder, applying pressure again, etc., until the mold was filled. This process must be classified an art, since the application of too great a pressure to any particular slug of powder caused a fissure between that slug and the next one in the final product. During the packing process, the stainless-steel wire slid back and forth through the packed powder. After sufficient teflon was in the mold, the packing screw was tightened to near the rupture point for the mold; then the screw was loosened, since the weight on the end of the steel wire over the pulley exerted enough pressure during the heating process.

The mold was placed in a 340°C oven for 20 minutes. After this time the mold was removed from the oven and the packing screw again tightened. As the teflon cooled, it contracted away from the walls of the mold and from the steel wire running through its center. A section was machined from each end of the molded tube to assure that the diameter through the length of the tube was as nearly constant as possible.

Tube 7 is quite different from the others. Since the comparison of results between different tubes is handicapped by the fact their previous histories, and hence their displaceable surplus charge per unit area, have a greater chance of being different, it was decided to study the streaming potential between different points along the same tube. It was calculated that a tube with a diameter of about 3 mm and a length of about 1 meter would have nonestablished flow for one-third its length at maximum

streamline flow. The modification of tube 4, the 3.08-mm borosilicate-glass tube, was considered, but rejected because the boring of holes in the glass would probably result in rough edges which might affect the flow pattern. Also, the fusing of the side tubes over the holes through which the streaming potential and pressure differences were to be measured would probably result in an appreciable distortion of the bore of the streaming potential tube.

As a compromise, a butyl acetate tube (tube 7) with a diameter of about 4.9 mm and a length of 93.75 cm was selected. Because it is an extruded plastic tube, its diameter is probably not constant. Seven 1-mm holes were drilled along its length. Side tubes were sealed over the holes to the outer surface of the streaming potential tube by plastic solvent; consequently, the diameter of the streaming potential tube was unaffected by this operation.

Since the greatest variations of the velocity distribution occur close to the entrance of a tube, most of the taps were placed near one end. One hole was located as close to the end as was physically possible, 0.35 cm from the entrance to the center of the hole. The next three were placed at 1.50-cm intervals. The other three taps were placed at 12.70, 15.24, and 30.38 cm intervals, which made them approximately one-sixth, one-third, and two-thirds of the tube length from that end at which the closely spaced taps were located.

Also, since the electrode chambers were needed at the taps when the streaming potential was being measured there, an enlarged section, 10 cm long and with a 4-cm inside diameter, was sealed onto each end of tube 7.

tap was placed midway in this enlargement so that the overall streaming potential and pressure difference could be measured.

(2) Electrode Chambers: Two vertical cylindrical chambers, whose inside diameter is 2.5 cm and whose inside height is 5.5 cm, are located between the ends of the streaming potential tube and the tubes containing the stopcocks. These chambers were machined from 2-inch teflon rods and have threaded outlets into which threaded plugs of teflon can be screwed. These plugs, in turn, may be solid or have precision-fitted holes for each particular connecting piece, usually a pyrex glass tube. The top of the chamber is a 1-inch section of 2-inch teflon rod, which is held tightly to the rest of the chamber by four bolts whose heads rest on an external brass ring and which extend through the teflon cover down into the wall of the chamber. The outer edges between the cover and the body of the chamber were machined down so that a seal exists at the interior edge of the body with the cover. Therefore, the solution cannot come into contact with the four brass bolts.

Each chamber has six outlets. Two 7/8-inch holes on opposite sides of the chamber as near to the base as possible admit plugs to which are fitted the streaming potential tube and the tube containing the stopcock, permitting the liquid flow to pass directly through the bottom of the chamber. Two 1/2-inch outlets are located on opposite sides of the chamber at right angles to the 7/8-inch holes. One of these holes is used as the outlet for measuring the pressure. The other admits the thermocouple, and it is centered at a higher level than the larger holes so that the small pyrex tube containing the thermocouple is not in the liquid path between the larger holes.

Only one of the two holes in the cover is threaded. The smooth-bore hole is fitted to the tube through which all the gas which may be in the liquid system can be removed through a stopcock, since the top of the electrode chamber has the highest elevation of any point in the solution system. The plug holding a silver-silver chloride electrode is mounted in the threaded outlet. The electrode is above the direct path for the liquid flow.

The seal between the chamber and the teflon plugs is accomplished by having a flat surface around each hole on the outside of the chamber and a flat surface perpendicular to the threads on each plug. These two surfaces make a snug fit when the plug is screwed into the chamber.

(3) Reservoirs: Two 14-liter heavy-walled pyrex bottles are used as reservoirs to store the solution at either end of the solution system. Rubber stoppers, which do not come into contact with the solution, are held in place by brass plates which cover the top of the stoppers and which are bolted to brass rings around the necks of the bottles. Each stopper has (1) a hole for the 15-mm bore tubes through which the solution flows, (2) a hole for connections to the nitrogen control valves, and (3) a hole for a lead to the manometers.

In addition to these holes, the right reservoir has another hole through which the solution was connected by siphon to a solution-level indicator.

The pressure difference across the solution system is the algebraic sum of the pressure differences of the nitrogen in the reservoirs and the difference of the hydrostatic level of the solution in the reservoirs. Therefore

the liquid level of the reservoir had to be read for each streaming potential measurement. After reading the solution level in the reservoir directly proved difficult, particularly for the larger streaming potential tubes when the level was changing more rapidly, the solution-level indicator was installed along the outside of the reservoir.

A tube was extended from the bottom of the solution, up through the stopper, curved down the outside of the reservoir to a level below the base of the reservoir, then U-turned upwards to connect to a straight 1-mm bore tube which extended in a vertical position to the level of the top of the reservoir. The top of this straight tube was connected into the right-reservoir lead to the manometer. When the solution is siphoned into this tube, the liquid level of the 1-cm bore portion is identical with that of the reservoir. By placing a scale behind the tube, the solution level can be read more accurately and quickly than reading the level within the reservoir.

(4) Thermometers and Thermocouples: The temperature recorded in the data is that of the solution in the electrode chamber. Due to physical limitations of the steel shielding, a thermometer could not be mounted into the chamber. Consequently, two thermocouples were constructed by soldering two copper wires to a length of "Advance" wire. "Advance" is a Driver-Harris alloy of copper and nickel whose thermal e.m.f. against copper is 0.043 mv/°C.

One of the thermocouples was sealed into a thin-walled glass tube which was mounted in a teflon plug, which in turn was screwed into the side of the electrode chamber. The other thermocouple was used as a reference by placing it in a glass tube which was inserted into a thermos filled with

chipped ice and distilled water, whose temperature would always be 0°C.

Initially the thermos was placed inside the steel shield. But when it was discovered that the thermos absorbed sufficient heat to lower the temperature of the air in the closed shield as much as 2°C, it was placed outside the shield.

The copper leads from the thermocouples were connected to a Brown Electronik Circular Chart Recorder, Model 152X12V-X-16, a recording potentiometer which also has a rotating pointer. A scale at the tip of the pointer was calibrated so that the temperature of the electrode chamber could be read directly. The sensitivity of the potentiometer and the thermocouple was such that the scale was about 1°C/cm.

Thermometers were placed in the solution of the left reservoir and in the air space of the steel shield of the solution system.

Nitrogen System: The solution being studied may be propelled through the flow system in either direction. The motivating force for this flow is furnished by high-pressure nitrogen. Nitrogen is used because of its inertness, for it has been found that even the smallest quantity of dissolved material, particularly carbon dioxide, will greatly reduce the streaming potential.

(1) Nitrogen Flow Components: A 250-liter tank is used as a pressure stabilizer between the high-pressure nitrogen and the control values. Four Hoke needle valves, which are mounted in series with pipe tees between them, are the mechanism for control of the pressure in each solution reservoir. The center tee is connected to the stabilizing tank. The other two tees are connected directly to the top of liquid reservoirs.

The outside outlets of the end valves are open to the atmosphere. Therefore, by adjustment of the needle valves, the pressure in either reservoir can be any pressure between atmospheric and that of the pressure-stabilizing tank. The various components of the nitrogen system are connected with 5-mm heavy-walled rubber tubing, which is also used to connect the manometers to the solution reservoirs.

(2) Manometers: In the initial experiments, manometers made from 5-mm bore glass tubing were used. These manometers were read, as an approximation, to the nearest 0.01 cm Hg. In early 1952 it was discovered that these manometers did not give reproducible pressures to 0.1 cm Hg. Manometers were then constructed from 15-mm bore tubing and filled with double-distilled mercury.

One mercury manometer was constructed with three tubes. The two outside tubes were connected directly to the top of the solution reservoirs at each end of the solution system; therefore, the difference in level of these two tubes indicates the nitrogen pressure difference across the flow system. The center tube was left open to the atmosphere, permitting the reading of the gauge pressure in each reservoir.

The reason that it is desirable to know this gauge pressure is that it was found necessary to maintain the pressure in the streaming potential tube and the electrode chambers at slightly above atmospheric pressure. Since the liquid level of the reservoirs is lower than the level of the electrode chambers, a pressure of about 5 cm Hg had to be maintained in the reservoirs for the pressure in the electrode chambers to be atmospheric.

The electrode chambers had to be slightly more than atmospheric pressure, particularly just after each time the equipment was reassembled, because with less than atmospheric pressure small leaks in the glass-teflon fittings would permit air to enter the system. Since most glass tubing is not exactly circular and since the holes drilled in the teflon plugs are necessarily circular, the holes were drilled slightly smaller, e.g., about 0.003 inch for a 1/4-inch hole, than the size of the glass tubing to be inserted into it. However, it usually required several days for the teflon to conform to the noncircular tubing, and until that time small leaks resulted. As long as solution ran out, and as long as no air got into the streaming potential tube, no significant effect is caused by the leak.

A water manometer is connected in parallel with the outside tubes of the triple-tube mercury manometer so that small pressure differences between the reservoirs can be read more accurately. Tightening screw clamps on the rubber tubing between the manometers isolates the water manometer when high pressure differences exist between the reservoirs.

To measure the pressure difference between the electrode chambers, or between the taps of tube 7, the outlets are connected to the bottom of two vertical glass tubes, each of whose levels can be controlled independently by nitrogen pressure. The pressure from the nitrogen stabilizing tank, which is connected by two leads to the tops of the vertical tubes, is controlled by screw clamps on the connection tubes. Side taps from these leads connect to the tubes of a mercury manometer. Therefore, the pressure difference between the outlets is the algebraic sum of the difference of the mercury manometer and the difference in levels of the solution in the

vertical tubes. For low pressures, the leads to the mercury manometer are interconnected so that the pressure difference between the outlets is the difference in the levels of the solution in the vertical tubes.

Electrical Measurement Equipment: The key component of the equipment used to measure the streaming potential is the electrometer detector. It is different from other streaming potential detecting devices in that it has a higher frequency response, permitting the observation of the oscillations of the streaming potential in turbulent and transient flow.

The streaming potential is detected by the electrodes in the electrode chambers. As can be seen in Figure 6 and partly in Figure 7, the leads from the electrodes pass through the small pipes mounted in the steel shielding of the solution system. The highest chassis in Figure 7, to which the electrode leads are connected, is the resistance box. The resistance box is the switching device for connecting a selected resistor or leaving an open circuit between the leads.

The left electrode and its circuit are maintained at a maximum resistance above ground. The right electrode is closer to the right solution reservoir, which cannot be as completely shielded as the left reservoir because the level of the right reservoir must be read each time a streaming potential is recorded. Consequently, more 60-cycle interference should be expected at the right electrode than at the left electrode. The left-electrode lead is connected to the upper left receptacle of the resistance box, which is internally shorted to the lower right receptacle. Then it is connected to the shorting mechanism, where its circuit may be left floating or may be connected to the control grid of the electrometer detector. All its

connecting cables are light-colored in Figure 7.

The right-electrode circuit also passes through the resistance box, but it is connected through the variable-voltage supply before being connected to the shorting mechanism. From the shorting mechanism this circuit is connected to the upper left receptacle of the electrometer detector. The cables connecting the different components of the right-electrode circuit between the resistance box and the electrometer detector are black in Figure 7. Another strand of these cables is the common ground.

The electrometer detector is essentially an impedance-matching device. Its output is amplified and recorded on the tape of a Sanborn "Twin-Viso" Amplifier and Recorder, which has been slightly modified for this study.

The electrical equipment is described in more detail in the following order: (1) electrodes, (2) electrometer detector, (3) Sanborn Amplifier and Recorder, (4) shorting mechanism, (5) variable-voltage supply, (6) resistance box, and (7) shielding.

(1) Electrodes: To minimize the effect of polarization, silver-silver chloride electrodes are used to detect the streaming potential.

These electrodes were made in groups of four following the electroplating process of Smith and Taylor (58), since that appeared simpler to execute than their thermal process or the thermal-electroplating process. Smith and Taylor showed that silver-silver chloride electrodes made by each of the three processes are equally reproducible. Initially, platinum wires of various sizes were used, but no preference could be detected for any special size, as far as polarization voltages between electrodes are concerned.

The final group, which has been used for the data recorded in the Appendix, was made from No. 22 platinum wire. Approximately 1 inch of platinum wire was sealed in the end of a 2-mm pyrex tube with approximately 13 mm of wire extending from the end of the tube and about 8 mm of bare wire extending into the tube. The wire was alternately heated to brightness and immersed in boiling concentrated nitric acid. The pyrex tube was then filled about half full of mercury, making it possible to insert a lead wire into the mercury so that a good electric contact could be established with the electrode.

An electrode and a thin sheet of pure silver were placed in each of four beakers. The free ends of three of the copper wires, which had been soldered to the tops of the silver sheets, were immersed in the mercury of an electrode tube in another beaker. The fourth copper wire was connected in series with a battery, a galvanometer, a control potentiometer, and the mercury of the fourth electrode tube. The beakers were then filled to a level so that the extending platinum wires were completely immersed and so that otherwise only pure silver was in contact with the following silver-plating solution:

AgCN	30 gm/liter
KCN	40.75 gm/liter
K_2CO_3	45 gm/liter
$(NH_4)_2S_2O_3$	0.0963 cc of 60% sol/liter

The electrodes were silver-plated by maintaining a 0.62-ma current (a current density of 5.4 ma/cm^2) for 20 hours at a temperature of approximately 25°C. After washing and soaking in changed baths of distilled water

for 2 weeks to remove any silver-plating solution, the electrodes were again placed in the plating apparatus but with the silver sheets replaced by platinum wires and the silver-plating solution replaced by 1N hydrochloric acid. The same intensity of current, 0.62 ma, was used, but for only 1 hour, and, of course, it flowed in the opposite direction with respect to the electrodes. The electrodes were then washed again in distilled water before being used in any chloride salt solution.

Several days were required for the electrodes to reach more or less stable voltages when they were placed in a solution of concentration different from that from which they had just been removed. It is believed that in this study the change of potential between the electrodes for a zero flow rate of solution was affected by other factors as well as by the polarization of the electrodes. This matter will be discussed in more detail under Shielding of the electrical equipment.

(2) Electrometer Detector: In order to measure a streaming potential, a measuring device must be used which has a high-input impedance; i.e., the measuring device must operate by drawing an extremely small quantity of power from the source. For electrometer circuits, this power is expressed as current, and it is usually less than 10^{-13} amp.

This current must be small when the streaming potential generated by the flow of dilute solutions is measured because in this case the source impedance is very high. Consequently, any appreciable current withdrawn from the source will reduce the electric potential across the tube. For example, when maximum current is withdrawn by an external, direct shunt of

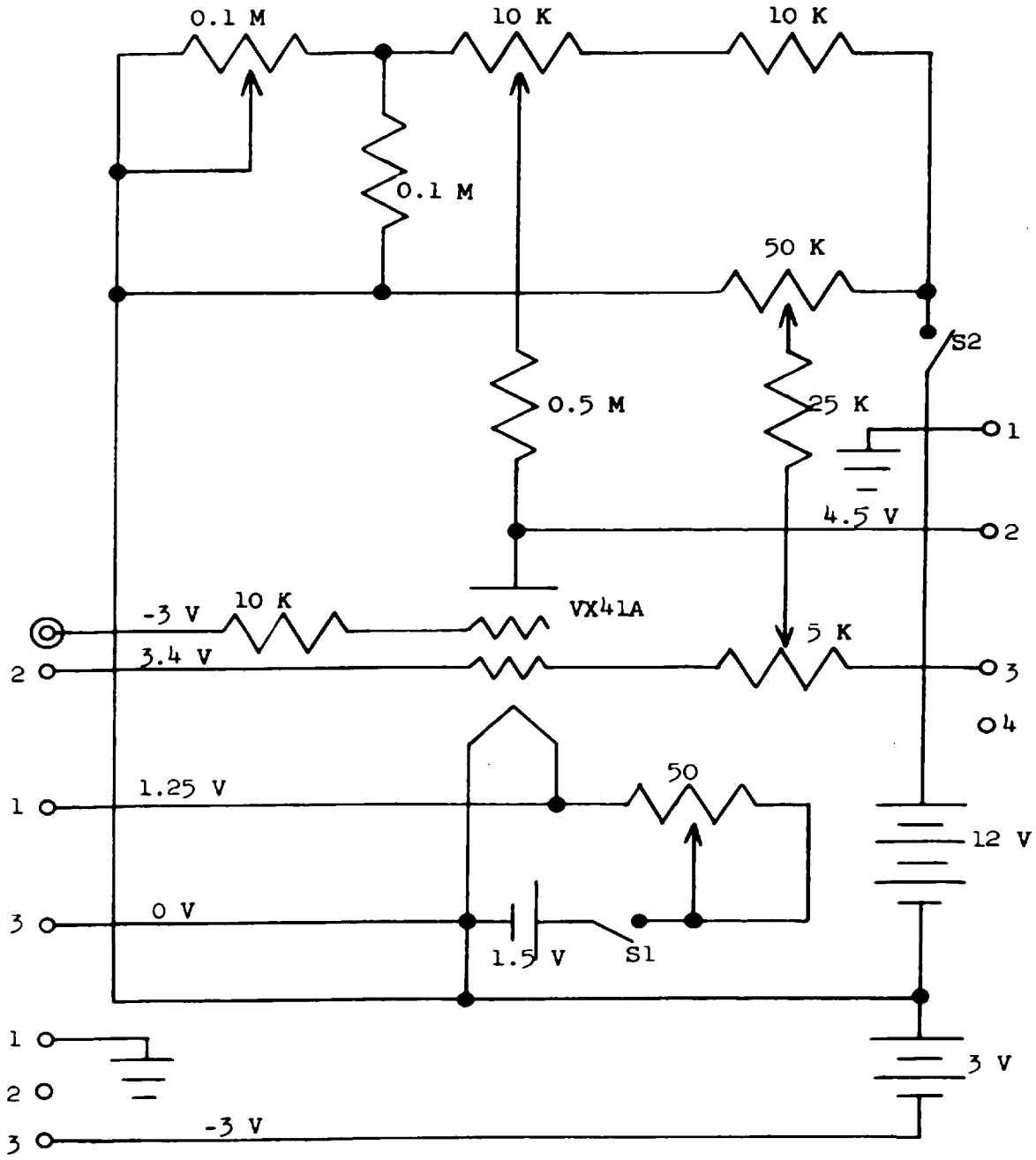


Figure 9. Circuit Diagram of Electrometer Detector

the tube ends, the potential will be zero. In this case the current which flows through the external circuit is equal to the streaming current.

When the streaming potential of more concentrated solutions is measured, this current must also be small, but for another reason. Silver-silver chloride electrodes are said to be reversible, or nonpolarizing, electrodes because the potential between the metallic silver of the electrode and a solution containing chloride ions remains more or less constant. This constancy is due to the fact that each layer of material has a common ion with its adjacent layer (the chloride ion for the solution and the solid silver chloride, the silver ion for the silver chloride and the metallic silver) which can be interchanged without appreciable change in the overall voltage, provided only very small currents flow between the layers.

However, if an appreciable current flows between a solution and an electrode, the potential between the center of the electrode and the solution changes in some haphazard way. The process of polarization is not completely understood, but the elimination of as much current as possible through the electrode is certainly a stabilizing factor for the potential between the solution and the electrode.

This stability is more necessary for the measurement of the streaming potential of concentrated solutions than for that of dilute solutions because the streaming potential is much smaller for the concentrated solutions and because electrodes polarize more readily in more concentrated solutions.

Both the quadrant electrometer and the modern vacuum-tube electrometer amplifier, such as Leeds and Northrup Thermionic Amplifier No. 7673, have an adequate input impedance. However, they are essentially direct-current

instruments without the frequency response which was desired for this study. Much correspondence and many inquiries failed to reveal any commercial instruments which met both requirements, high-input impedance and adequate frequency response.

After an industrial electronic concern failed to develop a suitable instrument, the electrometer detector, whose circuit diagram is Figure 9, was designed and constructed. It was based on the input circuit for a direct-current amplifier designed by Weller (65) for use in measuring atomic radiation. The electrometer detector is essentially a current amplifier, or an impedance matcher, since there is a voltage attenuation of approximately 10 percent.

Since a Victoreen electrometer subminiature tetrode VX-41A has essentially the same characteristics as the more expensive electrometer tubes, it was used. Its cost is $12.50, in contrast, for example, with the $75.00 for a G.E. "Pliotron" tube, FP-54. The operating conditions selected, along with some of its characteristics, for the VX-41A are as follows:

Filament Voltage	1.25 volts
Plate Voltage*	4.5 volts
Space Charge Grid Voltage*	3.4 volts
Control Grid Voltage*	-3.0 volts
Control Grid Current	3×10^{-15} amp
Filament Current	10 ma
Total Cathode Current	250 microamps
Plate Current	12 microamps

*Referred to the minus side of the filament, which may be considered the cathode connection.

The input signal to the electrometer detector is placed between the control grid and the cathode; therefore, it is essentially a change in the control grid bias voltage. The control grid bias voltage in an electrometer tube determines how much of the cathode emission will flow to the plate and how much will flow to the space charge grid.

The output of the electrometer is between a direct connection to the plate and a connection to a fractional part of the space charge grid resistor. This fractional part of the 5000-ohm potentiometer, which is connected directly to the space charge grid, is so adjusted that, with zero input signal, the potential difference across the fractional part is 1.1 volts. This voltage difference makes both output connections 4.5 volts above the minus side of the filament, or the voltage difference between the output connections zero.

One of the assumptions in the design of this circuit is that the drift of the electrometer tube is principally due to a change in cathode emission. Drift may be defined as the change of output voltage without a change in the input voltage. Also, it is assumed that the portion of any change in cathode emission flowing to the grid, or to the plate, will be proportional to the current which was flowing to the grid, or to the plate, before the change occurred.

Therefore, the plate load resistor, 0.5 megohm, and the part of the space charge resistor, the 25,000-ohm resistor, which is not directly connected to the grid were so selected that any change in cathode emission would produce an equal potential change at each output connection. Obviously, this result is idealized and will never quite be reached in practice

since changes of the plate voltage and space charge grid voltage will probably cause a proration of the cathode emission between the grid and plate which is different from that which existed before the cathode emission changed.

In the construction of the detector, potentiometers were used in place of fixed resistors to allow for changes in battery voltages, for differences in tube characteristics, and for convenience of circuit control. The 25,000-ohm space charge grid resistor was connected to the center tap of a 5000-ohm potentiometer, making it possible to adjust the resistance so that a 1.1-volt drop occurred between the space charge grid and the output connection for zero input signal without changing the resistance across which the changes of output voltage occur.

The plate voltage supply has both a coarse adjustment, the 0.1-megohm potentiometer, and a fine adjustment, the 10,000-ohm potentiometer. The voltage supply for the space charge grid is adjusted by a 50,000-ohm potentiometer. A 50-ohm potentiometer is used to adjust the filament voltage supply.

The 10,000-ohm resistance in the control grid is simply a protective precaution against excessive grid currents in case a positive bias voltage should accidentally occur. Switches are provided in the filament and plate voltage circuits, but the bias battery for the control grid is connected at all times, since no appreciable power is drawn from it.

The circuit was built on the front panel of a 5 x 6 x 9-inch chassis. Bare wire connections, IRC WW-4, 1% resistors, and Ohmite AB potentiometers were used in the construction. The tube is held in place

by its leads; no socket is used. The control grid bias battery is a Burgess F2BP, 3-volt "A" battery; the filament supply is two Burgess 2FBP, 1-1/2-volt "A" batteries connected in parallel; and the plate voltage supply is three Burgess F4BP, 4-volt batteries connected in series.

The control grid is connected to the panel with an Amphenol 75-PC1M, single-contact, chassis mount in which the original spacer had been replaced by a teflon one in order to increase the resistance between the center contact and the grounded mount. The panel outlet for the minus side of the control grid bias is through an Amphenol 91-PC3F, three-contact, chassis receptacle, one of the other contacts of which is the common ground.

The electrometer output is connected through an Amphenol 91-PC4F, four-contact, chassis receptable, of whose other contacts one is the common ground and one is not connected. The contacts of another Amphenol 91-PC3F, three-contact, chassis receptable on the panel are connected to the opposite sides of the filament and to the space charge grid so that their voltages can be measured when the circuit is in operation.

The concensus of opinion is that the control of an electrometer tube should be connected as directly as possible to one of the electrodes. In particular, switches should be eliminated if possible. The basis for this opinion is the identical reason for using an electrometer with its high-input impedance in the first place.

For an accurate direct measurement of the streaming potential, the resistance of the solution between the electrodes must be small when compared to any other electrical path between the electrodes. An indirect measurement of the streaming potential can be obtained by measuring a known

part, or all, of the streaming current. This measurement can be accomplished by shunting, or shorting, the electrodes with known resistances.

However, for this electrometer detector, it became necessary to devise a method for checking the drift of the circuit. Also, it seemed expedient to have some switching device so that known resistors can be placed between the electrodes in parallel with the resistance of the solution. By measuring the potential generated by the flowing liquid with and without a known resistance across the tube, the resistance of the solution can be evaluated.

Perhaps it would be best to have all the circuits between the lead from the electrode and the control grid of the electrometer in the same chassis. However, for this study each component was constructed in a separate chassis, necessitating modification of the usual cable and its connectors. Belden 8401, single-conductor, polyethylene-insulated, copper-shielded cable was used to connect the various components between the left electrode and the control grid. After the shielding had been removed from about an inch of the polyethylene surface at the end of a cable, the surface was cleaned with methyl alcohol and, after drying, coated with Dow Corning liquid silicone before the end was soldered to the receptacle contact. Amphenol series 75, pressure-type, single-contact, female receptacles and chassis mounts were modified by replacing the original spacer with a teflon one to increase the impedance between the contact and ground.

(3) Sanborn Amplifier and Recorder: Since the electrometer detector output has a relatively low impedance, about 0.5 megohm, several of the commercial amplifiers or voltmeters could have been used to amplify and record

its output. The "Twin-Viso" Recorder manufactured by the Sanborn Company, Cambridge, Massachusetts, was selected because it would meet the requirements of this study and could also be used for other experiments in the Physiology Laboratory. At the time of purchase, it was hoped that the pressure difference could be recorded on one channel while the streaming potential was being recorded simultaneously on the other. Technical difficulties in connecting the pressure outlets of the electrode chambers to the Sanborn Electromanometer Bridge through a high-electrical-impedance path were never successfully overcome, however.

Only minor modifications of the amplifiers were necessary to record the streaming potential. The circuit of the amplifier case was modified by cutting the output leads from channel "A" of the direct-current preamplifier to the input of channel "A" of the direct-current amplifier. A four-wire cable was used to connect these cut leads to a switch box mounted on the bottom of the amplifier case. Connections were then made to a triple-throw double-pole switch so that the output of channel "A" of the direct-current preamplifier could be (a) fed in its original path to the input of channel "A" of the direct-current amplifier; (b) left open; or (c) fed to a receptacle on the panel of the switch box, from whence it could be fed by cable to any point. During these experiments, the switch was at the "c" position, and the output of channel "A" of the direct-current preamplifier was fed to the input of channel "B" of the direct-current preamplifier by a connecting cable.

Shielding of perforated aluminum sheets was placed over the exposed sides of the direct-current preamplifier and the initial stage of

channel "B" of the direct-current amplifier.

The 60-cycle 110-volt power supply for the amplifiers was separated from that of the recorder and lead to an external receptacle on the amplifier case. This separation became necessary because the University power was very unstable and because the capacity of the Sola constant-voltage regulator, which was available, was not sufficient (500 watts) to operate both the amplifier and the recorder and, at the same time, regulate the voltage properly.

To reduce the 60-cycle vibrations of the galvanometers, 0.05-microfarad condensers were placed across the output of channel "B" of the direct-current preamplifier and across the output of the first stage of channel "B" of the direct-current amplifier. The condensers reduced the overall frequency response of the amplifying system, but were a necessity since this 60-cycle vibration was thought to be the cause of one galvanometer becoming inoperative.

The output of the amplifying system is recorded on a tape 5 cm wide. The speed of this tape can be varied, by the change of gear combinations, from 0.5 mm/sec to 100 mm/sec. The maximum sensitivity of the amplifying system is such that a deflection of about 4 cm is equivalent to an input voltage to the electrometer detector of 1 mv, making it possible to read 0.1 mv with comparative ease and to approximate even lower units of voltage.

The system can be attenuated in approximate steps of 1, 4, 20, 100, 400, or 1000-fold. Therefore, it is possible to observe streaming potentials as large as 1 volt on the tape. However, no numerical

measurements of the streaming potential were read at the higher attenuations because the accuracy of the measurement is limited by the reading of the tape. The measurements of the data were made by using the amplifying system as a null instrument to detect only the difference between the streaming potential and another known counterpotential, as is usually done in streaming potential measurements.

(4) Shorting Mechanism: The simplest method of detecting the drift of an amplifying system is to compare the output of the system for a period of time for zero signal input. Zero signal input can be easily accomplished by shorting the bias battery to the control grid. In the measurement of the streaming potential, the design is complicated by the fact that it becomes necessary to disconnect one of the leads to the electrodes before the control grid is shorted because a short between the electrodes might cause their polarization.

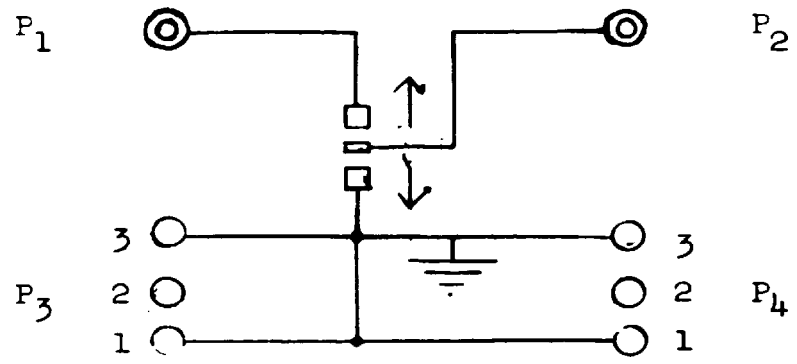


Figure 10. Circuit Diagram of Shorting Mechanism

This disconnection of the electrode prior to shorting the control grid can be accomplished if the control grid can be permitted to "float", i.e., not to be connected electrically, for that moment between disconnection

from the electrode and connection directly to the bias battery. If the control grid of an ordinary electronic tube is disconnected in this way, a considerable time will be required for the tube to regain normal operation after the grid is connected again. Since the current of the control grid of an electrometer tube is so small, it was deemed possible that the voltage of the control grid would not change if it were floated for a very short time because there is such a limited source of energy to activate the change. Since electrometer tubes are not so "mishandled" in the ordinary circuit, no reference could be found to substantiate or contradict this possibility.

A mechanical switching device has to be used because the drift of the first stage must be included in the drift of an entire direct-current amplifying system. Usually, the drift of the first stage is the only drift which appreciably affects the drift of the system, since it is amplified before being added to the drift of the following stages. In this amplifying system the first stage, the electrometer detector, has a voltage amplification of approximately unity; therefore, the drift of the second stage will be of equal importance. But, of course, it is not necessary to discriminate where drift occurs in the system. For accurate measurement, only value needs to be known, or a circuit devised to cancel its effect.

If a voltage of opposite sign, exactly equal to the streaming potential, is applied in series with the streaming potential and the bias battery, the potential at the control grid will be that of the bias battery; i.e., the input signal to the electrometer will be zero. Therefore

a checking device for the drift can also be used to denote when the streaming potential has been exactly annulled by an opposing voltage. The opposing voltage can be from a low-impedance source which can be measured accurately by any precision voltmeter or potentiometer. The opposing voltage becomes a measure of the streaming potential.

Therefore, it is desirable to compare the difference between the streaming potential and the opposing voltage with a zero input at very short intervals, i.e., every few seconds, so that the opposing voltage can be adjusted quickly until the difference is exactly zero.

Since the control grid should be left floating as short a time as possible and since a manually operated switch could probably not be thrown fast enough, a relay-operated single-pole switch as shown in Figure 10 was used. When it was found that the 6-volt direct-current relay did not operate fast enough, its spring was shortened to increase its opening speed and 12 volts were applied to close it at a faster rate. When the relay switch closed, the control grid was shorted to its bias battery.

It was found that the amplifying circuit stabilized immediately when the zero signal, and a zero impedance, was applied to the control grid. Therefore, the period for which the relay was closed could be much shorter (about one-tenth) than that for which it was open. Particularly for the very-high-impedance sources, greater than 1000 megohms, about 5 seconds were required for the amplifying circuit to stabilize each time the relay was opened. This time of instability was proportionally less as the source impedance decreased.

Since it was believed that the flux from the relay was affecting the input signal, the switch and relay were encased in separate shields, and a lucite arm was used to connect the two mechanically. The original insulation which supported the contact points was replaced by teflon to insure a higher impedance between the points and the common ground.

The relay is controlled by a continuously rotating switching device which was driven by a variable-speed electric motor. It is possible to vary the length of the exciting pulse as well as its frequency. The motor was placed at the far end of the room to limit the possibility of its electrical interference with the streaming potential. For convenience of operation, a toggle switch was placed near the shorting mechanism (it is in the small light-colored chassis just to the left of the shorting mechanism in Figure 7) so that the rotating switch could be disconnected and the relay activated by connection to a 6-volt battery so that the input could be left shorted. For example, it was desirable to leave the input shorted any time the shield of the solution system was opened.

(5) Variable-Voltage Supply: As a source for the voltage with which the streaming potential is annulled, a variable-voltage supply was constructed. This supply is essentially a device in which the number and size of the resistances between the inlet and outlet receptacles can be selected by rotary switches. Each of these resistors can have a calibrated 0.1-ma current flowing through it. The direction of this current can be reversed by a toggle switch. In other words, the voltage supply was designed with an impedance of 10,000 ohms/volt.

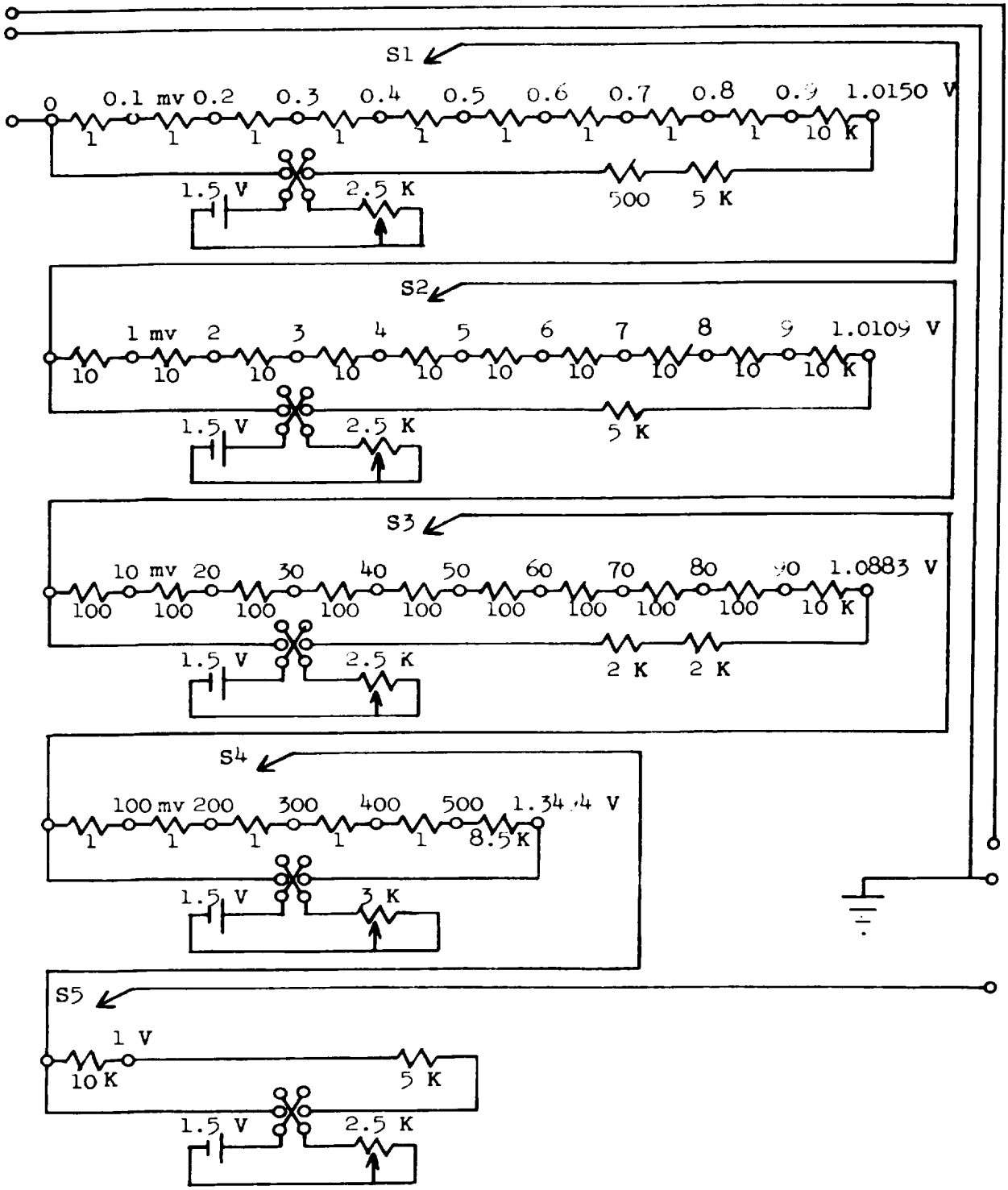


Figure 11. Circuit Diagram of Variable-Voltage Supply

Figure 11 is the circuit diagram for the variable-voltage supply. The five switches, S1 through S5, are Mallory 1211L shorting rotary switches. Each one is connected so that changing the rotary arm to an adjacent position changes the total voltage by one increment for which the circuit of that particular switch was designed. These increments for switches S1 through S5 are 0.1 mv, 1 mv, 10 mv, 100 mv, and 1 volt, respectively.

Consequently, the switch S1 with its 0.1-mv increments has 1-ohm resistors connected between each pair of its first ten positions. A 10,000-ohm resistance was placed between positions 10 and 11, and position 11 is used for calibration of the circuit of switch S1. The other switches were wired in essentially the same way, but with larger resistors between the positions. However, only seven positions of switch S4 with its 100-mv increments and only two positions of S5 were wired, since a sufficient range of voltage was obtained for this study with their being connected in this manner.

The separate voltage supply for each rotary switch was a Burgess 2FBP 1-1/2-volt battery, which was connected in series with a potentiometer to a Switchcraft 3037 double-pole double-throw three-position toggle switch. A potentiometer is used to adjust the current to 0.1 ma for each rotary-switch circuit for any change in battery voltage. The toggle switch is so connected that when it is in its central position the battery is disconnected from the circuit. At its other two positions, the battery is connected, but each position permits a current flow in the opposite direction from that of the other position.

Position 1 of each rotary switch was wired to the rotating contact arm of the switch with the next lowest voltage increments, except position 1

of switch S1, which was connected to a contact on a panel receptacle. The rotating arm of switch S5 was connected to a contact of the other panel receptacle. No matter at which position the rotary switches may be, there is always a continuous electric circuit between position 1 of switch S1 and the rotary arm of switch S5.

Since the current drawn from the variable-voltage supply is equal to the control grid current, less than 10^{-10} amp, of the electrometer tube, the voltage between the receptacles is not appreciably affected when its voltage opposes the streaming potential.

The polarity of the voltage across all the resistors of each rotary switch is controlled as a unit; however, it is not necessary for all the rotary-switch circuits to have the same polarity at the same time. Therefore, for example, +8 mv can be produced by two independent selections. One selection is to turn rotary switch S1 to its position 9 (8 mv) and the toggle switch of its circuit to plus polarity. All the other rotary switches must be at their position 1 or the toggle switches of their circuits must be in their central position; i.e., their batteries must not be connected to the circuits. The second selection is to turn rotary switch S2 to its position 2 (10 mv) with plus polarity and rotary switch S1 to its position 3 (2 mv) with minus polarity.

The variable-voltage supply was originally constructed without this two-selection system; i.e., a maximum of only seven positions of each rotary switch was used. The other positions were added to the circuits with the three lower voltage increments because the pressure difference and, consequently, the streaming potential decreased at a relatively rapid

rate for the larger pressure differences across the tubes with the larger diameters. The added positions expedited adjusting the variable-voltage supply to the amount needed to annul the streaming potential.

The variable-voltage supply was mounted on the 7 x 12-inch front panel of a 6 x 7 x 12-inch aluminum chassis. The potentiometer, which is used to adjust the current through the circuit of a given rotary switch, was placed directly above the control for that rotary switch on the panel. Two Amphenol 91-PC3F three-contact chassis receptacles were used as outlets. One contact of each receptacle was connected to the circuits. The other contacts were connected in pairs between the receptacles. One pair is the common ground, and the other is used in the calibration of the voltage supply. IRC WW-4 1% resistors and Ohmite AB potentiometers were used in the construction of the circuits.

The original electrical insulation of the switches and other components of the variable-voltage supply are satisfactory, since this unit is placed in the system by connecting it directly to the bias battery, through the shorting device. Actually one of the measures taken to minimize the 60-cycle interference was to connect the common ground between the bias battery and the variable-voltage supply, i.e., in the shorting mechanism.

(6) Resistance Box: In accord with the particular principles involved in White, Monaghan, and Urban's (67) method for measurement of solution conductance, in Lauffer and Gortner's (35) method for the measurement of the streaming potential in liquids of very low conductivity, and in one of Neale and Peter's (42) methods for the determination of the streaming

current, the following method is used to evaluate the resistance of the solution between the electrodes.

The streaming potential E_s was measured, and then after a known resistance R_x was connected between the electrodes, the potential E was measured. The difference in these two measurements for the same flow rate will be equal to the product of the resistance of the solution and the difference of the conduction current which flows through the solution during each of the measurements. Since the difference of this conduction current is equal to the quotient of the second measurement of potential E divided by the external resistance R_x, the resistance R of the solution in the tube can be calculated from the simple equation,

$$R = (E_s - E)R_x/E \quad . \tag{38}$$

In order to be able to connect various sizes of resistance between the electrodes, a resistance box was constructed. Figure 12 is its circuit diagram. It consists of three Mallory 172C nonshorting ceramic rotary switches which were mounted on the front panel of a 6 x 6 x 6-inch aluminum chassis. All resistances were connected between the contact positions on the rotary switches and a common point which was connected to the right-electrode circuit through a contact on each of two Amphenol 91-PC3F three-contact chassis receptacles on the panel. These two receptacles had other contacts which were the common ground.

The three rotary arms of the switches were connected to the left-electrode circuit through two Amphenol 75-PC1M single-contact chassis mounts which had the original spacers replaced by teflon ones. The ceramic bases

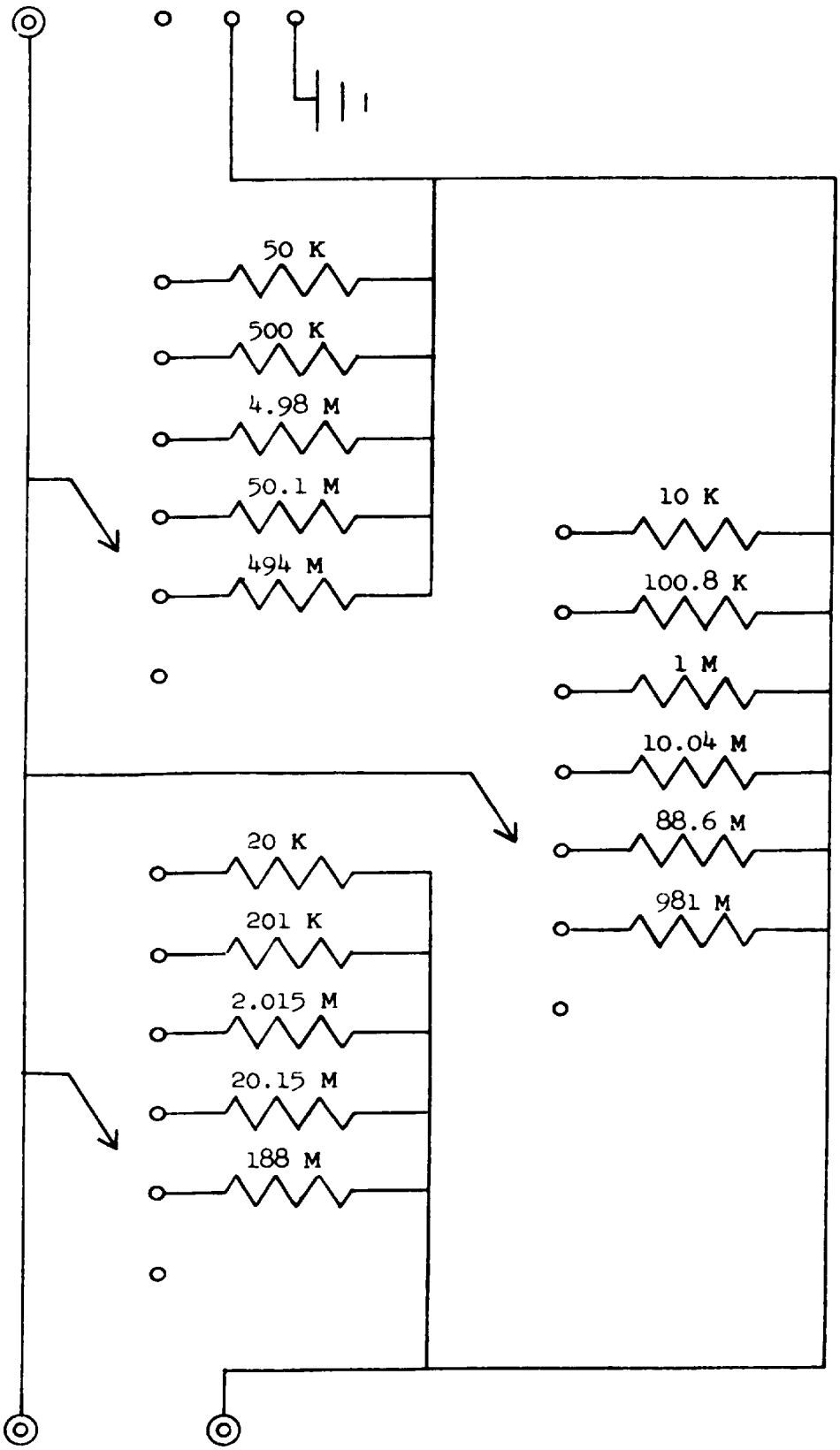


Figure 12. Circuit Diagram of Resistance Box

the switches were cleaned with methyl alcohol to insure maximum resistance between the contact points and the rotating arms, as well as between ground and the rotating arms.

The 981-megohm, the 494-megohm, the 188-megohm, and the 88.6-megohm resistors are Victoreen "Hi-Meg" 1% resistors. The 50.1-megohm, which is two 20-megohm and one 10-megohm resistors connected in series, the 20.15-megohm, and the 10.04-megohm resistors are IRC Type DCH resistors. All the other resistors are IRC WW-4 1% resistors.

When the streaming potential is being measured, each of the rotary switches is at an unconnected position. To place a resistance between the electrodes, a switch is turned to the desired position.

(7) Shielding: The voltage which can be built up across a resistance from electromagnetic propagation is approximately proportional to the size of the resistance. For the more dilute solutions and tubes with smaller diameters, the resistance between the electrodes is quite large, even up to thousands of megohms. Since the 60-cycle power system is the source of this propagation, it is impractical to eliminate the source.

It is necessary to reduce this propagation, however. The potential, and its positive peaks, could conceivably be large enough to drive the control grid of the electrometer tube sufficiently positive from its 3 volts bias to cause the control grid current to increase, i.e., for the grid to pick up electrons within the tube. Since the resistance between the electrodes is effectively a grid leak resistor, this grid current causes a reduction of the grid potential. When the grid current is appreciable as compared to the streaming current, the measurement of the streaming potential is low

if the electrode connected to the control grid, i.e., the left electrode, is positive with respect to the other electrode. Conversely, the measurement is high if the electrode connected to the control grid is negative with respect to the other electrode.

Due to the arbitrary selection of reference points, the minus streaming potentials of the data occurred when the electrode connected to the grid was positive with respect to the other electrode. Since the absolute value of the minus streaming potentials of the data is consistently higher, sometimes several millivolts, than the positive streaming potentials for the same pressure difference, another mechanism than the one described above must be used to explain this inconsistency. If the control grid current is due to the emission of electrons from the grid and is appreciable with respect to the streaming current, this grid current can cause the results observed in the measurements of this study.

However, the effect of the 60-cycle pickup is not limited to the electrometer tube. Since the Sanborn amplifiers are push-pull direct-coupled amplifiers, the effect of driving a grid positive with the peaks of the 60-cycle is to reduce the gain of the amplifying system. Since the amplifying system is used as a null instrument, a loss in gain simply reduces its sensitivity.

Particularly when the instrument was used at full gain, it was necessary to limit the 60-cycle pickup to several tenths of a millivolt. Not only does the 60-cycle interfere with the reading of the tape record, but it was thought to be the cause for one of the recorder galvanometers becoming defective.

To limit the propagation that could get to the amplifying system, the streaming potential tube, the electrode chambers, and stopcock tubes were housed in a box 6 feet long, 12 inches wide, and 14 inches high made of 1/4-inch sheet steel. The front and top panels were hinged to facilitate the handling of the flow apparatus. Openings for the tubes connecting to the solution reservoirs were fitted with 2-inch bore pipes 4 inches long. The box was connected to a common ground at its rear.

Initially both reservoirs were wrapped in several layers of aluminum foil, which was held in place by interconnected copper wires which were also connected to the pipe-fitted openings of the large steel shield. On April 25, 1952, the left reservoir was placed in a steel box 1 x 1 x 3 feet made of 1/4-inch sheets. The front panel was hinged. While this change did not appreciably affect the amount of 60-cycle pickup, the frequency response of the amplifier was increased.

This increase in frequency response is desirable, since a consequent reduction in the time required to adjust the opposing voltage, which annuls the streaming potential, is attained. Since the left reservoir is at the same end of the flow apparatus as the electrode which is connected directly to the control grid of the electrometer, this increase of frequency response is attributed to a decrease in the distributed capacity at that end of the solution system.

When the reservoir was wrapped in aluminum foil, the distance between the solution and the grounded foil was the thickness of the glass. Since the connecting tube out of the top of the reservoir, which was also foil-wrapped, had thinner walls than those of the reservoir, perhaps the

distributed capacity here was controlling. In any case, since the left reservoir has been placed in the steel box, none of its glass is in contact with the shielding. The smallest spacing is at the base of the reservoir, which was placed on a cardboard pad.

The right reservoir was wrapped in aluminum foil, but this foil is apparently adequate shielding, since this end of the solution system is essentially grounded electrically.

Calibration of Equipment

Since the amplifying system is used as a null instrument, the accuracy of the streaming potential measurement is dependent on the sensitivity of the amplifying system and the accuracy of the nulling voltage from the variable-voltage supply. Since the voltage of a battery decreases slowly from use, the variable-voltage supply is calibrated each day the streaming potentials are measured.

The resistors of the resistance box were calibrated just once, but agreement between measurements of the resistance of a solution in a tube by several resistors indicates that these resistors did not change appreciably.

The thermometers were also calibrated just one time; however, the thermocouples were checked from time to time without noting any change.

Variable-Voltage Supply: Each day the variable-voltage supply is used it is calibrated by measuring its output on a Leeds and Northrup Type K Potentiometer. After selecting the standard cell from a group of four which gave the most consistent comparison to the other three over a

period of several weeks, it was used for the Type K potentiometer standardization. Voltages up to 1.5 mv from the Type K were checked on the Brown Electronik Circular Chart Recorder with a push-button calibration using an internal standard cell.

The circuits of each rotary switch of the variable-voltage supply were so designed that each circuit could be calibrated separately. That is, when a rotary switch is turned to its calibration position and only its toggle switch is to an "on" position, the entire output of the voltage supply will come from that circuit. The circuit of rotary switch S1 of Figure 11 (0.1-mv increments) and the circuits of increasing increments were designed to have the following calibration voltages: 1.0009, 1.009, 1.09, 1.35, and 1.00 volts. However, the resistor used in the circuit had a 1 percent tolerance, and some of them varied slightly more than this tolerance from their marked value.

The voltage output of each position of the rotary switches was measured on the Type K potentiometer and, if the voltage was less than 1.5 mv, on the Brown Electronik Circular Chart Recorder. The most accurate outputs for the variable-voltage supply were obtained when the following calibration voltages were used, in the same order as above: 1.0150, 1.0109, 1.0883, 1.3494, and 1.0000 volts.

Resistance Box: The resistors of the resistance box were calibrated by checking them with a Beckman Ultra Ohmeter. The calibrated value is recorded as the R_x of the data. These values are well within the tolerance value specified on the resistors with one exception. The 88.6-megohm resistor is specified to be a 96-megohm resistor with 1 percent tolerance.

Thermometers and Thermocouples: The thermometers and the thermocouples were calibrated against a reference thermometer, Princo 224272, National Bureau of Standards 89808. Since the temperature of the solutions is always essentially room temperature, the thermometers and thermocouples were calibrated in total immersion in a circulating bath whose temperature was controlled by a thermostat to $\pm$ 0.01°C.

The thermocouples were checked periodically by removing the electrode-chamber thermocouple from its well and comparing the reading on the Brown Electronik Circular Chart Recorder with that of the thermometer in the air of the large steel shield.

Procedure

The portion of the procedure which was performed prior to the beginning of taking data on a given tube and solution will be referred to as the experimental preparation. The part of the procedure which is performed on the day on which data are taken will be referred to as experimental operation.

Preparation: The method of cleaning the equipment, particularly the streaming potential tubes, is probably one of the controlling factors in the reproduction of a double layer. While many techniques for cleaning surfaces have been presented, no exact reproduction in streaming potential experiments has been obtained by using any one of them.

Probably the best experimental results that have been reported were obtained when the tubes were cleaned in volatile solutions, such as nitric acid, and then heated to a dull red glow by passing superheated

steam through them. However, even with this method results of a series of experiments varied from 10 to 20 percent.

For this reason and because the larger tubes of this study would have required a large amount of superheated steam, this method was deemed unwarranted and impractical. Also, the seal between the glass tubes and the teflon plugs would have been damaged by removing the plugs each time the tubes were cleaned. If the tubes are heated to a dull red glow, the teflon plugs canot be left on the tubes, since the decomposition temperature of the teflon is about 350°C.

As a container for the cleaning solutions and the tubes, large test tubes were made from 4-cm bore glass tubing. The following process was used to clean the tubes in which the streaming potential was to be measured:

1. A tube was placed in a sulfuric acid-potassium dichromate cleaning solution for a period of at least a day. During this time the solution in the tube was changed several times by raising the tube out of the solution and letting it drain.

2. The tube was then rinsed by flowing tap water through it for several hours.

3. Step No. 1 was then repeated with the test tube filled with Alconox, a detergent consisting primarily of a homogeneous blend of patented hydrocarbon sulphonates (wetting agents) and polyphosphates (sequestering agents), instead of the acid cleaning solution.

4. Step No. 2 was repeated.

5. The tube was stored in a test tube which was filled with distilled water. The distilled water was changed every few days, and the storage period lasted from one week to several months.

To clean the other glassware and teflon components of the solution system, they were soaked overnight in Alconox, rinsed with tap water, and then rinsed with distilled water and drained until dry.

The solutions used in the streaming potential studies are prepared from reagent-grade solutes. Merck sodium chloride, reagent for biological work, and Mallinckrodt potassium chloride, analytical reagent, are used. Distilled water whose specific resistance was greater than 0.5 megohm/cm was obtained from the University Chemical Stores. All the normalities of the solutions are evaluated at 25°C. The solution to be studied is mixed in one of the reservoirs by bubbling nitrogen through it.

The components of the solution system are assembled as described in the Equipment section. The left reservoir and its shield are mounted on a movable platform so that the distance between the reservoirs can be adjusted to compensate for the various tube lengths. For the very short tube, an additional length of Fisher and Porter 1/2-inch bore glass pipe is inserted between two glass-to-glass couplings as shown in Figure 8.

After the solution system is assembled but before the solution is forced through the streaming potential tube, the electronic equipment has to be stabilized. This stabilization is necessary so that the initial measurements of the streaming potential can be made in a matter of minutes after the solution enters the tube. The stabilization of the electronic

equipment is discussed in more detail under operation.

The electrodes, which were stored in a container filled with the solution being studied, are the last component to be placed in the equipment. If they had been placed in the empty electrode chamber for an appreciable time, their drying out would have a marked effect on their polarization. As the solution is forced through the system by nitrogen gas under pressure, all the trapped air is accumulated in the top of the electrode chambers, from which it is released through a stopcock.

The four control valves for the nitrogen are so connected that the nitrogen in either reservoir can be maintained at any pressure between slightly more than atmospheric and slightly less than that of the pressure stabilization tank. The pressure loss due to the flow of nitrogen through the rubber tubing and the control valves makes it impossible to obtain exactly atmospheric pressure or the pressure of the stabilization tank when there is a flow. This loss is, of course, much greater when the liquid flow is through the larger streaming potential tubes.

A separate tap was connected through the reservoir's rubber plugs for the manometers so that the flow rate would have a minimum effect on the accuracy of the pressure difference as recorded in the data.

The purity of the solution is checked by measuring its electrical resistance with a Fisher Conductivity Bridge Model RC-1B. It is impractical to return the sample, which is used to determine the electrical resistance, because of the possibility of contamination. Consequently, since the sample contained about 50 cc, the frequency of checking the resistance of the solution has to be limited. It is checked when a new solution is made and any

time the ratio of the streaming potential to the pressure difference showed a marked decrease.

Operation: The following procedure is carried out to obtain a record of the streaming potential and the pressure difference simultaneously:

1. The input to the electrometer detector is shorted to obtain a zero signal input by flipping the toggle switch in the small chassis just to the left of the shorting mechanism in Figure 7. Then the electrometer detector and Sanborn amplifiers are turned on. During the period required for stabilization (about 1/2 hour) the entire electronic system is balanced several times so that the recorder indicator is maintained in the center of the tape with the system at maximum gain.

2. The thermos is filled with chipped ice and distilled water. The glass tube containing the reference thermocouple is immersed in the ice so that the thermocouple rests about one-third of the depth of ice from the bottom of the thermos.

3. The solution is forced through the streaming potential tube until the thermocouple temperature of the right electrode chamber is within 0.1°C of the temperature of the left reservoir and within 0.5°C of room temperature. Data were not recorded if the temperature changed more than 0.1°C when the flow direction was reversed.

4. After stabilization of the electronic equipment and of the temperature of the solution, and after making certain the leads to the electrodes and the remainder of input circuit to the electrometer detector were properly connected, the front and top panels of the large shield are closed.

5. The electric motor operating the rotating switch which controls the relay of shorting mechanism is turned on, and the toggle switch mentioned in step 1 for the shorting mechanism is flipped from the 6-volt battery connection to the rotating switch and its 12-volt supply.

6. The nitrogen control valves are then adjusted to produce a pressure difference between the reservoirs. A short period of time, which varies with the size of the streaming potential tube and the liquid level of the reservoirs, is required for the nitrogen to flow to and from the reservoirs until it becomes more or less stable. Particularly with the larger tubes, a constant pressure difference cannot be maintained because the pressure stabilization tank is not sufficiently large. Also, with the flow of liquid in a closed system, the change of hydrostatic head between the reservoirs would oppose the flow and would decrease the pressure difference between the reservoirs.

7. The motor driving the Sanborn Recorder is turned on. Then simultaneously the variable-voltage supply is adjusted to keep the recorder arm in the central portion of the tape as the gain of the amplifying equipment is increased. Maximum gain could not always be used because of the oscillations of the streaming potential due to the effects of turbulence. Figure 13 is a photograph of a tape recording.

Data from Figure 13 are recorded in Table 14 (4/21/52). Amplifier system attenuation is x 4; tape speed is 0.5 mm/sec. The short, solid lines represent the time when the relay is closed and the input to the electrometer detector is shorted. Point A: variable-voltage supply set at 283 mv. B: streaming potential equal and opposite to variable-voltage supply, or

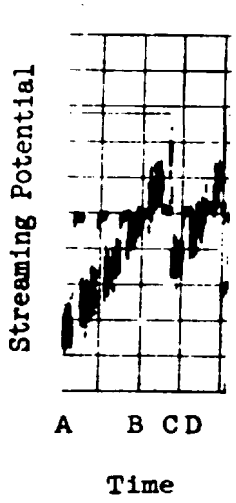


Figure 13. Streaming Potential vs Time
Reading the Tape for Data

the streaming potential is - 283 mv. C: variable-voltage supply reset at 281 mv. D: streaming potential again equal and opposite to variable-voltage supply, or the streaming potential is - 281 mv.

In this particular example, the - 283 mv reading was inadvertently missed; consequently, the recorder was left running so that the - 281 mv reading could be made. The reference point for all streaming potential measurements in the recorded data is the left electrode. Therefore, in this case the potential at the right electrode is 281 mv less than that of the left electrode.

8. At the instant a streaming potential can be read (either point B or point D), the recorder motor is usually snapped off and the liquid level of the right reservoir is read and recorded. This level is read on the solution-level indicator. At point D of the above example this level was 6.48 cm above a fixed reference point. From a previous calibration of the levels of the two reservoirs, the level of the left reservoir can be determined and in this case was 12.88 cm

above the same reference point as that for the right reservoir. Using the left reservoir as the reference point, the hydrostatic difference of the reservoirs is - 6.40 cm H_2O or - 0.47 cm Hg. The left pressure outlet is the reference point for all recorded pressure differences. As soon as possible after the level of the right reservoir is read, the manometer showing the pressure difference of the nitrogen in the two reservoirs is read. In this case the two readings were 80.15 and 26.67 cm Hg, left and right tube of the manometer, respectively. Therefore, the total pressure difference producing the flow was the algebraic sum of difference of pressure of the nitrogen and the difference of the hydrostatic pressure of the reservoirs. For this example, the total reservoir pressure difference was 53.48 - 0.47 = 53.01 cm Hg.

Actually, in recording the data of steps 7 and 8, the level of the right reservoir is recorded first, then the manometer readings, and then the variable-voltage supply, whose dials were designed to read the streaming potential directly. The pressure differences are not usually calculated until a complete series of measurements has been taken.

9. Particularly for the larger tubes and at greater pressure differences, the flow has to be shut off or reversed as soon as the manometer is read to prevent a reservoir from emptying and letting nitrogen reach the streaming potential tube.

10. The temperature of the right electrode chamber is read at any spare moment in the experimental procedure on the dial of the Brown Electronik Circular Chart Recorder. No fixed time was necessary, since the temperature did not change appreciably between runs.

11. For the measurements made when the solution has first entered the tube, the time is also recorded. After the first day, there is no longer the minute-to-minute change in the ratio of the streaming potential to the pressure difference that occurs when the solution first enters the tube. Consequently, the time is not recorded after the first day.

12. In order to evaluate the resistance of the solution in the tube, the potential generated when part of the streaming current is shunted through a fixed resistance R_x is measured. Once the resistor is selected by turning the dial on the resistor box, the procedure for the measurement of the potential and the pressure difference is identical to that of steps 6, 7, 8, 9, and 10.

Accuracy of Measurements

Streaming Potential: The deviation of the streaming potential measurements from their true value is determined by (1) the deviation of the variable-voltage supply, (2) the sensitivity of the amplifying system, which is dependent to some extent on the human limitations in reading the tape record, (3) the changing polarization of the electrodes or the changing of the control grid current of the electrometer detector, and (4) the effect of the oscillations due to turbulent flow and of pulsations due to transient flow. Each of these is discussed in the following paragraphs.

Since the variable-voltage supply is the source of potential to null the streaming potential, any divergence of this source from the actual value of the indicated voltage is reflected directly in the reading of the streaming potential voltage. Since care was taken in the selection of the

standard cells for calibration of the variable-voltage supply, the probable error for the supply will be about one percent, since the resistors used in its construction have a one-percent tolerance.

The sensitivity of the amplifying system for very small signals is about 4 cm/mv. If the tape is read to within 1 mm, the potential should be accurate to within 0.025 mv. For the small tubes and for small laminar flows, the streaming potential could be read within such limits, but this accuracy is not obtained for most readings.

The principal factor in the operation of the electrometer detector which affects the accuracy of the streaming potential measurements is the flow of control grid current. Particularly when the source impedance is very large, the voltage generated by this flow may be appreciable when compared to the streaming potential. Also, the control grid bias battery can be a source of current, which cannot be discriminated from the control grid current, if there is an appreciable leakage resistance between the control grid and the cathode of the electrometer tube. Since the source impedance does not change for any given solution and tube, the voltage due to these currents can be assumed fixed with regard to both intensity and polarity.

The polarization voltage of the electrodes is also fixed both as to intensity and as to polarity if there is no appreciable current flow through the electrodes and if they have reached equilibrium with the solution.

Consequently, the error due to the performance of the electrometer tube and the polarization of the electrodes can be evaluated, since it is

added to the streaming potential when the streaming potential has one polarity and is subtracted when the polarity of the streaming potential is reversed by reversing the direction of liquid flow. Or it may be evaluated by determining the voltage required to null the input for zero flow.

Therefore, after the streaming potential measurement for laminar flow is corrected for asymmetry of the detecting mechanisms, it should be accurate within one percent, or $\pm$ 0.1 mv, whichever is greater.

However, in the turbulent and transient regions, the streaming potential pulsates with the oscillations of the pressure difference. The recorded measurements for these regions of flow which are found in the appendix are for the potential which was visually determined to be the center of the pulsation of the writing arm of the recorder. Since for turbulent flow the oscillation has an amplitude of approximately 1 mv when the streaming potential was 100 mv, no appreciable error occurs in its reading. For the transient region, however, the amplitude of the pulsation of the streaming potential may be several millivolts when the average streaming potential is also several millivolts.

Besides just the visual selection of the center of the oscillation, the reading of an average streaming potential in the transient region is further complicated by the fact that particularly near the laminar end of the region the streaming potential appears to have a steady value with intermittent pulsations to a higher value, as seen in Figure 14. These pulsations are in contrast to the oscillations of the streaming potential for turbulent flow, which appear to be evenly distributed, above and below some average value. Because of these complications, very few readings were actually made

in the transient region. The curves through this region are principally extrapolations from the laminar and turbulent regions.

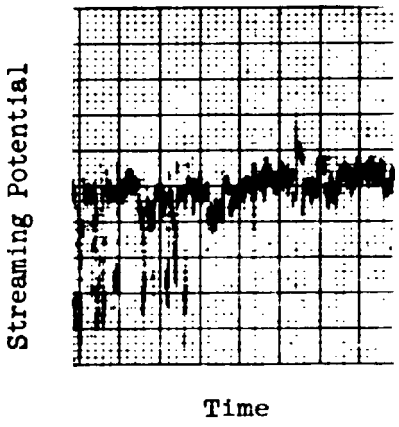


Figure 14. Streaming Potential vs Time.
Change from Transient to Laminar Flow.

Pressure Difference: The pressure differences recorded in the data are between the reservoirs, except as noted for tube 7. These pressure differences are the algebraic sum of the difference due to the liquid levels of the reservoirs and the difference of the reservoir gas pressures as read on a manometer.

For the small-bore tubes, the pressure difference, even at maximum flow rates, had steady values. That is, it required several minutes to detect a slight change even in the liquid level in the reservoirs. Therefore, for these tubes the probable error of the pressure difference is simply the error in reading the liquid level of the reservoirs and the manometer. The liquid level could probably be read within 0.5 mm and the manometer within 0.3 mm. If the reservoir gas pressure difference was less than 7.0 cm Hg, a water manometer was used to measure it. Therefore, for the higher pressure differences, the maximum probable

error for the small-bore tubes is of the order of 0.03 cm Hg and for the lower pressure differences (less than 7.0 cm Hg) the probable error is of the order of 0.006 cm Hg. For the lowest pressures (less than 1.2 cm Hg) the total pressure difference is the difference in the levels of the solution reservoirs, so the probable error is reduced to less than 0.004 cm Hg.

For the larger tubes, particularly at maximum flow rates, the accuracy of the pressure difference was completely dependent on the speed with which it could be read. The reading of the liquid level of the reservoir was probably always within 2 cm and the manometer within 2 mm. Therefore, the maximum probable error for the reservoir pressure difference for the large-bore tubes is about 0.30 cm Hg. Two men took the pressure readings at the higher flow rates in the larger tubes, but the determination of the exact time that the writing arm of the recorder would indicate a nulled streaming potential depended on a visual interpretation, and hence an experimental error is introduced into the readings which cannot be evaluated.

Also, the pressure differences between the taps of tube 7 are read for the entire range of reservoir pressure differences. In order for the streaming potential measurements between the taps to be accurate, the holes had to be very small; they were 1-mm bore. The manometers were sufficiently large, 1-cm bore, to prevent errors due to capillary rise. Since the pressure difference is steadily decreasing during the reading, a small flow of solution takes place through the 1-mm hole. The sum of the pressure differences along tube 7 for any reservoir pressure difference was about 10 percent less than the reservoir pressure; therefore, the technique of measurement is not satisfactory.

However, the pressure differences between the taps are recorded, since they indicate an order of magnitude of the pressure gradient along the tube.

Resistance of Solution: As shown in Analysis 3 of the appendix, the measurement of the potential generated by the flow of a solution through a tube both with and without a known resistor connected between the electrodes permits the determination of the macroscopic resistance between the electrodes. This macroscopic resistance or its reciprocal value, conductance, will include the electroosmotic countereffect and the surface conductance in the exact relation in which they affect the streaming current.

The accuracy of this measurement is dependent on (1) the tolerance of the resistor which is placed between the electrodes and (2) the accuracy of the potential and pressure-difference measurements.

The resistors of the resistor box are resistors with a 1-percent tolerance. Their calibration is included under Calibration of Equipment. The accuracy with which the potential can be measured is identical to that which has been discussed in the preceding section on the streaming potential.

For the determination of the resistance of the solution in the tube, the flow rate should theoretically be identical for all potential measurements. However, the pressure difference is used in this study as a basis for extrapolating the potential measurements to the same flow rate. The accuracy of this method depends on the accuracy with which the pressure differences are measured, which has been discussed in the preceding section.

The specific resistance of the solutions is measured with an Industrial Instruments Conductivity Bridge, Model RC-1B. The accuracy of this instrument is several percent. The human limitations of reading an electric eye are the controlling factor.

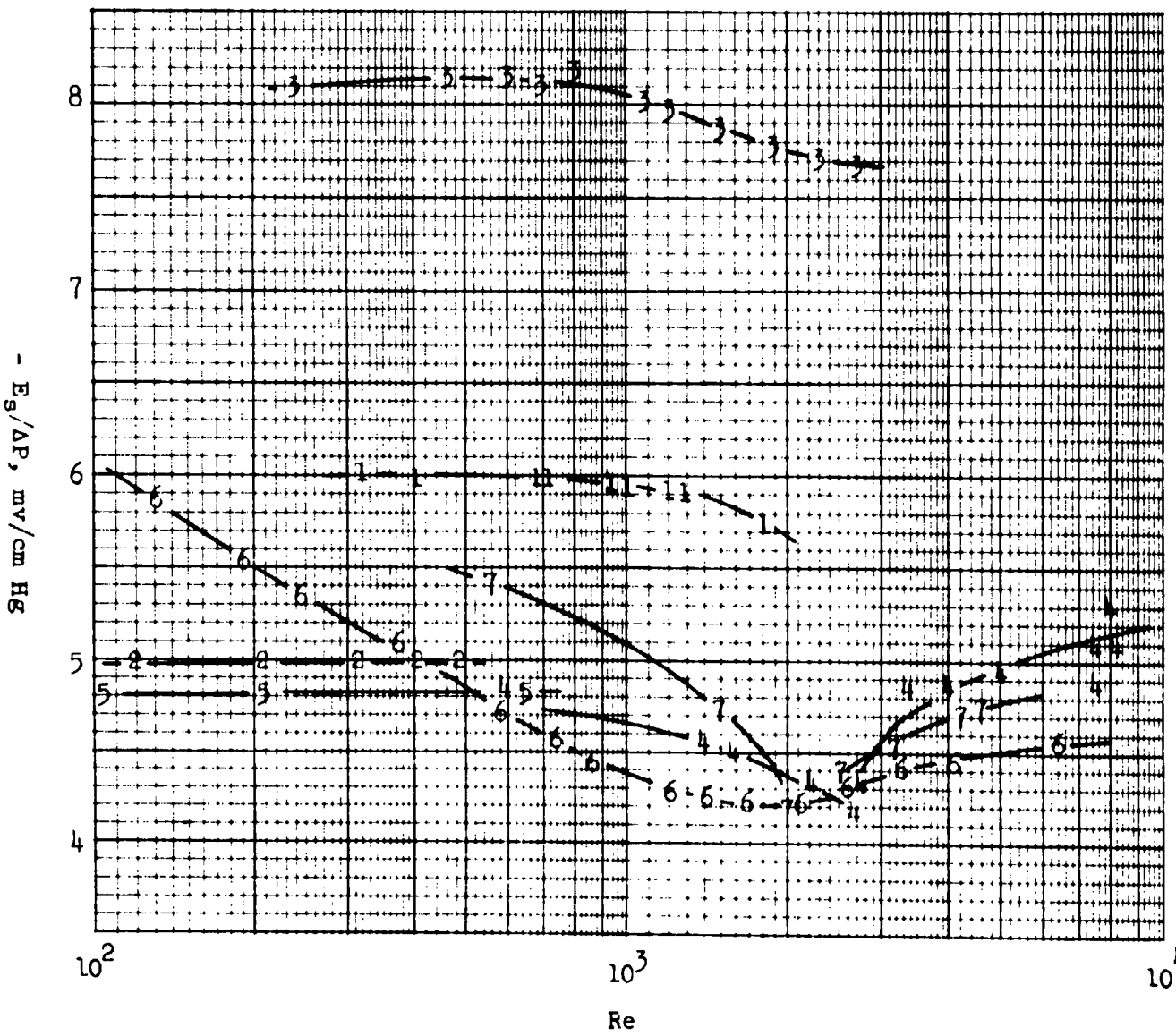
Temperature: The accuracy of the temperature measurements is dependent on the reading of thermometers which are divided into 0.1°C increments. Therefore, the temperatures should be accurate to within $\pm$ 0.1°C.

RESULTS AND DISCUSSION

All the experimental data which was recorded during this study is tabulated in the Appendix. In this section samples of the data are presented in graphs which illustrate the effect of the flow rate, the diameter, and the length of the tube on the streaming potential. Other pertinent points are discussed in their relation to each particular graph.

Effect of the Flow Rate on the Ratio of the Streaming Potential to the Pressure Difference Measured between Points in Front of the Entrance and beyond the Exit of the Tube.

As demonstrated in Figure 15, the ratio of the streaming potential to the pressure difference producing the flow is not always constant, even in the laminar region. For every tube in which the flow rates are such that the flow approached or passed through the transient region, i.e., for Reynolds numbers of approximately 2000, the ratio of the streaming potential to the total pressure difference producing the flow always decreases to a minimum value in this transient region. Tubes 2 and 5 have small diameters, 0.475 and 0.31 mm respectively. Because of these small diameters and because of limiting factors of the equipment, such as the size of the manometers, sufficiently high flow rates are not attained in these tubes to reach the transient region.



SOURCE OF DATA

Streaming Potential:

1. Table 2 (3/23/52)
2. Table 10 (4/7/52)
3. Table 12 (10/20/50)
4. Table 14 (4/14/52)
5. Table 15 (5/9/52)
6. Table 16 (4/29/52)
7. Table 17 (5/20/52)

Flow:

1. Table 23
2. Table 24
3. Table 25
4. Table 26
5. Table 27
6. Table 28
7. Table 29

Figure 15. Ratio of Streaming Potential to Pressure Difference Measured between Points in Front of Tube Entrance and Beyond Exit vs Reynolds Number

The Reynolds numbers of Figure 15 and subsequent figures are obtained from the extrapolations of curves of the pressure difference vs the Reynolds numbers on log-log paper. The points on these curves are calculated from the flow data of Tables 23-29.

For the Helmholtz-Smoluchowski streaming potential equation to be valid, the ratio of the streaming potential to the pressure difference must be equal for all flow rates. Following Helmholtz' concept, the equation is valid if the flow rate is sufficiently small so that the entrance conditions do not appreciably affect the overall flow through the tube. The entrance conditions have a greater effect at the higher flow rates. Consequently, there must be some maximum flow rate at which the equation is still valid and which cannot be exceeded.

From Figure 15 the Reynolds number at which the Helmholtz-Smoluchowski streaming potential equation looses validity can be approximated only for tubes 1 and 3.

The results obtained for tubes 2 and 5 show that the highest flow rate studied is smaller than the one for which the Helmholtz-Smolowchowski equation is no longer valid. Tubes 4, 5 and 7 are studied at flow rates so high that the results cannot be applied directly to the Helmholtz-Smoluchowski equation.

The results from tube 6 are particularly interesting in that the usually accepted criterion for the validity of the Helmholtz-Smoluchowski equation is that the Reynolds number be less than 2000, or that the flow is laminar. However, in this case it is evident

that even a Reynolds number of 100 exceeds the limits of applicability in this tube.

An attempt to establish a dimensionless empirical criterion based on the flow rate and the dimensions of the tube proved unsuccessful. However, as shown in Figure 16 some relation is apparent when the diameter of the tube is plotted on log-log paper against the ratio of the maximum Reynolds number, (for which the Helmholtz-Smoluchowski equation is valid) to the length of the tube.

Also plotted are some points from the data of Jones and Wood (34) and of Bishop, Urban, and White (4). If we assume the relation between the coordinates of this graph is a straight line, the equation for the value of the maximum Reynolds number Re for which the Helmholtz-Smoluchowski equation is valid becomes,

$$Re = CL/D^n \qquad (39)$$

where C is a constant; L, the length of the tube, and n, the power to which the diameter D must be raised. To satisfy the points on Figure 16, n must have a value between two and four.

Since the deviation of the Bishop, Urban and White (4) point (for their 0.125 mm-bore tube) is very great, the value of n should probably be about two. If n is placed equal to two and if the length and diameter are expressed cm, the relation becomes

$$Re = 0.065\ L/D^2. \qquad (40)$$

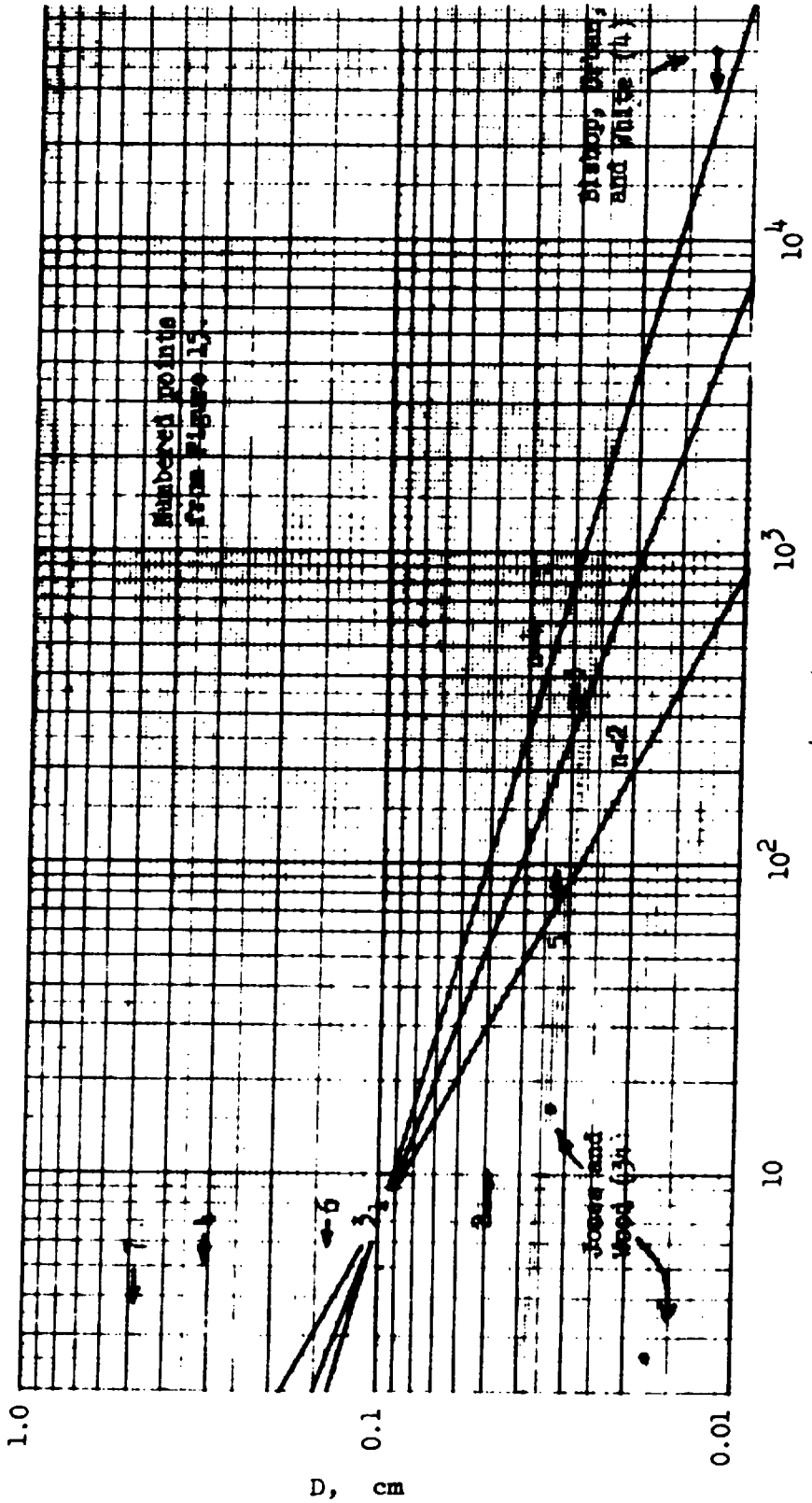


Figure 16. Tube Diameter vs Ratio of Maximum Valid Reynolds Number for Helmholtz-Smoluchowski Streaming Potential Equation to Tube Length

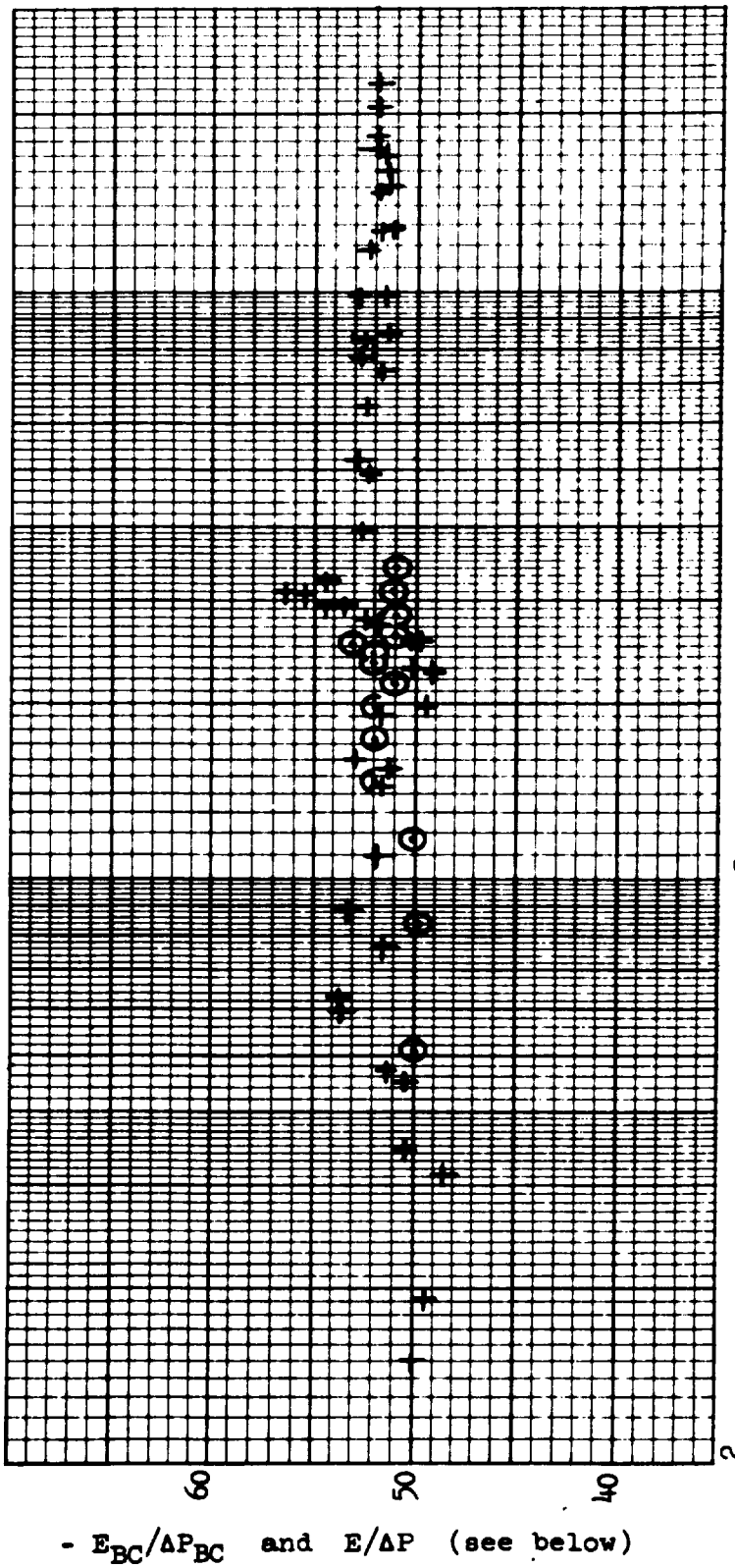
It should be noted that only two points, which are very close to one another, fit this equation. Furthermore, the equation (if valid at all) is probably limited to a laminar flow since all the points of Figure 16 are for a laminar flow.

Theoretically, if a tube is sufficiently long with respect to its diameter so that the entrance and exit losses are negligible with respect to the total flow losses, there is no limit to the type of flow or to the flow rate for which the Helmholtz-Smoluchowski equation is valid. Limits must be placed for actual apparatus since it has finite dimensions.

Effect of an Established Flow on the Ratio of the Streaming Potential to the Pressure Difference

In one of the experiments of this study, the streaming potential and pressure difference is measured between taps along tube 7. Taps were so located that these measurements can be made across the center third of the tube length. The ratios of these measurements are plotted on Figure 17 as a function of the Reynolds number.

While it cannot be verified that the flow is completely established through this section of tube length, particularly for the higher laminar and the transient flow rates, the deviation from an established flow should not be very great. The greater deviations occur very near the tube entrance, and the deviations diminish as the distance from the entrance is increased.



Source of Data: + $E_{BC}/\Delta P_{BC}$, mv/cm Hg, Table 19 (6/10/52), Table 20 (5/23/52); Flow Rate, Table 29

⊙ scale units · 10/cm Hg, Reichardt (48).

Figure 17. Ratio of Streaming Potential to Pressure Difference for an Established Flow vs Reynolds Number

The streaming potential E_{BC} and the pressure difference ΔP_{BC} could not be measured simultaneously because of apparatus limitations, but each is measured for various reservoir pressure differences as recorded in Tables 19 and 20. To obtain the ratio $E_{BC}/\Delta P_{BC}$, the ratio of the streaming potential E_{BC} to the reservoir pressure difference from Table 19 is divided by the ratio of the pressure difference ΔP_{BC} to the reservoir pressure. Since the two measurements are not recorded for exactly the same reservoir pressure differences, the ratio of the pressure difference ΔP_{BC} to the reservoir pressure difference is taken from a smooth curve through the more-or-less scattered points of a graph from Table 20.

The ratio of the streaming potential to the pressure difference can be read as 52.5 ± 4 mv/cm Hg for all flow rates of Figure 17. The spread of the points is attributed to experimental error, which is discussed under Accuracy of Measurements. As the flow rate decreases, the proportion of the experimental error to the measured quantities increases.

These results confirm the findings of Reichardt (48) (whose data is also plotted on Figure 17) that the condition for the flow for which the Helmholtz-Smoluchowski streaming potential equation is valid is not that the flow be laminar, but that the flow must be established.

Laminar Film in Turbulent Flow

In 1949 Miller (40) wrote, "It seems that the presence of the viscous film on the wall of a pipe through which fluid is flowing turbulently is still to be demonstrated by actual velocity measurements. The

difficulty of making such measurement is not to be minimized." Miller's requirement for positive proof of the existance of a laminar film is probably more exacting than is usually demanded. No one has successfully shown that a laminar film does not exist during turbulent flow, but on the other hand, most velocity measurements and theoretical analyses only point to the existance of a laminar film.

Reichardt apparently accepted the concept of the laminar film without needing further proof. In his 1935 article (48), he simply stated that if all flow rates are established the ratio of the streaming potential to the pressure difference is independent of the flow rate because of the existence of the laminar film for any type of flow. From his discussion, it becomes apparent that he believed that the existance of the laminar film for turbulent flow has been adequately confirmed by other investigators. In a 1940 article, Reichardt (49) does not refer to his 1935 article and Miller (see above) maintained the 1940 article is ambiguous.

Furthermore, the findings of this study are in complete agreement with those of Reichardt as shown in Figure 17. Since the ratio of the streaming potential to the pressure difference is independent of the flow rate as long as the flow is established, the same mechanism of flow must take place near the wall for either a laminar or turbulent flow. That is to say, surely a laminar film exists for a laminar flow; consequently, a laminar film must exist for a turbulent flow.

Effect of Expansion and Contraction Losses on Ratio of The Streaming Potential to the Pressure Difference

An attempt is made to correct the ratio of the streaming potential to the pressure difference when each is measured between points in front of

the entrance and beyond the exit of the tube. Possibly by subtracting all the pressure losses not directly related to the flow along the tube wall from the total pressure loss, a correct empirical pressure loss would result which could be used to give the same ratio for all flow rates.

Deciding just what constitutes the pressure losses not directly related to the flow at the wall is a complex problem because of the nonestablished flow near the entrance of the tube. In this treatment both experimentally measured pressure losses at the tube entrance and pressure losses based on the kinetic energy of the average velocity are subtracted from the total pressure.

As a generalized rule, the expansion loss at the exit of a tube is considered to be equal to the change in kinetic energy as the liquid leaves the tube. Consequently, there is no appreciable drop of pressure at the exit.

However, at the entrance of the tube, the shape of the entrance, the type of flow, i.e., laminar, transient, or turbulent, as well as the change in kinetic energy affect the loss due to the contraction of cross-section area. For a sharp-cornered entrance, the contraction loss is generally assumed to be about 0.5 of the change in kinetic energy, but the 0.5 coefficient is probably correct only for flow rates well into the turbulent region.

For tubes 1 - 6, it is not possible to measure the various pressure differences between points along the tubes. However, tube 7 is tapped at seven different points so that both the streaming potential

and pressure-difference gradients can be evaluated along the tube. Tap H is a one-mm hole centered only 0.35 cm from the end I of tube 7. This distance (less than the 0.49-cm diameter of the tube) is so short that the pressure loss due to the flow along it may be neglected if compared to the other pressure losses between I and H when end I is the entrance of the tube. Actually, the tap I is 5 cm from the end of the tube in the wall of the enlarged section sealed to the end of the tube. The pressure loss due to the flow along the 5 cm of the enlarged section is also negligible when compared to other losses. ΔP_{IH} represents the pressure losses due to the contraction of the cross-sectional area and due to the increase in the kinetic energy.

A jet concentrating the flow of liquid near the axis is inherent for a sharp-cornered entrance. Particularly for a laminar flow, this jet is very pronounced. When end I is the entrance of the tube, the kinetic energy of the flow at tap H may well be greater than at any other point in the tube. The reason for this greater kinetic energy is that the velocity distribution to be expected at this point is nonuniform to a greater degree than at any other point.

Presumably, the formation of such a jet, as well as a nonestablished flow for an entrance distance, is not as pronounced for turbulent flow as for laminar flow. For a turbulent flow the kinetic energy at tap H is probably very nearly the kinetic energy of that in the tube at the exit A. In this case, the pressure loss due to an increase in kinetic energy between taps I and H will be approximately equal to the loss of energy at the exit due to expansion. Consequently, the total pressure loss between taps I and

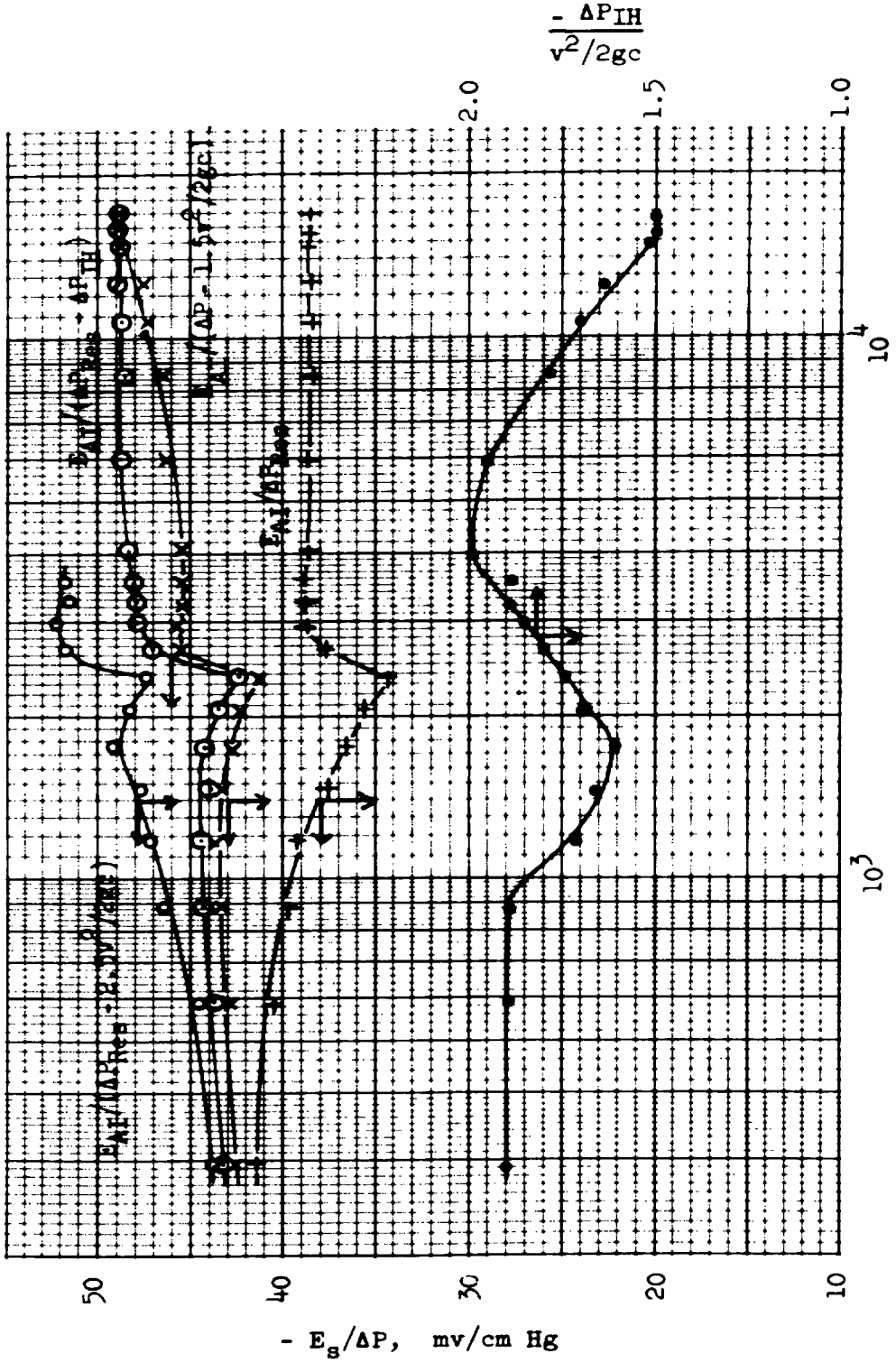
H represents the expansion and the contraction losses for turbulent flow to a more exact degree than for laminar flow.

The ratio of the streaming potential to the pressure difference across the entire tube is plotted against the flow rate on Figure 18 both before and after attempted corrections. The ratios are evaluated when ΔP_{IH} and the pressure differences (calculated from 1.5 and 2.5 times the kinetic energy of the average velocity) are subtracted from the total pressure. ΔP_{IH} is also included as a ratio to the kinetic energy of the average velocity.

Before subtraction of any pressure loss, the ratio of the streaming potential to the pressure difference has a maximum value at the lowest Reynolds number. After subtraction, the maximum value for the three cases treated occurs at the highest Reynolds number.

The ratio of the streaming potential to the pressure difference is relatively constant for turbulent flow before any pressure difference is subtracted, but this constant value is less than that for the lowest laminar flows. This smaller value indicates that it should be corrected. When ΔP_{IH} is subtracted from the total pressure difference, a relatively constant ratio results. Perhaps, this value is the correct one to use in the Helmholtz-Smoluchowski streaming potential equation.

In this case, a means is presented for using the streaming potential measurements for turbulent flow in the evaluation of zeta-potentials from the Helmholtz-Smoluchowski equation. Furthermore, if this case is correct, it confirms the belief that a turbulent flow becomes established almost at the entrance of the tube.



Source of Data: Table 30

Figure 18. Attempted Corrections for Ratio of the Streaming Potential to the Pressure Difference for Various Flow Rates

In addition, if this case is correct, the ratio of the streaming potential to the pressure difference across the tube for flows smaller than those studied here (approaching zero) must be equal to this corrected ratio of the turbulent region. The smaller flow rates show an increase of the ratio of the streaming potential to the pressure difference across the tube with decreasing flow. At the smallest flow rate (for a Reynolds number of 290) the ratio is only 41.4 mv/cm Hg. An extrapolation of the curve for smaller flow rates until the ratio is 49.0 mv/cm Hg (the corrected ratio of the turbulent region) appears possible from the data. However, in this case the pertinent curve of Figure 18 should probably have a greater slope for the lower Reynolds number than is shown. Consequently, the ratio at the Reynolds number of 1180 is probably too great because of experimental error and should be ignored.

The solution for subtracting a portion of the total pressure difference for a laminar flow is not simple. If the 49.0 mv/cm Hg is the correct ratio for an established flow, it would appear that 2.5 times the kinetic energy of the average velocity is the proper correction for a Reynolds number of 1800. For all flows with smaller Reynolds numbers, the correction would have to be greater than 2.5 times the kinetic energy of the average velocity, if the correction is a function of this kinetic energy.

The Streaming Potential Gradients of Tube 7

In Figure 19a, the streaming potential gradient determined between the various taps of tube 7 is presented as a function of the axial distance from end A of the tube. Since the spacing between taps

E, F, G, and H is only 1.50 cm and that between H and end I of the tube is only 0.35 cm, the scale for axial distance of Figure 19a is greater for that end than for the remainder of the tube. The streaming potential gradients are plotted on a log scale so that a wider range of flow rates can then be compared.

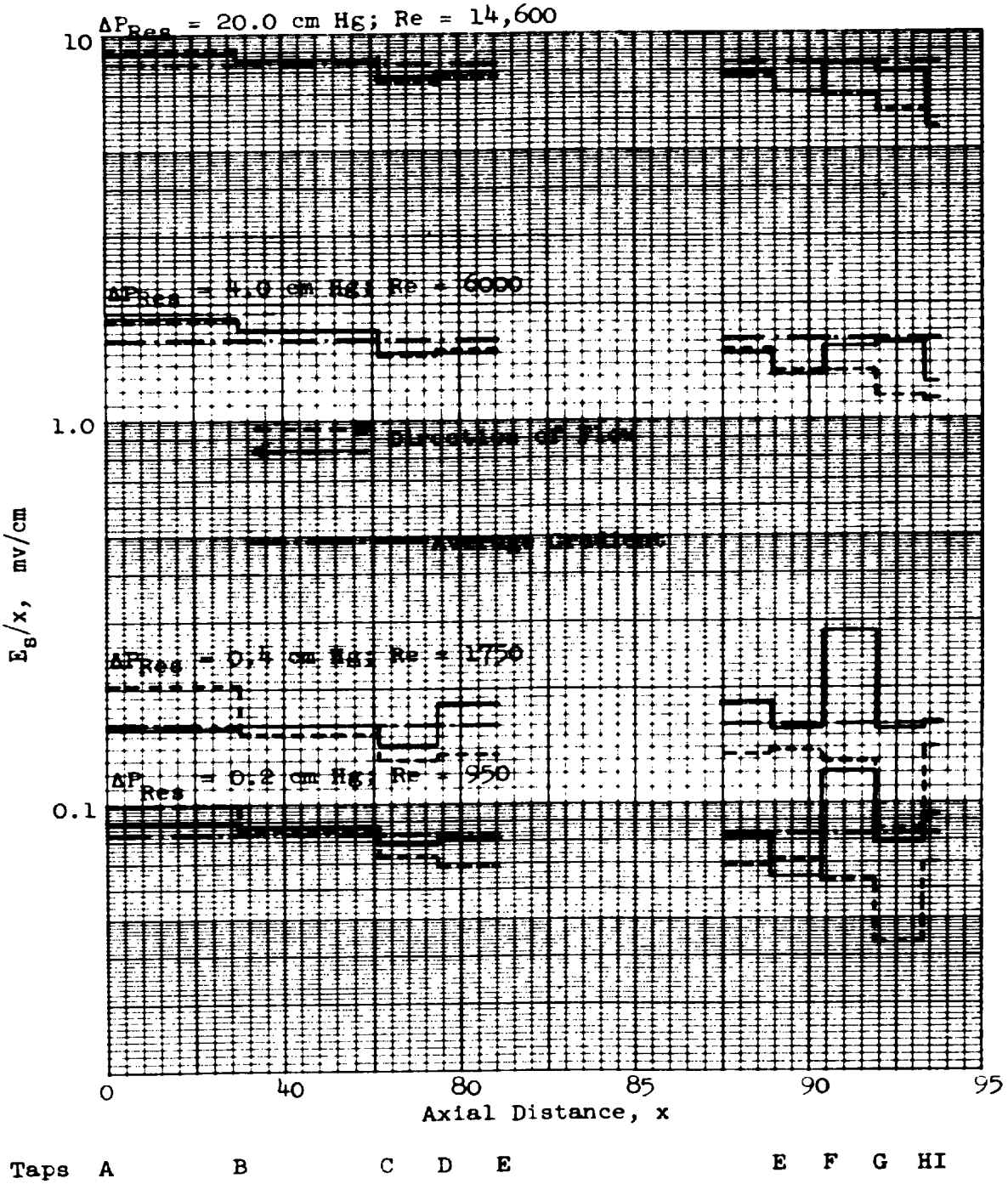
In order to interprete Figure 19a in its relation to fluid flow, equation (34), which relates the velocity gradient at the wall to the streaming potential gradient, should be reexamined. For the streaming potential

$$(du/dr)_a = -(E_s/x)\, a(k + 2k_s/a)/2\sigma_s \delta \qquad (34)$$

to be directly proportional to the velocity gradient, the other factors of the right side of equation (34) must be constant.

From previous studies, it has been found that regardless of how dilute the solution may be the surface conductance is negligible when compared to the total conductance if the radius of the tube is greater than several tenths of a millimeter. Since the radius of tube 7 is about 2.45 mm, the surface conductance will not appreciably affect the total conductance of the solution. Also, since the solution flowed back and forth through the system many times, it is well mixed. Therefore, the conductance should have no effect on changing the proportionality of the streaming potential gradient and the velocity gradient at the wall for different portions of the length of the tube.

Tube 7 is an extruded plastic tube. Its radius is not constant, and its cross section is not exactly circular. However, only the radius



Source of Data: Tables 1 and 19

Figure 19a. Streaming Potential Gradient between Points along the Length of Tube 7 for Four Flow Rates

near the ends of the tube could be directly measured without destruction of the tube. End I is only about one percent smaller than end A, and the deviation from circularity is about one percent near the ends. A mean diameter, which is in close agreement with measured diameter at the ends of the tube is evaluated from measurements of measuring the flow rates and of the pressure difference. The usual trial-and-error method, involving a Moody friction factor graph and allowance for entrance and exit losses based on the kinetic energy of the average velocity, is used. This mean diameter is needed for the evaluation of the Reynolds numbers which are used in the figures of this section.

As can be observed on Figure 19a, a comparison of the streaming potential gradients for both directions of flow (the dashed line indicates flow from end A to I and the solid line, flow from end I to A) to the average streaming potential gradient (the dash-dot-dash line) for any of the flow rates shows that the streaming potential gradients have a marked decrease from end A to end I. This deviation along the tube is much greater than the expected effect due to variation of the radius alone. In fact, this deviation is opposite to that expected from the measurement of the tube radius near its ends. Therefore, the cause of the decreasing streaming potential gradient from end A to end I must be attributed to the variation in the surplus charge density σ_s and the thickness δ of the double layer.

There have been some investigators of electrokinetics who consider that the thickness of the double layer is essentially the same between any solid-liquid interfaces. For example, Smoluchowski (59)

maintained that the thickness of the double layer can be evaluated by comparing the results of electrokinetic experiments in which there is quartz-nitrobenzene interface with those in which quartz solid and a good-conducting aqueous salt solution are used.

Considering the fact that the thickness of the double layer is defined as the distance from the tube wall to the electrical center of gravity of displaceable surplus charge (see equation (7) of analysis 2 of the Appendix), the thickness of the double layer must be some function of the quantity of displaceable charge. In all probability, the surplus charge density varies more percentagewise than does the thickness of the double layer, but, at least with our present knowledge, they cannot be separated into independent functions.

Then, both the surplus charge density and the thickness of the double layer are some function of the quantity of charge adsorbed immovably on the tube wall. As has been discussed in more detail above, the quantity of the adsorbed charge is greatly affected by the previous history of the surface. Therefore, the results, as presented in Figure 19a, indicate that the previous history of the entire surface was not the same and that the distribution of adsorbed charge is not homogeneous over the entire surface in the study of tube 7.

Notwithstanding the fact that the failure to obtain a homogeneous distribution of charge will prevent an exact analysis of Figure 19a, unique and interesting interpretations of the velocity gradient near the wall can be postulated from it.

To compensate for the effect of the day-to-day change in the quantity of adsorbed charge on the wall, the streaming potential E_{AI} (across the entire length of the tube) is measured each day that the streaming potential is measured between any of the taps. For standardization a reservoir pressure difference of 4.0 cm Hg was arbitrarily selected. The streaming potential E_{AI} at this pressure difference of the sixth day after the solution first entered the tube was also choosen. Then to correct a streaming potential for change of adsorbed charge, the streaming potential is multiplied by the ratio of this sixth-day streaming potential E_{AI} to the streaming potential E_{AI} which is measured on the same day as the corrected streaming potential and which is measured at the standard 4-cm Hg pressure difference. The accuracy of this correction is dependent on the assumption that the adsorbed charge of some particular section of the tube changes in the same way that the total adsorbed charge changes.

Because the sum of the pressure difference between the taps of tube 7 is about 10 percent less than the overall pressure difference, the validity of the procedure used for these measurements can be questioned. However, they can be used to determine the order of magnitude of the pressure gradient between the taps of tube 7.

The streaming potential gradients for equal flows in opposite directions deviate less from one another for a turbulent flow than for a laminar flow. This deviation is especially evident at the ends of the tube. Therefore, it can be said that the velocity distribution is less affected by entrance conditions in turbulent flow than in laminar flow.

The data for each interval of axial length was recorded on the same day; therefore, the most accurate interpretations of Figure 19a will result from the comparison of the streaming potential gradients between two taps at different flow rates and for flow in opposing directions. The magnitude of the gradients between taps H and I must be ignored since the experimental error is large compared to the measured streaming potential. However, the polarity of the streaming potential is important as will be shown in subsequent paragraphs so this gradient is included on Figure 19a.

The velocity gradient at the wall is shown to be greater for an entrance flow than for an exit flow for seven of the eight end conditions presented. End A for a Reynolds number of 6000 does show a greater velocity gradient for the exit condition than for the entrance flow, but this deviation is very small.

As has been found in previous studies of entrance flows, a sharp-cornered entrance causes a jet of fast moving liquid to form at the core of the liquid very near the entrance. The concentration of the liquid at the axis is due to the converging flow of the liquid just outside the entrance. When the velocity of the jet reaches a maximum, the kinetic energy of the flow in the cross section at this point is greater than the kinetic energy at any other cross section of the tube.

As a liquid flows through a tube, any velocity distribution will tend to be transformed into that velocity distribution which requires the least motivation energy for that flow rate. The ultimate distribution of velocity which can be attained in a tube is an established flow, which occurs when the shearing stress is proportional to the radial distance.

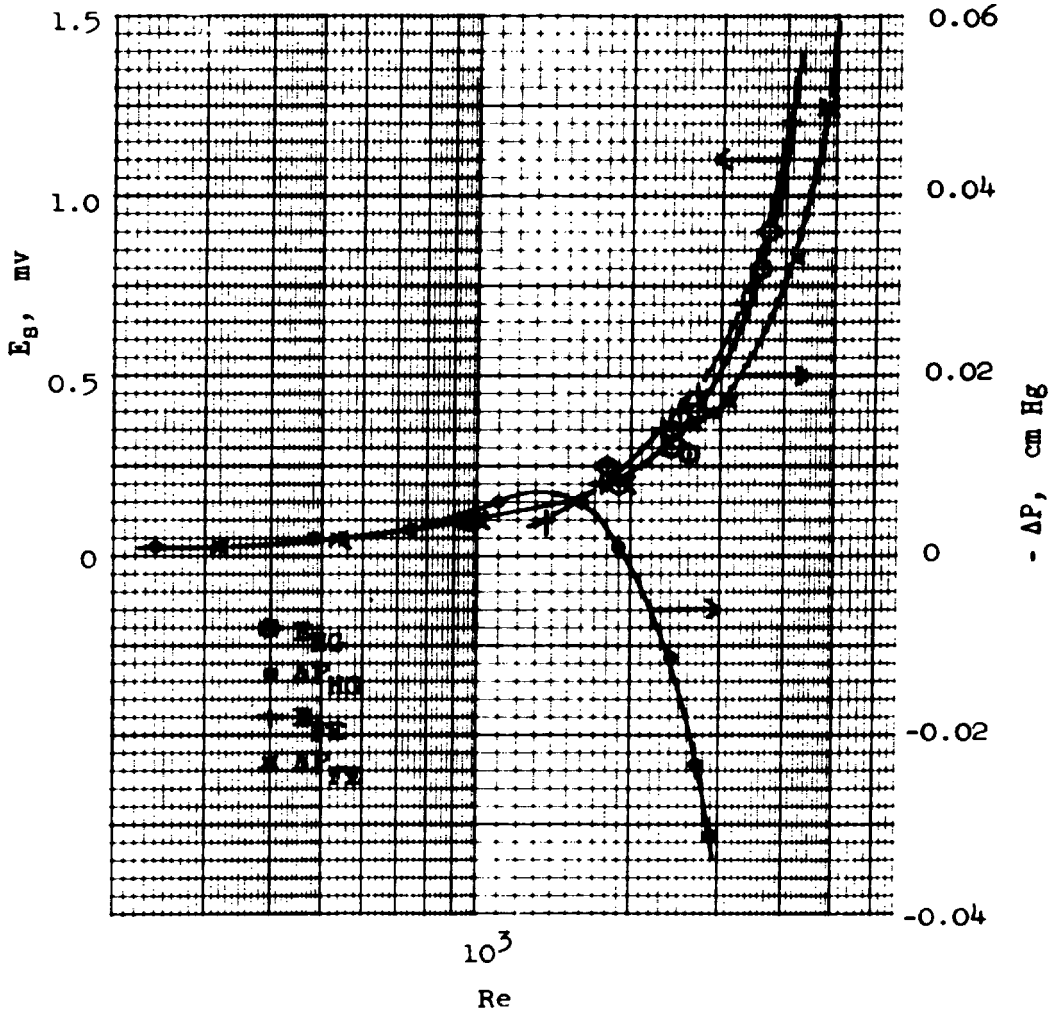
The loss of energy for an established flow is certainly less than for the flow along an entrance length.

For this reason, the jet formed near the entrance will spread to be transformed into a more efficient type of flow.

As the jet forms, there is a greater pressure gradient along the tube axis than for an established flow since the increasing kinetic energy, as well as the loss due to the irreversibilities of the change in kinetic energy, reduces the pressure. This reduction in pressure may be thought of as additional losses to that which is due to irreversibilities of the viscous and inertial forces which are related to any flow.

At least two types of forces combine to cause the jet to spread. (1) The increasing pressure gradient tends to accelerate all the laminae which have a velocity less than they would have for an established flow with the same pressure gradient, and (2) The exchange of energy by the shearing stress will slow the laminae of the jet and increase the velocity of the adjacent laminae.

The jet spreads very quickly and the decrease of kinetic energy tends to cause a pressure increase. Of course, there are losses of energy from the irreversibilities due to the decrease in kinetic energy and due to the flow itself. As seen in Figure 19b, if an appropriate interval of tube length is selected near the entrance of the tube, the decrease in pressure due to this type of energy loss may be smaller than the increase in pressure due to the loss of kinetic energy of the jet. Consequently, for the interval from H to G, when the flow is from H to G, the recorded pressure at G exceeds that at H for flow rates with a Reynolds number in



Source of Data: Tables 19, 20, and 29

Figure 19b. Streaming Potential and Pressure Difference between Taps F and E and between Taps H and G of Tube 7 vs Reynolds Number

excess of 2000. Streaming potential measurements between taps H and G are also presented as a function of the Reynolds number on Figure 19b.

For purposes of comparison, the same measurements for the same conditions are arbitrarily selected between taps E and F for Figure 19b. The spacing between taps E and F is 1.5 cm, which is identical to the spacing between taps G and H.

It should be noted that the quantities presented on Figure 19b have the usual reference point for a fluid flow. For example, the streaming potential is E_{HG}, since the flow is from H to G. This reference point is different from that of the data in the appendix, where G is always the reference point between taps G and H regardless of the direction of flow. Consequently, on Figure 19b a pressure difference of -0.02 cm Hg at a Reynolds number of 2600 for $-\Delta P_{HG}$ indicates that there is a pressure increase from H to G.

For the smallest flow rates, $-\Delta P_{HG}$ increases with increasing flow until a Reynolds number of about 1400 is reached. Then it decreases with increasing flow. As shown on Figure 19b, it is zero for a Reynolds number of about 2000. For all flows with a Reynolds number greater than 2000 which were studied here, the pressure increases from H to G for a flow from H to G. This pressure increase continues at about the rate shown in Figure 19b for increasing flow, until a Reynolds number of about 4500 is reached. Near this flow reproducible pressure differences are not obtained. For all the higher rates of flow, the pressure increase continues, but at a much slower rate.

Therefore, if the pressure difference alone controlled the direction and rate of flow near the wall, the streaming potential gradient between taps H and G for a flow from H to G should have a sign opposite to the streaming potential gradient in the remainder of the tube when the Reynolds number is greater than 2000. However, there are viscous forces due to movement of the liquid in the center of the tube which tend to pull the liquid near the wall in the direction in which the liquid in the center is moving.

All the streaming potential gradients for all intervals of axial distance and at all flow rates studied have the same sign; e.g., note that E_{HG} and E_{FE} have the same polarity on Figure 19b. Therefore, the average velocity near the wall for all intervals is in the direction of flow of the center liquid. Since the velocity is in the direction of the center flow, the viscous forces pulling the liquid near the wall must be greater than the forces near the wall due to the pressure gradient between taps H and G for a flow from H to G which has a Reynolds number greater than 2000. Since the average velocity near the wall and the velocity in the center of the tube have the same direction, any backflow from eddy currents must be limited to a small segment of the intervals between the taps.

The streaming potentials and the pressure differences between E and F when end I is the tube entrance have the same signs as those measurements between the ends of the tube for a flow with end I as the entrance. The conditions between E and F will be discussed further in subsequent paragraphs.

The streaming potential gradient from H to G for all flow rates presented in Figure 19a is slightly less than the average streaming potential

gradient for the entire tube. However, the streaming potential gradient from G to H (with the flow in the opposite direction or when end I is the exit) is smaller than that for any other interval in either direction of flow. This decrease cannot be readily explained as a function of the flow, since the flow is presumably not greatly affected by the conditions at points ahead of a flow.

If it can be assumed that the laminae near the tube axis are accelerated as they approach the exit of a tube because the resistance of the flow just outside the tube is much less than inside the tube, then the laminae near the wall must be decelerated, since the volume rate of flow is constant. This deceleration near the wall could be an explanation for the large decrease in the streaming potential gradient between G and H when end I is the exit of the tube.

However, this explanation appears inadequate in that the decrease is so large. Consequently, at least part of the decrease for the streaming potential gradient between G and H for both directions of flow is probably due to a decrease in the displaceable surplus charge density.

It should be mentioned that because of the reference points which have been selected the ratio of the streaming potential to the pressure difference has a negative value for the tubes and solutions in this study when the values across the entire tube are considered. However, for an entrance flow from H to G and for Reynolds numbers over 2000, this ratio decreases from positive infinity to positive finite numbers.

Proceeding to the next interval of axial length FG, one notes that the streaming potential gradient is much greater for the entrance flow than

for the exit flow. Even without accounting for the apparent decrease in the displaceable surplus charge density, the streaming potential gradient from G to F for laminar flow is the largest in the tube.

To conform with these results, one must assume that when the jet spreads the velocity of the laminae near the wall increases to a value greater than that further down the tube where the flow is more nearly that of an established flow. Also, it is true that the pressure gradient from G to F for an entrance flow is found to be greater than the pressure gradient at any other place in the tube. However, the streaming potential gradient is proportionally less than the pressure gradient when each is compared to that in the remainder of the tube.

In fact, the proportion is so much less that the ratio of the streaming potential to the pressure difference for an entrance flow from G to F has a value about one-half this ratio for the flow in the center of the tube.

Perhaps the decrease in the streaming potential gradient from F to E when end I is the entrance can best be explained by reconsidering the forces at the entrance of the tube. The converging forces at the entrance cause the liquid to be concentrated at the tube axis to form the jet discussed above. Perhaps this jet is broken up by the converging liquid rebounding toward the tube wall to increase the velocity near the wall, and hence the increasing streaming potential gradient between G and F. Conceivably, the liquid could rebound from the wall to decrease the velocity near the wall, as is reflected in the decreasing streaming potential gradient betweeen F and E.

This rebounding motion could continue with diminishing intensity for the entire length of the tube. And perhaps the increase in streaming

potential gradient from E to D at a Reynolds number of 1750 can be explained by a rebound toward the wall. The entire entrance effect should penetrate further into the tube for the higher laminar flow, since it has been found to be so for a tube with a trumpet-shaped entrance.

The axial distance between B and C is approximately the center third of the entire length. However, it is not exactly centered and perhaps it is far enough off center so that the rebounding motion of the liquid can be the cause of the streaming potential gradients' not being identical for the flow in opposite directions, particularly for the higher laminar flow rates.

The decreasing streaming potential gradients when end I is the exit have been discussed above. If there is a decrease of the velocity gradient at the wall as the flow approaches the exit, this decrease cannot be detected from the results when end A is the exit for turbulent flow. When the streaming potential gradients of the interval AB are compared to those of BC, the increase in the gradient due to the displaceable charge density (which apparently increases from end I to end A) must be considered. This increase is superimposed on any decrease of the gradient between the intervals which may be due to the flow near the exit.

For an exit flow at end A, there is a small decrease in the streaming potential gradient between intervals AB and BC for a Reynolds number of 1750. Furthermore, the increase of the gradient between the same intervals for a Reynolds number of 950 is proportionally smaller than the increase for the same value for turbulent flow.

The comparison of this small decrease and this smaller increase of the laminar flow rates with the larger increase for turbulent flow

indicates that near the exit there is a decrease in the velocity near the wall for a laminar flow and that this decrease is greater for the higher laminar rates.

Shearing Stress along Tube 7

The streaming potential is a surface phenomenon. Consequently, only the relation of change of the velocity gradient at the wall, equation (34), and the shearing stress at the wall τ_a, equation (36), can be evaluated between points along the tube from streaming potential measurements. If the tube is long enough so that the flow in one particular region is established, the shearing stress at the wall can be evaluated as a close approximation along the entire tube from streaming potential measurements.

The shearing stress at the wall for an established flow is equal to one-half the product of the pressure gradient and the radius of the tube. Then the shearing stress at the wall for any other section of the tube is evaluated by multiplying the shearing stress at the wall for the established flow by the ratio of the streaming potential gradient for the particular section to the streaming potential gradient for established flow.

Since the shearing stress is proportional to the energy loss of the flowing solution, the shearing stress in the interior of the solution can be approximated from the pressure loss. The fact that the velocity is maximum at the axis, zero at the wall, and some continuous function of the radial distance of the tube aids in this approximation. Therefore, Figure 20, which is a plot of the shearing stress vs the radial distance, is accurate only at the axis of the tube and at the wall. Even the accuracy at the wall can be questioned , since it is evaluated from the streaming potential

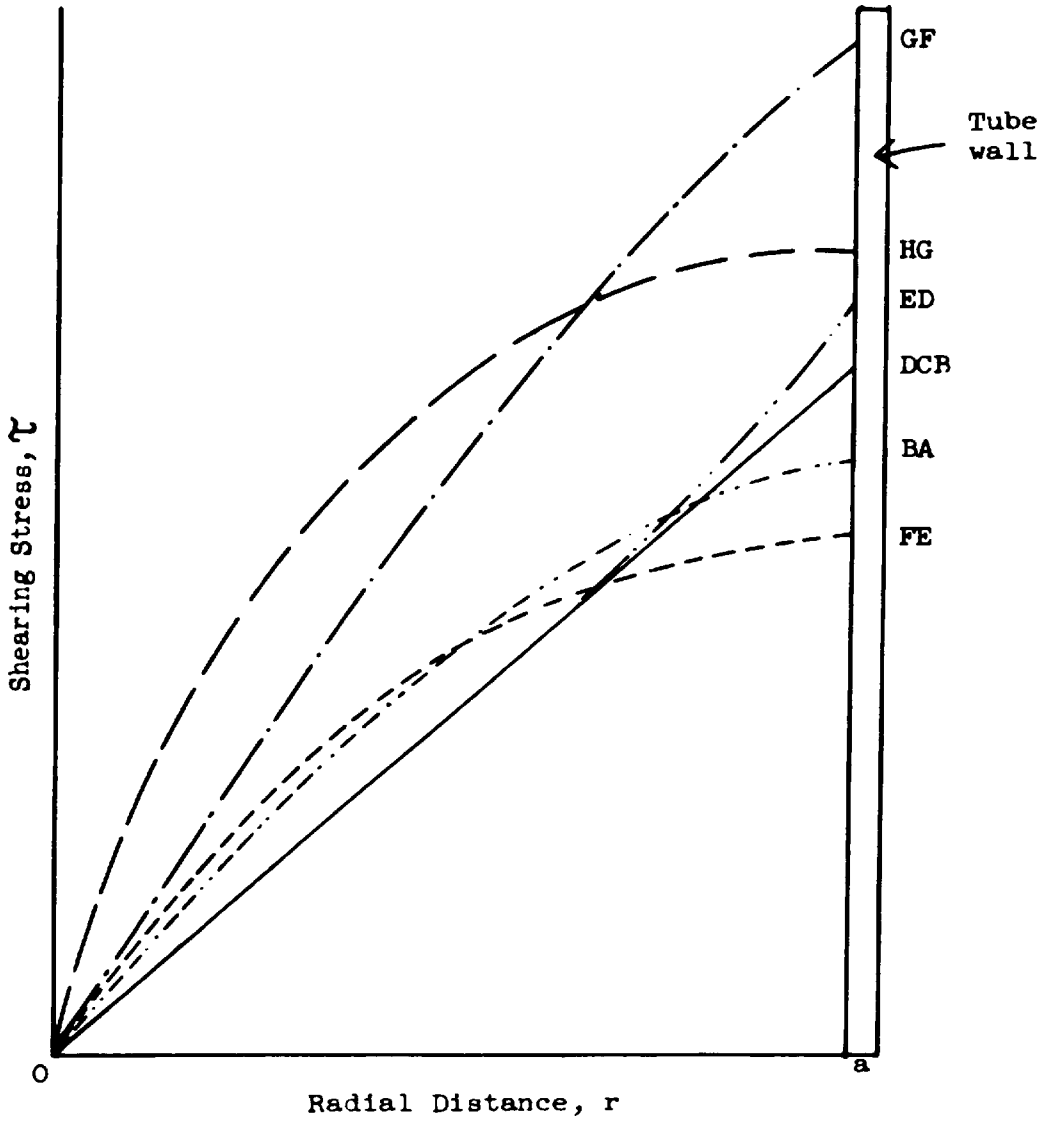


Figure 20. Hypothetical Shearing Stress vs Radial Distance for Entrance Flow at End I of Tube 7 for a Reynolds Number of 950.

gradients which are subject to the deviations discussed under the streaming potential gradients of tube 7.

Use of Streaming Potential in Evaluating the Boundary Conditions

As discussed in the two preceding sections, a method for determining the velocity gradient du/dr at the wall is presented by the measurement of the streaming potential gradient dE_s/dx, since the two gradients are directly proportional to one another. Helmholtz (31) apparently understood this, since in his discussion of the deviations in the wider tubes he maintained that the differential quotient du/dr is decisive for the "electrical conditions."

If there is both an established flow and a nonestablished flow in different sections of the same tube of constant radius, the velocity gradient at the wall between any points in the nonestablished flow can be evaluated. The velocity gradient at the wall is evaluated by multiplying the velocity gradient for the established flow by the ratio of the streaming potential gradient between the nonestablished-flow points to the streaming potential gradient for the established flow.

Perhaps Reichardt (48) had such a technique in mind when he delayed publication of some of his experimental results from 1928 to 1935 because (translated from the German), "... it was intended to improve the electrokinetic method to a technique so that the shearing stress could be determined at the wall. However, it has turned out that the difficulty of producing an electrically homogeneous surface makes an electrokinetic determination of the shearing stress out of the question as a general method of hydrodynamic measurement. Only in special cases is it possible to make hydrodynamic application of the electrical measurements."

Reichardt's concern for the difficulty in producing an electrically homogeneous surface is not unwarranted. As discussed under Theoretical Background of the Experimental Work, the assumption that the entire surface of any one tube has a homogeneous distribution of adsorbed charge should be more reliable than the assumption that two tubes have an identical homogeneous distribution of adsorbed charge. Consequently, if Reichardt had intended to perfect a method for determining the shearing stress at the wall directly from a single measurement of the streaming potential, the variation of the adsorbed charge from tube to tube and from day to day, which has been observed in all electrokinetic experiments, would make the method impractical.

What is proposed here is the comparison of the streaming potential gradient between different points of the same tube. No doubt, variations in the distribution of the adsorbed charge will occur along the tube. But there is no basis to assume that the adsorbed charge density will always be less on one particular spot than on the rest of the tube surface. By comparison of the results for flows of opposite direction, as well as by comparison of results for opposite ends of a tube, the effect due to a lack of homogeneous distribution of charge can be averaged out on a statistical basis. Also, repeated experiments, i.e., with thorough cleaning of the tube between series of measurements, will further eliminate this effect.

The initial investigation of the possibilities of such a method is presented in the preceding two sections, with tube 7 of this study. Certain changes in design and procedure should be made in future studies. (1) Either the diameter of the tube should be smaller or the length longer, so that the flow in the exit portions can be more nearly established for the

higher laminar flow rates. (2) A precision-bore tube with better circularity should be used. (3) For better comparison of results to offset the lack of homogeneous charge distribution, the taps should be located so that they are symmetrical about the center of the tube. (4) For a more accurate measurement of the pressure difference between taps, either the tube should be removed from the present equipment and the pressure differences between the taps determined for steady known flow rates, or a differential pressure meter requiring a minimum volumetric displacement should be used to measure the pressure difference between the taps.

With these changes, several repetitions of a series of measurements, with a cleaning of the tube between each such series, should make it possible to evaluate the velocity gradient and the pressure gradient along the tube. With these boundary conditions evaluated, at least an empirical solution can be made of the approximate velocity distribution in any cross section of the tube.

The significance of such a solution is not necessarily limited to the flow in tubes. Actually, the deviation of the nonestablished flow in the entrance of tubes is usually not appreciable when compared to the total flow. However, since the entire flow through a porous bed is probably nonestablished, any knowledge of the nonestablished flow may prove useful in the ultimate solution of the problem of flow through porous beds.

Change of the Ratio of the Streaming Potential to the Pressure Difference with Time

The change of the zeta-potential with time has probably been the greatest single handicap in the correlation of electrokinetic data. Since

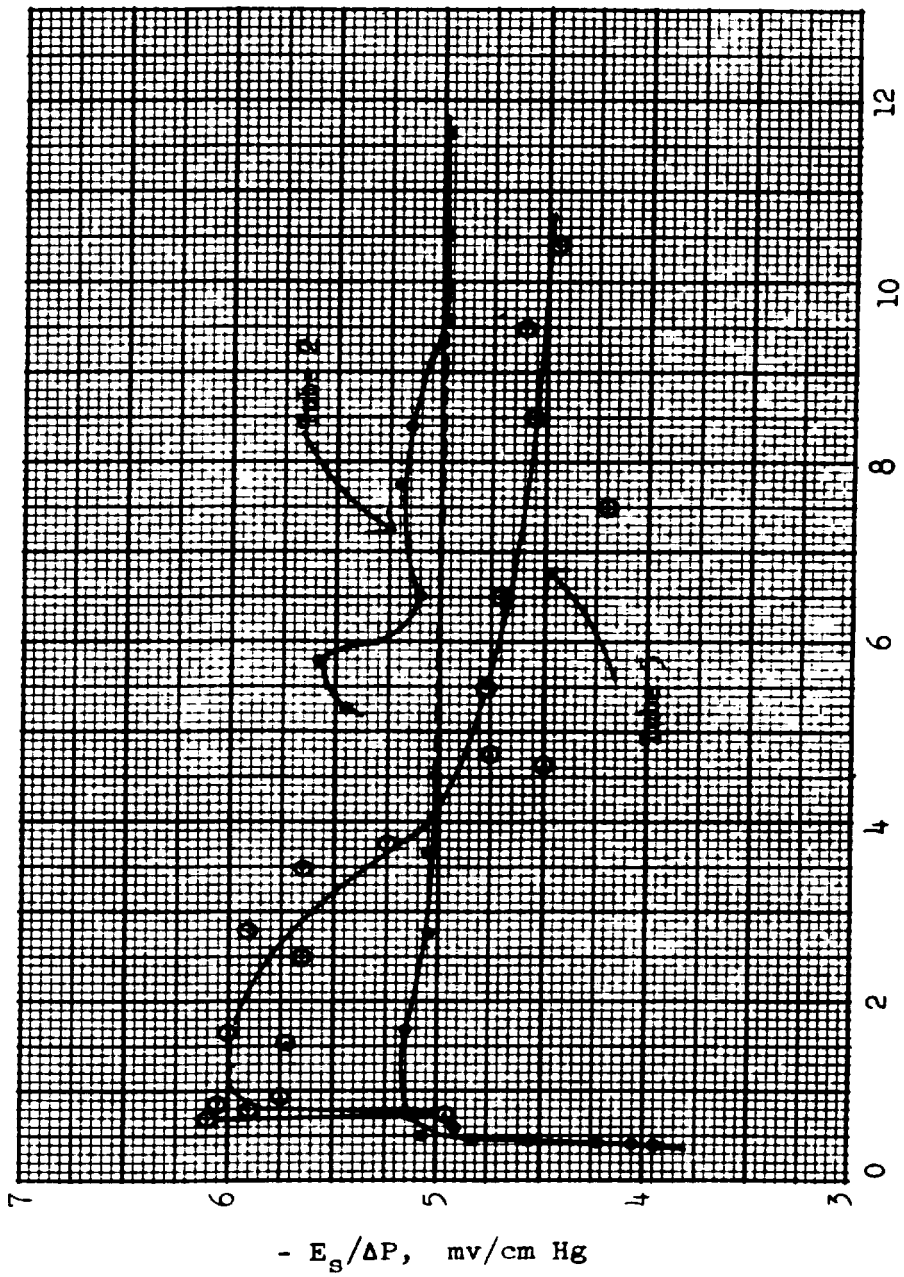
the ratio of the streaming potential to the pressure difference for tubes 2 and 5 is constant for all flow rates (see Figure 15), this ratio is directly proportional to the zeta-potential for these tubes. Figure 21 is a plot of the variation of this ratio with time.

The graph shows a sharp initial increase for the ratio. However, in the time between the solution first entering the tube and the first measurements being made, the streaming potential increases so rapidly for a fixed pressure difference that it is not possible to null it so that a measurement can be made. Part of this rapid change can be attributed to polarization of the electrodes, since the electrodes could have dried somewhat between the time that they were removed from storage in a separate container of solution and the time that they became immersed when the solution first flowed through the equipment.

As a general rule, the ratio of the streaming potential to the pressure difference increases very rapidly for an hour or so after the solution first enters the tube. Then it continues to increase for several days. After that time, it decreases at a very slow rate as long as the experiment lasts, which is sometimes as long as a month.

As can be seen on Figure 21, there are day-to-day variations. Tube 2, a 0.475-mm bore, borosilicate-glass tube, is sufficiently small so that a flow can usually be maintained in it overnight without the solution reservoir becoming empty. The reservoir was inadvertently emptied during the fifth night, and nitrogen flowed through the streaming potential tube, drying its surface.

No doubt a thin layer of sodium chloride was formed on the surface of the tube as the water was evaporated by the nitrogen. The study was continued the next morning without removing the tube from the equipment. From



Source of Data: Tables 10 and 15

Figure 21. Ratio of the Streaming Potential to the Pressure Difference vs Time

Figure 21 it appears that the effect of the discontinuing solution flow became negligible after four days. The measurements from the fifth day to those of the tenth day are connected by the dashed line, since the measurements for the three days before the reservoir emptied and for the three final days are consistent with what is theoretically expected. This slow decrease is further discussed under Rate of Formation of the Double Layer.

Tube 5 was a molded teflon tube with a 0.31-mm diameter. Unnoticed before the tube was placed in the equipment, a small burr of teflon covered one opening and interferred with the entrance flow. Consequently, the tube had to be removed from the equipment during the study and the end scraped. Perhaps the removal of the tube and its consequent drying out can be considered the cause of the continued variation of the ratio as shown in Figure 21.

The classic explanation for the decrease in the zeta-potential with time is that the glass dissolves, interferring as a simple impurity to lower the conductivity or by chemically combining with the solution for form a gel. Perhaps the dissolving of the glass is controlling when pure water is the liquid. But when solutions, for example 0.01 N NaCl, are present, it seems another explanation is necessary.

Observations made in the current study substantiate the view that the decrease in the zeta-potential is not due to the dissolving of the wall. Similar changes in zeta-potential occurred with time regardless of the composition. Tubes made of vitrous silica, borosilicate glass, teflon, and butyl acetate all displayed a gradual decrease in zeta-potential after passing an initial peak. Since all four compounds are usually considered to be insoluble,

no data are available on their solubilities, or even their relative solubilities. But since no silicate is present in teflon and butyl acetate tubes, it is impossible for a silicic acid gel to form and effect the change in the zeta-potential. Because of the above results and reasons, another hypothesis is presented in subsequent sections.

Formation of the Double Layer

The formation of the double layer on an inert solid such as glass is probably dependent on the adsorption of a surplus of either positive or negative ions. Both positive and negative ions can be adsorbed. A surplus of opposite charge equal to the adsorbed surplus of one charge remains in the solution. The migration of the ions which constitute the surplus of charge in the solution, and the attraction between the two surpluses of charge, cause the surplus of charge in the solution to form a diffused layer. The concentration of this layer is greatest nearest the solid and asymptotically approaches zero within a distance from the wall whose order of magnitude is 10^{-7} cm.

Figure 22 is this author's concept of the formation of the double layer for a negative zeta-potential. The diffused layer is in agreement with Verwey's (64) figure for the formation of a colloidal double layer. In his case, the solid actually has a charge. He maintained that there is a good basis to assume that iodine ions of his silver iodide solution force their way between the silver and iodide ions of the solid.

The Nernst potential between an inert solid such as glass and an aqueous solution does not change appreciably with the addition of an electrolyte. However, the zeta-potential decreases very markedly as an electrolyte is added to a solution at this interface. In order for the zeta-potential

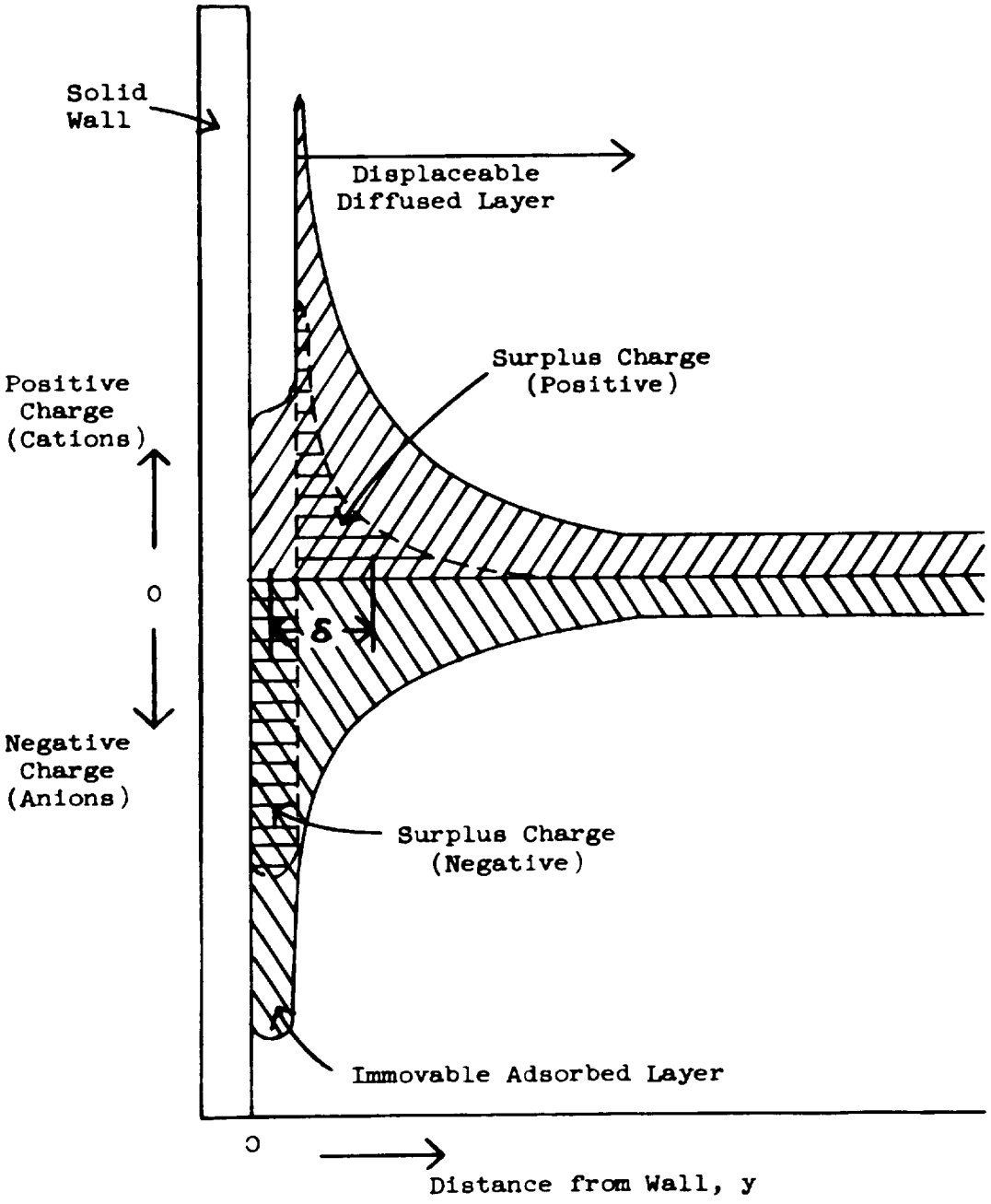


Figure 22. Hypothetical Distribution of Charge of the Double Layer for a Minus Zeta-Potential

to change when the Nernst potential does not, the difference in potential must occur in the immovable adsorbed layer. Therefore, it is given a finite thickness, but the distribution of charge within this immovable adsorbed layer is not attempted.

As indicated in the figure, the diffused layer has a greater thickness than the value of the thickness δ of the double layer as evaluated from the results of electrokinetic measurements; e.g., see Reichardt (47). Equation (7) of Analysis 2 of the appendix is the definition of the thickness of the double layer as related to electrokinetic effects. That is, the electric moment of the double layer is the product of the thickness of the double layer and the displaceable surplus charge. The forces which resist the displacement of the charge are the viscous forces. The viscosity is assumed constant from Analyses 1 and 2, but if it changes with relation to the distance from the wall, this change will affect the thickness of the double layer when evaluated from electrokinetic measurements.

Perhaps the controlling factor in the evaluation of the thickness of the double layer from electrokinetic measurements is the thickness of the immovable layer. The electrokinetic phenomena will still occur if even a part of the surplus charge (positive) of Figure 22 were held immovably at the wall, but the thickness δ of the double layer would then be smaller than the one indicated.

Rate of Formation of the Double Layer

The variation of the zeta-potential, both from point to point on the surface and with time, has probably been the principal reason for poor results in electrokinetic experiments. The point-to-point variations have been accredited to variations in the previous history and impurities at points

in the solid surface. The day-to-day variations have been accredited either to the dissolving of the glass to reduce the conductance of the solution or to the formation of silicic gels by the glass and solution.

When the usual day-to-day variations were observed in this study in two tubes made of teflon, a DuPont resin, which is a polymer of tetrafluoroethylene, and in the tube made of butyl acetate, the formation of silicic gels must be classed at least as the cause of the variations only for special cases. Many momentary variations of the surplus charge have been observed in previous studies. No doubt part of these variations can be attributed to inadequate measuring devices and, possibly, to the effect of such factors as a change of temperature.

Since the ratio of the streaming potential to the pressure difference is directly proportional to the displaceable surplus charge density, any observed change in the streaming potential for a given pressure difference can be interpreted as a change in the adsorbed surplus charge. The displaceable surplus charge and the adsorbed surplus charge are equal but have opposite polarity. The variations detected in this study are more or less in accord with those of previous studies. However, the increase in charge does not last as long in this study as those observed by Jones and Wood (34), i.e., two or three days compared to as long as several weeks. The rates of decrease of the surplus charge of this study are neither as great as, nor do the decreases begin as soon as, some of those reported by Bishop, Urban, and White (4).

In this study the usual attempt to obtain accurate measurements of the streaming potentials for the initial flows of the solutions through the tubes should have been sacrificed in at least one case so that the rapid

increase of the streaming potential for a constant pressure difference could have been recorded on the output tape. However, this rapid increase following the initial contact of the solution is observed and actually interferes in making an accurate measurement of the streaming potential.

The ratio of the streaming potential to the pressure difference continues to increase at a slower and slower rate until it reaches a maximum which may occur after a few hours or after several days. For examples, see Figure 21. The rate of the decrease which then occurs is slower than that of the increase, but apparently it continues at a slower and slower rate as long as the solution remains in contact with the solid.

If it is assumed, in accord with the Stern theory, that each ion has an adsorption potential (some maximum quantity which can be adsorbed per unit surface), the net rate of adsorption of an ion should be some direct function of the difference in the equilibrium concentration of its adsorption potential and the concentration just adjacent to the surface, i.e., the region occupied by the diffused layer.

For an example, let us take a sodium chloride solution and a glass surface. Based on the results of this study and those of previous studies, the adsorption potential for the Cl^- ion is greater than that for the Na^+ ion.

Therefore, at the initial contact of the solution and the solid, the concentration of the Cl^- and Na^+ ions will be identical, and the adsorption rate of the Cl^- ion will be greater than that of the Na^+ ion because the adsorption potential of the Cl^- ion is greater. As more and more Cl^- ions are adsorbed, there is an increase in the concentration of the Na^+ ions near the surface, tending to cause an increase in the rate of adsorption of the Na^+ ion. The rate of adsorption of the Cl^- ion begins to decrease because

an equilibrium is being approached between its concentrations on the solid and in the solution. When the rates of adsorption of the two ions become equal, the surplus of the adsorbed Cl^- ions in excess of the adsorbed Na^+ ions will be at a maximum; consequently, the zeta-potential, or the moment of the double layer, attains a maximum value at this time.

Just when the rate of adsorption of the Na^+ ion begins to decrease cannot be readily predicted. It is true that a maximum concentration of Na^+ ions occurs in the solution near the surface at the time of equal rates of adsorption, but an approach to the equilibrium concentration of the Na^+ ion may have caused a rate decrease prior to this time.

At least after the time of equal rates of adsorption, the rate of adsorption of the Na^+ ion will decrease because the concentration of the Na^+ ion in the diffused layer becomes less and because equilibrium is being more closely approached. However, the rate of adsorption of the Na^+ ion will have to be greater than that of the Cl^- ion until equilibrium is reached to be in accord with the observed results from streaming potential measurements. In the measurements of this study the ratio of the streaming potential to the pressure difference continues to decrease as long as the experiment lasts; that is, once a maximum is reached after the first few days, the ratio continues to decrease. For examples, see Figure 21.

Following the reasoning presented above, Figure 23 is a sketch of the adsorption of charge at a solid-liquid interface for a negative zeta-potential as a function of time. The glass-sodium chloride solution used as an example in the preceding paragraphs has a negative zeta-potential. The area crossed by lines with a positive slope represents the quantity of adsorbed positive charge. Therefore, the slope of the curve enclosing this area is the rate of adsorption of the positive ions.

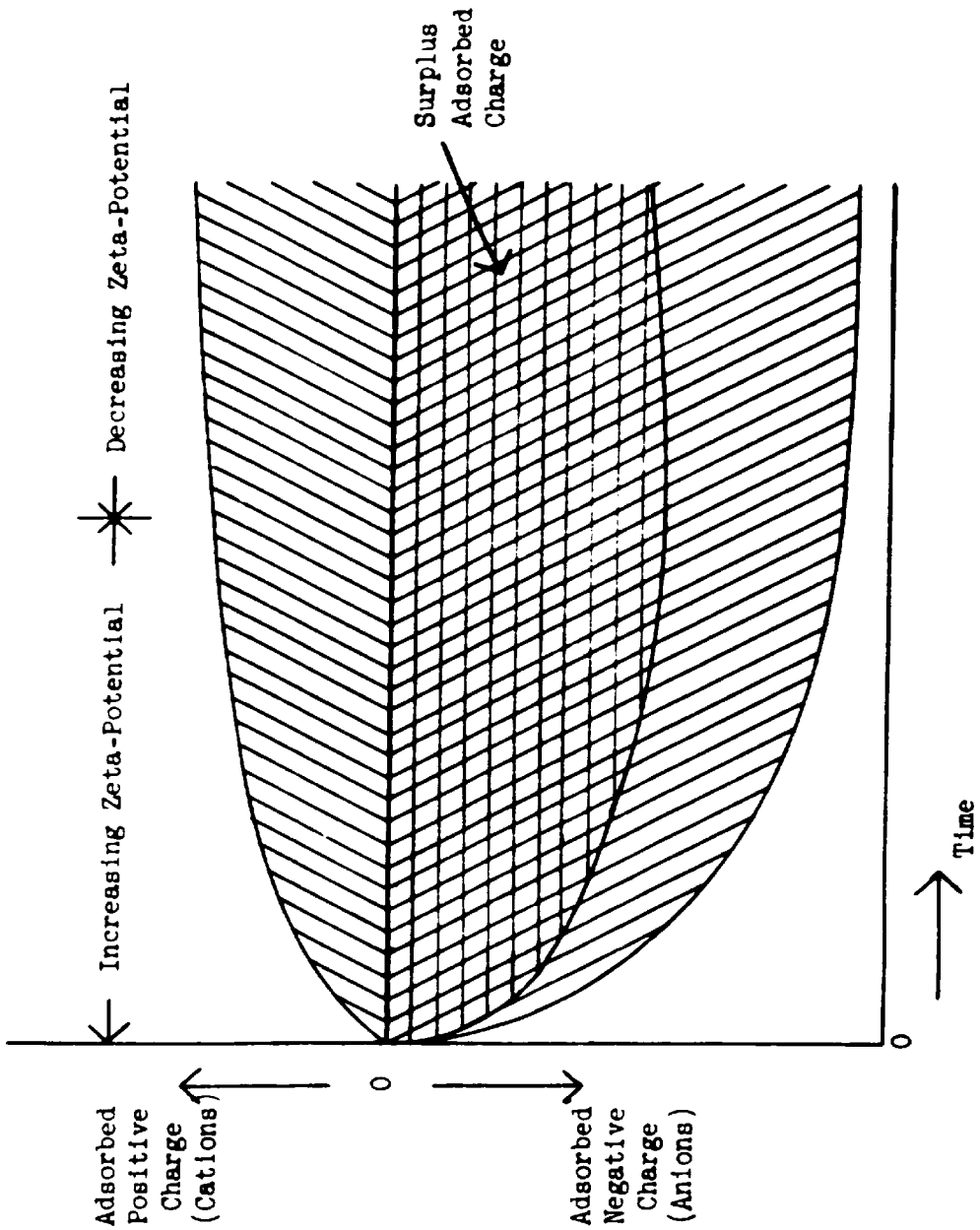


Figure 23. Hypothetical Adsorption of Charge at a Solid-Liquid Interface for a Negative Zeta-Potential vs Time

The area crossed by lines with a negative slope represent the quantity of adsorbed negative charge. The slope of the curve enclosing this area is the rate of adsorption of the negative ions.

The difference in the quantities of adsorbed negative and adsorbed positive charge, or for the case presented the surplus of negative charge, is crossed by horizontal lines. Therefore, the slope of the curve enclosing this area is the rate at which a surplus of charge is formed. Consequently, the slope of this curve is directly proportional to the rate of formation of the double layer.

To be in accord with this concept, the surface conductance should increase with time because more and more ions are always being adsorbed on the surface. Figure 2 of Wood's (73) article on the measurement of the interface potential between vitrous silica and pure water showed that initially the zeta-potential increases with increasing conductance. Then with a further increase in conductance, the zeta-potential begins to decrease. The data of Wood's Figure 2 are in close agreement with the rate of adsorption hypothesis for the formation of the double layer. However, no given relation of the zeta-potential and the conductance to time is apparent in Table I of the same article. For the initial measurements between silica and water, there is a wide divergence for his values of the zeta-potential and the conductance. This divergence could be attributed to the previous history of the surface and/or to the purity of the water.

Of course, it should be noted that the increase in the conductance does not necessarily have to be attributed to the surface conductance, since the smallest contamination in the bulk solution also greatly increases the total conductance. However, the effect of the surface conductance is always greater in the more dilute solutions.

In noting the relation between the zeta-potential and the conductance to time in the data of Jones and Wood (34) on vitrous silica-potassium chloride solutions, the zeta-potential always increased to a maximum, and then the experiments were discontinued. For most cases, solutions of sufficient concentration were used so that the surface conductance does not appreciably affect the total conductance. The conductance of these solutions does not change with time.

For the 10^{-5} N KCl solutions (34, Table VIII), the conductance steadily increased with time (one exception in sixteen points). For their 0.032-cm bore capillary, the zeta-potential also steadily increased, but for the 0.016-cm bore capillary the zeta-potential first decreased with time (from 149 to 140 mv) and then increased to a maximum of 150.6 mv. The increase in conductance of this solution could be attributed to the increase of the total adsorbed charge. But the variations of the zeta-potential for the 0.016-cm bore capillary do not agree with the hypothesis presented in this section on the rate of formation of the double layer.

In addition, the conductance of the 10^{-4} N KCl in the 0.016-cm bore capillary (34, Table VII) decreased with time. An explanation for a decrease in conductivity appears rather difficult from any viewpoint. Perhaps the surface of the tube could have been coated with a material which would dissolve. It could reduce the conductance in the tube, since the total volume of the solution in the system is large compared to that in the streaming potential tube, where the conductance is measured. Since a meticulous cleaning method was used by Jones and Wood, however, this explanation appears impossible.

Use of Streaming Current to Measure the Resistance of the Solution in the Streaming Potential Tube

The streaming potential is defined here as the potential generated by the streaming current when all this current is converted into a galvanic conduction current which flows through the solution of the tube. However, if part of the streaming current is shunted through a known resistor, the resulting potential across the tube will be reduced by the portion of the streaming current which is shunted.

The measurement of the streaming potential and the potential with a known shunt for the same flow rate offers a simple solution to the evaluation of the resistance in the tube. The streaming current is simply considered a fixed current source which, in the case of the streaming potential, flows through the unknown resistance and which, in the case of the potential with a known shunt, flows through two parallel resistances, one known and the other the same unknown. Consequently, there are two equations with two unknowns, the resistance of the solution in the tube and the streaming current. Neale and Peters (42) used a similar technique to evaluate some of the streaming currents in their experiments.

As shown in Analysis 3 of the appendix, the conductance calculated in this way includes the effect of surface conductance and the electroosmotic countereffect in exactly the proportions in which these effects reduce the streaming potential. Equation (10), the final result of Analysis 3, shows that for a tube of constant radius

$$R(1 - Q) = (E_s - E) R_x/E \quad ,$$

where R is the resistance of the solution in the streaming potential tube,

Q is the proportion by which the streaming potential is reduced by the electroosmotic countereffect, E_s is the streaming potential, and E is the potential measured across the tube when the shunt of resistance R_x is connected across the tube.

However, this equation can be generalized to be valid for any tube as shown by equation (9) of Analysis 3. When the macroscopic resistance R(1 - Q) which is measured by this method is used for the evaluation of the conductance of the solution in the Helmholtz-Smoluchowski streaming potential equation (10), the zeta-potential calculated by this equation will be properly corrected for both the effect of the surface conductance and the electroosmotic countereffect.

Zeta-potentials are not calculated in this study. The resistance R of the solutions is measured so that the radius of the tube, which is a very important factor in fluid flow, can be evaluated by another, independent method. The simple equation relating the radius a to the resistance of the solution is

$$R = LR_s/\pi a^2 , \qquad (41)$$

where L is the length of the tube and R_s is the specific resistance which is measured on the conductivity bridge.

The radii evaluated by this method are in close agreement both with the specifications by the manufacturers of the precision-made tubes (note the exception for tube 2 mentioned in the section on Equipment) and with the dimensions evaluated from the liquid flow measurements.

If the electroosmotic countereffect or surface conductance is appreciable, equation (41) is no longer valid if R is evaluated by the use of

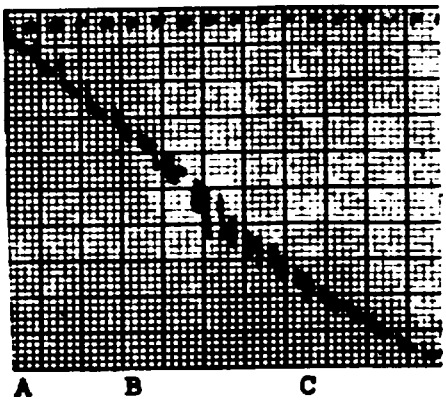
the streaming current as the source of energy. When these effects are appreciable, the relationship between the macroscopic resistance and the radius of the tube is dependent on the degree to which the electroosmotic countereffect and the surface conductance affect the macroscopic resistance. It is not a simple relationship.

Observations of Streaming Potential Oscillations in Turbulent Flow and Streaming Potential Pulsations in Transient Flow

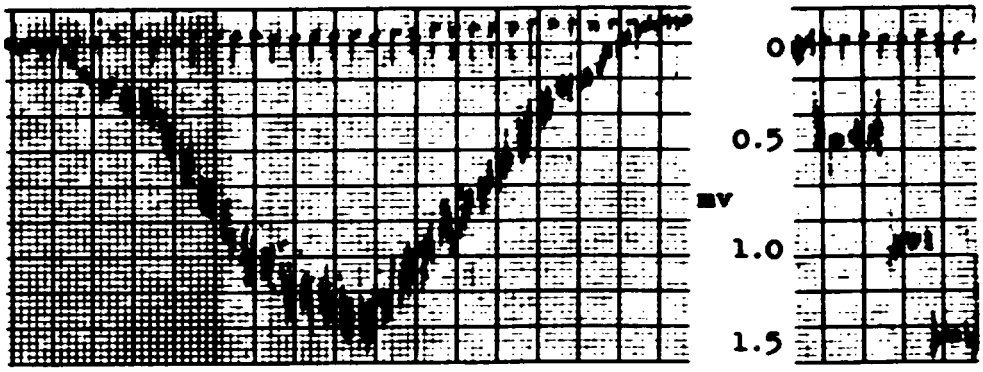
As predicted by Reichardt (48), the oscillations of the pressure difference variations due to turbulence cause the streaming potential to oscillate. Reichardt was unable to observe these oscillations because of the high moment of inertia of his quadrant electrometer. As illustrated by Figure 13, a photograph of a tape record, in the section on Experimental Procedure, these oscillations are a small source of error in this study. In the case illustrated, the oscillations have an amplitude of only about 1 mv compared to the streaming potential of 281 mv. The center of the oscillation is selected as the reading which is recorded in the data.

Three other photographs of tape records constitute Figures 24a, b, and c. A tape record is a measure of the streaming potential vs time. The short dashes across the base or top of the figures represent a zero potential. The rate at which the tape travels can be varied, but all the records presented in this study are for a speed of 0.5 mm/sec.

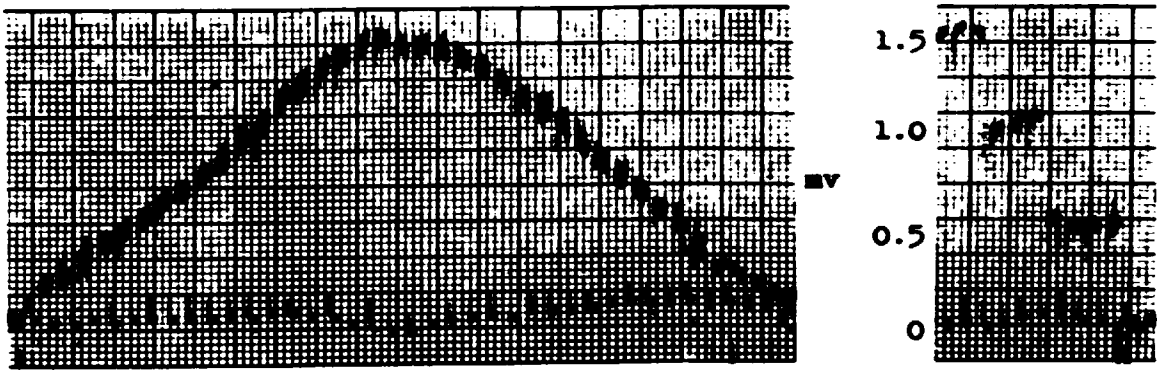
Figure 24a is for the streaming potential of a 0.001 N NaCl solution across tube 4 (the 3.08-mm bore borosilicate-glass tube) when the flow is from right to left. The pressure difference was steadily increased with time to produce this tape. The attenuation of the amplifier is 20 times.



a. A, Laminar; B, Transient; and C, Turbulent Flow in Tube 4



b. Increasing and Decreasing Entrance Flow from Tap H to G of Tube 7



c. Increasing and Decreasing Exit Flow from Tap G to H of Tube 7

Figure 24. Tape Record of Streaming Potential vs Time

From time A to time B the flow is laminar. From B to C, it is transient. From C to the end of the record, there is a turbulent flow. The streaming potential at time B is about 10 mv and at time C about 25 mv. It is apparent that the oscillations are greatest in the center of the transient region and that they gradually decrease as either the laminar or turbulent region is approached.

Figures 24b and c are presented for a comparison of entrance and exit effects. Both figures are recordings of the streaming potential between taps G and H of tube 7 for a 0.0001 N NaCl solution. The amplifier is at full gain. The laminar and transient regions constitute a small portion of the total tape. It can be noted that the oscillations due to turbulence are much greater for the entrance flow of Figure 24b than for the exit flow of Figure 24c. This effect is expected from other studies of entrance conditions.

The small length of tape to the right in Figures 24b and c pictures a calibration potential. While the streaming potentials pictured for the flow in opposite directions have about equal amplitude, the flow rates are not the same. The flow rates for the same streaming potential for the entrance flow are smaller than for the exit flow. For example, at a streaming potential of 0.5 mv, the Reynolds number for entrance flow is 3000 compared to a Reynolds number of 3300 for the exit flow; at 1.0 mv, 3800 compared to 4100; and at 1.5 mv, 4100 compared to 4500.

The most unique of the observations of the variations in the streaming potential for different flow rates occurs just as the flow changes from a transient to a laminar flow. The variations here are not oscillations about one point, but pulsations in the direction of increasing streaming potential.

This effect is demonstrated in Figure 14 under Accuracy of Measurements because it is impossible to compensate accurately for these pulsations by visual interpretation. They occur at haphazard intervals and with varying amplitude. In Figure 24 a (with its attenuation of 20 times), one of these pulsations occurs in the last segment in which laminar flow also exists.

Reichardt (48) found that the ratio of the streaming potential to the pressure difference was greater in the transient region than in either the laminar or turbulent region. In the explanation of his results, he maintained that the flow in the transient region probably could never be an established flow, since it was constantly alternating between a laminar flow and a turbulent flow.

It is known that for the same tube, the same solution, and the same pressure difference, the velocity at the tube axis for an established laminar flow is greater than the velocity at the axis for an established turbulent flow. Under the same conditions, the velocities very near the wall should be equal for either an established laminar or an established turbulent flow. However, in the opinion of this author in the transient region when the greater velocity at axis for a laminar flow decreases because it changes to a turbulent flow, the decrease at the axis may cause a surge producing a greater than normal velocity very near the wall. This surge is then an explanation for the pulsation of streaming potential observed in this study.

Adequate time has not been given for the analysis of the observations of the oscillations and pulsations of the streaming potential which they apparently warrant. However, the use of streaming potential measurements appears to be a new method for the analysis of the transient and

turbulent regions of flow. Perhaps a detector and amplifying system with a higher frequency response than the one of this study should be used. The observations presented here may be only the low-frequency part of a more complicated wave pattern.

OTHER THEORETICAL CONSIDERATIONS

While reviewing the literature for the development of his ideas on electrokinetics, the writer noted conflicts of opinion and ambiguities. Part of these factors have already been included in this presentation, for they pertain to the experimental work of this study. The following sections are concerned with theory which does not pertain directly to the experimental work. However, this theory is relevant to electrokinetics and to a broader concept of the streaming potential.

Electroosmotic Countereffect in Electroosmosis and in Streaming Potential

The conductance of a solution, or the bulk conductance, is considered to be dependent on (1) its concentration of ions, (2) the valance of the ions, and (3) the speed of migration of the ions, or the ionic mobility, e.g., see Bull (9) or Glasstone (20). The difference of the surface conductance from the bulk conductance has been attributed to three factors: (1) the increase in the concentration of ions near the surface, (2) the altered ionic mobility, and (3) the electroosmotic convection current.

In this study, the symbol k_s has been used to represent the surface conductance, but it has been limited to the effect of the first two factors listed above. This definition is arbitrary, but it appears to be more explicit since the first two factors are simply changes in the accepted factors affecting the bulk conductance.

It can be said that the increase in concentration of ions and the altered mobility are directly dependent on the formation of the double layer. However, the important difference in the electroosmotic convection current

and the other factors of conductance near the surface is that the electroosmotic convection current is composed of ions of one charge, while an electrolytic conduction current has an equal positive and negative charge.

In contrast to this interpretation of surface conductance, Bull and Gortner (10), following Smoluchowski's (59) concept, have at least implied that the surface conductance was completely due to the electroosmotic convection current. Perhaps the electroosmotic current is the controlling factor in the experimental measurement of surface conductance, but even today experimental error is so large with respect to the quantities being measured that no definite conclusions can be made. However, theoretical analyses can be made of the effect of the electroosmotic convection current on the electroosmosis and the streaming potential.

Effect on Electroosmosis: For electroosmosis, Smoluchowski's (59) expression for the ratio of the electroosmotic convection current I_{eo} to the conduction current I_c is

$$\frac{I_{eo}}{I_c} = \frac{\epsilon^2 \zeta^2}{8\pi^2 a \delta \mu (k + 2k_s/a)} , \qquad (42)$$

where ϵ is the dielectric constant, ζ the zeta-potential, a the tube radius, δ the thickness of the double layer, μ the viscosity, k the bulk conductance, and k_s the surface conductance (not including the effect of the electroosmotic current).

From the development of the Helmholtz-Smoluchowski electroosmosis equation, the I of this equation (4) is actually the conduction current within the tube; therefore, it can be written,

$$\frac{V_e}{I_c} = -\frac{\epsilon \zeta}{4\pi \mu (k + 2k_s/a)} , \tag{43}$$

where V_e is the electroosmotic volume rate of flow. If I symbolizes the current entering the tube to maintain the external potential across the tube,

$$I = I_c + I_{eo} . \tag{44}$$

Since I_c cannot be experimentally separated from I_{eo}, it is desirable to express the electroosmotic volume rate as a function of the measurable current I. Eliminating I_{eo} from equations (42) and (44), and substituting the resulting value of I_c into equation (43), one obtains

$$\frac{V_e}{I} = -\frac{\epsilon \zeta}{4\pi \mu (k + 2k_s/a)\left[1 + \epsilon^2 \zeta^2 / 8\pi^2 a \delta \mu (k + 2k_s/a)\right]} . \tag{45}$$

Therefore, when there is an electroosmotic flow in a tube, this equation accounts for that portion of the current I which flows into the tube and becomes the convection current, and consequently prevents the total entering current from producing electroosmosis. It is in this sense that the convection current can be thought of as an electroosmotic countereffect.

Effect on Streaming Potential: Now, in the generation of the streaming potential, the convection current is developed because the displaceable surplus charge is a part of a lamina near the wall whose velocity is determined by the usual hydrodynamic factors, such as the pressure gradient and the viscous forces. As this convection current is converted into the conduction current, a potential gradient is generated along the tube. This potential gradient, in turn, tends to retard the motion of the charge in the

convection current with a force identical to that of the potential gradient in electroosmosis.

Since the displaceable surplus charge is a part of a lamina, the velocity of every lamina between it and the axis of the tube is retarded an equal velocity because of the interconnection of the lamina by viscous forces. The reduction in the velocity of the charge of the convection current resulting from the electrical force of the streaming potential is then the electroosmotic countereffect.

This reduction has been expressed as a function of several of the terms of the flow equation, as well as of terms of the streaming potential equation. For example, Abramson (1) expressed it as the ratio of the amount the volume rate would be retarded to the volume rate theoretically expected for a given pressure difference. Elton (18) expressed the retardation as a function of the viscosity, and called the electroosmotic countereffect an electroviscous effect. He called the apparent increase in the viscosity the electroviscosity.

In his analysis, Elton assumed that the apparent viscosity was equal to the sum of the true viscosity and the electroviscosity. However, an error results in his development of the relationship between the apparent viscosity and the true viscosity in that he expressed the electroosmotic countereffect in terms of the apparent viscosity. Since the viscous forces between the laminae containing the convection current and the other laminae are dependent on the true viscosity and since these are the forces which oppose any electroosmotic movement, the true viscosity should have been used.

For another example, Bull and Moyer (13) expressed the electroosmotic countereffect as a ratio of the electrical work required to drive

the streaming current against the streaming potential gradient to the mechanical work producing the liquid flow.

If the results of any one of these analyses are used to modify the particular term upon which the analysis is based, and if the modified term is then substituted into the streaming potential equation, the resulting equation will be identical in each case. Of course, the error in Elton's development must be corrected to produce agreement with the results from the other analyses.

When the streaming potential equation is corrected for the electroosmotic countereffect, it becomes

$$\frac{E_s}{\Delta P} = \frac{\epsilon \zeta [1 - \epsilon^2 \zeta^2 / 2\pi^2 a^2 \mu (k + 2k_s/a)]}{4\pi \mu (k + 2k_s/a)} \quad . \tag{14}$$

Relationship between the Effect on Electroosmosis and the Effect on Streaming Potential: If the portion of the ratio of the streaming potential to the pressure difference which is reduced by the electroosmotic countereffect is indicated by Q,

$$Q = \frac{\epsilon^2 \zeta^2}{2\pi^2 a^2 \mu (k + 2k_s/a)} \quad . \tag{46}$$

That is, the right side of the Helmholtz-Smoluchowski equation, equation (13), must be multiplied by (1-Q) to correct it for the electroosmotic countereffect. In contrast to the accepted opinion that the right side of the electroosmosis equation (45) and the streaming potential equation (14) should be identical under any condition, the right side of the electroosmosis equation (4) must be multiplied by $1/(1 + aQ/4\delta)$ to correct

it for the electroosmotic countereffect.

Since, for practical application, the radius a will be very large compared to 4 times the thickness δ of the double layer, the electroosmotic countereffect will be much greater in electroosmosis than in streaming potential. The reason for this difference is that for electroosmosis, the entire liquid cross section has the same velocity, identical to that of the convection current; therefore, the change of velocity of every lamina is directly proportional to the applied voltage. In contrast, the effect of the streaming potential on the convection current is to retard the velocity of each lamina a small fixed amount of its total velocity; i.e., only those laminae containing the surplus displaceable charge are changed in a direct proportion to the streaming potential.

Consequently, if the conductance of a solution in a tube is measured by the application of a voltage across the tube, this conductance will include the effect of the electroosmotic convection current. However, it becomes apparent from this analysis that if the effect of the electroosmotic convection current is appreciable, this conductance cannot be used to evaluate the zeta-potential in the Helmholtz-Smoluchowski streaming potential equation.

Therefore, since the electroosmotic countereffect is different for the electroosmosis and for the streaming potential and since it is a function of the dimensions of the tube, it appears more explicit to express the effect as a modification of an equation than to express it as a modification of one of the terms of the equation. The evaluation of the conductance for use in evaluating the zeta-potential from streaming potential measurements

is most accurate when the streaming current is used as the only source of energy for the measurement of conductance.

Also, it should be pointed out that the measurement of both streaming potential and electroosmosis in the same tube of known, constant radius, under the conditions where the electroosmotic countereffect is appreciable, will offer a means to evaluate the thickness of the double layer. But the experimental technique, particularly for electroosmosis, will have to be improved so that more accurate measurements can be obtained.

Overbeek and Wijga (43) maintained that Wijga's (71) measurements of the streaming potential and the electroosmosis on the diaphragms showed that the ratio of the streaming potential to the pressure difference was always identical to the ratio of the electroosmotic volume rate to the electric current. Such an interpretation can be made of Wijga's results because the experimental error is usually large for electroosmosis.

However, if the zeta-potentials calculated from his streaming potential measurements (Wijga's Tables XX and XXI) for potassium nitrate solutions flowing through powdered-glass diaphragms are compared with those from his electroosmosis measurements (Wijga's Table XXIV) of the same solution and the same type of diaphragm, a different interpretation results, as can be seen in Figure 25.

For the more dilute solutions, but for any fixed concentration, the zeta-potential calculated from the streaming potential measurements was always greater than that calculated from electroosmosis measurements. The difference between the zeta-potentials became less and less as the concentration of the solution was increased. When the concentration was greater

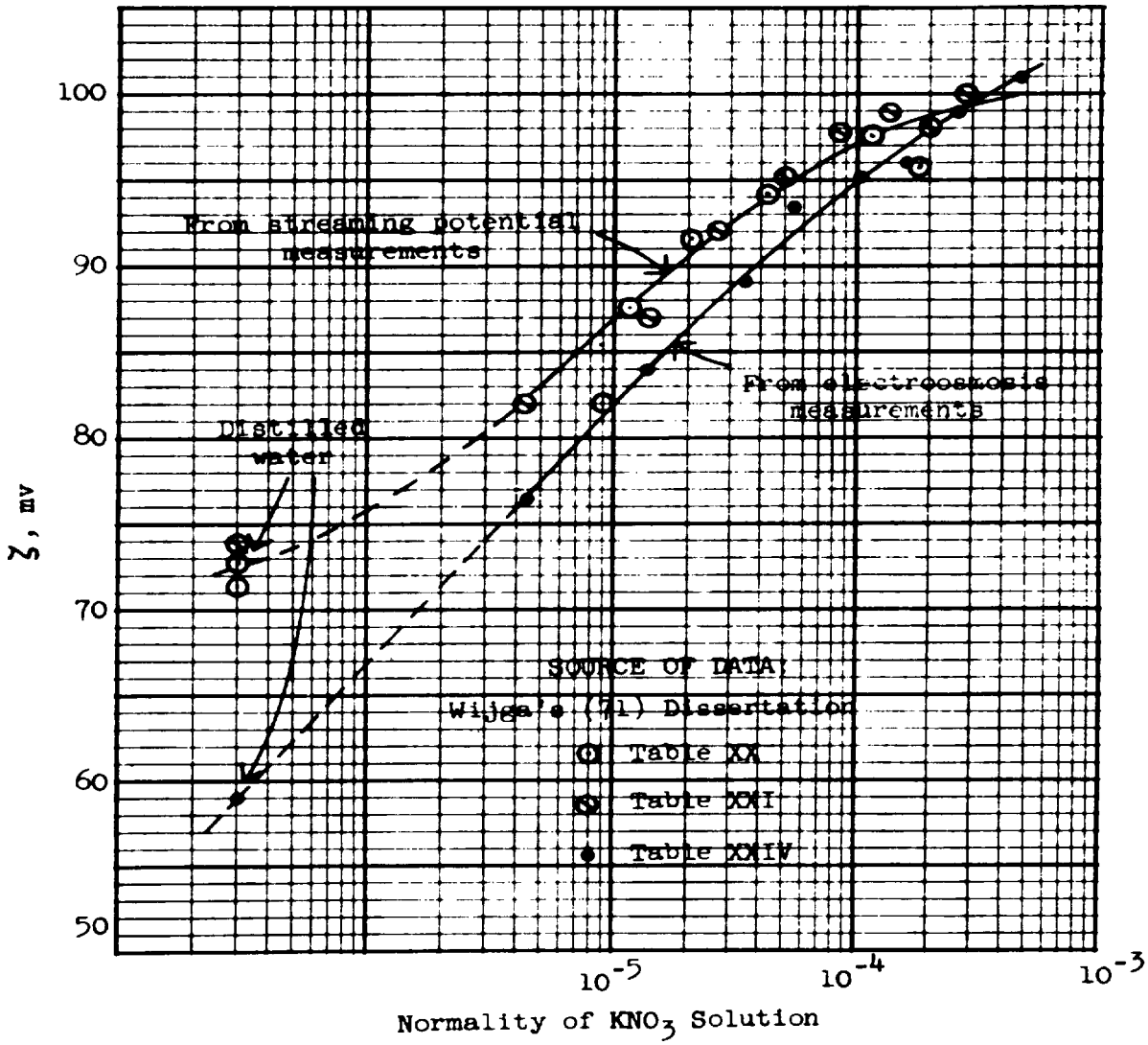


Figure 25. Wijga's Zeta-Potentials vs Concentration of Solutions from Measurements of Streaming Potentials and of Electroosmosis through Porous Diaphragms

than about 10^{-4} N, the zeta-potential was essentially the same from both the streaming potential and the electroosmosis measurements.

The difference of zeta-potentials for the more dilute solutions can be attributed to the fact that the electroosmotic countereffect is greater for electroosmosis than it is for streaming potential. The agreement of the zeta-potentials for the more concentrated solutions can be attributed to the electroosmotic countereffect being negligible.

It should be noted that the decrease of the zeta-potential from both streaming potential and electroosmosis measurements for decreasing concentration is probably due to the effect of surface conductance on the flow through diaphragms as analyzed by Overbeek and Wijga (43).

Effect of the Surface Conductance on the Streaming Current through Porous Diaphragms

In 1946 Neale (41) presented an analysis of the streaming current in which he maintained that the streaming current through porous diaphragms is independent of the surface conductance. In order to confirm Neale's analysis, Neale and Peters (42) evaluated the "surface potential," i.e., presumably the zeta-potential, from the measurements of the streaming current and pressure difference across a fiber diaphragm with various concentrations of solutions. When the solution was sufficiently dilute (about 5×10^{-5} M) for the surface conductance to have an appreciable effect on the total conductance, the zeta-potential was less than theoretically expected.

A mathematical analysis of this problem is presented in Analysis 4 of the appendix. The results of this analysis show that the surface conductance has an identical effect on the streaming current that it has on the

streaming potential through porous diaphragms. The problem is not easily discussed because of the complicated interrelationships of the electricity and the fluid flow through porous diaphragms.

First, a diaphragm must be thought of as a vast number of small pores, each pore having a constant radius. These pores are connected in parallel, in series, and at angles to one another. The analysis is simplified to consider only pores in parallel as one case and only pores in series as the other case.

From equation (11), it can be seen that the ratio of the streaming current to the pressure difference is directly proportional to the square of the radius of a tube. Therefore, if all the pores do not have an identical radius, the streaming currents in some of the pores must be different from those in the others.

When the pores of a diaphragm are connected in parallel, the potential across each of them is zero. Consequently, there can be no conduction current, and the conductance of the solution does not enter the analysis. The complications arise when the pores are connected in series.

For example, let us assume that several pores of different radius are connected in series and that a negative zeta-potential exists at the solid-liquid interface. The current drawn from the end of the series must flow through each of the pores. It may be either a streaming current or a conduction current, but the sum of these two currents must always be equal to the current withdrawn from the ends of the series. If there is one pore in which there is no conduction current, the streaming current will be equal to the current withdrawn at the end of the series. The voltage across this particular pore will be zero.

If another pore has a radius larger than this particular pore, a conduction current in the direction opposite to that of the streaming current must occur in the larger pore. The difference in the values of these two currents will be equal to the current withdrawn at the end of the series. A positive gradient in the direction of the flow results.

If still another pore has a smaller radius than the pore with no conduction current through it, a conduction current must occur in the direction of the streaming current in the smaller tube so that their sum will be equal to the current withdrawn at the end of the series. The potential gradient in the smaller pore will be negative with respect to the direction of fluid flow.

From these examples, it becomes apparent that the usual concept that the potential must be zero across a tube for the streaming current to be measured must be modified for the case of streaming currents through diaphragms.

As stated above, the streaming current is directly proportional to the square of the radius. If the bulk conductance is the controlling factor in the conduction of the solution, the conduction current is also proportional to the square of the radius. Therefore, in a sense, the surplus streaming current of the larger pores compensates for the deficiency of the streaming current in the smaller pores. This relation is not exact because it is the potentials which must add to zero, since the potential across the diaphragm is zero.

When the surface conductance is the controlling factor in the evaluation of the total conductance, the streaming current is still proportional to the square of the radius, but the conduction current becomes

directly proportional to the radius, i.e., the radius to the first power. Consequently, the relationship of the streaming current and the conduction current in the various pores must change. The larger pores need more conduction current or the smaller pores need less conduction current for the overall potential to remain zero. The net effect is that the pore which has no conduction current must now be a smaller pore.

For each case, the pore with no conduction current has the mean radius of the diaphragm. If the mean radius is based on the porosity of the diaphragm when the bulk conductance controls the conductance of the solution, an additional factor must be added when the surface conductance controls the total conductance.

No solution to this problem is apparent at this time. As shown by Analysis 4 of the appendix, the surface conductance affects only the streaming current through pores connected in series. Consequently, a knowledge of how the pores of a diaphragm are interconnected is also essential for the solution of this problem.

AN INTERPRETATION OF OTHER EXPERIMENTS IN VIEW OF THE RESULTS OF THIS STUDY

As stated in the introduction to this dissertation, electrokinetics is not an easily understood subject. Too often, investigators have accepted the viewpoint of others simply because the expressed concepts seemed logical and could be associated by analogy to facts with which the investigators were familiar. It appeared logical to accept Helmholtz' (31) conclusion that the flow must conform to the Poiseuille law for fluid flow because his equations had been confirmed by many investigators. In this very article there is much to be learned about electrokinetics, for Helmholtz' knowledge of many fields of science was much more extensive than that of the usual investigator of electrokinetics.

The following sections are concerned with particular points about other experiments with which the results of this study do not agree. Several pertinent studies are selected from a large group. They are presented in chronological order.

Clark (16), 1877

Clark measured the streaming potential generated by flowing water using the full pressure of the Heidelberg water supply through glass capillaries of different lengths and diameters. He maintained that the pressure generating the streaming potential was constant at 1285 mm Hg. Since the dimensions of the tubes, along with the flow rates, were measured and recorded, the theoretical pressure difference across each tube can be calculated.

This writer calculated the pressure differences necessary to produce the recorded flow rates with the assumption that for each case the flow was established. An established flow requires a minimum pressure difference. The pressure differences calculated for half of the circular tubes are greater than the 1285 mm Hg pressure of the Heidelberg water supply.

This lack of agreement can be attributed to (1) a variation in the supply pressure, (2) errors in measuring the dimensions of the tubes, and/or (3) errors in measuring the flow rates.

A further handicap in correlating Clark's data is that his flow system had an outlet which prevented air from entering the system by tapering to a small hole whose dimensions were not recorded. Apparently, for his largest tube the pressure drop across this hole represented the principal loss of energy for the entire flow.

Consequently, only generalized statements can be made on Clark's experiments. When he broke a tube into two parts, the streaming potential across a remaining part was always less than that across the whole tube. This decrease can be explained in terms of the concepts emphasized in the current study. With the shorter tube the pressure difference generating the streaming potential is smaller if the overall pressure difference is maintained constant. Since with the shorter tube at the same overall pressure difference the flow rate increases, the losses in the parts of the flow system other than the tube itself, along with the exit and entrance losses, must increase.

Cameron and Ottinger (14), 1909

These investigators measured the streaming potential across intervals of length of a 0.65-mm bore capillary. Electrodes were fused into the

wall of the tube at four points. The flow pattern of the liquid was disturbed both by the electrodes and by the enlargement of the cross section of the tube at the point where the electrodes were fused into the wall of the tube.

In their report of this experiment, Cameron and Ottinger calculated the ratio of the streaming potential to the pressure difference by multiplying the streaming potential gradient across the particular section by the ratio of the total length of the tube to the total pressure difference. There was a small decrease in the ratio of the streaming potential to the pressure difference from the entrance end to the exit. But this deviation from the Helmholtz-Smoluchowski equation was maintained to be negligible and was explained as a lack of homogeneous distribution of charge, which it might well have been.

However, by a closer examination of their data, it can be noted that the streaming potential gradient along the tube deviated from the average streaming potential gradient more for the highest laminar flow than for any other flow. Such a deviation agrees with the findings of the present study for it is with maximum laminar flows that the effects of the entrance extend a maximum distance into the tube.

The effect of the enlargement of the cross section at the point of the electrodes on the flow pattern, and consequently on the streaming potential, cannot be readily explained. Actually, the deviations of their study are probably due to (1) the lack of homogeneous distribution of charge, (2) the entrance and exit effects, and/or (3) the effect of the enlargement of the cross section at the electrodes.

Bishop, Urban, and White (4), 1931

In an attempt to evaluate the effect of the diameter on the streaming potential, these investigators measured the streaming potential of 0.0005 M KCl solution flowing through three glass capillaries with sharp-cornered entrances for the same pressure difference of 60 cm Hg. The three capillaries selected had inside diameters of 0.040, 0.080, and 0.125 mm, respectively; the 0.040-mm bore capillary was 5 cm long, the others 1 cm long.

The measured streaming potentials, which would have been identical if the Helmholtz-Smoluchowski equation were valid for their studies, were 392, 681, and 333 mv, respectively. In a discussion of this deviation the authors wrote, "From this series alone one might conclude that there is an optimum diameter for the development of a stream potential, lying between 0.040 and 0.125 mm. We are not ready to state, however, that this is the case; we can only say that there appears to be a relation between capillary diameter and stream potential but it apparently is not a simple one."

The irony of the authors' statements lies in the fact that they quoted Helmholtz' analysis of 1879 on the very page on which these statement occur. Certainly Helmholtz' reasoning is more specific in that the ratio of the streaming potential to the pressure difference would be reduced as the diameter increased because the formation of the jet in the entrance would be more pronounced for the larger tube. Or, as Helmholtz has stated, "Under these conditions in the entrance of the tube, or if it is short, in the entire tube, the motion at the wall and the differential quotient, du/dN, which is decisive for the electrical conditions, will be much smaller than in the steady state of eddy currents."

In defense of the authors, they continued their work and performed other useful experiments which aided in developing our concepts of the effect of surface conductance and the electroosmotic countereffect.

The deviations of the streaming potentials measured across the three capillaries appear sufficiently great that part of them probably should be attributed to different surplus charge densities. However, all the capillaries are sufficiently small and the solution used sufficiently dilute so that the effect of the surface conductance and the electroosmotic effect are appreciable. If the surface conductance determines the total conductance of the solution in a tube, and if the electroosmotic effect is negligible, the ratio of the streaming potential to the pressure difference is directly proportional to the radius of the tube. The ratio of the surface area to the volume increases as the radius decreases. If the electroosmotic countereffect is also appreciable, the ratio of the streaming potential to the pressure difference is dependent to a greater degree on the radius of the tube.

Consequently, for the case of the two smaller capillaries, a possible explanation can be based on these effects, since the streaming potentials of 392 and 681 mv were nearly proportional to the diameters of 0.040 and 0.080 mm, respectively.

On the other hand, an explanation for the streaming potential of the 0.125-mm bore capillary being less than that of the 0.080-mm bore capillary must be attributed to (1) the more pronounced effect of the entrance jet and (2) the increase in the losses due to contraction and expansion of the cross-sectional area at the entrance and exit of the larger tube.

Jones and Wood (34), 1946

Using meticulous methods to clean the capillary tubes, Jones and Wood developed a procedure for measuring the streaming potential generated by flowing solutions between 1-liter bottles. The same electrometer amplifier was used to measure the streaming potential, first in one solution flow system and then in a second independent flow system. The capillary tubes of each flow system had different diameters, 0.168 and 0.322 mm, but essentially the same length, 19.2 and 19.1 cm.

When the streaming potential reached the same maximum value across each flow system, it was maintained that equilibrium had been attained and that the zeta-potential calculated from this measurement would be the most definitive. Also, the small difference in the value of the streaming potential for flow in opposite directions was attributed to an asymmetry of the electrodes, presumably a polarization potential.

As discussed in more detail under the design and operation of the electrometer detector used in the present study, the difference in the streaming potential for flow in opposite directions cannot be attributed solely to the asymmetry of the electrodes. This asymmetry well might be the cause of the difference, but the effect of a control grid current or the effect of a current from the bias battery due to leakage resistance at the high-impedance end of the streaming potential tube cannot be isolated from the effect of the asymmetry of the electrodes.

Jones and Wood calculated and recorded the zeta-potentials to four figures, and sometimes to five figures. Meticulous care was exercised in all preparations, such as using recrystallized potassium chloride to make

the solutions and maintaining the temperature at 25°C ± 0.03°C. Consequently, it seems worth while to mention that a small error results from their using the gauge pressure of their ballast tank as the pressure difference producing the streaming potential.

In order to force air bubbles out of the liquid system of their equipment, a 1-mm bore tube was used as a delivery tube from the capillary to one reservoir. Assuming the length of this delivery tube to be about 20 cm, the pressure difference across it will be equal to slightly more than 1 percent of the pressure difference across the 0.322-mm bore capillary.

The flow system for the 0.168-mm bore capillary differed in some details from that for the 0.322-mm bore capillary; perhaps it was found necessary to use a delivery tube of less than 1-mm diameter for the smaller capillary to force the air bubbles from the solution system. If a smaller delivery tube is used, the pressure difference across it could be appreciable when compared to the pressure difference across the streaming potential tubes. If the delivery tube for the smaller-capillary system had a 1-mm diameter, no appreciable pressure difference occurred across the delivery tube.

Also, Jones and Wood's method of measuring the conductance of the solution in the streaming potential tubes can be questioned. The error of their method is probably small when compared to experimental error except for very dilute solutions and distilled water.

Their equipment consisted of a bridge, one of whose arms was the streaming potential tube through which the solution was flowing during the conductance measurement. With no external voltage applied to the bridge,

the streaming potential generated by the flow produced an unbalance of the bridge. Consequently, instead of the usual zero voltage between null points of a bridge, a counterpotential E_A (their symbolization) was used to zero the current between the null points to indicate balance. When the external voltage E_B was applied, the variable-resistance arm was adjusted so that no current flowed and so that the same counterpotential existed between the null points.

According to their schematic circuit diagram, the current i_a through the bridge detector can be zero only if the resistance R_a of the detector is infinite. Yet, after expressing the current i_a as a ratio of two determinants in their analysis, Jones and Wood assume that the determinant in the numerator is zero, even though the R_a of the determinant in the denominator cannot be eliminated. In order to assume that the numerator is zero of any fraction whose value is zero, it is first necessary to show that the denominator is finite.

The actual assumption necessary for the presented analysis is that the voltage drop i_aR_a is zero. Since E_A is less than 10 mv, the assumption that i_aR_a is diminishingly small when compared to E_A is not as exact as the assumption that i_a is zero. Apparently the instrument they used was sufficiently sensitive, since their results were always reproducible.

However, their assumption that the streaming potential E_2 (their symbolization) is unaffected by the application of an external voltage appears incorrect, particularly for those solutions sufficiently dilute so that the electroosmotic countereffect may be appreciable. Since the velocity of the charges which constitute the convection current or streaming

current is affected by a potential gradient as well as by a hydrostatic pressure gradient, the application of an external potential to the bridge alters the convection current, and consequently their E_2.

When the polarity of the streaming potential and the external voltage are such that the hydrostatic forces and the electrical forces on the displaceable charge oppose one another, the macroscopic electrical resistance of the solution in the tube as measured by Jones and Wood's method will be greater than the macroscopic resistance if the hydrostatic force and the electrical force act in the same direction. A maximum macroscopic resistance will occur when the hydrostatic and electrical force on the displaceable surplus charge are equal and opposite.

The circuit diagram of Jones and Wood's equipment showed that the polarity of the external voltage as well as the polarity of the streaming potential could be reversed. But they do not mention whether or not the resistance of the solutions flowing in one direction was evaluated by using both polarities or external voltage. If the same value was obtained with both polarities of external voltage, it would indicate that the electrical force on the displaceable charge was not appreciable when compared to the hydrostatic force.

CONSIDERATIONS OF THE STREAMING POTENTIAL AS A TOOL IN THE MEASUREMENT OF BLOOD FLOW

The initial intent of this study was to investigate the possibility of using the streaming potential as a measure of the blow flow *in vivo*. The experimental work and part of the theoretical analyses presented in this dissertation have constituted a necessary preliminary investigation of this problem. However, further experimental work, requiring the development of new equipment and techniques, will be necessary before it can be ascertained whether or not the streaming potential can be used to measure the blood flow through its vessels.

That the earliest investigators realized that electrokinetics has a physiological significance becomes apparent when one reads Porrett's (45) opinion of his electroosmosis experiment in 1816, "I think that by the above experiment I have demonstrated the existence of a power ... that of conveying fluid through minute pores not otherwise pervious to them, and of overcoming the force of gravity.

"Is not this electro-filtration, jointly with electrochemical action, in constant operation in the minute pores of the animal system?

"... I cannot help thinking that an affirmative answer to the above question is capable of a good defence."

That the affirmative answer has not been confirmed also becomes apparent in Bull's (9) recent book, *Physical Biochemistry*, where it is stated, "The utility of streaming potential and electroosmotic experiments would be greatly expanded if such measurements could be made on membranes. In spite of a a large amount of work along these lines the situations remains ambiguous."

In another excerpt, a positive opinion is presented by Bull, "There is in living tissue a constant ebb and flow of fluids, and every such motion must result in a streaming potential."

The questions, then, to be investigated are (1) how large is the streaming potential in blood flow, and (2) what is the relation between the streaming potential and the volume rate of flow.

The Streaming Current in Blood Flow

The magnitude of the streaming current in blood flow will depend on (1) the surplus displaceable charge density, or the zeta-potential between the vessel wall and the blood and (2) the velocity of the blood near the wall.

The Zeta-Potential: In 1928 Gortner and Briggs (21) found that for a glass-water interface the zeta-potential was approximately - 30 mv. But when the same surface was coated with paraffin, the zeta-potential between the coated surface and water became "essentially" zero. Also, they noted that blood clotted rapidly on a glass surface, but much more slowly on a paraffin-coated surface. On the basis of these observations, they postulated that the higher zeta-potential was related to the blood-clotting process. Since blood does not clot in its vessels, perhaps the conclusion should follow from Gortner and Briggs' postulate that the zeta-potential between the vessel walls and blood is essentially zero.

More recent measurements of the zeta-potential for a vitrous silica-water interface by Wood (73) showed the value to be about - 180 mv. There is a difference in a vitrous-silica and a glass surface, but this difference should not account for the sixfold increase of the later measurement.

Consequently, this inconsistency offers grounds to believe that the zeta-potential for a paraffin-coated glass-water interface may be greater than "essentially zero".

However, the facts that blood has many constituents and that the vessel wall is impregnated with many of the same constituents, e.g., potassium salts and, to a lesser degree, sodium salts, leads one to expect that the zeta-potential between the vessel walls and the blood is very small.

In 1950 Horan and associates (32) found in their study relating the zeta-potential to the blood-clotting process that it was necessary to dilute the blood or its constituents from their original concentration of 0.15 M to solutions of about 0.001 M KCl or KH_2PO_4-KOH, which was also about 0.001 M with respect to the potassium ion. With these dilutions the zeta-potential was sufficiently large so that it could be evaluated by a streaming potential method.

Of course, the value of the zeta-potential between the vessel wall and blood must await experimental measurement, which has been delayed by problems of instrumentation.

It appears that it may be possible to evaluate the zeta-potential by measuring the pressure difference and the streaming potential developed by flowing blood through an isolated gland, e.g., a modification of the preparation of the salvary gland of a dog as presented by Bohr and associates (5).

Since it is necessary for the silver-silver chloride electrodes to be in the solution for a day or so before they become electrically stable, they should be mounted in the electrode chambers and the chambers filled with physiological saline several days before the potential is to be measured. A

catheter and a physiological-saline supply can be connected to outlets of the two electrode chambers. An electrode can then be connected through physiological saline to the inlet and outlet of the blood supply for the gland by inserting the filled catheters into branches of the arterial and venous supply of the gland.

At the time of measurement the flow of physiological saline through the catheter can be stopped by controlling the pressure of the physiological-saline supplies. The difference in the pressure of the two physiological-saline supplies, corrected for difference of hydrostatic levels, will be a measure of the pressure difference generating the streaming potential.

Since the sensitivity of the amplifying equipment used in this study at maximum gain, as recorded on the output tape, is only 4 cm/mv, the gain of the present equipment will probably have to be increased. Since the Sanborn DC Preamp, Model 60-400, proved to be very stable even though it was connected in series, which amplifies the instability of the first stage ten-fold, perhaps the simplest way to increase the gain of the present equipment is to add another DC Preamp to the equipment. A Sanborn Power Supply, Model 60-1000, will be needed for the additional preamp.

The Velocity Near the Wall: In that arterial blood flow is pulsatile, and in that the vessel walls are flexible, the relation between the velocity at the wall and volume rate of flow is different from that for a steady flow through rigid-walled tubes. The velocity distribution in the larger vessels, particularly the arteries near the heart is, no doubt, very unstable. The pulsatile flow probably tends to cause the flow to be nonestablished, while the flexible walls will adsorb some of the transverse energy tending to produce an established flow more quickly.

However, by measuring the streaming potential gradient and pressure gradient along a flexible tube with a pulsatile flow, along with an evaluation of the radius of the tube from the measurement of the electrical resistance, the boundary conditions for the flow in a flexible tube can be determined. Such a procedure will follow from the theoretical considerations presented under the experimental work of this dissertation.

The Streaming Potential in Blood Flow

In this study, the term streaming potential has been limited by definition to mean the potential generated when all the streaming current is converted into a conduction current through the flowing solution. By this definition the vessel wall would have to be an insulator when compared to the conductance of the blood.

If the blood-vessel wall has an appreciable conductance compared to that of the solution, it can be considered in an identical way to that of the surface conductance k_s. This wall conductance will depend on the conductance of the cells and of the fluid between them. The potential gradient along the blood vessel will be less because the conductance of the vessel wall and the surrounding media is a parallel conductance to that of the blood itself.

Complications of Catheterization

The anticipated method for introducing electrodes into the blood vessels is by vascular catheterization. The electrodes could be mounted on the outside of the catheter near its tip with a short interval of length between the electrodes. Insulated leads through the core of the catheter could connect the electrodes to the measuring device. At least two complications

affect this method. One is the effect of the streaming current generated by the blood flowing past the catheter. The other complication is more serious, for the velocity distribution of the blood flow may be greatly affected by the introduction of the catheter.

Since the same pressure gradient will exist along the catheter as that along the vessel wall, their relative streaming currents become a ratio of the products of their zeta-potentials and their circumferences. Therefore, if the product of the zeta-potential and the circumference of the catheter is large when compared to the same product for the vessel, or if the converse is true, the problem is somewhat simplified because the course of the streaming current is then known. If that of the catheter is the controlling factor, the time for the zeta-potential to develop becomes important, as well as the determination of what constituents of the blood control the amplitude of the zeta-potential. If that of the vessel is controlling, the constituents of the blood which control the magnitude of the zeta-potential are the important factors. In consideration of the fact that the varying zeta-potentials, which have been observed in many studies, are probably the fundamental cause for lack of agreement among the many studies, the zeta-potential of the blood flow in each animal will probably have to be evaluated individually. Perhaps the zeta-potential of a vessel in an extremity can be evaluated and then used throughout the blood system.

The velocity distribution, particularly for the pulsatile flow of the arteries, is so complicated that the effect of catheterization on it can best be shown by some simplifying assumptions. If we assume that a flow is an established laminar flow in a rigid-wall tube, the introduction of a catheter whose radius is diminishingly small compared to that of the tube along the

axis of the tube will increase the resistance to flow through the tube three times. If the same catheter lies along the wall of the tube, the resistance to flow is not affected by the catheter. When the catheter has a finite radius, the displacement of the catheter reduces the cross section of the tube. This reduction consequently increases the resistance to flow. The flexibility of the blood-vessel walls probably partly compensates for these increases of resistance to flow by expanding, but this compensation cannot completely offset the increase.

Conclusions

The problem of determining whether or not the streaming potential can be used to measure blood flow appears merely complicated, not impossible. The measurement of the streaming current may be an alternative answer. However, any answer must await additional experimental study.

This writer, because of his limited knowledge of the subject, like Porrett in 1816, can only suggest that the streaming potential and electroosmosis probably play important roles in the transmission of fluids through the minute pores of the animal system. Does electroosmosis affect the filtration in the kidneys? Do streaming potential and electroosmosis play a role in the transmission of nerve impulses? The answers to these questions are still indefinite and are enveloped in ambiguities.

CONCLUSIONS

The conclusions developed in this study are based on the results of the experimental work as they apply to the fundamental mechanisms responsible for the generation of the streaming potential. Additional conclusions are included which have been drawn from studies of the literature as well as from theoretical analyses of both the methods used in this study and those used by other investigators. These conclusions are:

1. The validity of the Helmholtz-Smoluchowski streaming potential equation is dependent on the flow through the tube being established, but not necessarily laminar. An established flow is defined as one whose pressure gradient is independent of the axial distance along a tube.

2. The validity of the Helmholtz-Smoluchowski streaming potential equation for an established turbulent flow confirms in the most adequate manner the existence of a laminar film in turbulent flow.

3. The hydrodynamic boundary conditions, the velocity gradient at the wall in particular, for any nonestablished flow can be further defined by the measurement of the streaming potential between points along this flow. For example, the flow of a liquid against an increasing pressure gradient near the sharp-cornered entrance of tube 7 generates a streaming potential which shows that the average velocity near the wall is in the direction of the axial velocity.

4. The variation in the displaceable surface charge density, and consequently the day-to-day variation in zeta-potential, can be explained

by a hypothesis based on the variation in the relative rates of adsorption of the positive and negative ions on the surface.

5. The zeta-potential, or the moment of the double layer, is most accurately calculated when the conductance, which is to be used in the Helmholtz-Smoluchowski streaming potential equation, is evaluated from measurements which use the streaming current as the source of energy.

6. The electroosmotic countereffect on the streaming potential is more explicit when expressed as a modification of the Helmholtz-Smoluchowski equation or a fluid flow equation instead of as a modification of one of the terms of these equations.

7. The electroosmotic countereffect is much greater on the electroosmosis than on the streaming potential.

8. The effect of the surface conductance on the streaming current through a porous diaphragm is identical to the effect of the surface conductance on the streaming potential through a porous diaphragm.

9. The problem of determining whether or not the streaming potential can be used to measure the blood flow is very complicated, not impossible.

SYMBOLIZATION

A	area
a	radius of tube
C	capacity of conductance or reciprocal of cell constant
D	diameter of tube
d	differential operator
E	electrical potential
E_s	streaming potential
f	Moody friction factor
g	acceleration due to force of gravity
g_c	factor which converts pounds force into poundals
h	height of liquid
I	electric current
I_s	streaming current
K	electric conductance
k	specific electric conductivity
k_s	specific surface conductivity
L	length of tube
ℓ	Prandtl mixing length
lw	energy lost in fluid flow
M	electric moment (minus when adsorbed layer has a surplus of minus charges)
N	surplus electric charge present in a lamina per unit length
P	absolute pressure
ΔP	pressure difference
Q	proportion which streaming potential is reduced due to electroosmotic countereffect
R	electric resistance
R_{exp}	measured resistance
R_{calc}	theoretical resistance in absence of surface conductance
R_s	specific resistance
R_x	external resistance connected between electrodes
Re	Reynolds number
r	radial distance from axis of tube
T	temperature
t	time
u	point velocity parallel to tube axis
u_s	velocity near the wall
V	volume rate of flow
v	average velocity
W	hydrostatic resistance
X	electric force parallel to tube axis
x	distance parallel to tube axis
y	distance from wall

Z M/μ, electrokinetic coefficient

δ thickness of double layer

ϵ dielectric constant

ζ zeta-potential

θ angle about tube axis

μ coefficient of viscosity

ρ density

σ charge density

σ_s displaceable surface charge density

τ shearing stress

τ_v viscous shearing stress

τ_i inertial shearing stress

ψ point potential between axis and wall of tube

APPENDIX

APPENDIX

Included in the appendix are one table showing composition and dimensions of the streaming potential tubes, twenty-eight tables of experimental data, one table whose figures are calculated from experimental data, and four theoretical analyses.

In the tables, the potentials and pressure differences are recorded with the left point, of the points between which they are measured, as the reference point. Regardless of the direction of liquid flow through the apparatus, the recorded streaming potential is equal to the potential at the right electrode minus the potential at the left electrode. For example, a minus E indicates that the potential of the right electrode is negative with respect to the left electrode. The pressure difference is equal to the pressure at the right reservoir, or tap, minus the pressure at the left reservoir, or tap. For example, a plus ΔP indicates that the pressure at the right point is greater than that at the left point, and flow is from right to left.

TABLE 1

COMPOSITION AND DIMENSIONS OF THE STREAMING-POTENTIAL TUBES

Tube Number	Composition	Diameter (mm)	Length (cm)
1	Quartz	0.86	89.35
2	Boro silicate Glass	0.475	83.82
3a	Boro silicate Glass	1.00	83.82
3b	Boro silicate Glass	1.00	76.53
4	Boro silicate Glass	3.08	83.82
5	Teflon	0.31	11.57
6	Teflon	1.33	12.75
7	Butyl Acetate	4.9	93.75
	Tap A		0
	Tap B		30.48
	Tap C		60.96
	Tap D		76.20
	Tap E		88.90
	Tap F		90.40
	Tap G		91.90
	Tap H		93.40
	Tap I		93.75

TABLE 2

10^{-3} N KCl in Tube 1
Quartz D = 0.86 mm L = 89.35 cm

t	E_s (mv)	ΔP (cm Hg)	T (°C)	R_x (megohms)
2/26/52	Solution first entered tube.			
3/8/ 52				
	-195.6	29.2	24.3	
	-176.2	29.1		981
	-160.2	29.1		494
	-123.7	29.1		188
	-87.4	29.1		88.6
	-195.0	29.1		
	-172.6	-26.0		
	153.1	-26.0		981
	140.9	-26.0		494
	108.7	-26.0		188
	77.1	-26.0		88.6

TABLE 2 (cont.)

t	E_s	ΔP	T	R_x
	170.7	-26.0		
	-149.0	21.6		
	-133.9	21.6		981
	-121.6	21.5		494
	-94.0	21.5		188
	-66.5	21.5		88.6
	-148.3	21.5		
	125.4	-19.2		
	112.8	-19.2		981
	102.7	-19.1		494
	79.0	-19.1		188
	56.0	-19.1		88.6
	124.0	-19.1		
	-106.1	15.5	24.3	
	-95.3	15.5		981
	-86.7	15.4		494
	-67.0	15.4		188
	-47.2	15.4		88.6
	-105.6	15.4		
	89.1	-13.4		
	80.0	-13.4		981
	72.8	-13.4		494
	56.1	-13.3		188
	39.8	-13.3		88.6
	88.4	-13.3		
	-42.7	5.9		
	-38.5	5.9		981
	-35.2	5.9		494
	-27.0	5.9		188
	-19.2	5.9		88.6
	-42.8	5.9		
	27.5	-4.25		
	24.8	-4.25		981
	22.6	-4.25		494
	17.3	-4.25		188
	12.4	-4.25		88.6
	27.3	-4.25		
3/9/52	-40.0	5.83	24.3	
	-35.9	5.83		981
	-32.8	5.83		494
	-25.3	5.83		188
	-18.0	5.83		88.6
	27.3	-4.4		
	24.7	-4.4		981



TABLE 2 (cont.)

t	E_s	ΔP	T	R_x
	22.6	-4.4		494
	17.5	-4.4		188
	12.4	-4.4		88.6
	27.6	-4.4		
	-104.2	15.6		
	-93.8	15.6		981
	-85.6	15.6		494
	-66.0	15.6		188
	-46.0	15.6		88.6
	-104.5	15.6		
	90.1	-13.5		
	80.8	-13.5		981
	73.7	-13.5		494
	57.0	-13.5		188
	40.5	-13.5		88.6
	90.1	-13.5		
	-223.5	35.3		
	-211.2	35.3		981
	-192.3	35.3		494
	-148.1	35.3		188
	-104.8	35.3		88.6
	-233.7	35.3		
	216.8	-32.4		
	195.1	-32.4		981
	177.5	-32.3		494
	136.7	-32.3		188
	96.8	-32.2		88.6
	215.3	-32.2		
	-313.7	47.4		
	-281.6	47.3		981
	-255.6	47.2		494
	-197.2	47.1		188
	-139.5	47.0		88.6
	-311.5	46.9		
	292.1	-44.3		
	262.4	-44.0		981
	238.4	-43.9		494
	184.0	-43.8		188
	130.2	-43.7		88.6
	290.1	-43.6		
3/23/52	309.6	-53.64	21.5	
	309.6	-53.44		
	309.1	-53.26		
	308.8	-53.01		

TABLE 2 (cont.)

t	E_s	ΔP	T	R_x
3/23/52	226.4	-38.13		
	226.5	-28.09		
	226.1	-27.85		
	-212.3	35.57		
	-211.3	35.49		
	-210.6	35.43		
	178.6	-30.03		
	178.7	-30.00		
	178.7	-29.98		
	-166.6	27.84		
	-166.6	27.84		
	-166.4	27.80		
	128.4	-21.49		
	128.4	-21.47		
	128.4	-21.42		
	-119.6	19.89		
	-119.6	19.85		
	70.4	-11.85		
	70.5	-11.76		
	-61.0	10.07		
	-61.0	10.08		

TABLE 3

10^{-3} N KCl in Tube 3a

Boro silicate Glass D = 1.00 mm L = 83.82 cm

t	E_s	ΔP	T
11/1/50	336	-59.2	24.3
	-316	-56.6	
	310	-55.4	
	-282	49.9	
	292	-51.9	
	-280	49.6	
	283	-50.2	
	-268	47.5	24.3
	264	-45.4	
	-255	44.8	
	245	-43.0	
	237	41.5	
	233	-40.4	
	-222	38.6	

TABLE 3 (cont.)

t	E_s	ΔP	T
	219	-37.7	
	-188	32.7	
	195	-33.8	
	-180	31.2	
	181	-31.0	24.3
	-170	29.4	
	168	-28.6	
	-153	26.2	
	154	-25.7	
	-135	22.9	
	132	-21.7	
	-129	21.2	
	123	-19.2	
	-110	18.6	
	105	-17.1	
	-96	16.1	
	93	-15.4	
	-88	14.6	
	90	-14.6	
	-76	12.8	
	72	-11.9	
	-66	10.9	
	60	-9.9	
	-58	9.7	
	55	-9.1	
	-47	7.8	
	45	-7.2	24.3
	-33	5.6	
	34	-5.5	
	-22	3.7	
	21	-3.4	
	-11	1.7	
	10	-1.4	
	0	0	

TABLE 4

10^{-3} N KCl in Tube 3b

Boro silicate Glass D = 1.00 mm L = 76.53 cm

t	E	ΔP	T
1/18/51	Solution first entered tube		
1/24/51	-469	75.2	29.1
	446	-73.2	

TABLE 4 (cont.)

t	E	ΔP	T
	-430	69.5	
	405	-67.4	
	-397	64.4	
	383	-62.3	
	-365	59.3	
	347	-57.8	
	-325	54.2	29.1
	307	-52.9	29.0
	-308	50.4	
	285	-49.1	
	-283	46.4	
	267	-45.1	29.0
	-246	42.2	28.9
	243	-40.7	
	-230	37.9	28.9
	219	-36.1	
	-205	32.9	
	194	-32.1	
	-181	29.6	
	170	-27.1	
	-149	24.7	
	146	-24.3	
	-129	21.1	
	122	-19.4	
	-103	16.7	
	98	-15.8	28.9
	-77	12.3	28.8
	75	-11.8	
	-52	8.4	
	42	-6.4	
	-18	3.1	
	15	2.7	
	3	0	28.8
2/1/51	406	-67.5	27.8
	-392	64.2	28.3
	367	-61.5	
	-353	59.2	
	332	-56.2	
	-323	53.3	
	321	-53.9	
	-315	51.0	
	277	-48.5	
	-282	46.8	
	-398	65.6	
	373	-62.3	



TABLE 4 (cont.)

t	E_s	ΔP	T
	-366	60.5	28.3
	345	-58.0	28.4
	-340	55.9	
	323	-54.1	
	-304	50.7	
	286	-50.5	
	-290	48.2	
	269	-46.7	28.4
2/2/51	-422	69.8	29.6
	407	-67.1	
	-387	64.5	
	372	-62.7	
	-360	59.6	29.6
	344	-58.2	29.7
	-331	55.2	
	320	-54.2	
	-307	51.5	
	277	-49.6	
	-273	47.8	
	259	-46.3	
	-256	43.4	
	234	-41.3	29.7
	453	-76.3	29.6
	-435	72.5	
	420	-70.1	
	-397	66.8	
	378	-64.4	
	401	-68.1	
	390	-66.4	
	-384	64.6	
	353	-60.3	
	-338	56.8	
	308	-52.9	
	278	-50.3	29.6
	292	-51.6	29.5
	-293	49.8	29.5

TABLE 5

10^{-3} N KCl in Tube 4

Boro silicate Glass D = 3.08 mm L = 83.82 cm

t	E_s	ΔP	T
2/3/51	-325	59.7	30.0
	274	-55.1	
	-286	52.5	30.0

TABLE 5 (cont.)

t	E_s	ΔP	T
	262	-52.6	30.1
	-252	46.3	
	223	-40.5	
	-208	38.4	
	192	-35.2	
	-178	32.5	
	169	-30.8	
	-158	28.9	30.1
	352	-65.5	30.0
	-350	65.6	
	311	-58.0	
	-300	56.5	
	288	-54.0	
	-265	50.1	
	254	-47.8	30.0
	-254	47.7	29.9
	226	-42.3	
	-208	39.4	
	198	-37.1	
	184	34.6	
	173	-32.6	
	-163	30.6	29.9
2/12/51	310	-62.7	23.4
	-280	59.2	
	268	-55.4	
	-253	52.1	23.4
	238	-48.8	23.3
	-255	46.6	
	215	-43.6	
	-210	41.1	
	191	-38.8	
	-162	37.3	
	179	-36.0	
	-153	31.3	
	297	-60.2	
	-292	59.9	
	327	-66.8	
	-312	63.7	
	291	-60.1	
	-282	57.5	
	263	-53.8	
	-254	52.0	
	241	-49.0	
	-226	46.2	
	218	-43.5	

TABLE 5 (cont.)

t	E_s	ΔP	T
	-203	40.9	
	189	-38.5	
	-177	35.9	23.3

TABLE 6

Physiological Saline in Tube 1

Quartz D = 0.86 mm L = 89.35 cm

t	E_s	ΔP	T
7/22/50	-0.85	26.8	
	-1.02	21.1	
	-0.8	16.9	
	-0.69	12.4	
	-0.65	6.2	
	-0.35	2.4	
	-0.4	0	
	-1.05	30.7	
	-0.64	27.9	
	-0.65	24.6	
	-0.64	19.9	
	-0.25	17.2	
	-0.33	13.1	
	-0.11	9.2	
	-0.30	7.0	
	-0.22	4.4	
	-0.19	2.5	
	-0.29	1.1	
	-0.095	0	
	-0.032	-0.8	
	0	-2.4	
	0.016	-5.2	
	0.22	-7.2	
	-0.063	-10.0	
	0.11	-14.3	
	0.25	-17.4	
	0.32	-22.9	
	0.41	-27.3	
	0.55	-28.9	
	0.52	-25.5	
	0.32	-21.9	

TABLE 6 (cont.)

t	E_s	ΔP	T
	0.19	-17.4	
	0.21	-12.5	
	-0.063	-8.3	
	0.032	-3.7	
	0.079	-2.2	
	-0.032	-0.6	
	-0.079	0	

TABLE 7

Physiological Saline in Tube 2

Boro silicate Glass D= 0.475 mm L = 83.32 cm

t	E_s	ΔP	T	R_x
6/11/52	2.2	0		
	3.0	-45.0		
	2.9	-33.1		
	2.8	-20.2		
	2.8	-19.6		
	2.6	-10.6		
	2.4	0		
	2.3	9.0		
	2.0	21.0		
	1.9	27.6		
	1.8	34.9		
	1.6	38.8		
	1.9	22.1		
	2.0	11.6		
	2.1	5.1		
	2.2	0		
	2.2	-3.9		
	2.3	-14.5		
	2.4	-23.3		
	2.6	-32.3		
	2.6	-35.0		
	2.3	-34.8		20.15
	2.1	-20.2		20.15
	2.0	-11.0		20.15

TABLE 7 (cont.)

t	E_s	ΔP	T	R_x
	1.9	3.4		20.15
	1.7	0		20.15
	1.7	7.2		20.15
	1.6	15.1		20.15
	1.5	23.8		20.15
	1.4	33.2		20.15
	1.0	47.6		10.04
	1.2	38.7		10.04
	1.3	25.5		10.04
	1.4	15.4		10.04
	1.4	9.4		10.04
	1.5	3.7		10.04
	1.5	0		10.04
	1.6	-9.7		10.04
	1.6	-18.3		10.04
	2.0	-44.7		10.04
6/12/51	1.6	0		
	1.95	-13.0		
	2.0	-21.2		
	2.2	-29.9		
	2.45	-41.8		
	2.6	-51.5		
	2.4	-38.3		
	2.2	-26.3		
	2.2	-10.7		
	1.85	3.5		
	1.9	0		
	1.7	10.2		
	1.55	19.3		
	1.45	28.0		
	1.4	39.0		
	1.25	48.9		
	1.45	40.2		
	1.6	29.7		
	1.7	21.4		
	1.9	10.8		
	1.9	5.8		
	2.0	0		
	1.8	-10.7		20.15
	1.9	-23.8		20.15
	2.0	-29.3		20.15
	2.05	-37.8		20.15
	2.2	-46.9		20.15
	2.1	-38.4		20.15

TABLE 7 (cont.)

t	E_s	ΔP	T	R_x
	2.0	27.4		20.15
	1.9	-19.7		20.15
	1.8	-10.5		20.15
	1.75	-3.6		20.15
	1.7	0		20.15
	1.65	14.0		20.15
	1.5	24.5		20.15
	1.45	33.6		20.15
	1.2	53.4		20.15
	1.45	41.0		20.15
	1.55	28.9		20.15
	1.6	21.4		20.15
	1.6	11.0		20.15
	1.7	0		20.15
	1.6	-10.2		10.04
	1.7	-20.7		10.04
	1.8	-31.3		10.04
	1.9	-41.6		10.04
	1.95	-52.8		10.04
	1.95	-46.1		10.04
	1.8	-35.7		10.04
	1.7	-16.5		10.04
	1.6	0		10.04
	1.7	10.6		10.04
	1.65	19.7		10.04
	1.55	30.2		10.04
	1.5	40.2		10.04
	1.3	53.6		10.04
	1.4	40.7		10.04
	1.5	31.8		10.04
	1.6	20.8		10.04
	1.65	11.8		10.04
	1.75	0		10.04

TABLE 8

10^{-2} N NaCl in Tube 1

Quartz D = 0.86 mm L = 89.35 cm

t	E_s	ΔP	T
7/20/50	-7.5	13.6	
	-6.0	10.2	

TABLE 8 (cont.)

t	E_s	ΔP	T
	-5.5	8.8	
	-4.5	4.3	
	-2.5	2.2	
	0	0	
	-7.5	12.8	
	-4.5	7.9	
	-2	4.7	
	-0.5	2.4	
	0	0	
7/21/50	-16	24.6	
	-15	22.2	
	-13.5	19.2	
	-11.5	16.3	
	-9.5	14.0	
	-7	11.7	
	-5.5	7.8	
	-4	5.3	
	-1.5	3.0	
	-1	1.1	
	0	0	
	-15.9	27.9	
	-15.5	25.7	
	-13.8	22.8	
	-10.4	17.8	
	-8.7	14.0	
	-6.5	11.2	
	-4.6	7.5	
	-3.0	4.7	
	-1.8	2.0	
	-1.2	0.5	
	0	0	
	15	-24.6	
	13.5	-20.8	
	12	-16.9	
	9	-11.9	
	5.5	-8.7	
	4	-5.6	
	1.5	-3.2	
	0.5	1.6	
	0.2	0	

TABLE 9

10^{-3} N NaCl in Tube 1

Quartz D = 0.86 mm L = 89.35 cm

t	E_s	ΔP	T
7/20/50	-154	21.5	
	140	19.2	
	-125	16.5	
	-110	14.9	
	-95	12.6	
	-82	10.5	
	-69	8.5	
	56	7.0	
	-46	5.8	
	-38	4.5	
	-31	3.4	
	20	2.3	
	-13	1.5	
	-8	0.7	
	-4	0	
	-23	0.5	
	-33	1.5	
	-40	2.7	
	-53	4.5	
	-73	7.3	
	-87	9.9	
	-109	12.8	
	-130	15.2	
	-153	18.4	
	-179	21.8	
	163	19.6	
	-148	17.8	
	-130	15.1	
	-95	10.7	
	-75	7.4	
	-55	4.8	
	-38	2.1	
	22	0.4	
	-18	0	
	-10	-0.9	
	0	-2.3	
	15	-4.3	
	33	-6.8	
	58	-10.2	
	91	-14.5	

TABLE 9 (cont.)

t	E_s	ΔP	T
	113	-17.5	
	131	-20.2	
	118	-18.2	
	105	-16.0	
	90	-14.2	
	75	12.7	
	60	-10.4	
	48	-8.8	
	33	-6.6	
	21	-4.9	
	10	-3.3	
	0	-1.8	
	-10	-0.6	
	-13	0	

TABLE 10

10^{-3} N NaCl in Tube 2

Boro silicate D = 0.475 mm L = 83.82 cm

t	E_s (mv)	ΔP (cm Hg)	T (°C)	R_x (Megohms)
3/27/52				
A.M.				
10:06	Solution first entered tube.			
10:18	166.2	-42.02	24.6	
10:25	178.9	-42.02		
10:28	182.7	-42.02		
10:32	172	-42.02		
10:35	177	-42.02		
10:36	179	-42.02		
10:39	184	-42.02		
10:45	182	-42.01		
10:50	187	-42.01		
10:55	192	-42.08		
11:05	199	-42.08		
11:10	200	-42.08		
11:15	202	-42.08		
P.M.				
12:46	208	-41.53		
1:09	234	-45.93	24.3	

TABLE 10 (cont.)

t	E_s (mv)	ΔP (cm Hg)	T (°C)	R_x (Megohms)
2:00	231.6	-45.60		
3:00	227.6	-44.86		
3:50	219.1	-44.51	24.3	
	158.0	-44.51		981
	123.7	-44.51		494
5 00	226.7	-44.25		
	163.0	-44.25		981
	127.7	-44.25		494
7 00	206.7	-43.60	24.2	
	147.5	-43.60		981
	115.2	-43.60		494
	210.7	39.43		
	-152.0	39.43		981
	-119.3	39.43		494
3/28/52				
A.M.				
11:15	129.4	-26.08	23.7	
P.M.				
1:10	134.5	-25.94		
4.30	126.5	-25.47	23.6	
	90.5	-25.47		981
	70.9	-25.47		494
	-137.8	25.76		
	-99.1	25.76		981
	77.6	25.76		494
	178.0	-36.03		
	128.4	-36.03		981
	100.6	-36.03		494
	179.0	-36.03		
	-198.7	35.91		
	-143.0	35.91		981
	-112.4	35.91		494
	198.9	35.91		
3/29/52				
P.M.				
3:00	-359.3	69.93	23.0	
	-257.0	69.87	23.0	981
	-358.6	69.82	23.0	
	-200.8	69.75	23.0	494
	-357.5	69.66	23 0	
	-116.7	69.60	23.0	188
	-356.8	69.57		
	66.4	69.58		88 6

TABLE 10 (cont.)

t	E_s	ΔP	T	R_x
	-355.6	69.51		
	-40.7	69.45		50.1
	-358.2	70.23		
	-17.7	70.16		20.15
	-358.0	70.11		
	-9.1	70.05		10.04
4:30	-358.1	70.01	23.0	
8:00	288.3	-77.60	23.4	
	278.8	-77.59	23.4	981
	388.7	-77.55	23.4	
	218.1	-77.55	23.4	494
	388.6	-77.54	23.4	
	127.2	-77.50	23.4	188
	388.4	-77.50	23.4	
	72.4	-77.48	23.4	88.6
	387.9	-77.45	23.4	
	44.6	-77.43	23 4	50.1
	388.3	-77.39	23.4	
	-379.4	74.31	23 4	
	-271.8	74.31		981
	-378.5	74.29		
	-212.3	74.27		494
	-378.0	74.27	23.4	
3/30/52 P.M.				
6:00	-360.2	68.09	23.8	
	-257.3	68.06		981
	-356.7	68.05		
	-200.7	68.03		494
	-354.8	67.99		
	-116.3	67.97		188
	-352.7	67.96		
	-10.1	0		
	318.7	-65.23		
	230.5	-65.29		981
	320.5	-65.27		
	181.2	-65.25		494
	320.9	-65.25		
	106.3	-65.20		188
	321.8	-65.10		
	-7.1	0		
	-6.6	0		
	312.5	-62.87		
	225.2	-62.87		981

TABLE 10 (cont.)

t	E_s	ΔP	T	R_x
	312.5	-62.86		
	-6.3	0		
	-312.9	60.79		
	-224.7	60.89	23.8	981
	-312.1	60.89		
	-5.2	0		
3/31/52	284.0	-58.49		
	205.6	-58.48		981
	285.8	-58.48		
	162.5	-58.47		494
	287.0	-58.49		
	-290.5	56.86		
	-208.9	56.86		981
	-289.8	56.86		
	-163.7	56.84		494
	-288.6	56.81		
	-95.6	56.81		188
	-288.2	56.79		
	0	-1.21	23.9	

The tube unintentionally emptied of solution when there was not sufficient solution in the left reservoir to maintain an overnight continuous flow.

4/1/52 A.M.			
9:00	Tube refilled		
9:03	-250.2	41.06	
9:06	-241.0	40.45	
9:09	-236.3	40.18	24.2
9:13	-232.0	39.78	
9:16	-228.6	39.39	
9:18	-34.6	4.04	
9:21	-223.6	38.59	
9:27	-222.4	38.85	
9:30	-32.4	3.96	24.2
9:32	-108.5	17.79	
9:35	-181.7	31.16	
9:38	-217.6	38.26	
9:40	-266.6	47.23	
9:48	-263.5	47.02	
10:54	-260.0	46.49	
10:57	-222.6	39.22	
11:00	-149.4	25.44	
11:03	-62.8	9.35	24.2

TABLE 10 (cont.)

t	E_s	ΔP	T	R_x
P.M.				
8:00	-251.3	45.25	23.7	
	-181.2	45.22		981
	-252.2	45.21		
	-142.2	45.20		494
	-251.8	45.15		
	-352.4	64.13		
	-253.9	64.06		981
	-352.0	64.01		
	-200.0	63.98		494
	-353.0	63.98		
	294.5	-60.79		
	212.8	-60.79		981
	292.1	-60.79		
	166.0	-60.79		494
	288.3	-60.79		
	175.6	-42.87		
	63.0	-16.83		
	-33.2	-2.42		
	-142.1	14.95		
4/1/52				
P.M.				
	-205.5	26.28		
	-276.5	42.00		
	-386.8	59.26	23.7	
4/2/52	218.2	-42.87	24.4	
	257.1	-49.79		
	184.4	-49.63		981
	256.0	-49.61		
	144.1	-49.55	24.1	
	256.5	-49.49	24.2	
	187.9	-36.32	24.2	
	95.2	18.78	24.2	
	0	-1.12	24.2	
	-100.5	18.49	24.2	
	-199.5	37.42	24.2	
	-252.6	47.66	24.1	
4/3/52	376.9	-73.40	23.7	
	270.0	-73.38		981
	377.5	-73.34	23.6	
	211.8	-73.32	23.6	494
	377.5	-73.29		

TABLE 10 (cont.)

t	E_s	ΔP	T	R_x
	123.2	-73.23	23.5	188
	377.4	-73.21		
	245.6	-47.83	23.5	
	129.6	-25.46	23.5	
	0	-0.56	23.5	
	-137.4	26.06	23.5	
	-252.4	48.18		
	-374.2	71.58	23.5	
4/4/52	-402.1	66.67	23.7	
	-291.3	66.64	23.7	981
	-397.2	66.61	23.7	
	-227.2	66.56	23.7	494
	-394.6	66.54	23.7	
	-134.0	66.51	23.7	188
	Air bubble removed from near left electrode			
	-348.0	66.20	23.7	
	-208.6	39.36	23.7	
	0	-0.91	23.7	
	126.3	-25.37	23.6	
	234.0	-46.18	23.7	
	336.0	-65.99	23.7	
4/5/52	293.2	-59.09	23.0	
	209.9	-59.06	23.0	981
	293.2	-59.04		
	164.0	-59.03	23.0	494
	293.1	-59.00	23.0	
	95.1	-58.99	23.0	188
	293.0	-59.00	23.0	
	229.4	-46.18	22.9	
	113.7	-22.93	22.9	
	0	-0.03	22.9	
	-106.4	21.30	22.9	
	-199.9	40.12	22.9	
	-282.6	56.57	22.9	
4/6/52	395.0	-79.53	23.6	
	282.6	-79.33	23.6	981
	392.4	-78.98	23.6	
	219.5	-78.76	23.6	494
	390.4	-78.59	23.6	

TABLE 10 (cont.)

t	E_s	ΔP	T	R_x
	289.2	-58.25	23.5	
	199.9	-40.33	23.5	
	96.5	-19.57	23.5	
	-0.1	-0.14	23.5	
	-89.5	17.86	23.5	
	-195.5	39.12	23.5	
	-279.0	56.01	23.5	
	-363.1	72.95	23.5	
4/7/52				
P.M.	397.1	-79.95	23.5	
	284.6	-79.92		981
	297.2	-79.95	23.5	
	222.6	-79.90	23.5	494
	397.1	-79.90		
	129.5	-79.87		188
	397.1	-79.85	23.4	
	323.5	-65.03	23.3	
	253.6	-51.02	23.3	
	170.9	-35.40	23.3	
	93.1	-18.82	23.3	
	0.5	-0.25	23.2	
	-92.8	18.54	23.2	
	-160.8	32.21	23.3	
	-234.2	47.01	23.3	
	-310.2	62.29	23.3	
	-379.9	76.32	23.3	
	-213.2	76.36	23.3	494
	-380.5	76.39	23.4	
4/9/52	366.6	-73.66	23.8	
	263.1	-73.68	23.7	981
	366.9	-73.70	23.7	
	259.6	-52.15	23.7	
	102.8	-20.80	23.7	
	1.0	-0.34	23.7	
	-105.5	21.15	23.7	
	-253.3	50.75	23.7	
	-348.9	69.99	23.7	

TABLE 11

10^{-3} N NaCl in Tube 3a

Boro silicate Glass D = 1.00 mm L = 83.82 cm

t	E_s	ΔP	T
9/6/50	Solution first entered tube.		
9/8/50	-63	31.6	21.8
	-32	38.9	
	-25	26.5	
	0	21.2	
	37	18.1	
	87	15.6	
	103	10.9	
	150	7.5	
	130	4.4	
	185	1.4	
	240	0	
	445	-29.9	
	410	-23.8	
	350	-17.8	
	300	-12.8	
	208	-6.7	
	229	-4.4	
	205	-0.9	
	183	0	
	-158	36.0	
	-111	33.3	
	-42	30.8	
	-76	28.8	
	-63	26.3	
	-54	23.7	
	-17	20.4	
	0.5	17.9	
	45	15.7	
	64	10.6	
	86	8.0	
	120	5.8	
	149	2.9	
	168	0.8	
	178	0	
	178	-1.4	
	182	-2.3	
	205	-5.4	
	241	-8.3	
	285	-14.1	

TABLE 11 (cont.)

t	E_s	ΔP	T
	338	-19.5	
	372	-24.9	
	437	-32.4	
9/14/50	23	0	20.1
	0	1.5	
	-21	3.1	
	-37	4.8	
	-63	10.4	
	-98	16.3	
	-128	19.5	
	-148	25.8	
	-223	33.4	
	-259	38.9	
	-316	47.2	
	-365	52.6	
	-382	58.5	
	-358	55.1	
	-350	50.7	
	-282	45.6	
	-260	41.2	
	-228	36.5	
	-153	29.7	
	-124	25.8	
	-75	19.6	
	-45	16.2	20.1
	73	0	20.1
	90	-1.9	
	135	-6.6	
	187	-13.5	
	225	-17.8	
	300	-26.5	
	335	-32.4	
	360	-36.0	
	375	-39.2	
	421	-45.7	
	488	-53.0	
	440	-47.0	
	393	-42.6	
	364	-38.3	
	337	-33.9	
	274	-26.9	
	225	-19.5	
	150	-12.3	
	116	-6.7	

TABLE 11 (cont.)

t	E_s	ΔP	T
	75	-2.8	
	44	-0	
9/15/50	3	0	
	15	-1.6	
	42	-5.0	
	58	-6.9	
	83	-10.4	
	141	-17.1	
	168	-21.7	
	221	-27.4	
	263	-31.8	
	322	-39.2	
	333	-41.9	
	375	-48.7	
	431	-54.0	
	468	-59.6	
	500	-63.8	
	513	-67.1	
	358	-45.4	
	339	-41.9	
	310	-38.2	
	277	-35.0	
	263	-31.2	
	224	-26.4	
	179	-21.9	
	146	-17.2	
	125	-14.0	
	78	-9.0	
	53	-5.9	
	23	-2.5	
	0	0	
9/19/50	28	0	18.6
	10	1.5	
	-55	10.2	
	-89	20.5	
	-160	29.3	
	270	41.9	
	-378	49.9	
	-465	60.1	
	-566	70.4	



TABLE 12

10^{-3} N NaCl in Tube 3a

Boro silicate Glass D = 1.00 mm L = 83.82 cm

t	E_s	Δp	T
10/9/50	46.5	-5.15	21.9
	43.5	-4.78	
	40	-4.41	
	38	-4.05	
	35	-3.68	
	31.5	-3.31	
	28.5	-2.94	
	25.5	-2.57	
	22.5	-2.21	
	20	-1.84	
	17.5	-1.47	
	14.5	-1.10	
	12	-0.920	
	10.5	-0.735	
	9	-0.552	
	7.5	-0.368	
	6	-0.184	
	4	0	
	0	0	
	2	-0.184	
	4	-0.368	
	4.5	-0.552	
	7	-0.735	
	8.5	-0.920	
	10	-1.10	
	13.5	-1.47	
	16.5	-1.84	
	19.5	-2.21	
	23	-2.57	
	25.5	-2.94	
	28.5	-3.31	
	31.5	-3.68	
	35	-4.05	
	38	-4.41	
	41	-4.78	
	44.5	-5.15	21.9
	-44.5	5.15	21.9
	-41.5	4.78	
	-37	4.41	
	-34.5	4.05	

TABLE 12 (cont.)

t	E_s	ΔP	T
	-31.5	3.68	
	-28	3.31	
	-25.5	2.94	
	-23	2.57	
	-18.5	2.21	
	-16	1.84	
	-12.5	1.47	
	-9	1.10	
	-7.5	0.920	
	-6.5	0.735	
	-4.5	0.552	
	-3.5	0.368	
	-2	0.184	
	0	0	
	-5	0	
	-6.5	0.184	21.9
	-7.5	0.368	
	-9	0.552	
	-10.5	0.735	
	-12	0.920	
	-13.5	1.10	
	-16.5	1.47	
	-20	1.84	
	-22.5	2.21	
	-25	2.57	
	-28.5	2.94	
	-31.5	3.31	
	-35	3.68	
	-38.5	4.05	
	-41	4.41	
	-44.5	4.78	
	-48	5.15	
10/10/50	485	-58.8	21.7
	-466	55.3	
	454	-53.6	
	-433	50.0	
	412	-48.2	
	-389	45.5	
	378	-44.9	22.0
	-360	41.4	
	347	-40.4	
	-336	38.0	
	322	-37.1	
	-308	34.6	



TABLE 12 (cont.)

t	E_s	ΔP	T
	286	-33.5	
	-273	31.1	
	261	-30.2	
	-253	28.7	
	241	-27.3	
	-223	24.7	
10/20/50	448	-58.0	22.4
	-415	54.0	
	399	-51.8	
	-377	48.9	
	365	-47.1	
	-341	44.0	
	326	-42.0	
	-313	40.1	
	303	-38.7	
	-281	36.1	
	272	-34.0	
	-252	32.1	22.3
	243	-30.5	
	-239	30.2	
	210	-26.4	
	-211	26.5	
	201	-25.2	
	-189	23.7	
	177	-21.9	
	-168	21.0	
	175	-21.7	
	-156	19.4	
	119	-16.7	
	-146	18.4	
	136	-16.8	
	-131	16.4	
	135	-16.4	
	-116	14.2	
	112	-13.8	
	-104	12.9	
	110	-13.3	
	-100	12.5	
	98	-11.9	
	-88	10.8	
	85	-10.2	
	-77	9.6	
	76	-9.1	
	-66	8.4	
	65	-7.7	

TABLE 12 (cont.)

t	E_s	ΔP	T
	-57	6.9	
	46	-5.4	
	-33	4.4	
	21	-2.1	
	-18	2.4	
	0	0	22.3
10/21/50	1	0	22.0
	21	-2.4	
	36	-4.3	
	63	-7.4	
	90	-11.0	
	132	-16.0	
	184	-22.1	
	229	-28.0	
	273	-33.2	
	315	-38.8	
	357	-44.0	
	401	-50.1	
	451	-56.3	
	514	-63.1	
	553	-67.9	
	-509	63.8	
	-462	58.4	
	-431	54.3	
	-386	48.1	
	-334	41.3	
	-286	34.8	
	-215	26.1	
	-152	18.5	
	-127	15.2	
	-99	11.7	
	-65	7.5	
	1	0	22.0

TABLE 13

10^{-3} N NaCl in Tube 4

Boro silicate Glass D = 3.08 mm L = 83.82 cm

t	E_s	ΔP	T
9/23/50	20	0	
	29	-2.1	
	68	-7.1	

TABLE 13 (cont.)

t	E_s	ΔP	T
	130	-16.0	
	285	-37.7	
	23	0	
	-75	16.0	
	-260	37.7	
	-363	52.1	
	19	0	
	370	-48.2	
	375	-49.2	
	-320	46.9	
	-200	30.3	
	13	0	
	325	-41.0	
	240	-32.0	
	115	-13.7	
	17	0	
	-273	38.7	
9/24/50	3	0	18.8
	-250	31.3	
	0	0	
	240	-30.0	
	1	0	
	-213	36.2	
	-183	26.2	
	-187	25.2	
	-180	24.7	
	200	-25.2	
	220	-25.6	
	210	-25.9	
	210	-25.9	
	-175	24.0	
	-168	23.0	
	165	-18.6	
	163	-18.4	
	157	-18.6	
	-123	16.5	
	-120	16.3	
	-120	16.3	
	135	-14.4	
	130	-14.4	
	127	-14.6	
	-93	13.2	
	-90	13.2	
	-88	13.0	
	115	-12.5	

TABLE 13 (cont.)

t	E_s	ΔP	T
	105	-11.0	
	15	0	
	107	-11.2	
10/2/50	-13	2.21	22.2
	13.5	1.84	22.2
	-10	1.47	22.3
	11.5	-1.47	
	-5.8	1.10	
	5.6	-0.735	
	-2.5	0.368	
	2.5	-0.368	
10/4/50	435	-58.0	
	-421	55.8	
	343	-45.6	
	-363	48.5	
	344	-45.6	
	304	-39.8	
	-286	37.3	
	264	-35.6	
	-258	33.5	
	242	-31.7	
	-209	28.9	
	185	-23.8	
	-169	21.9	
	155	-20.3	
	-147	18.6	
	132	-17.1	
	-123	15.5	
	113	-14.3	
	-105	13.2	
10/5/50	-418	54.8	20.5
	388	-51.3	
	-378	49.1	20.4
	342	-44.6	
	-310	40.1	20.5
	285	-37.8	
	-273	35.5	
	245	-32.1	
	-236	30.6	
	222	-28.8	
	-205	26.7	
	190	-25.0	20.5

TABLE 13 (cont.)

t	E_s	ΔP	T
	-184	23.5	
	170	-21.8	
	-159	20.4	
	147	-18.8	
	-137	17.5	
	126	-16.0	
	-119	15.1	
	110	-14.1	
	-104	13.2	
	92	-12.1	
	-86	11.1	
	78	-10.0	
	-72	9.2	
	70	-9.1	
	-59	7.8	
	59	-7.4	
	-53	6.3	
	43	-5.3	
	-35	4.6	
	32	-4.3	
	-25	3.2	
	22	-2.7	
	-22	2.8	
	7	-1.1	
	-14	1.7	
10/6/50	-42	5.52	20.8
	-38	5.15	
	-44	5.88	
	-43	5.52	
	-38	5.15	
	-35	4.78	
	-34	4.41	
	-30	4.05	
	47	-5.88	
	44	-5.52	
	41	-5.15	
	38	-4.78	
	35	-4.41	
	31	-4.05	
	29	-3.68	
	25	-3.31	
	22	-2.94	
	20	-2.57	
	17	-2.21	

TABLE 13 (cont.)

t	E_s	ΔP	T
	-34	4.41	
	-30	4.05	
	-28	3.68	
	-25	3.31	
	-21	2.94	
	-18	2.57	
	-16	2.21	
	-14	1.84	
	-12	1.47	
	-10	1.10	
	-7	0.735	
	-4	0.368	
	-1	0	
	29	-3.68	20.7
	25	-3.31	
	22	-2.94	
	19	-2.57	
	17	-2.21	
	15	-1.84	
	12	-1.47	
	9	-1.10	
	10	-0.735	
	3	-0.368	
	0	0	
10/7/50	-16	2.21	20.6
	-14.5	2.02	
	-13.5	1.84	
	-12.5	1.65	
	-11.5	1.47	
	-11	1.29	
	-9.5	1.10	
	-8	0.920	
	-6.5	0.735	
	-5.5	0.552	
	-4.5	0.368	
	-2.5	0.184	
	-1	0	
	17	-2.21	
	16	-2.02	
	14.5	-1.84	
	13.5	-1.65	
	12.5	-1.47	
	11	-1.29	
	9.5	-1.10	



TABLE 13 (cont.)

t	E_s	ΔP	T
	8	-0.920	
	6.5	-0.735	
	5	-0.552	
	3.5	-0.368	
	2	-0.184	
	0	0	

TABLE 14

10^{-3} N NaCl in Tube 4

Boro silicate Glass D = 3.08 mm L = 83.82 cm

t	E_s	ΔP	T	R_x
4/9/52				
A.M.				
10:46	Solution first entered tube.			
11:02	-186.4	35.98		
11:04	-175.4	33.84		
	-160.1	30.94	23.5	
11:12	173	-31.98		
11:14	158.5	-30.58		
	153.0	-29.64		
	174.0	-28.43		
11:18	142.0	-27.53	23.5	
11:21	-148.0	28.55		
11:22	-143.0	27.62		
11:23	-138.0	26.65		
	-124.0	24.00	23.5	
11:33	128.0	-24.92		
	123.0	-23.90		
	117.0	-22.73		
	106.0	-20.74	23.5	
P.M.				
2:10	-112.0	21.23	23.7	
	-94.0	20.12		88.6
	-99.0	19.08		
	-95.0	18.43		
2:17	-92.0	17.80	23.6	
	97.0	-18.83		
	78.0	-18.59		50.1
	88.0	-17.15		

TABLE 14 (cont.)

t	E_s	ΔP	T	R_x
	85.0	-16.54		
	54.4	-15.62		20.15
	75.0	-14.59	23.5	
9:00	3.7	-0.855	24.1	
	2.5	-0.628		
	1.9	-0.503		
	1.2	-0.366		
	0.6	-0.273	24.0	
	-4.9	0.890		
	-4.4	0.771		
	-3.7	0.628		
	-2.95	0.478		
	-2.3	0.330		
	-1.7	0.208		
	3.3	-0.798		
	2.2	-0.506		
	1.5	-0.388		
4/10/52				
A.M.				
10:00	5.1	-1.153	23.5	
	4.4	-1.093		
	3.0	-0.706	23.5	
	2.0	-0.468		
	1.0	-0.259		
	0	-0.042		
P.M.				
1:00	-4.7	0.955		
	-4.0	0.778	23.5	
	-3.0	0.543		
	-2.0	0.333		
	-1.0	0.145		
	0	-0.037		
1:30	5.2	-1.213	23.5	
	4.3	-1.044		
	3.7	-0.905		
	2.8	-0.709		
	2.2	-0.568		
	1.5	-0.435		
	0.7	-0.276		
	-0.3	-0.044		
	-4.7	0.922		
	-4.0	0.763		
	-3.2	0.617		
	-2.3	0.410	23.4	
	-1.5	0.245		



TABLE 14 (cont.)

t	E_s	ΔP	T	R_x
	-0.7	0.086		
	0.4	-0.093		
3:00	55.2	-10.92	23.4	
	47.9	-9.79		
	-44.3	8.92		
	-40.5	8.22		
	-29.9	6.22		
	-27.8	5.81	23.4	
	-24.8	5.06		
	36.0	-6.03		
	27.4	-5.63		
4/11/52	-49.0	9.68	22.0	
	-45.0	8.96	22.0	
	45.0	-8.97		
	28.0	-5.71	22.1	
	24.0	-5.00		
	-29.0	5.77		
	-26.0	5.23	22.2	
	-10.0	2.28	23.5	
	-7.9	1.64	23.5	
	-6.3	1.26		
	-5.3	1.02		
	6.6	-1.54	23.6	
	4.8	-1.14		
	-4.2	0.789	23.7	
	-3.7	0.667		
	-2.5	0.440	23.7	
	-1.4	0.246		
	-0.5	0.078		
	5.4	-1.183		
	4.4	-1.055		
	3.4	-0.772		
	2.0	-0.474		
	0.8	-0.296		
	0.1	-0.084	23.8	
4/12/52	-133.0	26.01		
	-129.0	25.14		
	-124.0	24.26		
	-121.0	23.65		
	124.0	-24.24		
	120.0	-23.45	22.5	
	111.0	-21.75		
	-108.0	21.14		
	-101.0	19.77	22.5	
	-92.0	17.99		

TABLE 14 (cont.)

t	E_s	ΔP	T	R_x
	95.00	-18.67	22.4	
	84.0	-16.55		
	-80.0	15.71		
	-76.0	14.92		
	-65.0	12.87	22.5	
	-60.0	11.90	22.5	
	67.0	-13.28		
	57.0	-11.37		
	42.0	-8.48		
	40.0	-8.14		
	-47.0	9.33		
	-42.0	8.43		
	-37.0	7.48		
	-30.0	5.95		
	30.0	-6.12		
	25.0	-5.18		
(Trans)	-25.0	5.04		
(Lam)	-11.0	2.65		
(Lam)	10.0	-2.50		
	7.1	-1.72		
	5.8	-1.36		
	-8.4	1.81		
	-7.3	1.55		
	-5.8	1.16		
	-4.4	0.82		
	3.5	-0.94	22.8	
	-5.0	1.065		
	-4.8	0.910		
	-4.1	0.722	22.8	
	-3.4	0.580		
	-2.7	0.425		
	-1.5	0.143		
	-0.7	0.058	22.8	
	5.5	-1.254		
	5.0	-1.173		
	4.5	-1.059		
	4.0	-0.958		
	3.5	-0.849		
	3.0	-0.740		
	2.5	-0.631		
	1.5	-0.410		
	0.3	-0.157		
	0.3	-0.035		

TABLE 14 (cont.)

t	E_s	ΔP	T	R_x
4/14/52	141.0	-27.66	23.5	
	135.0	-26.55	23.5	
	-138.0	25.36	23.5	
	-123.0	24.24	23.5	
	119.0	-23.83		
	57.0	-21.81		10.04
	106.0	-20.92	23.5	
	-108.0	21.15		
	-52.0	19.72		10.04
	-95.0	18.73	23.5	
	94.0	-18.51		
	-83.0	16.35		
	79.0	-15.75	23.5	
	-73.0	14.33		
	67.0	-13.39		
	-64.0	12.51		
	58.0	-11.59		
	-56.0	11.13	23.5	
	50.0	-10.10		
	-47.0	9.51		
	41.0	-8.33		
	-36.0	7.27		
	30.0	-6.39	23.5	
(Trans)	-23.0	4.74		
(Trans)	21.0	-4.38		
	8.6	-2.09		
	8.8	-2.14		
	-10.8	2.45		
	-9.4	2.10		
	-7.9	1.72		
	-6.3	1.27		
	-5.0	1.00		
	8.0	-1.95		
	6.5	-1.59		
	5.0	-1.23	23.5	
	-5.5	1.087		
	-4.4	0.793		
	-2.5	0.418		
	-0.8	0.103		
	5.5	-1.308	23.5	
	4.3	-1.032		
	2.6	-0.735		
	1.3	-0.368		
	-0.6	0.012	23.5	

TABLE 14 (cont.)

t	E_s	ΔP	T	R_x
4/15/52	167.0	-32.41	23.7	
	160.0	-31.03		
	-158.0	30.74	23.7	
	-146.0	28.42		
	145.0	-28.09	23.7	
	133.0	-25.85		
	-129.0	25.04	23.7	
	117.0	-22.82		
	-111.0	21.58		
	100.0	-19.58		
	-91.0	17.77		
	82.0	-16.13	23.7	
	-74.0	14.49		
	63.0	-12.95		
	-58.0	12.39		
	49.0	-9.76		
	-43.0	8.51	23.7	
	37.0	-7.47		
	-35.0	6.99		
	30.0	-6.11		
(Trans)	-28.0	5.62		
(Trans)	26.0	-5.33		
	9.2	-2.25		
	-10.5	2.36		
	7.5	-1.85		
	-7.8	1.68		
	6.3	-1.474	23.7	
	5.5	-1.328		
	4.2	-1.033		
	2.8	-0.710	23.7	
	1.0	-0.339		
	-5.0	0.970		
	-3.8	0.658		
	-1.2	0.145	23.7	
4/18/52	8.2	-2.21	24.2	
	7.0	-1.826		
	6.0	-1.571	24.2	
	5.0	-1.342		
	4.3	-1.160	24.2	
	2.7	-0.787		
	-8.7	1.833		
	-7.7	1.551		
	-6.9	1.425	24.2	
	-6.1	1.240		
	-5.5	1.104	24.2	



TABLE 14 (cont.)

t	E_s	ΔP	T	R_x
	-4.7	0.879		
	-4.0	0.739		
	-3.3	0.615	24.2	
	0.3	-0.214		
	9.0	-2.22		
	-9.7	2.26		
	222.0	-43.65		
	213.0	-41.94		
	-205.0	40.34		
	-195.0	38.35		
	187.0	-36.69		
	175.0	-34.40		
	-168.0	33.02		
	-154.0	30.32		
	136.0	-26.89		
	-117.0	23.14		
	108.0	-21.37		
	-90.0	17.86		
	73.0	-14.62		
	-46.0	9.38		
	33.L	-6.80		
4/19/52	8.7	-2.16	25.3	
	8.0	-1.937		
	7.0	-1.690		
	6.2	-1.495		
	5.0	-1.232		
	4.0	-0.975		
	-9.7	2.16		
	-8.9	1.941		
	-7.9	1.734		
	-7.0	1.502		
	-6.1	1.284		
	-5.1	1.031		
	-3.6	0.706		
	0.4	-0.202		
	8.0	-1.940		
	5.2	-1.293		
	4.3	-1.102		
	-9.2	1.963		
	-8.2	1.719		
	-7.4	1.605	25.2	
4/20/52	8.8	-2.12	26.3	
	8.0	-1.894		

TABLE 14 (cont.)

t	E_s	ΔP	T	R_x
	7.5	-1.764		
	7.0	-1.639		
	6.5	-1.503		
	5.7	-1.340	26.3	
	5.0	-1.164		
	4.0	-0.985		
	3.5	-0.881		
	3.0	-0.769	26.3	
	2.5	-0.673		
	-9.9	2.145		
	-8.8	1.889		
	-8.3	1.761		
	-7.5	1.577		
	-6.5	1.345	26.3	
	-6.0	1.216		
	-5.5	1.117		
	-5.0	0.984		
	-4.5	0.874		
	-3.5	0.647		
	-7.0	1.430		
	-6.2	1.258	26.2	
	-5.5	1.088		
	-5.0	0.980		
	-4.5	0.869		
	-3.5	0.672		
	-4.0	0.765		
	-3.0	0.535		
	-2.5	0.416		
	-2.0	0.324		
	8.5	-2.06		
	7.5	-1.792		
	7.0	-1.654		
	6.3	-1.488		
	5.5	-1.294		
	4.5	-1.073		
	4.0	-0.955	26.2	
	3.5	-0.848		
	3.0	-0.717		
	2.5	-0.625		
	2.0	-0.514		
	1.5	-0.411		
	0.5	-0.214		
	1.0	-0.318		
	0	-0.114		
	-2.5	0.438		



TABLE 14 (cont.)

t	E_s	ΔP	T	R_x
	-2.0	0.311		
	-1.5	0.201		
	-1.0	0.088	26.2	
	-194	36.82		
	187	-35.49		
	179	-33.99		
	-168	31.92		
	150	-28.59		
	-138	26.31		
	123	-23.48		
	-112	21.37		
	100	-19.19		
	-89	17.04		
	80	-15.46		
	-69	13.29		
	60	-11.72		
	-48	9.33		
	41	-8.09		
	-33	6.51		
	31	-6.22		
	-28	5.55		
	24	-4.83	26.2	
4/21/52	350	-65.94		
	-334	63.02		
	-325	61.30		
	314	-59.16		
	301	-56.64		
	-290	54.78		
	-281	53.01		
	268	-50.58		
	257	-48.54		
	-249	47.04		
	228	-43.19		
	-219	41.43		
	204	-38.63		
	-194	36.66	26.2	
	177	-33.59		
	-173	32.74		
	154	-29.21		
	-144	27.28		
	127	-24.22		
	-119	22.56		
	101	-19.30		
	-98	18.67		



TABLE 14 (cont.)

t	E_s	ΔP	T	R_x
	80	-15.40		
	-77	14.68		
	67	-12.99		
	-55	10.62		
	47	-9.24		
	-34	6.64	26.2	
	36	-7.19		
	-28	5.41		
	29	-5.91		
	7.4	-1.861		
	-9.5	2.105		
	-9.0	1.922		
	-7.0	1.425		
	-6.5	1.322		
	-6.0	1.189		
	-5.5	1.084	26.2	
	-5.0	0.962		
	-4.5	0.858		
	-4.0	0.735		
	-8.8	1.899		
	-8.4	1.769		
	-8.0	1.640		
	8.0	-1.988		
	7.5	-1.853		
	7.0	-1.720		
	6.5	-1.581		
	6.0	-1.469		
	5.5	-1.375		
4/23/52	-73.0	13.67		
	-34.0	12.39	24.1	10.04
	-61.0	11.65		
	-29.5	10.86		10.04
	60.0	-11.49		
	29.0	-10.73		10.04
	53.0	-10.28		
	47.0	-9.19		
	22.7	-8.59	24.1	10.04
	78.0	-14.88		
	38.0	-14.05		10.04
	69.0	-13.28		
	-67.0	12.66		
	-32.1	11.78		10.04
	-59.0	11.23		
	-29.0	10.60		10.04

TABLE 14 (cont.)

t	E_s	ΔP	T	R_x
	-53.0	10.14		
	-77.0	14.56	23.9	
	-37.5	13.73		10.04
	-67.5	12.86		
	-33.0	12.12		10.04
	-60.0	11.46	23.9	
	67.0	-12.78	23.9	
	33.0	-12.20		10.04
	60.0	-11.56		
	28.0	-10.50		10.04
	51	-9.88	23.9	

TABLE 15

10^{-3} N NaCl in Tube 5

Teflon D = 0.305 mm L = 11.57 cm

t	E_s	ΔP	T	R_x
5/5/52 P.M.				
4:20	Solution first entered tube.			
4:25	322.3	-51.11	23.9	
4:40	-265.0	53.63	23.9	
4:44	-277.0	53.56		
4:46	-282.0	53.57		
	-0.5	-0.02		
4:50	282.6	-51.93		
4:54	288.9	-52.03	23.0	
4:58	294.0	-51.98		
5:02	182.0	-29.01		
	-0.6	0.01		
5:07	-292.8	50.12		
5:10	-295.5	50.18	24.0	
5:14	-298.1	50.17		
5:17	-301.0	50.11		
5:19	-268.6	50.10		981
5:21	-302.6	50.11	24.1	
5:26	293.5	-47.88		
7:05	286.9	-47.34	24.3	
7:10	402.3	-70.99		
7:22	-374.6	66.16		

TABLE 15 (cont.)

s t	E_s	ΔP	T	R_x
7:27	373.4	-64.95		
	301.0	-65.09		494
7:31	373.6	-65.08	24.3	
	-358.0	62.01		
	-218.3	62.01	24.3	188
	-347.4	62.00		
5/6/52 A.M.				
10:30	-417.0	73.51		
	-384.3	66.15		
	-321.3	53.14		
	-246.7	38.59		
	-188.1	28.10	22.8	
	-146.7	21.17		
	-102.2	14.38		
	-44.4	6.18		
	-3.2	0.39		
11:30	406.2	-71.51	22.8	
	408.2	-71.45		
	410.0	-71.42		
	313.5	-53.64		
	217.5	-36.81		
	109.0	-18.37		
	32.1	-5.25		
	-3.0	0.45		
11:55 P.M.	-409.0	69.57	22.8	
1:00	-401.8	68.68	23.0	
	-307.3	51.93		
	-229.5	38.58		
	-157.9	26.42	23.0	
	-64.9	10.87		
	-1.4	0.16		
	41.6	-6.87	22.9	
	85.2	-14.14		
	144.5	-23.75		
	215.1	-35.32		
	389.7	-65.33	22.9	
5/7/52	291.1	-56.06	22.0	
	232.5	-44.50		
	146.5	-28.03		
	82.0	-15.45		
	38.8	-7.18		
	0.6	-0.12		

TABLE 15 (cont.)

t	E_s	ΔP	T	R_x
	-49.4	8.60	22.0	
	-108.0	18.29		
	-183.0	31.88		
	-268.0	47.86	22.0	
	-350.2	59.83		
	-308.5	59.85	22.1	981
	-351.1	59.88		
	-309.0	59.86		981
	-351.3	59.83		
	-276.1	59.82	22.1	494
	-351.4	59.79		
	-276.0	59.76		494
	-351.6	59.75		
	-203.7	59.71	22.1	188
	-351.5	59.66		
	-137.4	59.65		88.6
	-351.3	59.63	22.1	
	-202.4	59.60		188
	-350.8	59.61		
	-316.4	59.58		88.6
	-350.3	59.56		
	-372.5	67.89	22.5	
	346.9	-64.60		
	-340.9	63.17		
	327.3	-59.34	22.5	
	-326.3	57.01		
	313.4	-54.56	22.4	
	-304.1	52.36		
	294.0	-50.05	22.4	
	-283.0	48.02		
	230.5	-39.19		
	-209.5	35.07		
	200.6	-33.28		
	-199.7	32.76	22.4	
	-335.4	55.86		
	307.0	-51.50		
5/8/52	-397.0	70.03	21.0	
	372.1	-66.23	21.0	
	-358.3	63.59	21.0	
	342.5	-61.03	21.0	
	-329.4	58.80		
	315.4	-56.00	21.0	
	-301.4	53.81	21.0	
	290.7	-51.99		

TABLE 15 (cont.)

t	E_s	ΔP	T	R_x
	-268.0	47.92	21.0	
	253.3	-45.30	20.9	
	-242.4	43.40	20.9	
	226.2	-40.58	20.9	
	-210.5	37.71		
	201.0	-36.12	20.9	
	-188.2	33.80	20.9	
	174.4	-31.35	20.9	
	-162.1	29.16		
	147.1	-26.56	20.9	
	-138.6	24.97	20.9	
	127.2	-22.97		
	-114.1	20.59	21.0	
	108.1	-19.59	21.0	
	-99.9	17.92		
	85.9	-15.58	21.0	
	-80.2	14.59		
	67.8	-12.39		
	-63.9	11.66	21.0	
	56.4	-10.34	21.0	
	-51.9	9.49	21.0	
	45.4	-8.36		
	-43.4	7.98	21.0	
	38.8	-7.21	21.0	
	-36.2	6.65		
	-29.2	5.44		
	27.7	-5.19		
	35.5	-6.61		
	-34.5	6.32		
	24.0	-4.55		
	-25.3	4.67		
	-19.7	3.65		
	17.7	-3.36		
	-16.5	3.04		
	14.9	-2.845	21.0	
	-11.9	2.21		
	10.4	-2.04		
	-8.3	1.530	20.9	
	7.4	-1.302		
	-9.9	1.832		
	8.9	-1.760	20.9	
	-5.7	1.036		
	4.9	-1.004		
	-4.2	0.749		
	3.5	-0.735		
	-2.5	0.418	20.9	

TABLE 15 (cont.)

t	E_s	ΔP	T	R_x
	1.5	-0.364		
	-1.3	0.184		
	0.5	-0.174		
	-0.3	0	20.9	
5/9/52	0.1	0	22.1	
	-1.0	0.250		
	1.1	-0.214		
	-2.1	0.497		
	2.0	-0.397	22.0	
	-3.0	0.681		
	5.2	-1.121		
	-5.0	1.109		
	3.3	-0.666		
	-7.1	1.531	22.1	
	6.8	-1.397		
	-10.3	2.205	22.1	
	10.1	-2.08		
	-14.0	2.97		
	13.1	-2.71		
	-21.0	4.44	22.2	
	22.0	-4.59		
	342.1	-71.20		
	205.7	-71.04	22.2	188
	341.5	-70.83		
	-324.3	67.53		
	-195.1	67.36		188
	-322 6	67.18	22 4	
	305.8	-63.93	22.4	
	-291.3	60.71		
	275.0	-57.63		
	-257.0	53.58		
	226.0	-47.24	22.5	
	-207.0	42.92	22 5	
	181.9	-37.72		
	-165.0	34.16	22 5	
	150.3	-31.15		
	-124.6	25.91		
	113.4	-23.52		
	-100.6	20.87		
	85.5	-17.72		
	-73.2	15.21		
	63.0	-13.09		
	-53.6	11.17	22.5	
	39.2	-8.25		
	-29.4	6.19		

TABLE 15 (cont.)

t	E_s	ΔP	T	R_x
	19.9	-4.08		
	-13.2	2.90		
5/10/52	0.1	0.013	22.0	
	-365.7	75.51		
	340.0	-71.02		
	-325.5	67.68		
	310.4	-64.76		
	-298.6	61.86		
	273.6	-57.00	21.8	
	-241.3	50.10		
	-144.6	49.90		188
	-240.4	49.82	21.8	
	225.8	-47.07		
	135.4	-46.91		188
	224.8	-46.79	21.8	
	-204.6	42.49		
	175.8	-36.53		
	-152.5	31.61		
	132.8	-27.64		
	-98.1	20.42		
	82.6	-17.15	21.8	
	-63.1	13.19		
	49.7	-10.32		
	-40.8	8.54	21.8	
	31.8	-6.63		
	-31.3	6.61		
	24.9	-5.20		
	-20.6	4.33		
	16.6	-3.48		
	-9.8	2.08		
	6.9	-1.441	21.8	
	-5.3	1.118		
	4.4	-0.919		
	-2.9	0.640		
	1.8	-0.390		
	-0.8	0.189		
	0.1	-0.001	21.8	
	-5.8	1.222		
5/11/52	0	0	21.8	
	-7.1	1.520		
	5.8	-1.240		
	-4.2	0.933		
	2.3	-0.484	21.7	
	-5.4	1.193		

TABLE 15 (cont.)

t	E_s	ΔP	T	R_x
	-2.4	0.554		
	332.7	-71.65	21.7	
	-313.1	66.73		
	294.4	-63.56		
	176.5	-63.38		188
	293.7	-63.18		
	-288.2	61.86		
	-172.8	61.59		188
	-287.4	61.43		
	249.3	-53.28	21.8	
	-214.0	45.67		
	-156.7	34.15		
5/12/52	306.7	-72.60	21.2	
	-278.5	66.24	21.2	
	281.0	-66.53		
	-268.3	63.62		
	-160.3	63.28		188
	-267.4	63.12	21.2	
	252.9	-59.86		
	151.3	-59.71		188
	252.4	-59.57	21.2	
	-242.2	56.67	21.4	
	223.7	-53.54		
	-193.0	45.46		
	120.9	-28.68		
	-77.1	18.26		
	81.4	-19.46		
	-41.5	9.87		
	43.2	-10.31		
	31.4	-7.50		
	-27.2	6.31		
	18.0	-4.10		
	-14.3	3.22		
	5.1	-1.168		
	-5.8	1.262		
	11.2	-2.41		
	-2.8	0.565		
	22.6	-4.89		
	-1.2	0.197	21.3	
	1.6	-0.382		
	3.8	-0.881		
	-3.2	0.681		
	-1.6	0.336		
	-0.8	0.149	21.2	

TABLE 15 (cont.)

t	E_s	ΔP	T	R_x
5/13/52	0.1	-0.039		
	-1.8	0.376		
	7.0	-1.600	20.1	
	-5.3	1.210		
	3.0	-0.705		
	322.7	-71.03	20.2	
	-303.0	67.09	20.2	
	292.5	-64.62		
	-279.2	62.09		
	-165.3	61.93		188
	-277.8	61.75	20.2	
	-262.0	56.53	21.2	
	237.1	-52.14	21.2	
	-196.5	42.63	21.2	
	181.1	-39.55		
	-137.0	29.64	21.2	
	132.7	-28.99		
	-88.0	19.06		
	84.8	-18.41		
	-35.0	7.70		
	32.2	-7.02		
	-29.6	6.46		
	20.6	-4.44		
	-13.5	2.96		
	5.9	-1.260		
	-5.3	1.183		
	2.7	-0.574	21 5	
	-2.0	0.485		
	0.1	0		
	-1.7	0.409		
5/14/52	331.1	-71.17	22.0	
	-313.6	67.60		
	296.0	-63.94		
	177.9	-63.63		188
	294.5	-63.51	22.1	
	-284.2	61.59		
	-170.9	61.41		188
	-283.1	61.29	22.2	
	228.6	-49.51		
	-223.6	48.40	22.2	
	-176.4	37.79		
	167.3	-36.10		
	129.3	-27.76		
	-125.8	27.11	22.2	
	-83.5	18.00		

TABLE 15 (cont.)

t	E_s	ΔP	T	R_x
	79.4	-17.11		
	35.2	-7.59		
	-30.2	6.50	22.3	
	26.5	-5.80	22.3	
	-19.3	4.24		
	10.7	-2.34	22.3	
	-5.4	1.220		
	5.3	-1.158	22.3	
	-11.7	2.60		
	1.7	-0.364		
	-1.7	0.371		
	0	-0.001		
5/15/52	-308.9	69.20	22.0	
	-309.4	-69.49	22.0	

TABLE 16

10^{-3} N NaCl in Tube 6

Teflon D = 1.33 mm L = 12.8 cm

t	E_s	ΔP	T	R_x
4/25/52 P.M.				
2:00	Solution first entered tube.			
2:15	124	-22.24	23.4	
2:17	120	-21.76	23.4	
2:20	-121.0	21.72		
	-67.5	21.18		10.04
	-117.0	20.93	23.4	
2:28	112.4	-19.71		
	62.5	-19.38		10.04
	107.5	-19.09	23.4	
2:35	-108.0	18.94		
	-76.7	18.57		20.15
	-104.0	18.26		
2:40	99.2	-17.27		
	70.2	-16.98		20.15
	95.0	-16.79	23.4	
8:45	124	-22.79		
	-122.2	22.22		
	-69.2	21.99		10.04

TABLE 16 (cont.)

t	E_s	ΔP	T	R_x
	-118.1	21.68		
	113.1	-20.70		
	63.5	-20.47		10.04
	108.3	-20.33		
	-101.8	18.73		
	87.9	-16.41		
	-81.9	15.19		
	70.6	-13.25		
	-69.9	13.09	24.3	
	58.1	-11.10		
	-50.1	9.70		
	43.5	-8.59		
	-39.4	7.89		
	-26.0	5.07		
	22.0	-4.57		
	-20.3	4.08	24.4	
	-14.5	2.87		
	11.7	-2.295		
	-10.6	1.966		
	7.9	-1.536		
	-6.8	1.213		
	4.9	-0.885		
	-3.6	0.579		
	1.8	-0.342	24.6	
5/26/52 P.M.				
2:00	-355.5	65.63	24.1	
	323.6	-61.43		
	-304.0	59.07		
	293.0	-56.46	24.1	
	-275.2	53.46		
	263.3	-50.85	24.1	
	-248.9	48.45		
	237.5	-46.01		
	134.1	-45.40		10.04
	230.2	-44.90	24.1	
	-224.7	43.97		
	-127.7	43.52		10.04
	-218.4	42.95	24.1	
	208.0	-40.66		
	-191.0	37.53	24.1	
	176.8	-34.72		
	-160.4	31.47		
	149.4	-29.32	24.1	
	-134.6	26.50		

TABLE 16 (cont.)

t	E_s	ΔP	T	R_x
	119.0	-23.46		
	-97.0	19.03		
	83.8	-16.61	24.1	
(Trans)	-72.7	14.36		
	-59.0	11.85		
	54.8	-11.17		
	-48.3	9.93		
	42.4	-8.80		
	-35.5	7.58	24.1	
	32.5	-7.11		
	-28.6	6.35		
	24.3	-5.71	24.3	
	-21.8	4.75		
	18.2	-4.28	24.3	
	-16.2	3.465		
	13.2	-3.055		
(Lam)	-12.0	2.38	24.3	
	10.8	-2.37		
	-11.2	2.125		
	9.5	-2.065		
	-9.8	1.897		
	8.7	-1.850	24.4	
	-8.7	1.680		
	7.7	-1.582	24.5	
	-8.2	1.500		
	5.7	-1.195		
	-5.3	0.882		
	3.1	-0.668		
	-2.8	0.396		
	1.5	-0.307	24.6	
	-0.3	-0.022		
4/27/52	188.4	-38.62	24.5	
	-187.7	38.26		
	-106.7	37.66		10.04
	-182.2	37.12	24.5	
	173.3	-35.08		
	97.7	-34.59		10.04
	167.1	-34.27		
	-162.8	33.27	24.5	
	146.6	-30.13		
	-139.0	28.52		
	124.9	-25.72	24.5	

TABLE 16 (cont.)

t	E_s	ΔP	T	R_x
	-118.7	24.34		
	106.7	-22.05		
	-99.2	20.37		
	89.7	-18.66	24.5	
	-83.5	17.21		
	75.2	-15.76		
	-67.7	14.44	24.5	
	62.0	-13.15		
(Trans)	-57.1	11.99	24.5	
	50.7	-10.87		
	-45.0	9.65		
	39.3	-8.65	24.6	
	-34.3	7.57		
	28.3	-6.45		
	-25.0	5.66	24.6	
	21.3	-5.04		
	-18.9	4.22		
	17.4	-4.11	24.6	
	-15.5	3.38		
	12.5	-2.92		
	-11.5	2.395		
	8.5	-1.927	24.7	
	-7.6	1.473	24.7	
	5.3	-1.118		
	-5.0	0.862		
	2.8	-0.676		
	-3.1	0.435		
	1.2	-0.307		
	-0.5	-0.010		
4/28/52	274.4	-57.63	26.0	
	-260.9	55.49	26.0	
	245.4	-51.84	26.0	
	-235.7	50.29		
	-136.2	49.79		10.04
	-229.2	49.11	26.0	
	221.6	-47.18		
	-27.4	-46.59		10.04
	214.6	-46.08		
	-205.5	44.38	26.0	
	194.2	-41.80		
	-178.7	38.80		
	165.2	-35.77	25.9	
	-153.1	33.29		
	139.0	-30.23	25.9	

TABLE 16 (cont.)

t	E_s	ΔP	T	R_x
	-128.7	28.03		
	115.3	-25.17	25.9	
	-103.9	22.40		
	92.0	-20.22		
	-86.3	18.85	25.9	
	77.3	-17.08		
	-72.3	15.83	25.9	
	63.8	-14.18		
	-58.6	12.97	25.9	
	50.7	-11.48		
(Trans)	-46.0	10.36		
	40.8	-9.40	25.9	
	-36.2	8.36		
	31.3	-7.43		
	-27.9	6.44		
	22.8	-5.70		
	-19.3	4.55	25.9	
	15 9	-3.98		
	-13.0	2.92		
	9.7	-2.34		
(Lam)	-9.3	1.967		
	6.7	-1.588	25.9	
	-7.9	1.519		
	5.1	-1.172		
	-5.2	1.018	25.9	
	3.5	-0.728		
	-3.8	0.621		
	2.0	-0.411		
	-2.3	0.321		
	-0.6	-0.021	25.9	
4/29/52	-329.0	70.72	23.7	
	318.5	-67.92	23.7	
	-296.3	64.01		
	286.3	-61.26		
	-268.8	58.24	23.7	
	258.2	-55.48		
	146.5	-54.97		10.04
	252.0	-54.45	23.7	
	-243.2	53.01		
	-138.1	52.50		10.04
	-237.4	52.01	23.7	
	207.4	-45.75	23.8	
	-199.0	44.34	23.8	
	183.0	-40.50	23.8	
	-172.3	38.42		

TABLE 16 (cont.)

t	E_s	ΔP	T	R_x
	157.2	-34.91	23.8	
	-147.5	33.02		
	132.7	-29.60	23.8	
	-121.3	27.22		
	109.5	-24.49		
	-102.9	22.81		
	92.6	-20.80	23.8	
	-85.6	19.27		
	76.3	-16.23		
	-70.3	15.73	23.8	
	62.0	-14.08		
	-53.8	12.14		
(Trans)	47.2	-10.92		
	-42.4	9.74	23.8	
	34.8	-8.23		
	-32.4	7.54	23.8	
	26.8	-6.47		
	-24.5	5.66		
	20.0	-4.86	23.8	
	-18.4	4.19		
	15.2	-3.70	23.8	
	-14.2	3.12		
	10.8	-2.545		
	-10.1	2.13		
	8.8	-2.07	23.9	
	-8.2	1.693		
	7.0	-1.622		
	-7.8	1.528		
	6.4	-1.448	24.0	
	-6.9	1.347		
	5.8	-1.288		
	-5.6	1.036		
	4.0	-0.995		
	-4.9	0.914	24.0	
	3.7	-0.851		
	-4.8	0.821		
	3.3	-0.722		
	-3.9	0.622	24.1	
	2.2	-0.523		
	-3.0	0.451		
	1.6	-0.398		
	-2.6	0.361		
	1.0	-0.270		
	-1.9	0.228	24.1	
	0.7	-0.194		



TABLE 16 (cont.)

t	E_s	ΔP	T	R_x
	-1.5	0.150		
	-0.5	0		
	241.0	59.53	30.9	
	226.5	-55.76	31.2	
	-215.6	53.50	31.2	
	204.1	50.98	31.2	
	-194.9	48.53	31.2	
	184.3	45.90		
	110.7	-45.39	31.2	10.04
	179.0	-44.86		
	-175.3	44.09		
	-105.6	43.73	31.2	10.04
	-170.7	42.99		
	161.1	-40.50	31.3	
	-152.0	38.61		
	144.1	-36.47	31.4	
	-134.1	33.85		
	125.3	31.86	31.4	
	-117.3	29.83	31.4	
	109.2	28.93		
	-101.7	26.34		
	92.8	-23.79	31.4	
	86.8	22.20		
	78.3	-20.20		
	-73.0	18.69	31.4	
	65.2	-16.98		
	57.9	14.89		
	-49.4	12.82	31.4	
	46.3	11.99	31.4	
	40.6	10.89		
	33.5	-9.17		
	31.1	8.44	31.4	
	25.7	-6.63		
	-22.9	6.22		
	16.7	-4.78		
	-16.0	4.31	31.4	
	33.3	-3.73		
	-12.5	3.15		
	9.5	-2.495		
	9.2	2.085		
	6.1	1.533		
	-7.3	1.502		
	5.6	-1.382		
	-5.1	1.060	31.4	
	4.3	-1.008		

TABLE 16 (cont.)

t	E_s	ΔP	T	R_x
	-4.2	0.735		
	2.7	-0.684		
	-3.5	0.533		
	1.8	-0.484		
	-2.4	0.300		
	1.0	-0.256		
	-1.8	0.184		
	-0.7	0.015	31.4	
4/30/52	-292.0	68.25	23.4	
	282.5	-65.94	23.4	
	254.8	-59.96		
	143.4	-59.26		10.04
	246.5	-58.47	23.4	
	-234.0	56.20		
	-133.0	55.87		10.04
	-228.0	54.83	23.4	
	220.4	-52.88		
	193.2	-46.63		
	-180.4	43.91	23.3	
	171.2	-41.52		
	-155.0	37.84		
	138.2	-33.71	23.3	
	-115.6	28.21		
	102.1	-24.93	23.3	
	-87.8	21.37		
	71.0	17.56	23.3	
	-66.7	16.39		
	48.9	-12.32	23.3	
	-44.6	11.03	23.3	
	34.4	-8.88		
	-31.7	7.98	23.3	
	23.7	-6.25		
(Trans)	-19.9	4.98		
	16.0	-4.16		
	-14.4	3.55		
(Lam)	10.3	-2.52	23.3	
	-9.7	2.05		
	7.5	-1.762		
	-7.9	1.630		
	6.1	-1.313		
	-5.6	1.058		
	3.2	-0.787		
	-3.8	0.604		
	2.5	-0.566		

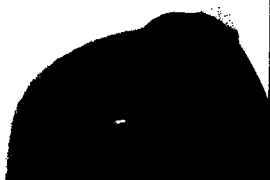


TABLE 16 (cont.)

t	E_s	ΔP	T	R_x
	-3.0	0.437		
	1.6	-0.416		
	-2.3	0.279		
	1.0	-0.271	23.3	
	-0.7	0		
5/2/52	-322.7	77.70	22.0	
	304.7	-73.66	22.0	
	-290.0	71.26	22.0	
	273.0	-66.99		
	152.0	-66.22		10.04
	266.0	-65.70	22.0	
	-255.3	63.88		
	-142.5	63.25	22.0	10.04
	-247.0	62.32		
	234.0	-58.71	22.0	
	-214.0	54.94		
	202.6	-51.09	22.0	
	-185.6	47.32		
	171.4	-43.36	22.0	
	-157.8	40.44		
	146.6	-37.35	22.0	
	-135.7	34.85		
	122.1	-31.21	22.0	
	-110.0	28.39		
	97.9	-25.22	22.0	
	-85.0	21.91	22.0	
	79.0	-20.44		
	-65.6	17.12		
	58.8	-15.42	22.0	
	-45.9	12.07		
	38.4	-10.33	22.0	
	-32.0	8.54		
	26.0	-7.12		
	-21.6	5.79		
	18.6	-5.11	22.0	
	-17.1	4.40		
	13.9	-3.77		
	-11.0	2.68		
	8.1	-2.07		
	-6.6	1.544		
	5.2	-1.272		
	-4.6	0.939		
	2.5	-0.661		
	-2.3	0.384		
	0.8	-0.222		

TABLE 16 (cont.)

t	E_s	ΔP	T	R_x
	-1.1	0.111		
	0	-0.066		
	-0.4	0.003	22.0	
5/3/52	-265.5	68.47		
	-226.5	67.80		50.1
	-259.0	67.09	21.5	
	246.4	-63.77		
	49.6	-63.23		2.015
	239.4	-62.53	21.5	
	-230.7	60.92		
	-2.8	60.05		0.1008
	-224.0	59.36	21.5	
	214.6	-56.71		
	110.0	-56.30		10.04
	211.0	-55.73	21.5	
	-200.3	53.85		
	-4.9	53.11		0.201
	-195.4	52.57	21.5	
	189.6	-50.74		
	72.6	-50.10		4.98
	184.9	-49.54		
	131.3	-49.54		20.15
	180.8	-48.53	21.5	
	-176.0	47.85		
	-19.5	47.24		1.000
	-171.2	46.75		
	-10.0	45.74		0.504
	-165.1	45.17	21.5	
	162.7	-44.35		
	0.3	-43.67		0.010
	157.8	-43.22	21.5	
5/5/52	233.3	-66.81		
	167.5	-66.20		20.15
	222.8	-65.69	22.2	
	-221.3	64.48		
	25.0	63.84		1.000
	-216.6	63.26		
	-83.8	62.43		4.98
	-211.8	61.86	22.1	
	205.8	-59.73		
	42.1	-59.05		2.015
	201.5	-58.49		
	113.5	-58.02		10.04
	198.6	-57.44	22.1	

TABLE 16 (cont.)

t	E_s	ΔP	T	R_x
	-191.4	56.31		
	-11.4	55.36		0.504
	-186.2	54.88		
	-4.6	54.13		0.201
	-181.6	53.59	22.1	
	177.6	-52.21		
	152.3	-51.53		50.1
	174.0	-51.01		
	2.2	-50.41		0.1008
	169.7	-49.84		
	-0.3	0		
	-14.0	4.23	22.7	
	12.0	-3.595	22.7	
	-11.2	3.08	22.7	
	8.6	-2.36		
	-7.3	1.789		
	6.5	-1.618		
	-5.9	1.410		
	4.3	-1.071	22.9	
	-4.3	0.887		
	2.8	-0.602	22.9	
	-2.6	0.462		
	1.2	-0.240		
	-1.3	0.184		
	-0.3	0.011		

TABLE 17

10^{-3} N NaCl in Tube 7

Butyl Acetate D = 5 mm L = 93.75 cm

t	E_{AI}	ΔP_{Res}	T
5/18/52 Noon	Solution first entered tube.		
5/20/52	-20.0	4.20	
	20.0	-4.30	
	-15.0	3.16	
	14.3	-3.09	
	-10.6	2.23	
	9.0	-1.933	
	-7.4	1.585	
	5.5	-1.182	

TABLE 17 (cont.)

t	E_{AI}	ΔP_{Res}	T
	-5.0	1.112	
	3.0	-0.677	
	-2.4	0.563	
(Lam)	1.5	-0.316	
	-1.6	0.336	
	2.0	-0.455	23.7
	-1.8	0.445	23.7
	1.1	-0.225	
	-0.6	0.118	
	0.6	-0.103	
	0	0.016	23.7
5/21/52	20.6	-4.97	23.1
	-17.2	4.20	
	14.0	-3.34	23.1
	-11.6	2.87	
	10.0	-2.45	
	-8.2	2.04	23.1
	7.5	-1.788	
	-6.2	1.513	
	5.4	-1.330	
	-4.0	1.022	
	3.0	-0.741	
	-2.3	0.646	
	1.7	-0.386	
	-1.2	0.300	
	1.0	-0.216	
	-0.7	0.186	
	0.7	-0.121	
	-0.4	0.102	
	0.3	-0.034	
	0	0	
5/22/52	115.0	-29.41	24.8
	-105.0	27.13	
	99.0	-25.46	
	-90.0	23.13	
	83.3	-21.17	
	-76.2	19.56	
	71.3	-18.19	
	-64.5	16.52	
	60.0	-15.32	
	-55.1	14.06	
	46.3	-11.68	
	-44.4	11.35	
	37.3	-9.44	

TABLE 17 (cont.)

t	E_{AI}	ΔP_{Res}	T
	-32.2	8.19	
	31.4	-7.87	
	-24.8	6.24	
	22.1	-5.57	
	-16.4	4.18	
	15.8	-4.02	
	-13.7	3.45	
	11.2	-2.86	
	-10.1	2.59	
	6.4	-1.629	
	-6.4	1.649	
(Trans)	3.5	-0.941	
	-2.3	0.633	
	2.0	-0.565	
	-1.5	0.356	24.9
	1.2	-0.341	
	-0.8	0.174	
	0.6	-0.148	
	-0.1	0.009	

t	E_{BC}	ΔP_{Res}	T
5/18/52 Noon	Solution first entered tube.		
5/19/52	-41.0	27.24	
	38.0	-25.04	
	-34.6	22.79	
	32.4	-21.10	
	-29.0	18.76	
	27.0	-17.64	
	-24.7	16.18	
	22.3	-14.28	
	-20.6	13.29	
	18.8	-12.07	
	-16.6	10.67	
	14.8	-9.58	
	-12.9	8.17	23.7
	11.4	-7.14	
	-10.0	6.28	
	8.0	-5.03	
	-6.1	3.83	
	5.3	-3.46	
	-4.8	2.91	
	3.6	-2.375	
	-2.9	1.618	

t	E_{BC}	ΔP_{Res}	T
	1.6	-1.288	
	-1.6	0.816	
	0.1	-0.364	
	-0.9	0.334	
	-0.6	0.018	
5/20/52	-5.5	3.56	
	6.6	-4.11	23.6
	-4.4	2.92	
	3.4	-2.16	
	-2.8	1.914	
	2.5	-1.537	
	-1.7	1.164	
(Trans)	1.6	-0.969	
	3.5	-2.21	
	-1.7	1.211	23.6
	2.0	-1.206	
	-0.6	0.486	
	0.7	-0.445	
	-0.3	0.221	
	0.4	-0.226	
	-0.1	0.094	
	0.2	-0.088	
	0	0.005	

t	E_{FI}	ΔP_{Res}	T
5/18/52 Noon	Solution first entered tube.		
5/20/52	-0.9	3.99	
	0.6	-4.15	
	-0.6	3.13	
	0.4	-2.81	
	-0.4	2.13	23.7
	0.2	-1.678	
	-0.3	1.479	
	-0.2	0.596	
	0	-0.013	
5/22/52	0.2	0	
	-3.3	29.45	25.0
	3.2	-27.80	
	-2.9	25.61	
	2.7	-23.58	
	-2.6	21.81	
	2.4	-20.35	

TABLE 17 (cont.)

t	E_{FI}	ΔP_{Res}	T
	-2.2	18.60	
	1.9	-17.03	
	-1.8	15.91	
	1.2	-9.85	
	-1.1	9.24	
	1.0	-8.13	
	-0.9	7.69	
	0.1	-0.006	
	-0.5	4.55	
	0.6	-4.78	
	-0.4	3.66	
	0.4	-3.14	
	-0.3	2.68	
	0.3	-2.09	
	-0.15	1.505	
	0.12	-1.022	
	-0.1	0.852	
	0.1	-0.502	
	0.02	0.245	
	0	-0.015	

t	E_{HI}	ΔP_{Res}	T
5/18/52 Noon	Solution first entered tube		
5/21/52	-0.12	18.8	
	0.28	-16.7	
	-0.17	34.5	
	0.31	-32.0	
	-0.10	20.0	
	-0.15	29.5	
	0.20	-20.0	
	0.28	-27.0	

TABLE 18

10^{-4} N NaCl in Tube 1

Quartz D = 0.86 mm L = 89.35 cm

t	E_s	ΔP	T
7/18/50	-1655	22.5	
	-1008	17.5	
	-715	11.3	

TABLE 18 (cont.)

t	E_s	ΔP	T
	-420	5.8	
	-177	2.2	
	-1233	17.6	
	745	-16.5	
	495	-11.0	
	283	-6.4	
	125	-3.1	
	10	0	
	118	-2.0	
	171	-4.4	
	355	-7.7	
	735	-12.4	
	1390	-22.6	
	1060	-17.6	
	813	-13.6	
	578	-9.6	
	333	-5.5	
	158	-2.9	
	33	0	
	-268	3.6	
	-528	7.7	
	-868	13.0	
	-1225	18.3	
	-1363	20.2	
	-828	12.2	
	-283	3.5	
	-55	0	
	1263	-20.3	
	927	-17.8	
	790	-15.0	
	863	-13.1	
	723	-10.7	
	565	-8.5	
	428	-6.0	
	269	-4.2	
	116	-1.9	
	33	-0.6	
	3	0	
7/19/50	-59	0.7	
	-159	2.3	
	-270	3.8	
	-408	5.9	
	-579	8.2	
	-773	10.9	
	-882	12.7	

TABLE 18 (cont.)

t	E_s	ΔP	T
	-1038	14.8	
	-1178	16.7	
	-1279	18.8	
	-1513	22.1	
	-1703	24.7	
	28	0	
	1030	-20.0	
	885	-17.7	
	751	-14.8	
	543	-10.9	
	253	-5.2	
	-260	4.8	
	-553	8.3	
	-1018	16.5	

TABLE 19

10^{-4} N NaCl in Tube 7

Butyl Acetate D = 0.49 mm L = 93.75 cm

t	E_{AI}	ΔP_{Res}	T
6/4/52	Solution first entered tube		
6/9/52	-1171	29.44	25.5
	1031	-26.30	
	-825	20.83	
	675	-17.07	
	-695	17.68	
	453	-11.41	
	-427	11.72	
	404	-10.39	
	-271	6.86	
	242	-6.23	
	-263	6.64	
	276	-6.95	
	-206	5.18	
	224	-5.67	
	-174	4.40	
	172	-3.64	
	-125	3.22	
	104	-2.70	

TABLE 19 (cont.)

t	E_{AI}	ΔP_{Res}	T
	-78	2.01	
	65	-1.723	25.6
	-36	0.925	
	-24	0.602	
	-17	0.429	
	-14.1	0.366	
	-10.8	0.278	
	-8	0.217	
	-5.8	0.141	
	-2.8	0.072	
	46	-1.182	
	34	-0.904	
	27	-0.736	
	23.1	-0.630	
	19.1	-0.522	
	16.1	-0.426	
	12.7	-0.333	
	10.1	-0.259	
	8.1	-0.199	
	6.1	-0.142	
	3.0	-0.066	25.6
6/10/52 (Initial)	-271	6.91	
	286	-7.32	
	-240	6.14	
	225	-5.80	
	-185	4.74	25.2
	173	-4.44	
	-116	2.96	
	124	3.25	
	69	1.779	
	67	-1.799	
	-44	1.110	25.2
	-32	0.835	
	-24	0.676	
	-16	0.437	
	-11	0.283	
	-6.0	0.141	25.0
	54	-1.395	
	44	-1.154	
	34	-0.920	
	24	-0.665	
	19.0	-0.522	
	14.0	-0.383	
	9.0	-0.234	25.0
	4.0	-0.091	

TABLE 19 (cont.)

t	E_{AI}	ΔP_{Res}	T
(Final)	-196	5.03	
	257	-6.70	
	-174	4.46	
	168	-4.37	
	-109	2.77	
	116	-2.98	
	-53	1.361	
	58	-1.508	25.0
6/11/52 (Initial)	-807	19.78	
	725	-18.74	
	-600	15.45	
	553	-14.32	
	-441	11.37	
	419	-10.74	
	-317	8.24	
	282	-7.30	24.8
	-258	6.68	
	276	-7.14	
	221	-5.71	
	-226	5.81	
	173	-4.49	
	-161	4.16	
	121	-3.22	
	-104	2.84	
	61	-1.516	
	-70	1.800	24.8
	44.0	-1.161	
	34.0	-0.875	
	24.0	-0.662	
	16.9	-0.474	
	11.9	-0.317	
	8.9	-0.230	
	4.8	-0.118	
	1.8	-0.044	
	0.8	-0.020	24.7
	-45.3	1.133	
	-36.3	0.936	
	-26.2	0.720	
	-17.2	0.481	
	-13.2	0.340	
	-9.2	0.231	
	-5.2	0.122	
	-1.7	0.042	

TABLE 19 (cont.)

t	E_{AI}	ΔP_{Res}	T
6/11/52 (Final)	-246	6.17	
	-267	6.61	
	271	-6.80	
	-231	5.76	
	223	-5.59	
	-171	4.30	
	175	-4.44	
	-122	3.08	
	111	-2.81	
	-73	1.828	
	73	-1.881	
6/20/52	254	-7.39	
	-205	5.75	
	202	-5.77	
	-155	4.44	24.3
	153	-4.36	
	-156	4.47	24.2
	99	-2.84	
	-104	2.96	
	65	-1.91	24.2
	-29.5	0.889	
6/21/52	-229	6.04	
	255	-6.72	24.6
	-174	4.59	
	168	-4.37	
	-113	2.95	
	118	-3.12	
	-70	1.66	
	64	-1.235	24.6

t	E_{AB}	ΔP_{Res}	T
6/10/52	-553	40.03	
	520	-36.87	
	-446	32.20	
	427	-30.23	
	-366	26.38	
	339	-24.22	
	-275	20.12	
	246	-17.57	
	-223	16.13	25.2
	193	-13.82	
	-149	10.73	
	150	-10.82	
	-100	7.45	

TABLE 19 (cont.)

t	E_{AB}	ΔP_{Res}	T
	107.8	-7.80	
	-84.0	6.06	
	87.9	-6.33	25.2
	-93.9	6.76	
	98.7	-7.09	
	-77.3	5.35	
	87.1	-6.27	
	-58.3	4.14	
	68.0	-4.84	
	-34.8	2.47	
	41.5	-2.96	
	-20.4	1.433	
	27.1	-2.04	
	-16.8	1.316	25.2
	-14.9	1.013	
	-12.4	0.825	
	-10.3	0.725	
	-7.3	0.588	
	-5.8	0.500	
	-4.8	0.402	
	-3.7	0.288	
	-2.7	0.199	
	-1.7	0.119	
	-0.95	0.064	
	-0.05	0.004	
	16.2	-1.235	25.1
	13.2	-1.026	
	10.3	-0.724	
	7.8	-0.509	
	6.3	-0.407	
	4.9	-0.305	
	3.4	-0.225	
	2.4	-0.152	25.1
	1.5	-0.086	
	1.0	-0.065	
	0.6	-0.036	

t	E_{BC}	ΔP_{Res}	T
6/10/52	-574	44.17	25.1
	485	-37.24	
	-475	36.61	
	397	-30.53	
	-365	28.10	
	346	-26.81	

TABLE 19 (cont.)

t	E_{BC}	ΔP_{Res}	T
	-313	24.34	25.1
	262	-20.13	
	-274	21.27	
	185	-14.17	
	-203	15.86	
	133	-10.03	
	-129	9.99	25.0
	87	-6.58	
	-100	7.78	
	95	-7.20	
	-89	6.80	
	77	-5.94	
	-77	5.92	
	59	-4.50	
	-56	4.29	
	40.3	-3.04	
	-37.3	2.84	
	16.0	-1.172	
	-24.8	1.880	
	-14.1	1.032	
	-10.1	0.831	
	-8.6	0.739	
	-6.6	0.579	
	-5.3	0.446	
	-4.6	0.374	
	-3.7	0.304	
	-3.0	0.236	
	-2.5	0.187	
	-1.8	0.127	24.9
	-1.2	0.087	
	-0.8	0.058	
	-0.4	0.027	
	17.7	-1.302	
	15.0	-1.130	
	12.5	-1.011	
	10.0	-0.861	
	8.0	-0.730	
	6.1	-0.569	
	5.1	-0.466	
	4.1	-0.346	
	3.1	-0.254	
	2.1	-0.158	24.9
	1.7	-0.119	
	1.3	-0.094	
	0.9	-0.064	
	0.5	-0.035	

TABLE 19 (cont.)

t	E_{CD}	ΔP_{Res}	T
6/11/52	-228	39.86	
	200	-34.95	
	-182	31.86	
	164	-28.72	
	-150	26.17	
	131	-22.97	
	-114	20.04	24.8
	102	-17.97	
	-88.0	15.38	
	83.5	-14.73	
	-63.9	11.24	
	58.6	-10.42	
	-45.3	8.07	
	38.7	-6.83	
	-28.2	4.97	
	28.3	-5.03	24.8
	-37.6	6.61	
	41.9	-7.48	
	-31.7	5.53	
	35.6	-6.29	24.9
	22.2	-3.89	
	-25.6	4.44	
	18.5	-3.26	
	-17.5	3.03	
	11.9	-2.09	
	-9.7	1.694	24.8
	6.9	-1.145	
	5.9	-0.974	
	4.9	-0.807	
	3.9	-0.714	
	2.6	-0.592	
	2.2	-0.478	
	1.7	-0.330	
	1.2	-0.218	
	0.8	-0.138	
	0.4	-0.069	24.8
	-5.8	1.139	
	-5.1	0.997	
	-4.1	0.832	
	-3.1	0.622	
	-2.6	0.484	
	-2.1	0.388	
	-1.6	0.274	
	-1.1	0.183	24.8
	-0.6	0.098	

TABLE 19 (cont.)

t	E_{DE}	ΔP_{Res}	T
6/10/52	-215	43.49	
	190	-39.09	
	-157	31.67	25.0
	158	-33.02	
	-132	26.87	
	108	-22.41	
	-110	22.52	
	100	-20.65	
	-84	17.41	
	78	-16.06	
	-71	14.78	
	65.0	-13.49	
	-50.8	10.62	
	54.1	-11.27	
	-41.7	8.70	
	39.7	8.16	
	-25.0	5.36	
	23.9	-4.89	
	-33.8	7.09	25.0
	34.0	-7.05	
	-26.5	5.32	
	26.7	-5.48	
	-21.5	4.41	
	21.9	-4.50	
	-13.0	3.06	
	14.4	-2.94	
	-6.4	1.610	
	8.5	-1.708	
	-4.5	1.050	24.9
	-3.5	0.745	
	-3.0	0.558	
	-2.5	0.427	
	-2.0	0.362	
	-1.5	0.286	
	-1.1	0.211	
	-0.7	0.144	
	-0.3	0.071	25.0
	6.4	-1.323	
	5.1	-1.059	
	4.1	-0.859	
	3.1	-0.714	
	2.1	-0.599	
	1.8	-0.444	
	1.3	-0.286	
	0.9	-0.207	
	0.6	-0.142	
	0.35	0.090	25.0

TABLE 19 (cont.)

t	E_{EF}	ΔP_{Res}	T
6/11/52	-22.7	43.74	
	-27.7	52.80	
	22.6	-47.82	
	-22.3	43.38	
	18.7	-39.28	
	-17.7	34.85	
	15.3	-32.52	
	-14.2	28.55	
	12.2	-25.84	
	-11.7	24.52	
	9.7	-20.50	24.8
	-8.4	18.32	
	7.6	-16.15	
	-7.3	15.43	
	7.6	-12.94	
	-5.3	11.51	24.7
	4.4	-9.38	
	-3.0	6.52	
	3.2	-6.95	
	3.2	-6.86	24.8
	-3.4	6.99	
	3.0	-6.55	
	-2.7	5.63	
	2.2	-4.59	
	1.9	-4.22	24.8
	-2.0	4.35	
	1.3	-2.62	
	-1.2	2.63	24.8
	1.1	-2.32	
	-0.7	1.492	
	0.6	-1.168	
	0.5	-0.928	
	0.4	-0.728	
	0.2	-0.485	
	0.1	-0.236	
	-0.5	1.052	
	-0.4	0.815	
	-0.3	0.609	
6/21/52	2.8	-6.27	
	-2.9	6.36	
	2.1	-5.02	24.4
	-1.9	4.41	
	1.2	-2.80	
	-1.2	2.74	24.4
	0.7	-1.56	

TABLE 19 (cont.)

t	E_{EF}	ΔP_{Res}	T
	-0.7	1.35	
	0.5	-1.033	
	0.4	-0.918	24.5
	0.3	-0.715	
	0.2	-0.515	
	0.1	-0.257	24.5
	-0.45	0.820	
	-0.4	0.699	
	-0.35	0.544	
	-0.2	0.387	
	-0.1	0.192	
	E_{FG}		
6/9/52	-0.6	0.710	25.6
	-0.4	0.414	
	-0.3	0.292	25.6
	-0.05	0.147	
	-0.03	0.088	
	-3.0	5.66	
	0.5	-1.078	
	0.4	-0.805	
	0.25	-0.586	
	0.2	-0.430	
	0.05	-0.162	25.5
	0.1	-0.116	
	2.9	-6.06	
	-3.7	6.50	
	2.5	-5.26	
	-3.0	5.45	25.6
	2.1	-4.36	
	-2.3	3.95	
	1.5	-3.04	
	-1.6	2.90	
	0.9	-1.911	
	-1.1	1.909	
	0.6	-1.251	25.5
	0.5	-1.043	
	0.4	-0.726	
	0.2	-0.537	
	0.1	-0.222	
	-0.7	1.051	
	-0.6	0.879	
	-0.5	0.653	
	-0.4	0.482	25.5
	-0.2	0.227	
	-0.07	0.109	
	26.4	44.03	

TABLE 19 (cont.)

t	E_{FG}	ΔP_{Res}	T
	28.5	45.03	25.1
	22	-43.67	
	-25	42.45	
	20.0	-40.12	
	-22.0	36.49	
	16.0	-32.18	
	-19.0	31.19	
	13.6	-26.56	
	-14.9	24.41	
	12.0	-24.30	25.2
	-12.9	21.83	
	8.8	-17.85	
	-9.8	16.72	
	7.4	-15.10	
	-9.6	16.57	
	5.8	-11.67	
	-5.3	9.27	
	3.9	-8.20	
	-0.7	1.039	
	-4.1	7.06	
	2.9	-6.20	
	2.2	3.71	
	1.3	-2.68	
t	E_{GH}	ΔP_{Res}	T
6/20/52	15.8	31.80	24.4
	11.4	-28.87	
	-13.1	26.10	
	9.1	-22.71	
	-11.1	22.03	24.4
	7.4	-18.99	24.4
	-0.35	0.654	
	-0.25	0.416	24.4
	-0.28	0.765	24.7
	-0.22	0.327	
	-0.1	0.203	24.7
	-2.8	5.67	24.7
	0.38	-0.987	
	0.25	-0.632	24.6
	0.12	-0.418	24.6
	2.2	-6.62	

TABLE 19 (cont.)

t	E_{GH}	ΔP_{Res}	T
	-3.2	6.30	24.5
	-2.1	4.41	
	1.7	-4.55	24.5
	-1.6	3.09	
	1.1	-2.98	
	-0.8	1.652	
	0.5	-1.613	24.4
6/21/52	-3.4	6.70	24.3
	2.5	-6.65	
	-3.0	5.83	
	2.2	-3.80	
	-2.3	4.70	
	-1.4	2.70	
	1.7	-4.62	
	-0.9	1.77	
	1.1	-3.07	
	0.5	-1.353	
	-0.4	0.824	
	-0.3	0.664	
	-0.2	0.449	
	-0.1	0.206	24.3
	0.3	-0.902	
	0.2	-0.678	
	0.1	-0.413	

t	E_{HI}	ΔP_{Res}	T
6/9/52	-3.7	43.94	25.4
	3.7	-39.12	
	3.0	36.45	
	2.8	-29.81	
	-2.4	30.96	25.4
	2.4	-25.94	
	-2.2	26.21	
	-1.7	20.27	
	1.7	-17.19	
	-1.3	16.44	
	-1.2	14.07	
	1.1	-12.03	
	-1.0	12.19	
	0.9	-9.57	
	-0.7	7.67	
	0.7	-8.03	
	0.6	-5.93	
	-0.6	7.27	25.5
	0.55	-6.29	

TABLE 19 (cont.)

t	E_{HI}	ΔP_{Res}	T
	-0.5	5.21	
	0.5	-5.95	
	-0.4	4.15	
	0.4	-4.45	
	-0.3	3.51	25.5
	-0.2	2.06	
	-0.1	0.728	
	0.2	-2.22	
	0.1	-0.91	25.5

TABLE 20

t	ΔP_{LA}	ΔP_{Res}	T
7/11/52	0.042	1.412	24.3
	0.039	1.232	
	0.032	0.998	
	0.017	0.666	
	-0.224	-6.70	
	0.041	1.391	
	0.036	1.123	
	0.028	0.859	
	0.009	0.473	
	0.001	0.228	
	-0.060	-1.628	24.3
	-0.053	-1.317	
	-0.041	-0.977	
	-0.032	-0.644	
	-0.015	-0.332	
	-0.007	-0.146	
	0.160	6.16	
	-0.299	-7.92	24.4
	0.144	5.57	
	-0.238	-6.43	
	0.103	4.07	24.3
	-0.187	-5.08	
	0.067	2.56	24.5
	-0.122	-3.20	
	0.057	2.02	
	-0.060	-1.60	
	0.963	37.95	
	-1.405	-34.62	
	0.792	31.82	

TABLE 20 (cont.)

t	ΔP_{LA}	ΔP_{Res}	T
	-1.103	-27.51	
	0.608	25.61	
	-0.888	-22.20	
	0.545	20.41	24.6
	-0.692	-17.55	
	0.368	13.98	
	-0.452	-11.46	
	0.233	8.95	

t	ΔP_{AI}	ΔP_{Res}	T
8/4/52	-29.05	-31.15	23.9
	26.25	28.08	
	-23.58	-25.21	23.9
	21.94	23.20	
	36.35	38.95	24.1
	-33.15	-35.72	
	30.70	32.82	
	-28.27	-30.48	
	25.93	27.77	
	-24.42	-26.18	24.1
	19.64	21.05	
	-18.19	-19.64	24.1
	15.34	16.34	
	-11.02	-11.83	
	-8.77	-9.63	
	6.11	6.57	24.1
	-6.28	-6.76	
	4.45	4.80	
	-4.43	-4.88	
	2.10	2.28	
	-1.59	-1.79	24.2
	-1.477	-1.585	
	-0.896	-0.976	
	-0.596	-0.631	
	-0.408	-0.438	
	-0.201	-0 217	
	-0.110	-0.113	24.2
	1.208	1.297	
	0.905	0.970	
	0.607	0.642	
	0.304	0.313	
	0.103	0.110	24.3

TABKE 20 (cont.)

t	ΔP_{AB}	ΔP_{Res}	T
5/27/52	-4.95	-11.71	
	2.38	10.42	24.3
	-2.76	-6.82	
	1.582	7.03	
	0.686	3.12	
	-0.529	-1.329	
	-0.441	-1.188	
	-0.392	-0.986	
	-0.313	-0.717	
	-0.236	-0.573	
	-0.136	-0.344	
	-0.075	-0.216	
	-0.023	-0.093	
	-0.015	-0.052	24.3
	-1.68	-4.96	
	0.251	1.053	
	0.175	0.803	
	0.087	0.448	
	0.060	0.285	
	0.034	0.137	24.3
	0.018	0.075	
	0.005	0.024	
	0.605	2.46	
	-0.334	-0.790	
	-0.235	-0.553	
	-0.144	-0.342	24.4
	-0.063	-0.177	
7/11/52	3.64	15.86	24.6
	-5.76	-13.40	
	-13.90	-31.93	
	6.49	29.06	24.6
	-11.56	-26.83	
	5.31	23.83	
	-9.42	-21.88	
	4.46	19.80	
	-7.60	-18.08	24.6
	-6.36	-14.86	
	3.24	14.10	
	-5.18	-12.18	
	2.44	10.63	
	-3.49	-8.31	
	1.696	7.20	24.8
	-2.45	-6.43	
	1.254	5.30	24.9
	-1.721	-4.18	

TABLE 20 (cont.)

t	ΔP_{AB}	ΔP_{Res}	T
	0.981	4.07	
	-0.956	-2.43	
	0.492	2.20	
	-0.585	-1.42	
	0.320	1.311	24.9
	0.252	1.028	
	0.159	0.739	
	0.097	0.508	
	0.058	0.263	
	0.021	0.080	24.9
	-0.618	-1.612	
	-0.508	-1.341	
	-0.416	-1.072	24.9
	-0.311	-0.725	
	-0.175	-0.416	
	-0.058	-0.165	
	-0.015	-0.044	24.9
t	ΔP_{BC}	ΔP	T
5/23/52	1.220	4.39	
	-0.162	-0.731	
	-0.119	-0.533	
	-0.012	-0.055	24.8
	-0.891	-3.58	25.0
	0.169	0.725	
	0.038	0.146	
	0.008	0.027	25.0
	1.225	4.89	
	-0.153	-0.691	
	-0.091	-0.404	
	0.745	2.97	
	-0.154	-0.705	
	-0.959	-3.96	
	0.089	0.352	
	0.032	0.123	
	0.781	3.14	25.0
	-0.060	-0.268	
	-0.033	-0.125	
	-1.242	-5.26	
	0.155	0.661	
	0.047	0.177	
5/24/52	1.49	5.80	
	-0.758	-3.02	
	0.667	2.66	
	-0.428	-1.73	

TABLE 20 (cont.)

t	ΔP_{BC}	ΔP_{Res}	T
	0.500	2.02	24.9
	-0.449	-1.79	
	0.971	3.86	
	-0.314	-1.284	
	-0.234	-1.012	
	-0.136	-0.639	
	-0.080	-0.340	
	-0.048	-0.192	
	-0.028	-0.107	
	-0.010	-0.031	
	-1.014	-4.41	
	0.251	1.010	
	0.192	0.814	
	0.159	0.692	
	0.126	0.560	
	0.104	0.456	
	0.077	0.325	
	0.051	0.198	
	0.032	0.124	
	0.017	0.074	
	0.007	0.029	
	-1.179	-4.77	
	0.292	1.130	
	-0.316	-1.253	
	-0.168	-0.800	
	-0.127	-0.592	
	-0.099	-0.439	
	-0.077	-0.341	
	-0.055	-0.216	24.7
5/25/52	-0.083	-0.379	24.4
	-0.060	-0.265	
	-0.043	-0.168	24.4
	-0.007	-0.018	
	0.061	0.257	
	0.036	0.140	
	0.018	0.067	
	0.009	0.031	
	0.002	0.004	
5/27/52	6.55	26.26	
	-5.76	-23.28	
	5.25	20.89	
	-4.66	-18.83	
	4.16	16.24	
	-3.80	-15.02	24.2

TABLE 20 (cont.)

t	ΔP_{CD}	ΔP_{Res}	T
	-0.645	-5.55	24.4
	0.106	1.047	
	0.086	0.810	
	0.059	0.466	
	0.031	0.252	
	0.015	0.125	
	0.009	0.063	
	0.581	5.06	
	0.316	2.64	
	-0.161	-1.298	
	-0.128	-1.051	
	-0.080	-0.793	
	-0.054	-0.581	
	-0.039	-0.386	
	-0.024	-0.220	
	-0.012	-0.088	24.5
	-0.004	-0.035	

t	ΔP_{DE}	ΔP_{Res}	T
	-0.678	-5.96	
	-0.350	-3.09	
	0.107	1.132	
	0.094	0.926	
	0.083	0.720	
	0.066	0.548	
	0.049	0.397	
	0.032	0.270	
	0.017	0.147	
	0.009	0.085	
	0.004	0.035	
	0.553	5.69	
	0.308	3.14	
	0.125	1.38	
	-0.151	-1.384	
	-0.126	-1.138	
	-0.099	-0.940	
	-0.072	-0.736	
	-0.046	-0.544	
	-0.031	-0.330	24.3
	-0.015	-0.145	
	-0.010	-0.080	
	-0.005	-0.043	
	-4.17	-40.21	24.3
	3.35	36.93	
	-3.71	-33.82	24.3

TABLE 20 (cont.)

t	ΔP_{DE}	ΔP_{Res}	T
	2.98	20.87	
	-3.12	-28.05	
	2.41	24.82	
	-2.46	-22.61	
	1.842	19.61	24.3

t	ΔP_{EF}	ΔP_{Res}	T
	0.050	5.83	24.4
	0.033	3.08	
	0.015	0.800	
	-0.015	-1.458	
	-0.013	-1.141	
	-0.008	-0.805	
	-0.004	-0.484	
	-0.002	-0.281	
	-0.001	-0.156	
	-0.001	-0.058	24.4
	-0.059	-6.21	
	-0.036	-3.62	
	0.017	1.191	
	0.016	0.977	24.3
	0.013	0.663	
	0.008	0.429	
	0.004	0.213	
	0.002	0.106	
	0.001	0.063	24.2

t	ΔP_{FG}	ΔP_{Res}	T
5/26/52	-0.053	-5.14	24.4
	0.118	4.74	
	-0.037	-3.81	
	0.081	3.60	
	-0.027	-2.56	
	0.054	2.42	
	-0.018	-1.62	
	0.033	1.34	
	-0.074	-6.20	
	0.028	1.030	
	0.023	0.783	
	0.017	0.598	
	0.012	0.379	
	0.007	0.240	
	0.003	0.142	
	0.002	0.091	

TABLE 20 (cont.)

t	ΔP_{FG}	ΔP_{Res}	T
	0.001	0.043	24.4
	-0.048	-4.66	
	0.115	4.75	
	-0.014	-2.233	
	-0.010	-0.905	
	-0.007	-0.673	
	-0.004	-0.530	
	-0.003	-0.392	
	-0.002	-0.242	
	-0.001	-0.097	

t	ΔP_{GH}	ΔP_{Res}	T
	-0.159	27.95	
	-0.559	-25.52	
	-0.136	22.84	24.5
	-0.391	-21.37	
	-0.133	18.85	
	-0.106	-6.55	
	-0.121	6.43	
	-0.016	-1.209	
	-0.011	-0.940	
	-0.005	-0.604	
	-0.003	-0.144	
	-0.073	-4.78	
	-0.031	1.020	
	-0.023	0.823	
	-0.011	0.653	
	0.001	0.470	
	0.006	0.326	
	0.006	0.230	
	0.003	0.154	
	0.002	0.095	
	0.001	0.044	24.6
	-0.173	3.35	24.7
	-0.053	-3.58	
	-0.113	2.33	
	-0.038	-2.70	
	-0.071	1.59	
	-0.024	-1.87	
	-0.035	1.05	
	-0.184	4.34	
	-0.013	-0.141	
	-0.010	-0.908	
	-0.007	-0.738	
	-0.004	-0.548	

TABLE 20 (cont.)

t	ΔP_{GH}	ΔP_{Res}	T
	-0.004	-0.395	
	-0.003	-0.270	
	-0.002	-0.169	
	-0.203	4.34	
	-0.150	5.25	24.3
5/27/52	-0.91	-44.01	
	-0.33	40.13	
	-0.73	-37.13	24.3
	-0.24	34.00	
	-0.62	-31.20	
	-0.18	28.62	
	-0.51	-25.49	
	-0.19	24.10	
7/11/52	-0.372	38.03	
	-0.278	31.06	
	-0.572	-27.72	
	-0.211	25.14	
	-0.394	-19.54	25.0
	-0.139	17.65	
	-0.310	-15.74	
	-0.144	14.30	
	-0.238	-12.46	
	-0.105	11.15	
	-0.178	-9.75	
	-0.139	7.23	
	-0.110	-6.39	
	-0.159	5.80	
	-0.060	-3.70	
	-0.138	3.55	
	-0.072	1.62	25.0
	-0.052	1.282	25.1
	-0.032	1.017	
	-0.020	0.786	25.1
	-0.012	0.562	
	0	0.415	
	0.005	0.290	
	0.003	0.184	
	0.001	0.072	25.1

t	ΔP_{HI}	ΔP_{Res}	T
5/25/52	0.428	5.30	
	0.332	4.65	
	0	-1.10	
	0.016	-5.15	

TABLE 20 (cont.)

t	ΔP_{HI}	ΔP_{Res}	T
	0.193	1.040	
	0.155	0.810	
	0.106	0.575	24.2
	0.029	0.256	
	0.011	0.147	24.4
	0.003	0.066	
	0.001	0.032	
	0.803	3.72	24.2
	0.723	3.40	
	0	-0.884	
	0.022	-5.89	
	0.181	0.973	
	0.150	0.783	
	0.109	0.561	
	0.072	0.444	
	0.042	0.320	
	0.018	0.174	24.2
	0.170	0.921	
	0.313	1.64	
	0.671	3.24	
	0.523	2.54	
	0.619	2.95	
	0.265	1.43	24.4
	1.087	5.15	
	0.242	1.30	
	0.434	2.13	
	0.570	2.72	
	0.021	-4.29	
	0.206	1.133	
	0.192	0.991	
	0.148	0.746	
	0.122	0.625	
	0.093	0.501	
	0.057	0.376	
	0.036	0.278	
	0.015	0.167	24.5
	0.346	1.750	
	0.412	2.04	
	0.162	0.800	
	0.136	0.689	
	0.117	0.596	
	0.094	0.511	
	0.074	0.435	
	0.055	0.364	
	0.041	0.302	
	0.027	0.236	

TABLE 20 (cont.)

t	ΔP_{HI}	ΔP_{Res}	T
	0.020	0.191	
	0.011	0.131	
	0.007	0.093	
	0.927	4.47	
	0.681	3.20	
	1.178	5.76	
	1.168	5.55	24.5
	1.428	7.09	
	0.162	-20.68	
	4.16	19.96	
5/26/52	3.37	16.20	24.5
5/27/52	0.32	-35.57	
	7.20	32.15	
	0.29	-29.27	
	5.85	26.84	
	0.22	-23.76	
	4.83	22.50	
	0.15	-20.26	24.3
	3.84	17.99	
7/11/52	9.87	42.03	25.0
	0.302	-33.75	
	7.01	31.94	
	0.282	-27.39	25.0
	5.70	25.87	
	0.207	-22.11	
	4.44	20.73	
	0.152	-17.43	
	3.24	14.92	
	0.097	-12.68	25.0
	2.39	11.76	
	0.078	-9.97	24.9
	1.88	9.02	
	0.040	-6.43	
	1.223	5.81	
	0.021	-4.56	
	0.922	4.32	
	0.008	-2.50	
	0.558	2.65	24.9
	0.224	1.145	
	0.262	1.292	
	0.198	1.029	25.0
	0.136	0.695	
	0.064	0.386	
	0.019	0.195	
	0.002	0.073	25.0

TABLE 20 (cont.)

t	ΔP_{IR}	ΔP_{Res}	T
5/27/52	1.86	41.78	24.5
	-1.21	-37.48	
	1.53	34.80	
	-1.02	-31.60	
	1.23	28.51	
	-0.860	-26.68	
	0.906	21.34	
	-0.578	-18.48	
	0.576	13.72	
	-0.326	-10.62	
	0.300	7.31	
	-0.194	-6.17	
	0.228	5.62	
	-0.152	-4.70	
	-0.075	-2.34	
	-0.030	-0.74	
	0.052	1.080	
	0.045	0.866	
	0.040	0.685	
	0.030	0.497	
	0.020	0.374	
	0.013	0.249	
	0.005	0.131	24.4
	0.004	0.070	
	0.001	0.031	
	0.132	2.94	
	0.058	1.340	
	0.069	1.416	24.5
	-0.054	-1.420	
	-0.049	-1.222	
	-0.039	-0.950	
	-0.034	-0.745	
	-0.024	-0.564	
	-0.015	-0.427	
	-0.007	-0.170	
	-0.003	-0.091	

TABLE 21

Specific Resistance of Solutions

Measured with Fisher Scientific Conductivity Bridge,

Model RC-1B, Serial Number 741.

t	R_s (ohm cm)	T (°C)
	10^{-3} N KCl	
11/1/50	6870	24.8
1/18/51	7120	23.2
2/1/51	6450	27.8
2/12/51	6960	23.6
2/21/52	7100	23.2
2/29/52	7100	23.2
	10^{-3} N NaCl	
9/6/50	8670	21.8
9/14/50	8850	20.4
3/28/52	8190	24.3
4/3/52	8300	23.9
4/23/52	8180	24.0
5/9/52	8250	23.4
	8300	23.0
5/22/52	7810	25.7
	10^{-4} N NaCl	
6/11/52	71100	25.2
	70200	24.4
6/26/52	65400	27.5
	67300	27.2
7/10/52	66500	24.9

TABLE 22

Calibration of Right Reservoir

Volume (liters)	h (cm)	Δh (cm)
1	0.86	
		2.37
2	3.23	
		2.36
3	5.59	
		2.37
4	7.96	
		2.35
5	10.31	
		2.33
6	12.64	
		2.33
7	14.97	
		2.33
8	17.30	
		2.32
9	19.62	
		2.31
10	21.92	
		2.30
11	24.23	
		2.30
12	26.53	
		2.31
13	28.84	
		1.31
13.5	30.15	
		2.64
14	32.79	

TABLE 23

Tube 1

Quartz D = 0 mm L = 89.35 cm

t (hr:min:sec)	Left Reservoir (liters)	Right Reservoir (liters)	ΔP (cm Hg)	T (°C)
3/12/52				
0:00:00		2.0	-52.73	24.0
07:24		2.5	-52.37	
08:42	6.0		-52.30	
15:30		3.0	-51.90	
16:20	5.5		-51.84	
23:12		3.5	-51.43	
24:30	5.0		-51.39	
31:00		4.0	-50.98	
32:35	4.5		-50.94	
39:00		4.5	-50.55	
40:28	4.0		-50.51	
47:28		5.0	-50.11	
48.35	3.5		-50.08	
55:35		5.5	-49.68	
56:40	3.0		-49.62	
1:04:00		6.0	-49.24	
05:20	2.5		-49.20	
11:52		6.5	-48.85	
12:20	2.0		-48.84	
20:15		7.0	-48.44	
21:15	1.5		-48.40	
28:28		7.5	-48.03	
30:00	1.0		-47.94	



TABLE 24

Tube 2

Borosilicate Glass D = 0.475 mm L = 83.82 cm

t (hr:min:sec)	Reservoir Volume (liters)	ΔP (cm Hg)	T (°C)	D (mm)
3/30/52				
2:00	8.3	71.92	23.6	0.475
12:28	8.2	71.85	23.6	0.475
23:08	8.1	71.70	23.6	0.475
33:33	8.0	71.57		0.475
44:40	7.9	71.44		0.475
55:51	7.8	71.30		0.475
1:07:10	7.7	71.17		0.475
1:18.33	7.6			0.475
1:27:59	7.5	70.90		0.475
1:38:54	7.4	70.77	23.7	0.475
1:49:20	7.3	70.66		0.475
2:00:32	7.2	70.57		0.475
2.12:26	7.1			0.476
4:12:50	6.0	68.61	23.8	0.476
4/1/52				
28:00	8.7	48.82	24.1	0.474
2:34:23	7.9	47.76	24.1	0.474
3:40:15	7.5	47.16	24.1	0.474
7:20:20	6.3	45.27	23.7	0.474
4/2/52				
1:05:17	3.5	- 44.52	24.4	0.474
1:22:35	3.6	- 44.44		0.474
2:33:30	4.0	- 44.14		0.474
3:07:45	4.2	- 44.02	24.6	0.474
3:59:30	4.5	- 43.67	24.4	0.474
4:35:00	4.7	- 43.50	24.3	0.474
6:56:30	5.5	- 42.90	24.4	0.474
4/3/52				
2.59:30	3.6	- 45.23	23.9	0.474
3:17:30	3.7	- 45.12	23.8	0.474
3.51:00	3.9	- 44.96	23.8	0.474
4:09:30	4.0	- 44.86	23.8	0.474
4:26:40	4.1	- 44.74	23.8	0.474
4:37:25	4.2	- 75.56	23.8	0.474
4:47:50	4.3	- 75.59	23.8	0.474
4:57:15	4.4	- 75.42	23.8	0.474
5:07:50	4.5	- 75.35	23.8	0.474
5:17:50	4.6	- 75.27	23.8	0.474
5:28:30	4.7	- 75.15	23.8	0.474
5:39:15	4.8	- 74.97	23.8	0.474

TABLE 25

Tube 3a

Borosilicate Glass D = 1.00 mm L = 83.82 cm

t (min:sec)	Left Reservoir (liters)	Right Reservoir (liters)	ΔP (cm Hg)	T (°C)
9/16/50				
19:30		3.5	41.3	18.1
31:30		2.5		
33:05	4.0			
37:50		2.0		
43:15		1.5		
44:45	5.0			
48:55		1.0		
50:30	5.5			
33:45	5.5		- 14.3	
39:00		1.0		
48:30	5.0			
55:55		1.5		
5:00	4.5			
12:45		2.0		
20:40	4.0			
27:40		2.5		
36:35	3.5			
43:45		3.0		
52:00	3.0			
59:10		3.5		
11:20	3.0		62.2	
13:15		3.0		
15:15	3.5			
17:35		2.5		
19:20	4.0			
21:20		2.0		
23:15	4.5			
25:20		1.5		

TABLE 26

Tube 4

Borosilicate Glass D = 3.08 mm L = 83.82 cm

t (min:sec)	h (cm)	ΔP (cm Hg)	T (°C)
4/18/52			
0	9.79	- 2.21	24.2
1:37	10.88	- 1.826	
3:06	11.85	- 1.571	24.2
4:49	12.80	- 1.342	
6:25	13.54	- 1.160	24.2
10:14	15.02	- 0.787	
0	13.82	1.833	
1:19	12.98	1.551	
2:37	12.19	1.425	24.2
4:00	11.45	1.240	
5:08	10.91	1.104	24.2
7:23	10.00	0.879	
8:59	9.44	0.739	
10:39	8.94	0.615	24.2
13:06	8.42	0.503	

TABLE 27

Tube 5

Teflon D = 0.305 mm L = 11.57 cm

t (hr:min:sec)	h (cm)	ΔP (cm Hg)	T (°C)
5/12/52			
3:18:55	8.20	- 59.15	21.2
4:24:58	9.50	- 54.16	21.3
4:50:20	10.00	- 52.25	21.4
4:57:15	10.00	61.14	21.4
7:06:35	7.40	51.45	21.4

TABLE 28

Tube 6

Teflon D = 1.33 mm L = 12.75 cm

t (min:sec)	Reservoir Volume (liters)	ΔP (cm Hg)	T (°C)
5/5/52			
0	3.4	47.13	22.2
3:10	2.1	46.05	22.2
0	2.5	- 64.67	22.2
7:18	6.0	- 61.37	22.2
0	5.5	59.62	22.2
6:31	2.5	57.18	
0	5 863	1.814	22.5
5:18	5.648	1.719	
11:38	5.390	1.589	

TABLE 29

Tube 7

Butyl Acetate D = 4.9 mm L = 93.75

t (min:sec)	h (cm)	ΔP (cm H_2O)	T (°C)
7/11/52			
24:00	23.00	17.76	25.2
24:40	22.00	14.89	
25:24	21.00	13.02	
26:10	20.00	11.14	
26:59	19.00	9.32	25.2
27.52	18.00	7.55	
28:53	17.00	5.82	
30:08	16.00	4.09	
32:03	14.90	2.23	
35.27	14:00	0.70	

TABLE 29 (cont.)

t (min:sec)	h (cm)	ΔP (cm H_2O)	T (°C)
38:00	1.00	- 22.32	
38:34	2.00	- 20.51	
39:10	3.00	- 18.70	
39:47	4.00	- 16.88	25.2
40:27	5.00	- 15.05	
41:09	6.00	- 13.22	
41:53	7.00	- 11.38	
42:40	8.00	- 9.58	
43:32	9.00	- 7.84	
44:31	10.00	- 6.11	
45:43	11.00	- 4.40	
47:00	24.00	18.61	25.3
47:37	23.00	16.76	
48:40	21.50	13.96	
49:02	21.00	13.02	
49:48	20.00	11.14	
50:37	19.00	9.32	
51:31	18.00	7.55	
52:32	17.00	5.82	
53:45	16.00	4.09	
55:29	15.00	2.23	
59:05	14.00	0.70	25.3
3:00	1.00	- 22.32	
3:52	2.50	- 19.60	
4:11	3.00	- 18.70	
4:47	4.00	- 16.80	
5:27	5.00	- 15.05	
6:09	6.00	- 13.22	
6:52	7.00	- 11.38	
7:55	8.30	- 9.05	
8:32	9.00	- 7.84	
9:30	10.00	- 6.11	
10:42	11.00	- 4.40	
12:32	12.10	- 2.55	
16:14	13.00	- 1.02	25.3

TABLE 30

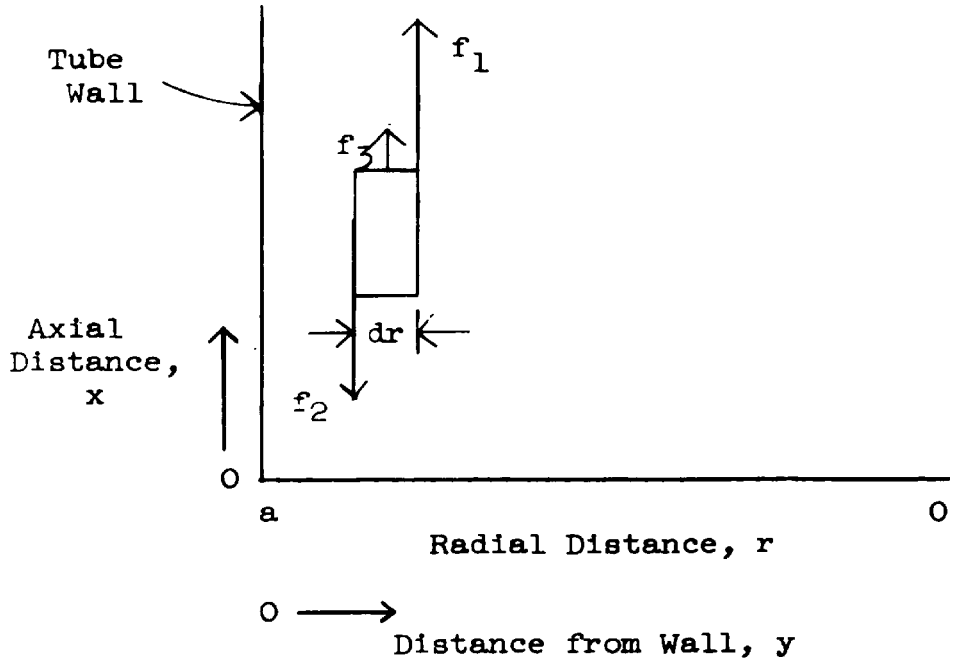
Calculated from Data in Tables 19, 20, and 29

ΔP_{Res}	Re	E_{AI}	ΔP_{IH}	$v^2/2g_c$	$\frac{\Delta P_{IH}}{v^2/2g_c}$	$\frac{E_{AI}}{\Delta P_{Res}}$	$\frac{E_{AI}}{\Delta P_{Res}-\Delta P_{IH}}$	$\frac{E_{AI}}{\Delta P_{Res}-1.5v^2/2g_c}$	$\frac{E_{AI}}{\Delta P_{Res}-2.5v^2/2g_c}$
cm Hg		mv	cm Hg	cm Hg	mv/cm Hg	mv/cm Hg	mv/cm Hg	mv/cm Hg	mv/cm Hg
0.0552	292	2.3	0.002	0.00115	1.90	41.6	43.2	42.8	43.7
0.118	585	4.8	0.008	0.0042	1.90	40.7	43.6	43.0	44.5
0.181	877	7.2	0.018	0.0095	1.90	39.8	44.2	43.2	46.6
0.247	1,170	9.7	0.029	0 0169	1.72	39.2	44.5	43.8	47.3
0.317	1,460	12.0	0.044	0.0263	1.67	37.9	44.0	43.3	47.7
0.391	1,755	14.6	0.061	0.0379	1.61	36.8	44.3	43.7	49.3
0.490	2,050	17.5	0.088	0.0516	1.70	35.7	43.5	42.5	48.5
0.611	2,340	21.0	0.118	0.0674	1.75	34.4	42.6	41.2	47.4
0.774	2,630	29.2	0.154	0.0854	1.80	37.8	47.1	45.2	52.0
1.031	2,920	40.1	0.196	0.1053	1.86	38.9	48.0	45.9	52.2
1.273	3,220	49.4	0.241	0.1275	1.89	38.8	47.9	45.6	51.7
1.503	3,510	58.2	0.285	0.1520	1.88	38.8	48.0	45.6	51.9
2.0	4,000	77.5	0.405	0.202	2.0	38.8	48.6	45.6	
4.0	5,900	154	0.860	0.438	1.96	38.5	49.0	46.3	
8.0	8,500	308	1.630	0.912	1.79	38.5	48.4	46.5	
12.0	10,800	464	2.50	1.47	1.70	38.6	48.8	47.4	
16.0	12,600	620	3.30	2.00	1.65	38.8	49.0	47.7	
20.12	14,700	781	4.20	2.77	1.51	38.8	49.0	49.0	
23.18	15,800	897	4.90	3.22	1.52	38.7	49.0	48.9	
26.47	16,900	1022	5.70	3.67	1.51	38.6	49.2	48.8	

ANALYSIS 1

VELOCITY DISTRIBUTION NEAR THE WALL OF A TUBE

Neglecting any electroosmotic countereffect and dividing the tube length into a sufficient number of increments so that the velocity u near the wall in the direction of x and the pressure gradient dP/dx can be considered constant for each increment, there will be three forces acting on each lamina with a thickness dr, as shown in the following diagram.



If the inner side of the lamina has a viscous force,

$$f_1 = 2\pi r \mu \, du/dr \quad , \tag{1}$$

where r is the radial distance, μ the viscosity, and u the velocity parallel to the wall. Then with the assumption that the viscosity is the same for any lamina near the wall, the outer side of the lamina will have an opposing viscous force.

$$f_2 = 2\pi\mu \left[r \frac{du}{dr} + \frac{d(r\, du/dr)}{dr} dr \right] . \qquad (2)$$

The force due to the pressure gradient will be

$$f_3 = 2 \pi r\, dr \frac{dP}{dx} . \qquad (3)$$

The viscous forces act in opposite directions, and their difference is equal to the force due to the pressure gradient, or

$$f_1 - f_2 = f_3 . \qquad (4)$$

Substituting equations (1), (2), and (3) into (4) and simplifying, one obtains

$$\mu \frac{d(r\, du/dr)}{dr} = r \frac{dP}{dx} . \qquad (5)$$

Integrating twice gives

$$u = \frac{r^2}{4\mu} \frac{dP}{dx} + M \ln r + N , \qquad (6)$$

where M and N are constants of integration.

Since only the velocity near the wall is to be considered here, let y be the distance from the wall. Then

$$r = a - y , \qquad (7)$$

where a is the radius of the tube.

Substituting equation (7) into (6), there results

$$u = \frac{a^2 - 2ay + y^2}{4\mu} \frac{dP}{dx} + M \ln (a-y) + N ; \qquad (8)$$

however, expressing the logarithm as a series gives

$$\ln (a-y) = \ln a + \frac{y}{a} - \frac{y^2}{2a^2} - \frac{y^3}{3a^3} - \ldots \qquad (9)$$

Substituting equation (9) into (8) and dropping M ln a since it is a constant which can be combined with the constant of integration N,

$$u = \frac{a^2 - 2ay + y^2}{4\mu} \frac{dP}{dx} + M\left(\frac{y}{a} - \frac{y^2}{2a^2} - \ldots\right) + N \; . \qquad (10)$$

When $y = 0$, $u = 0$; therefore

$$N = - \frac{a^2}{4\mu} \frac{dP}{dx} \qquad (11)$$

and since y can be considered diminishingly small compared to a, and after substituting of equation (11) into (10), the velocity near the wall can be expressed as

$$u = \left(- \frac{a}{2\mu} \frac{dP}{dx} + \frac{M}{a}\right) y \; . \qquad (12)$$

For an established flow the constant of integration M can be shown to be zero, but for a nonestablished flow its value is dependent on the experimental measurement of the velocity near the wall.

Since the terms which are the coefficients of y in equation (12) are in this analysis independent of y, the velocity gradient at the wall may be written

$$\frac{du}{dy} = - \frac{a}{2\mu} \frac{dP}{dx} + \frac{M}{a} \; . \qquad (13)$$

For an established flow, equation (13) is usually expressed

$$\frac{du}{dy} = \frac{a\,(-\Delta P)}{2\,\mu\,L} \; , \qquad (14)$$

where ΔP is the pressure difference across the length L.

It should be noted that the evaluation of M near the wall does not solve the problem of velocity distribution in the entire cross section of the tube for a nonestablished flow. In any nonestablished flow part of the liquid must have transverse motions as well as its motion in the direction of the tube axis. These transverse motions are very limited near the wall, so they have been considered as negligible in the above analysis.

ANALYSIS 2

THE STREAMING CURRENT EXPRESSED AS A PRODUCT OF THE VELOCITY AT A PARTICULAR DISTANCE FROM THE WALL AND THE TOTAL DISPLACEABLE CHARGE PER UNIT LENGTH

From equation (12) of the preceding analysis,

$$u = ky \quad , \tag{1}$$

where u is the velocity of any lamina of the double layer at a distance y from the wall and k is treated as a constant, since it is assumed independent of the distance from the wall; however, it will vary along the axial distance depending on the degree to which the flow is established.

Also, the distribution of charge in the double layer is assumed to be unaffected by the flow, and if it is assumed to be independent of the length

$$N = f(y) \quad , \tag{2}$$

where N is the surplus of charge per unit length contained in a lamina at distance y from the wall and f(y) is the function expressing this quantity.

The total displaceable charge per unit length is then

$$\sum_{1}^{j} N_j = 2 \pi a \sigma_s \quad , \tag{3}$$

where j is the number of lamina containing a displaceable charge, a is the radius of the tube, and σ_s is the displaceable charge density. Also, the streaming current I_s may be expressed as

$$I_s = \sum_{1}^{j} u_j N_j \quad . \tag{4}$$

Substituting equations (1) and (2) into (4), one obtains

$$I_s = \sum_1^j k\, y_j\, f(y_j) \quad . \tag{5}$$

Multiplying and dividing by the constant δ, some fixed distance from the wall, and factoring k from the summation, there results

$$I_s = k\delta \sum_1^j \frac{y_j}{\delta} f(y_j) \quad . \tag{6}$$

Then δ is evaluated by the relation

$$\sum_1^j y_j\, f(y_j) = \delta \sum_1^j f(y_j) \quad . \tag{7}$$

Each side of this equation is an expression for the moment M of the double layer. Equation (7) is not exact if the viscosity μ of equation (12) of the preceding analysis is not constant, but is some function of the distance from the wall. But in this case, k is also no longer a constant.

Then, by definition,

$$k\delta = u_s \quad , \tag{8}$$

where u_s is the velocity at distance δ from the wall, and also noting from equations (2) and (3) that

$$\sum_1^J f(y_j) = 2\pi a \sigma_s \quad . \tag{9}$$

Substituting equations (7), (8), and (9) into (6), one obtains

$$I_s = u_s (2\pi a \sigma_s) \quad . \tag{10}$$

This analysis shows that the streaming current can be expressed as the product of a velocity at a particular distance from the wall and

total displaceable charge, since the analysis is independent of the length of the tube.

It should be noted that the assumption that the distribution of charge of the double layer is independent of the length is probably not exact in most experimental studies. This assumption is dependent on there being a homogeneous charge distribution over the entire surface, which, in turn, probably cannot be accomplished because of the difficulty in reproducing a given surface upon which the ions of a solution are adsorbed to form a double layer.

Also, with our present knowledge of the distribution of charge of the double layer, i.e., f(y) is not known, δ cannot be numerically evaluated from equation (7). However, at least for an incremental length sufficiently short so that the distribution of charge can be independent of the length for the incremental length, equation (7) shows that δ does exist for that incremental length and that it must have a value between zero and the distance from the wall where the innermost displaceable surplus charge exists, since f(y) is a continuous function.

ANALYSIS 3

EVALUATION OF THE RESISTANCE OF THE SOLUTION BETWEEN THE ELECTRODES BY SHUNTING THE STREAMING POTENTIAL WITH KNOWN RESISTORS

The equation for the streaming potential E_s of j increments of tube length is

$$E_s = I_{s_1}R_1 + I_{s_2}R_2 + \ldots I_{s_j}R_j \quad , \tag{1}$$

where for each increment of length, I_s is the average convection current and R is the resistance.

When a resistance R_x of known value is placed between the electrodes and a current I flows through it, the potential may be expressed by two equations,

$$E = IR_x \tag{2}$$

$$E = (I_{s_1} - I)R_1 + (I_{s_2} - I)R_2 + \ldots (I_{s_j} - I)R_j \quad . \tag{3}$$

Substituting the I of equation (2) into equation (3) and rearranging, it results that

$$E = I_{s_1}R_1 + I_{s_2}R_2 + \ldots I_{s_j}R_j - E\left(\frac{R_1 + R_2 + \ldots R_j}{R_x}\right) \quad . \tag{4}$$

Substituting the streaming potential as expressed in equation (1) for the first series on the right-hand side of equation (4) and rearranging, one obtains

$$R_1 + R_2 + \ldots R_j = \frac{(E_s - E)\,R_x}{E} \quad . \tag{5}$$

Since the left side of equation (5) is the total resistance, the results are identical with those obtained by assuming a constant cross-sectional area and a constant convectional current throughout the length of the tube.

However, the results of this method are not independent of the electroosmotic effect, as can be shown by the following analysis.

If Q is the proportion by which the streaming potential is reduced due to an electroosmotic effect, the following equation for the streaming potential of j increments of tube length results:

$$E_s = I_{s_1}R_1 (1 - Q_1) + \ldots I_{s_j}R_j (1 - Q_j) \quad . \qquad (6)$$

The potential with the resistance R_x connected externally between the electrodes then becomes

$$E = IR_x \qquad (7)$$

$$I \quad (I_{s_1} - I R_1(1 - Q_1) + \ldots (I_{s_j} - I R_j(1 - Q_j) \qquad (8)$$

Substituting and rearranging as above, one obtains

$$R_1(1 - Q_1) + \ldots R_j(1 - Q_j) = \frac{(E_s - E R_x}{E} \quad . \qquad (9)$$

Obviously, equations (6) and (9) are not identical. The series comprising the left side of equation (9) is an exact expression for the total resistance across which the streaming potential is developed, combined with the electroosmotic counterpressure.

Since $Q = \epsilon \zeta / 4\pi\mu K + K_s a^2$, all the Q's of the series in equation (9) can be equal only if the radius a is constant throughout the tube. The other terms can be considered constant for any given tube and any given solution. Probably the greatest deviation from a constant value would occur for zeta-potential ζ, which is dependent on the previous history of each increment of length, which may be different along the tube.

Therefore, for a constant radius a, equation (9) may be reduced to

$$R(1 - Q) = \frac{(E_s - E) R_x}{E} . \qquad (10)$$

In any case, when the zeta-potential, or the moment of the double layer, is evaluated by using the resistance as measured by this method, the electroosmotic countereffect has been considered, and no further allowances should be made for it.

ANALYSIS 4

EFFECT OF THE SURFACE CONDUCTANCE OF STREAMING CURRENT IN POROUS DIAPHRAGMS

Following the method of Overbeek and Wijga's (43) analysis for the effect of the surface conductance on the streaming potential in porous diaphragms, the diaphragm may be thought of as composed of many small capillaries which are connected in parallel and in series.

For a single capillary j of length L and constant radius a, the resistance R of the solution filling it will be

$$R_j = \frac{L_j}{\pi a_j^2 (k + 2k_s/a_j)} , \qquad (1)$$

where k is the conductivity of the bulk solution and k_s is the surface conductance.

Capacity C per conductance for this capillary if the surface conductance is negligible is

$$C_j = \frac{\pi a_j^2}{L_j} . \qquad (2)$$

The rate of the streaming current I_s to the pressure difference ΔP for this capillary is

$$I_{s,j} = Z C_j (\Delta P)_j , \qquad (3)$$

where Z is the electrokinetic coefficient or

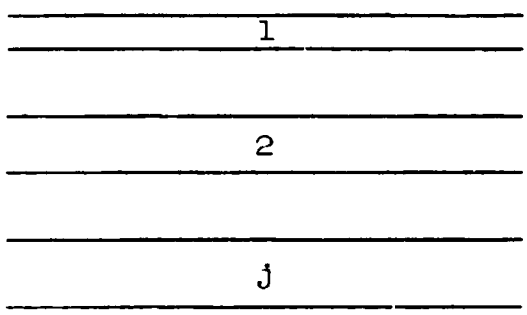
$$Z = \epsilon \zeta / 4 \pi \mu . \qquad (4)$$

The relation between the pressure difference and the volume rate of flow is

$$(\Delta P)_j = W_j V_j , \qquad (5)$$

in which W is the hydrostatic resistance and V is the volume rate of flow.

Case 1. Capillaries Connected in Parallel



The same pressure difference ΔP is applied across each capillary; consequently,

$$\Delta P = (\Delta P)_1 = (\Delta P)_2 = (\Delta P)_j \quad . \tag{6}$$

For the measurement of the streaming current, the potential E across the capillaries is zero, or

$$E = 0 \quad . \tag{7}$$

The total streaming current I_s drawn is the sum of the individual streaming currents, or from equation (3),

$$I_s = ZC_1(\Delta P)_1 + ZC_2(\Delta P)_2 + \ldots ZC_j(\Delta P)_j \quad . \tag{8}$$

From equation (6), all the pressure differences are equal to ΔP, so equation (8) becomes

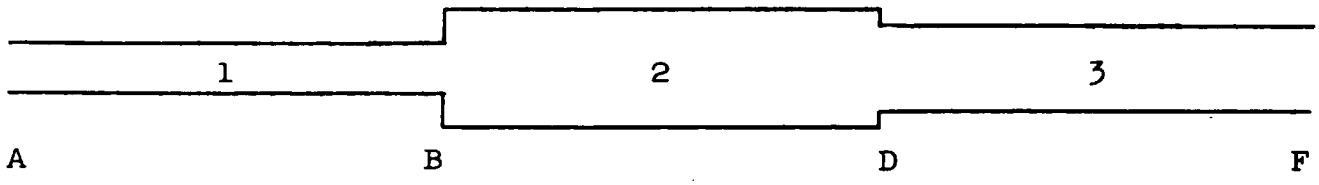
$$\frac{I_s}{\Delta P} = Z\,(C_1 + C_2 + \ldots C_j) \quad . \tag{9}$$

Since all the terms of the right-hand side of equation (9) are independent of the surface conductance, the streaming current is independent

of the surface conductance, and a mean radius a can be evaluated from the summation of the C's by the following equation

$$\frac{a^2}{L} = \sum_{1}^{j} \frac{a_j^2}{L_j} \quad . \tag{10}$$

Case 2. Capillaries Connected in Series



To measure the streaming current, the ends of the end capillaries are shorted; consequently, the potential across all the capillaries is zero, but it does not follow that the potential is zero across the individual capillaries.

$$E_{AE} = E_{AB} + E_{BD} + E_{DF} = 0 \quad . \tag{11}$$

If the potential across the individual capillaries is not zero, there must be a conduction current I_c to satisfy Ohm's law, $E = I_c R$.

$$I_{c_1} = E_{AB}/R_1 \tag{12}$$

$$I_{c_2} = E_{BD}/R_2 \tag{13}$$

$$I_{c_3} = E_{DF}/R_3 \tag{14}$$

Then, if there are conduction currents in the capillaries, the current I withdrawn from the ends of the capillaries must be equal for each of the capillaries and equal to the sum of the streaming current and the conduction current.

$$I = I_{c_1} + I_{s_1} = I_{c_2} + I_{s_2} = I_{c_3} + I_{s_3} . \qquad (15)$$

The six unknowns E_{AB}, E_{BD}, E_{DF}, I_{c_1}, I_{c_2}, and I_{c_3} may be eliminated from the six equations (one from equation (11), one each from equations (12), (13), and (14), and two from equation (15) above). Equation (15) then becomes

$$I = \frac{I_{s_1}R_1 + I_{s_2}R_2 + I_{s_3}R_3}{R_1 + R_2 + R_3} . \qquad (16)$$

The volume rate of flow V must be equal through all the capillaries; i.e.,

$$V = V_1 = V_2 = V_3 . \qquad (17)$$

The pressure difference across each of the capillaries is equal to the product of the hydrostatic resistance and the flow rate; therefore

$$\Delta P_{AB} = W_1 V_1 \qquad (18)$$

$$\Delta P_{BD} = W_2 V_2 \qquad (19)$$

$$\Delta P_{DF} = W_3 V_3 \qquad (20)$$

The total pressure difference is equal to the sum of the pressure differences across each capillary.

$$\Delta P = \Delta P_{AB} + \Delta P_{BD} + \Delta P_{DF} . \qquad (21)$$

The six unknowns V, V_1, V_2, V_3, ΔP_{BD}, and ΔP_{DF} may be eliminated from the six equations (two from equation (17), one each from equations (19) and (20), and one from equation (21) above). Equation (18) then becomes

$$\Delta P_{AB} = \frac{W_1(\Delta P)}{W_1 + W_2 + W_3} . \qquad (22)$$

Substituting equation (22) into equation (3), one obtains

$$I_{s_1} = \frac{Z\, C_1\, W_1\, (\Delta P)}{W_1 + W_2 + W_3} \tag{23}$$

By a like method, I_{s_2} and I_{s_3} can be evaluated. Then the substitution of the streaming current of the individual capillaries into equation (16) gives

$$\frac{I}{\Delta P} = \frac{Z\,(C_1W_1R_1 + C_2W_2R_2 + C_3W_3R_3)}{(W_1 + W_2 + W_3)(R_1 + R_2 + R_3)} \,. \tag{24}$$

If the flow in the individual capillaries is assumed to be an established laminar flow,

$$W = 8\mu L/\pi a^4 \,. \tag{25}$$

The substitution of C from equation (2), of W from equation (25), and of R from equation (1) and the generalization to an infinite number of capillaries, because if the above analysis is valid for three capillaries it can be shown to be valid for an infinite number, gives after simplification

$$\frac{I}{\Delta P} = \frac{Z\pi \sum_1^j L_j/a_j^4(k + 2k_s/a_j)}{\sum_1^j L_j/a_j^4 \cdot \sum_1^j L_j/a_j^2(k + 2k_s/a_j)} \,. \tag{26}$$

If the surface conductance is negligible compared to the total conductance, $k >> 2k_s/a$ and

$$\frac{I}{\Delta P} = \frac{\pi Z}{\sum_1^j L_j/a_j^2} \,, \tag{27}$$

and a mean radius a can be evaluated from the equation

$$\frac{a^2}{L} = \frac{1}{\sum_1^j L_j/a_j^2} \,. \tag{28}$$

There is a difference between equations (10) and (28), but the mean radius by both equations could have very nearly the same value.

If the surface conductance is the controlling factor in the total conductance, then $k << 2k_s/a$ and

$$\frac{I}{\Delta P} = \frac{\pi Z \sum_1^j L_j/a_j^3}{\sum_1^j L_j/a_j^4 \cdot \sum_1^j L_j/a_j} . \qquad (29)$$

A mean radius is evaluated from the equation

$$\frac{a^2}{L} = \frac{\sum_1^j L_j/a_j^3}{\sum_1^j L_j/a_j^4 \cdot \sum_1^j L_j/a_j} . \qquad (30)$$

The ratio of the streaming current when the surface conductance is the controlling factor of the total conductance to the streaming current when the surface conductance is negligible is found by dividing equation (29) by equation (27), or

$$\frac{I_{k<<2k_s/a}}{I_{k>>2k_s/a}} = \frac{\sum_1^j L_j/a_j^3 \cdot \sum_1^j L_j/a_j^2}{\sum_1^j L_j/a_j^4 \cdot \sum_1^j L_j/a_j} < 1 . \qquad (31)$$

Overbeek and Wijga (43) proved the right side of equation (31) is less than one.

This analysis shows that the surface conductance affects the streaming current through porous diaphragms because the same mean radius cannot be evaluated for the pores of a diaphragm both for the case when the surface conductance is controlling and for the case when the surface conductance is negligible.

BIBLIOGRAPHY

1. Abramson, H.A., "A Small but Constant Source of Error in Measurement of Viscosity," J. Gen. Physiol. 15, 279 (1932).

2. Bakhmeteff, B.A., The Mechanics of Turbulent Flow, Princeton University Press, 1941.

3. Bikerman, J.J., "Ionentheorie der Elektrosmose, der Strömungsströme und der Oberflächenleitfähigkeit," Z. physik. Chem., A163, 378 (1932).

4. Bishop, G.H., Urban, F., and White, H.L., "A Study of the Blocking Effect of Membranes," J. Phys. Chem. 35, 137 (1931).

5. Bohr, D.F., Paterson, R.R., Kenfield, W.J., Kitto, H.J., and Stroia, L.N., "Physiological Action of the Renal Vasoexcitor Material (VEM) with Reference to the Pathogenesis of Hypertension," U. of Mich. Med. Bull. 18, 77 (1952).

6. Briggs, D.R., "The Determination of the ζ Potential on Cellulose," J. Phys. Chem. 32, 641 (1928).

7. Brown, G.G., and associates, Unit Operations, John Wiley and Sons, 1950.

8. Bull, H.B., "Electrokinetic. XIV. A Critical Comparison of Electrophoresis, Streaming Potential, and Electroosmosis," J. Phys. Chem. 39, 577 (1935).

9. Bull, H.B., Physical Biochemistry, 2nd Ed., John Wiley and Sons, 1951.

10. Bull, H.B., and Gortner, R.A., "Studies on Electrokinetic Potentials. VI. Electrical Phenomena at Interfaces," J. Phys. Chem. 35, 309 (1931).

11. Bull, H.B., and Gortner, R.A., "Electrokinetic Potentials. XI. The Effect of Sodium Soaps on the Electric Moment of the Double Layer at an Aqueous-Cellulose Interface," Physics 2, 21 (1932).

12. Bull, H.B., and Gortner, R.A., "Electrokinetic Potentials. X. The Effect of Particle Size on the Potential," J. Phys. Chem. 36, 111 (1932).

13. Bull, H.B., and Moyer, L.S., "Electrokinetics. XVI. Streaming Potential in Small Capillaries," J. Phys. Chem. 40, 9 (1936).

14. Cameron, A., and Öttinger, J., "On the Electromotive Force Produced by Acid and Alkaline Solutions through Glass Capillary Tubes," Phil. Mag. (6) 18, 586 (1909).

15. Chapman, D.L., "A Contribution to the Theory of Electrocapillarity," Phil. Mag. (6) 25, 475 (1913).

16. Clark, J.W., "Über die beim Durchströmen von Wasser durch Capillarröhren erzeugte electromotorische Kraft," Ann. Physik. (3) 2, 335 (1877).

17. Dodge, R.A., and Thompson, M.J., Fluid Mechanics, McGraw-Hill, 1937.

18. Elton, G.A.H., "Electroviscosity I," Proc. Roy. Soc. (Lond.) A194, 259 (1948).

19. Freundlich, H., Kapillarchemie, Akademische verlagsgesellschaft m.k.h., 1909.

20. Glasstone, S., Physical Chemistry, 2nd Ed., Van Nostrand, 1946.

21. Gortner, R.A., and Briggs, D.R., "Glass Surfaces vs Paraffin in Blood-Clotting. Hypothesis," Proc. Soc. Exper. Biol. and Med. 25, 820 (1928).

22. Gouy, G., "Sur la constitution de la charge electrique a la surface d'un electrolyte," J. Physique (4) 9, 457 (1910).

23. Grahame, D.C., "New Techniques in the Measurement of the Capacity of the Electric Double Layer," Phys. Rev. 72, 522 (1947).

24. Grahame, D.C., "The Electric Double Layer and the Theory of Electrocapillarity," Chem. Rev. 41, 441 (1947).

25. Grahame, D.C., "Measurement of the Capacity of the Electrical Double Layer at a Mercury Electrode," J. Am. Chem. Soc. 71, 2975 (1949).

26. Grahame, D.C., "The Potential of the Electrocapillary Maximum of Mercury," J. Am. Chem. Soc. 71, 2978 (1949).

27. Grahame, D.C., "Thermodynamic Properties of the Electrical Double Layer," Tech. Report 1, Proj. No. NR-051-150, Office of Naval Research, Mar. 9, 1950.

28. Grahame, D.C., "Effects of Dielectric Saturation on the Diffuse Double Layer and Free Energy of Hydration of Ions," J. Chem. Phys. 18, 903 (1950).

29. Grahame, D.C., and Whitney, R.B., "The Thermodynamic Theory of Electrocapillarity," J. Am. Chem. Soc. 64, 1548 (1942).

30. Guggenheim, E.A., "The Helmholtz," Trans. Faraday Soc. 36, 139 (1940).

31. Helmholtz, H., "Studien über electrische Grenzschichten," Ann. Physik. (3) 7, 337 (1879). Gesammte Abhanglungen, I., 1882, p. 855, trans. by Bocquet, P.E., Two Monographs on Electrokinetics, Univ. Mich. Eng. Res. Bull. 33, 1951.

32. Horan, F.E., Hirsch, F.G., Wood, L.A., and Wright, I.S., "Surface Effects on Blood-Clotting Components as Determined by Zeta-Potential," J. Clin. Invest. 29, 202 (1950).

33. Hougen, O.A , and Watson, K.M., Chemical Process Principles, Part III, Kinetics and Catalysts, John Wiley and Sons, 1947.

34. Jones, G., and Wood, L.A., "The Measurement of Potentials at the Interface between Vitrous Silica and Solutions of Potassium Chloride by

Streaming Potential Method," J. Chem. Phys. 13, 106 (1945).

35. Lauffer, M.A., and Gortner, R A., "Electrokinetics. XX. Interfacial Energy and the Molecular Structure of Organic Compounds," J. Phys. Chem. 42, 641 (1938).

36. Lauffer, M.A., and Gortner, R.A., "Electrokinetics. XII. Electrokinetic Theory. Streaming Potential and the Electroosmotic Counter Effect," J. Phys. Chem. 43, 721 (1939).

37. Lorenz, P. B., "The Phenomenology of Electro-osmosis and Streaming Potential," a paper presented at Boston Meeting of the Am. Chem. Soc., Apr. 4, 1951.

38. Maturo, D., "Energetica del Equilibrio Electroosmotico," Rev. facultad quim. ind. agr. 6, 42 (1937). (Univ. na. cl. literal, Rosario, Santa Fe, Argentina.)

39. Mazur, P., and Overbeek, J. Th. G., "On Electro-osmosis and Streaming Potentials in Diaphragms. II. General Quantitative Relationship Between Electro-kinetic Effects," Recueil 70, 83 (1951).

40. Miller, B., "The Laminar Film Hypothesis," Trans. ASME 71, 357 (1949).

41. Neale, S.M., "Electrical Double Layer, the Electrokinetic Potential, and the Streaming Current," Trans. Faraday Soc. 42, 473 (1946).

42. Neale, S.M., and Peters, R.H., "Electrokinetic Measurements with Textile Fibres and Aqueous Solutions," Trans. Faraday Soc. 42, 478 (1946).

43. Overbeek, J. Th. G., and Wijga, P.W.O., "Electroosmosis and Streaming Potentials in Diaphragms," Rec. trav. chim. 65, 556 (1946).

44. Perrin, J., "Mecanisme de l'electrisation de contact et solutions colloidales," J. Chim. Phys. 2, 601 (1904).

45. Porrett, R., "Curious Galvanic Experiments," Annals of Philosophy 8, 74 (1816).

46. Quincke, G., "Über eine neue Art elektrischer Ströme," Ann. Physik (2) 107, 1 (1859).

47. Reichardt, H., "Über Abweichungen von der Helmholtzschen Theorie elektrokinetischer Erscheinungen," Z. physik. Chem. A154, 337 (1931).

48. Reichardt, H., "Elektrisches Strömungspotential bei turbulenter Strömung," Z. physik. Chem. A174, 15 (1935).

49. Reichardt, H., "Die Warmenbetragung in turbulenten Reibungsschichten," Z. angew. Math. und Mech. 20, 297 (1940); trans. in NACA Tech. Memo. No. 1047, 1943.

50. Reuss, F.F., Mémoires soc. imperiale naturalistes Maskau 2, 327 (1809).

51. Reynolds, O.E., "An Experimental Investigation of the Circumstances Which Determine Whether the Motion of Water Shall Be Direct or Sinistrous, and of the Law of Resistance in Parallel Channels," Phil. Trans.

174, 935 (1883).

52. Reynolds, O.E., "On the Dynamical Theory of Incompressible Viscous Fluids and the Determination of Criterion," Phil. Trans. A186, 123 (1895).

53. Riety, L., "Force electromotrice produite par l'ecoulement d'une solution de sulfate de cuivre dans un tube capillaire," Comp. rend. 152, 1375 (1911).

54. Rutgers, A.J., "Streaming Potentials and Surface Conductance," Trans. Faraday Soc. 36, 69 (1940).

55. Rutgers, A.J., and DeSmet, M., "Researches on Electro-Endosmosia," Trans. Faraday Soc. 41, 758 (1945).

56. Rutgers, A.J., and DeSmet, M., "Electroosmosis, Streaming Potentials, and Surface Conductance " Trans. Faraday Soc. 43, 102 (1947).

57. Saxen, U., "Über die Reciprocität der electrischen Endomose und der Stromungsströme," Ann. Physik (3) 47, 46 (1892).

58. Smith, E.R., and Taylor, J.K., "Reproducibility of Ag-AgCl Electrode," J. of Research, U.S. Bur. of Standards 20, 837 (1938).

59. Smoluchowski, M., "Elektrische endosmose und Stromungsströme," Handbuch der Elektrizitat und des Magnetismus, Vol. II, Graetz (ed.), Barth, 1921, p. 366. Trans. by Bocquet, P.E., Two Monographs on Electrokinetics, Univ. Mich. Eng. Res. Bull. 33, 1951.

60. Stern, O., "Zur Theorie der Elektrolytischen Doppelschicht," Z. Elektrochem. 30, 508 (1924).

61. Svensson, H., "Electrophoresis by the Moving-Boundary Method," Ark. Kemi. Mineral. Geol. 22A, No. 10 (1946).

62. Tietjins, O.G., Fundamentals of Hydro- and Aeromechanics, Engineering Society Monograph, McGraw-Hill, 1934.

63. Urban, F., and White, H.L., "Application of the Double Layer Theory of Otto Stern, I," J. Phys. Chem. 36, 3158 (1932).

64. Verwey, E.J., "The Electrical Double Layer and the Stability of Lyophobic Colloids," Chem. Rev. 16, 363 (1935).

65. Weller, B.L., "Direct Current Amplifier," U.S. Patent 2,455,718, held by U.S. Atomic Energy Commission.

66. White, H.L., Monaghan, B., and Urban, F., "Electrical Factors Affecting the Rate of Filtration of Aqueous Electrolyte Solutions through Cellophane Membranes," J. Gen. Physiol. 18, 515 (1935).

67. White, H.L., Monaghan, B., and Urban, F., "Stream Potentials and D.C. Surface Conductivities in Small Capillaries," J. Phys. Chem. 40, 207 (1936).

68. White, H.L., Urban, F., and Krick, E.T., "Stream Potential Determinations on Glass Capillaries of Various Sizes," J. Phys. Chem. 36, 120 (1932).

69. White, H.L., Urban, F., and Monaghan, B., "The Magnitude of the Surface Conductivity at Aqueous-Glass Interfaces," J. Phys. Chem. 45, 560 (1941).

70. White, H.L., Urban, F., and Van Atta, E.A., "A Correlation of Stream Potential and Surface Conductance," J. Phys. Chem. 36, 3152 (1932).

71. Wijga, P.W.O., "Stromingspotentialen, Electroendosmose en Oppervaktegeliding," Thesis, Utrecht, 1946.

72. Wood, L.A., "An Analysis of the Streaming Potential Method of Measuring the Potential at the Interface between Solids and Liquids," J. Am. Chem. Soc. 68, 432 (1946).

73. Wood, L.A., "Interface Potential of Vitrous Silica and Pure H_2O," J. Am. Chem. Soc. 68, 437 (1946).